CHAPTER 1

INTRODUCTION

1.1 Cancer overview

Cancer has been recognized throughout recorded history and was known to the ancient Egyptians, but it was not until the seventeenth century that the formal study of cancer (oncology) was first documented[1]. The incidence and spread of cancerous diseases are of growing concern to the National Health Services in South Africa, just as in other parts of the world. It is thought of as an unpredictable disease that strikes indiscriminately at rich and poor, fat and thin, old and middle-aged, as if it usually owed nothing to external causes[2]. One defining feature of cancer is the rapid creation of abnormal cells which grow beyond their usual boundaries, and which can invade adjoining parts of the body and spread to other organs, a process referred to as metastasis. Metastases are major causes of deaths from cancer[2.3].

Cancer poses a major threat to already overstretched healthcare services, and its global burden continues to increase. The World Health Organization (WHO) estimated that in the year 2000, 5.3 million men and 4.7 million women developed a malignant tumor and 6.2 million died from the disease. The number of new cases is projected to continue rising to reach 15 million by 2020[4].

Cancer classification is complicated by the variety of human cancers, with hundreds of different tumor types arising from almost every tissue and in every organ. This is further complicated by the ability of a cancer cell to invade surrounding tissues and metastasize to distant organs. Cancer biologists and oncologists have agreed on a classification based on the tissue of origin, regardless of organ location, focusing on the similarities in

cellular structure and function among these tumors[5,6]. Pathologically, cancers are classified as:

- Carcinoma, originating from epithelial cells in the skin or in tissues that line or cover the internal organs, and typically representing over 80% of diagnosed human cancer each year;
- Sarcoma, originating in bone, cartilage, fat, muscle, blood vessels, or other connective or supportive tissue;
- Leukemia, a cancer originating in blood-forming tissues such as the bone marrow, and causing large numbers of abnormal blood cells to be produced and enter the bloodstream; and
- Lymphoma, which originates in the cells of the immune system.

Cancer occurs because of changes in the genes responsible for cell growth and repair. These changes are the result of the interaction between genetic host factors and external agents which can be categorized as[6,7]:

- Physical carcinogens such as ultraviolet (UV) and ionizing radiation
- Chemical carcinogens such asbestos and tobacco smoke
- Biological carcinogens such as infections by viruses (Hepatitis B virus and liver cancer, Human Papilloma virus (HPV) and cervical cancer), and bacteria (Helicobater pylori and gastric cancer), and parasites (schistosomiasis and bladder cancer); and
- Contamination of food by mycotoxins such as aflatoxins (products of Aspergillus fungi) causing liver cancer.

People with HIV/AIDS have a high risk of developing certain cancers, such as Kaposi sarcoma, non-Hodgkin's lymphoma, and cervical cancer. The connection between HIV/AIDS and these cancers is not completely understood, but the link likely depends on a weakened immune system[8,9].

The four basic types of cancer treatment include: surgery, a primary form of treatment and preferred for localized disease; radiotherapy, a procedure in

which radiation is used to damage living cells; immunotherapy, aiming at stimulating and activating the patient's immune system to destroy cancer cells and finally chemotherapy, which is the use of anticancer drugs to kill cancer cells at the microscopic level, but as with radiation, it may produce damage to normal tissues. For a tumor which is confined and not metastasized, surgery alone or combined with local radiation may be curative. For the majority of patients, however, physicians are forced to rely on chemotherapy either as a primary treatment method or as a means to attack residual diseases following surgery and / or radiation[10].

Chemotherapy constitutes a major therapeutic approach for the treatment of cancer. It has played an important role in treating malignancies and solid tumors, though no effective chemotherapy for certain solid tumors and advanced tumors is available. This drug efficacy is further diminished by drug resistance and drug toxicity, frequently leading to premature treatment discontinuation (section 2.1.3). This situation inspired researchers world-wide to explore the utilization of polymeric drugs and polymeric delivery systems as possible means of enhancing the efficiency of antitumor agents (section 3.2). Within the framework of macromolecular drug research at the School of Chemistry of the University of the Witwatersrand, this dissertation represents a small contribution to the advancement in cancer drug development.

1.2 Objectives of the study

The primary objective of the research project was to address the problem of the poor drug efficacy by providing a vehicle for improved pharmacokinetic utilization of anticancer agents. This was achieved *via* bioreversible conjugation of selected anticancer drugs with water-soluble macromolecular carriers, designed in accordance with specific biomedical requirements. Specifically, the key feature of the research comprised of the development

of synthetic routes towards macromolecular carrier structures that comply with requisite biomedical requirements and to incorporate functionalities suitable for drug binding and release. Complementary research features included drug modification for polymer binding, the development of drug anchoring chemistry, conjugate and co-conjugate synthesis.

The second objective was the evaluation of the biological activity of the synthesized polymer-drug conjugates against human cancer cell lines. The motivation was to compare the potency of these conjugates with the parent drugs presently in clinical use. The principal drug systems used were based on metallo-organic (platinum) and organometallic (iron) structures.

The background to this work will be discussed in Chapter 2, with emphasis on cancer treatment modality, and the importance of water-soluble polymeric carriers. The development of the work done in order to achieve the objective of the thesis is discussed in Chapter 3 together with preliminary biological anticancer results. The experimental protocols for this work will be detailed in Chapter 4. The summary and conclusion are included in Chapter 5.

CHAPTER 2

LITERATURE REVIEW

2.1 Treatment of cancer: an overview

Treating cancer is one of the most complex aspects of medical care. It involves a team that encompasses doctors with various specialties (for example, primary care doctors, gynaecologists, medical oncologists, surgeons, radiotherapists, and pathologists) and many other groups of health care practitioners (for example, nurses, physiotherapists, social workers, and pharmacists). Treatment decisions take into account many factors, including the likelihood of cure or of prolonging life when a cure is not possible, the effects of the treatment on the disease, the side effects of treatment, and the patient's wishes. When the diagnosis of cancer is first made, the main goals of treatment are to remove the cancer if possible (through a single treatment or through a combination of surgery, radiation therapy or chemotherapy)[11]. Chemotherapy is usually the only way to treat any cancer cells that have spread (metastasized) beyond the original site.[12]

This chapter is organized around the four conventional treatment modalities available today; namely surgery, radiotherapy, chemotherapy and targeted therapy; with emphasis on chemotherapy since this is the object of this research. At the same time, some new therapies are also reviewed in this chapter.

2.1.1 Surgery

Surgery is a traditional form of cancer treatment used to physically remove malignant tissue[13]. If surgery is the only treatment, the assumptions are

made that the location of all malignant tissue is known, it can all be removed, and undetectable micrometastatic disease is not left behind, or if some is left behind, it will not re-grow to clinically detectable levels within the life expectancy of the patient.[13] Surgery is the most effective modality for treating localized disease, as long as the lesion can be localized and safely resected.[13] Diagnosis at the earliest possible stage minimizes the probability of local and distant spread and increases the probability of localized disease, resulting in a higher probability of surgical cure. The more common types of cancer surgeries are listed below[14-19]:

- Preventive surgery
- Diagnostic surgery
- Staging surgery
- Curative surgery
- Debulking surgery
- Palliative surgery
- Supportive surgery
- Restorative surgery

2.1.2 Radiation therapy

Radiation therapy or radiotherapy for cancer originated in the finding that x-rays sterilized rams by killing the proliferating germ cells in the testes that maintain spermatogenesis[20,21]. The historical understanding of cancer as a disease of overly rapid cellular proliferation made it logical to treat cancer patients with x-rays, and the initial tumor responses encouraged the development of this treatment[22]. During radiotherapy, malignant cells are exposed to ionizing radiation from either an external or implanted radiation source, and the resulting damage inhibits cellular division, leading to cell death, which leads to a gradual reduction in tumor mass[22].

In its most common form, radiation therapy uses an external beam of gamma radiation generated by a linear accelerator. Less commonly,

electron or proton beam radiation is used. Proton beam radiation, which can be focused on a very specific area, effectively treats certain cancers in areas in which damage to normal tissue is a particular concern, such as the eye, brain, or spinal cord. All types of external beam radiation are focused on a particular area or organ of the body that contains the cancer. To avoid overexposing normal tissue, several beam paths are used and surrounding tissues are shielded as much as possible. New technologies of focusing external beam radiation, called intensity modulated radiation therapy (IMRT), help protect surrounding tissues and allow a higher dose of radiation to be delivered to cancer cells[23].

In other radiation therapy strategies, a radioactive substance may be injected into a vein to travel to target the cancer (for example, radioactive iodine, which is used in the treatment of thyroid cancer). Another technique uses small pellets (seeds) of radioactive material placed directly into the cancer (for example, radioactive palladium used for prostate cancer). These implants provide intense radiation to the cancer, but little radiation reaches surrounding tissues. Implants contain short-lived radioactive substances that stop producing radiation after a period of time.

More recently, radioactive substances have been attached to monoclonal antibodies, which specifically target cancer cells and once attached to them[22], deliver the therapeutic agent to impede further cellular growth.

Radiation therapy plays a key role in curing many cancers, including Hodgkin's lymphoma, early-stage non-Hodgkin's lymphoma, squamous cell cancer of the head and neck, seminoma (a testicular cancer), prostate cancer, early-stage breast cancer, some forms of non-small cell lung cancer, and medulloblastoma (a brain or spinal cord tumor). Radiation therapy is sometimes combined with other forms of treatment[23].

Unfortunately, radiation can damage normal tissues near the tumor. Side effects depend on how large an area is being treated, what dose is given, and how close the tumor is to sensitive normal tissue. Sensitive tissues are those in which cells normally divide rapidly, such as skin, bone marrow, hair follicles, and the lining of the mouth, esophagus, and intestine. Radiation can also damage the ovaries or testes.

Symptoms depend on the area receiving radiation and may include fatigue, mouth sores, skin problems (redness, itching, peeling), painful swallowing, lung inflammation (pneumonitis), hepatitis, gastrointestinal problems (nausea, loss of appetite, vomiting, diarrhea), urinary problems (increased frequency, burning with the urination), and low blood counts. Radiation to head and neck tumors often causes damage to the overlying skin, as well as the lining of the throat. Doctors try to identify and treat such symptoms as early as possible, so the patient remains comfortable and can continue with treatments[23].

2.1.3 Chemotherapy

Chemotherapy involves the use of drugs to destroy cancer cells. The clinically useful antineoplastic agents are more toxic to sensitive malignant cells than to normal cells of the tumor-bearing host. They are therefore said to exhibit selective toxicity. Cancer chemotherapy inhibits cancer through several potential mechanisms, where it may induce cell death through nonspecific means (cytotoxicity), suppress cancer cells for variable periods of time without inducing cell death (cytostatic effects), and, rarely, it may induce cell differentiation[24,25].

Malignant tissues are largely composed of dividing cells that synthesize DNA at some point in their life cycle. Cancer cells use large amounts of glucose as a source of energy to permit the exaggerated utilization of amino

acids and nucleosides in the synthesis of DNA[26]. This pattern of metabolism is nonspecific, since it is also seen in fetal or regenerating tissue. What appears to be unique with neoplastic tissues, however, is an altered pattern of gene expression, especially a failure of the cancer cell to control or cease gene expression and to control the rate of cell division.

Cytotoxic chemotherapy works best against cells actively progressing through the cell cycle, and these drugs are generally less effective against the same cells in a quiescent state. As with radiotherapy, chemotherapy eradicates dividing cells in renewing tissue, and the anticancer drugs act as cytoreductants in both tumor tissue (efficacy) and in the gastrointestinal mucosa, bone marrow, hair follicles, and germ cells (toxicity). The most sensitive normal tissue in which life-threatening toxicity occurs is called the dose-limiting tissue, and the dose just below that which causes life-threatening toxicity is called the maximum tolerated dose (MTD). Usually the therapeutic index of chemotherapy (MTD to efficacious dose ratio) is quite small, and patients are dosed with the drugs to toxic levels in order to achieve maximum clinical benefit. Chemotherapeutics are administered by injection directly into the bloodstream, or are absorbed into the blood from the gastrointestinal tract after oral dosing, where it circulates through the body[27]. In contrast to surgery and radiotherapy, which are local and regional therapies, respectively, chemotherapy is a form of systemic therapy since the dose is distributed throughout the body. Although this means toxicity will be more extensive, systemic therapy is the only conventional modality that potentially can treat every malignant cell of a metastatic cancer, even in micrometastatic disease with unknown locations of tumor foci[28].

2.1.3.1 Chemotherapeutic agents

Cancer chemotherapeutic agents are usually discussed in groups that reflect either the origin of the drug or their predominant mechanism of

action. The major classes of agents include the alkylating agents, antitumor antibiotics, plant alkaloids, antimetabolites, hormonal agonists and antagonists, and a variety of miscellaneous agents[29,30]. Some of these groups are briefly discussed in this section with more emphasis on the drugs investigated in this research.

2.1.3.1.1 Alkylating agents and platinum antitumor compounds

The alkylating agents and the platinum antitumor compounds form strong chemical bonds with electron-rich atoms (nucleophiles), such as sulfur in proteins and nitrogen in deoxyribonucleic acid (DNA)[31]. Although these compounds react with many biological molecules, the primary cytotoxic actions of both classes of agents appear to be inhibition of DNA replication and cell division produced by their interactions with DNA. However, the chemical differences between these two classes of agents produce significant differences in their antitumor and toxic effects.

a. Alkylating agents

The alkylating agents are compounds that react with electron-rich atoms in biological molecules to form covalent bonds[31]. Traditionally these agents are divided into two types: those that react directly with biological molecules and those that form a reactive intermediate, which then reacts with the biological molecules. Although many cellular substances can be alkylated in this way, the alkylation of nucleic acids, primarily DNA, is the critical cytotoxic action for most of these compounds. Alkylation may produce breaks in the DNA molecule, cross-linking of its twin strands (interstrand cross-linking), cross-linking within the same strand of DNA (intrastrand cross-linking), or various combinations of these effects, thus interfering with DNA replication and the transcription of RNA[31]. Although the alkylating agents can react with virtually all the nitrogens in the DNA bases, there is

selectivity; the 7th position of guanine in DNA is most extensively alkylated[31]. The alkylating agents are cell cycle phase-nonspecific agents in that they exert their activity independent of the specific phase of the cell cycle. The nitrogen mustards and alkyl alkone sulfonates, for example, are most effective against cells in the RNA and protein synthesis phase (G_1 phase) or mitosis phase (M phase)[32]. Cellular resistance to antitumor agents is a critical determinant of the effectiveness of therapy. This includes decreased uptake of agents into or increased export out of the cell; increased inactivation of agents in the cell; enhanced repair of the DNA damage produced by the alkylating agents; and the absence of cellular mechanisms that produce cytotoxicity in response to DNA damage. The most frequently used alkylating agents in cancer therapy[31,32] include mechlorethamine, cyclophosphamide, ifosfamide, melphalan, and chlorambucil, (Figure 2.1).

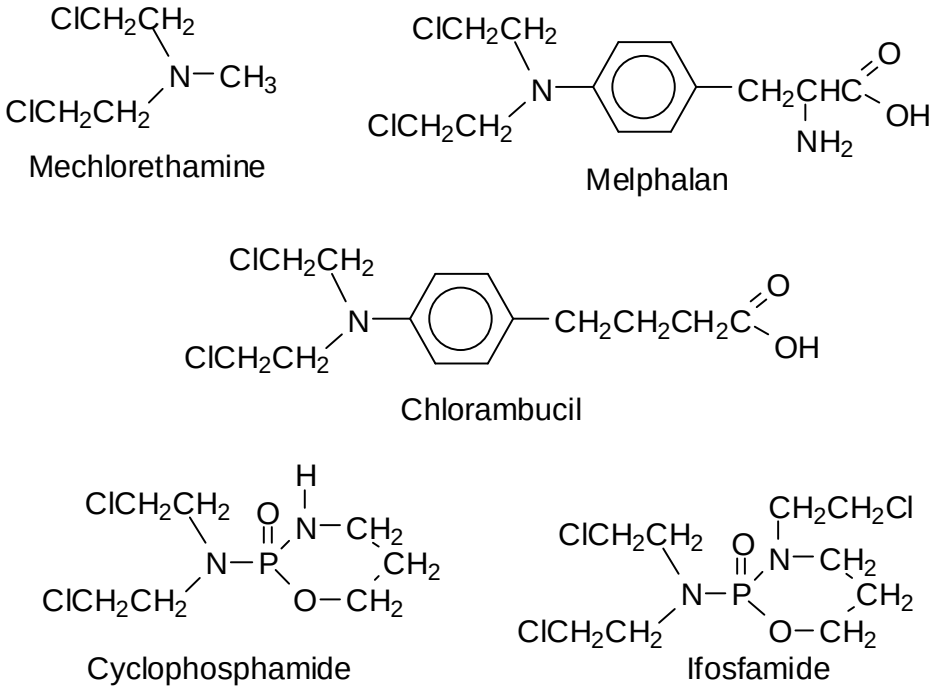

Figure 2.1. Structures of nitrogen mustards currently used in therapy[31,32].

b. Platinum-based drugs

History of platinum in medicine: The successful development of metal-containing anticancer drugs clearly starts with *cis*-diamminedichloroplatinum(II), often referred to as *cisplatin*. The compound was first described in 1845 as Peyrone's salt[33,34], and its anticancer properties were not discovered until 1964. The antitumor activity of the platinum complexes was discovered as the result of a fortuitous observation by Barnett Rosenberg and co-workers[35,36] during a study of the effects of electrical current on growing bacteria. When alternating current was delivered through platinum electrodes to a growing bacterial culture, the bacterial cells stopped dividing and grew into long filaments. The cause of the inhibition of cell division was found to be *cis*-diamminedichloroplatinum (II), also known as *cis*-DDP and *cisplatin*.

In the early 1970s, *cisplatin* went into clinical trials[37-40] and was found to have significant antitumor activity against testicular cancer, lymphoma, squamous cell carcinoma of the head and neck, ovarian cancer, and bladder cancer. Because of its significant therapeutic effect in these tumors and activity against a number of other solid tumors, it became the most frequently used antitumor agent. Because of the renal and neurotoxicities of *cisplatin*, there were intensive efforts to develop analogs with fewer of these toxicities. This work led to the development of carboplatin, which produces primarily hematopoietic toxicity and appears to have an antitumor effect similar to *cisplatin*[41-43] in the tumors against which it has been used.

While thousands of *cisplatin* analogs have been synthesized and screened, only about 28 platinum compounds have entered clinical trials as anticancer agents. Of these only three are currently approved. Those approved are *cisplatin*, carboplatin, and oxaliplatin (Figure 2.2)[33,44,45].

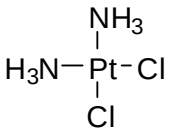

Cisplatin, *cis*-DDP
(*cis*-Diamminedichloroplatinum(II))

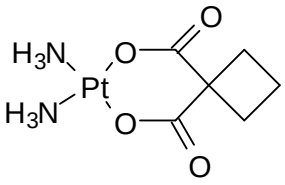

Carboplatin
(*cis*-Diammine-1,1-cyclobutane-dicarboxylato-platinum(II))

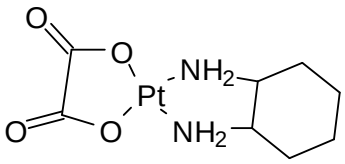

Oxaliplatin
(Oxalatoplatinum(II))

Figure 2.2: Structures of *cisplatin, carboplatin* and *oxaliplatin*[44,45].

In addition to *cisplatin*, carboplatin and oxaliplatin which are in wide clinical use throughout the world, some platinum agents have gained regional approval in a number of countries. Among these, nedaplatin, (*cis*-diammineglycolatoplatinum(II)) is approved for clinical use in Japan for the treatment of ovarian and cervical carcinomas, head and neck tumors, and esophageal and bladder cancer (Figure 2.3). Heptaplatin, *cis*-malonato [(4*R*,5*R*)-4,5-*bis*(aminomethyl)-2-isopropyl-1,3-dioxolane]platinum(II), is approved for use in South Korea for the treatment of gastric cancer and, in combination with paclitaxel, head and neck squamous cancers (Figure 2.4). While lobaplatin, (*R,R/S,S*)-(1,2-cyclobutanedimethanamine)[(2*S*)-2-hydroxypropanoato-*O,O'*]platinum(II), is approved for use in China for the treatment of non-small-cell lung cancer, breast tumors and certain forms of leukemia (Figure 2.3)[45].

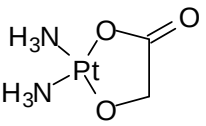

Nedaplatin
(*cis*-Diammineglycolatoplatinum (II))

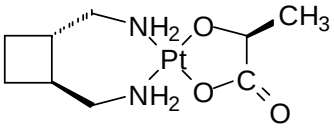

Lobaplatin

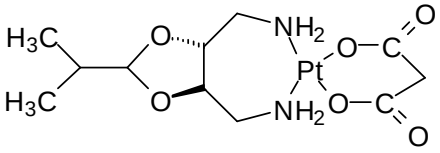

Heptaplatin

Figure 2.3: Structures of platinum antitumor agents that have gained regional approval for use as anticancer drugs[45].

Chemistry

Covalent bond character: Platinum is in the third row of transition metals in the periodic table and has eight electrons in the outer *d* shell. Palladium and nickel, which occupy analogous positions in the second and first transition series, have similar configurations of outer electrons, but little or no antitumor activity. Because the platinum atom has a much larger total number of electrons, however, the orbitals of its outer electrons are more polarizable, and bonds that are formed from these orbitals have more covalent character[46]. The special configuration depends on whether the oxidation state of platinum is +2 or +4; these oxidation states are usually designated as Pt(II) or Pt(IV), respectively. Because the bonds are fixed and not readily interchangeable, the complexes can have distinct isomers, such as *cis*- and *trans*-Pt(II)$(NH_3)_2Cl_2$ (Figure 2.4). The *cis*-isomer is the antitumor drug *cisplatin*. The importance of steric conformation is highlighted by the fact that the *trans*-isomer has virtually no antitumor activity[45]. Some platinum bonds, such as those to nitrogen, are essentially irreversible under physiological conditions; while others, such as the chloride-platinum(II) bond in *cisplatin*, are more labile[46].

Cisplatin *Transplatin*

Figure 2.4: *Cis*- and *trans*-platin(II) isomers[42].

Displacement reactions: Displacement reactions can occur in Pt(II) complexes in which one or both ligands are displaced by a competing nucleophile. The biological actions of Pt(II) complexes are due to displacement reactions, which cause the platinum to become stably bound to DNA, RNA, proteins, or other critical biomolecules[47]. The stability of the bonding of different ligands to Pt(II) varies greatly. Although the bonding to sulfur or nitrogen sites is essentially irreversible under physiological conditions, the stability of bonding to halogens is much lower, in the order I^- > Br^- > Cl^-, and the stability of bonding H_2O is weaker still[48].

The aqua (H_2O) ligand dissociates rapidly, whereas chloride dissociates more slowly. The dissociation rate can also be influenced by the identity of the other ligands in the complex, especially by the ligand located *trans* to the dissociating ligand[48]. The tendency of a ligand to leave the complex correlates inversely with the affinity for binding to platinum (II) and increases in the order: CN^- > NH_3 ≈ OH^- > I^- > SCN^- > Br^- > Cl^- ≈ Carboxylate > H_2O > NO_3^-, ClO_4^-.

Reactions in water and biological fluids: The pharmacological behavior of *cisplatin* is in part determined by its reactions in water, which are summarized in Figure 2.5. In blood plasma, the high chloride concentration of approximately 100 mM would keep *cisplatin* predominantly in the uncharged and relatively unreactive dichloro-form. This form may react to some degree with sulfhydryl groups of plasma proteins. The free dichloro form can enter cells by passive diffusion. In the cytoplasm, the relatively low

chloride concentration of approximately 4 mM would favor the reaction which would yield highly reactive species whose ionic charge may retard its exit from the cell[31,49]. Thus, the active form within the cell is believed to be the monohydrated structure, $[Pt(NH_3)_2(OH_2)Cl]^+$, the preferred extracellular species contains two *cis*-oriented leaving groups that are normally chloride ligands[49]. Before the molecule enters the cell, it will be electrically neutral due to the high concentration of chloride ion in blood.

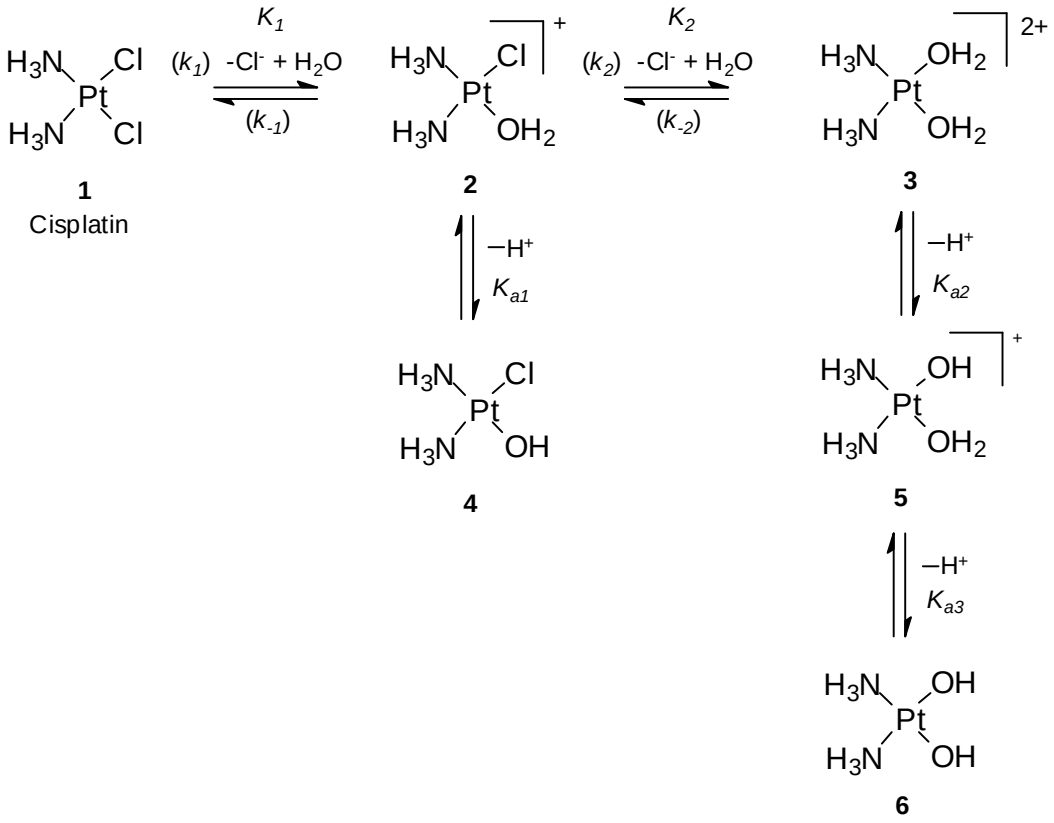

Figure 2.5: Speciation of *cisplatin* in aqueous solution[49].

Reaction with DNA: The mechanism of action of platinum drugs generally involves hydrolytic dissociation of the leaving groups in the lysosomal compartment in the intracellular space, leading to an aqua-complexed intermediate. This highly reactive compound is implicated as the active drug species, generally interacting with the cell's nuclear DNA. The intra- and

interstrand cross-links or DNA-protein crosslink (Figure 2.6) formed in such interactions create lesions in the double helix, which cannot be repaired in time prior to division of the rapidly proliferating cancer cell. As a result, the cells are unable to survive with such lesions in the nuclear material and will eventually die[31,49].

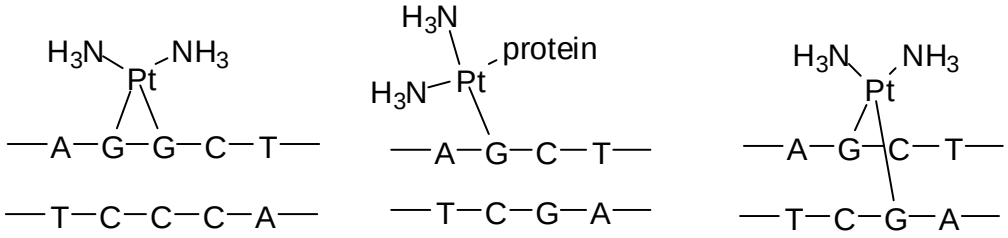

Intrastrand crosslink *DNA - protein crosslink* *Interstrand crosslink*

Figure 2.6: General crosslinked forms of DNA from reaction with *cisplatin*[31]*.*

Cisplatin has been noted to bind to all DNA bases, but there seems to be preferential binding to the N-7 positions of guanine and adenine bases, and the N-3 position of cytosine and uracil. Kinetic studies indicate that *cisplatin* cross-links to DNA through two successive pseudo-first-order reaction steps. In the first step, *cisplatin* is hydrolyzed in aqueous medium to the intermediate mono-aqua platinum complex. The intermediate migrates to the most favorable binding site of the DNA helix and binds to the N-7 atom of the guanine through displacement of water. The second chloro ligand is displaced by water in the second step, and the final step is the closure of the chelate complex (Figure 2.7)[31,49-55].

Toxicity of platinum compounds: Since the discovery by Rosenberg[35,36] that *cisplatin* is an effective anticancer drug, large synthesis and evaluation programs have been aimed at the creation of *cisplatin* derivatives that show greater and more widespread activity against cancer, but with lowered toxicity. Despite much progress in drug research, results on average have been highly discouraging. The major toxic manifestations of *cisplatin* include pronounced gastrointestinal problems such as acute nausea, vomiting, and

diarrhea; occasional liver dysfunction; myelosuppression involving anaemia, leucopenia, and thrombocytopenia; nephrotoxicity, and less frequently, cases of immunosuppression, hypomagnesia, hypocalcaemia, and cardiotoxicity. The most serious side effect is damage to the kidney. Much of the administered *cisplatin* is filtered out of the body within a few hours, exposing the kidneys to bursts of high concentrations of platinum. The rapid rate at which the kidneys filter the platinum from the blood is believed to be responsible for the nephrotoxicity. Another problem is the cumulative and irreversible hearing loss experienced initially in the 4000 – 8000 Hz range and then later in the 1000 – 4000 Hz range[31,34,56-58].

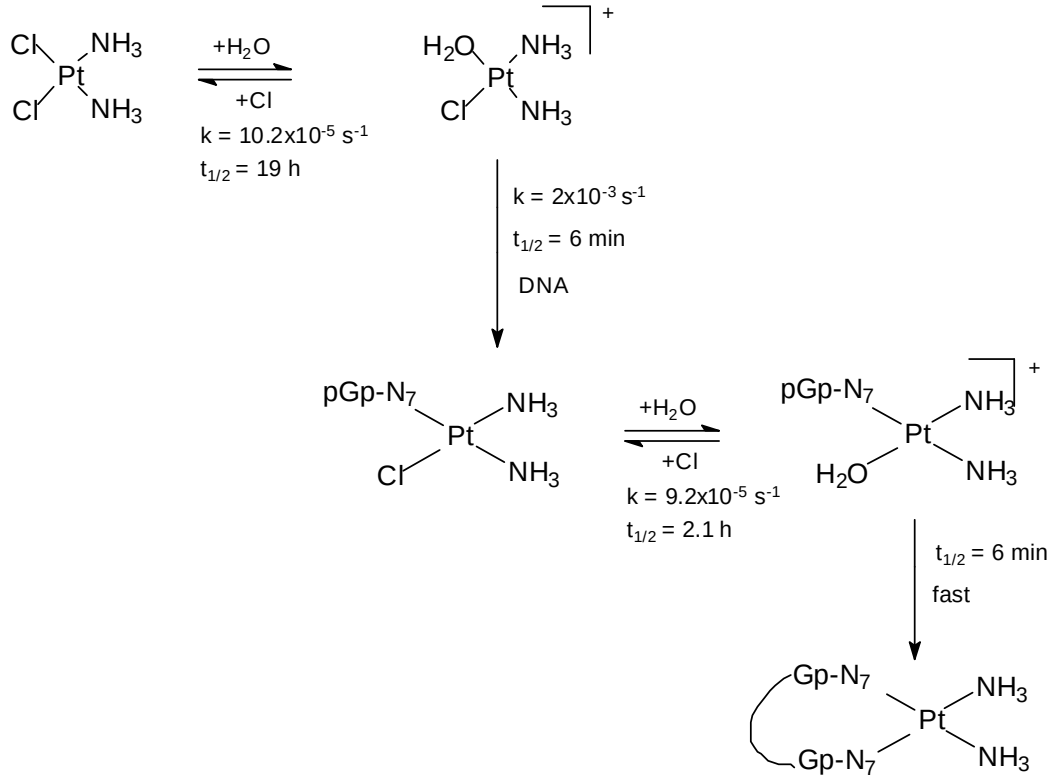

Figure 2.7: Schematic reaction of *cisplatin* with DNA[51].

2.1.3.1.2 Antibiotics

The antitumor antibiotics comprise a heterogeneous group of chemotherapy agents that have proven to be extremely successful in the treatment of a

wide variety of tumors, both epithelial and mesenchymal. Antibiotic agents have not only proven useful clinically, but also from the standpoint of the basic scientist; they have yielded a fascinating variety of structure-activity relationships that have provided insights into the mechanisms by which anticancer agents exert their effects on normal and malignant tissues. Many antibiotic agents bind to DNA through intercalation between specific bases and block the synthesis or interfere with cell replication or transcription[59].

Antitumor antibiotics: These drugs inhibit DNA topoisomerase II, by binding to DNA and nicking one of its strands, thus allowing the supercoiled macromolecule to relax as the opposite strand passes through the break. The enzyme then reattaches the broken ends. While varying in the mechanism of drug action and frequently in their pharmacokinetic pathways, the drugs have in common a cytotoxic effect resulting from interaction with endocytic nuclear material. Although isolated from natural sources, the antitumor antibiotics lack the specificity of the antimicrobial antibiotics, and therefore produce significant toxicity[59].

One of the representatives of the antitumor antibiotics in clinical use is dactinomycin (Figure 2.8) which is a product of the *Streptomyces* yeast species, discovered in 1940[59]. It has since been identified as an active anticancer antibiotic for gestational choriocarcinoma, Wilm's tumor, neuroblastoma, childhood rhabdomyosarcoma, and Ewing's sarcoma. Based on its structure, dactinomycin intercalates itself between DNA base pairs, while the polypeptide rings lie within the minor groove. The overall effect is to bind the two complementary strands of DNA together, preventing the synthesis of the corresponding RNA molecules. At low concentrations dactinomycin mainly inhibits DNA-directed RNA synthesis, whereas at high concentrations, both RNA transcription and DNA replication are affected[60-62]. The dose-limiting toxicity of dactinomycin is primarily myelosuppression, although nausea, vomiting, diarrhea, and mucositis also occur[59]. It can also

cause a radiation recall phenomenon by inhibiting DNA repair mechanisms[59]. The organs most prone to this effect are the skin and gastrointestinal tract, although late effects can be seen in the lungs and the liver.

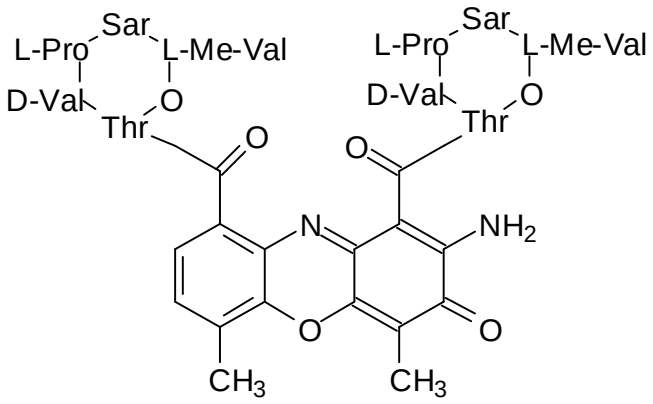

Me: Methyl
Pro: Proline;
Sar: Sarcosine;
Val: Valine;
Thr: Threoline

Figure 2.8: Structure of dactinomycin[59].

Anthracyclines: The anthracyclines are highly reactive in solution and create a panoply of effects on biological systems[59]. A major component of their cytotoxicity is a result of poisoning of topoisomerase II. Anthracyclines also intercalate into double-stranded DNA and produce structural changes that interfere with DNA and RNA synthesis. Before the effects of the anthracyclines on topoisomerase II were fully appreciated, it was their ability to participate in oxidation and reductions that was believed to produce the cytotoxicity. Anthracyclines generate reactive oxygen species, including oxygen-free radicals, hydroxyl radicals, and hydrogen peroxide that damage DNA, messenger ribonucleic acid (mRNA), proteins, and lipids[59]. This class of antibiotics includes doxorubicin, daunorubicin and idarubicin (Figure 2.9).

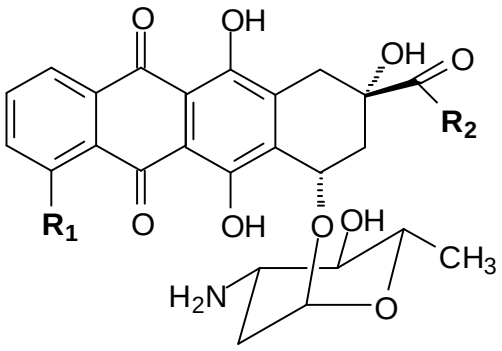

	R_1	R_2
Idarubicin	-H	$-CH_3$
Daunorubicin	$-OCH_3$	$-CH_3$
Doxorubicin	$-OCH_3$	$-CH_2OH$

Figure 2.9: Structures of the anthracycline class[59].

Doxorubicin is indicated in the treatment of many solid tumors (breast, sarcoma, bladder, thyroid, gastric, ovary, and small-cell lung cancers) and in the treatment of Hodgkin's and non-Hodgkin's lymphoma, as well as in the treatment of acute lymphoblastic and myeloblastic leukemias[59,63,64]. Daunorubicin is indicated for the treatment of acute lymphocytic and myelogenous leukemias; and it has limited activity against solid tumors and non-Hodgkin's lymphoma. Idarubicin, on the other hand, is given in combination with cytosine arabinoside for the treatment of acute myelogenous leukemia. All anthracyclines produce cardiac damage that can result in serious and even life-threatening complications.

Mitomycin C: In contrast to the anthracyclines, mitomycin C (Figure 2.10) is a prodrug and requires metabolic activation to achieve its cytotoxic potential. Mitomycin is considered the prototypical bioreductive alkylating agent, and the predominant mode of action is thought to be alkylation of DNA at the N-6 position of adenine or either the N-2 or N-7 position of guanine[59]. The drug has been active against a wide variety of solid tumors, including breast, non-small cell lung, gastric, pancreatic, gallbladder, colorectal, cervical, prostatic, and superficial bladder cancers. The most significant side effect of mitomycin C is a delayed myelosuppression. Other toxic adverse effects include mild and infrequent anorexia, nausea, vomiting, and diarrhea.

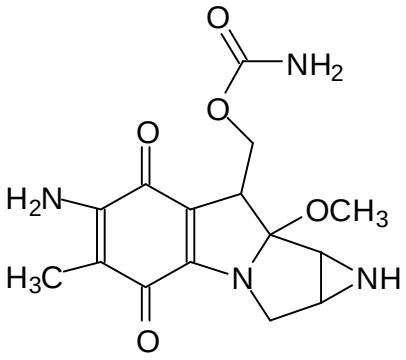

Figure 2:10: Structure of mitomycin C[59].

Epipodophyllotoxins: The epipodophyllotoxins (Figure 2.11) were synthesized in an effort to improve the activity of podophyllotoxin, an antimicrobial agent that is present in mandrake plant extract[65]. The epipodophyllotoxin group includes etoposide, tenposide and etoposide phosphate. Etoposide, on the one hand, has significant antitumor activity against a wide variety of neoplasms, including germ-cell malignancies, lung cancer, non-Hodgkin's lymphomas, leukemias, Kaposi's sarcoma, neuroblastoma, and soft-tissue sarcomas. Common etoposide toxicities include bone marrow suppression, mild nausea or vomiting and hair loss[66]. Etoposide phosphate is more water-soluble than etoposide and is a prodrug that is rapidly converted to etoposide *in vivo*. Teniposide, on the other hand, is used as a component of initial therapy for poor prognosis patients with acute lymphocytic leukemia. It is also used as therapy for advanced lymphoblastic lymphoma of childhood and other non-Hodgkin's lymphoma patients who relapse following initial therapy[59]. Teniposide toxicities are identical to those of etoposide in patients.

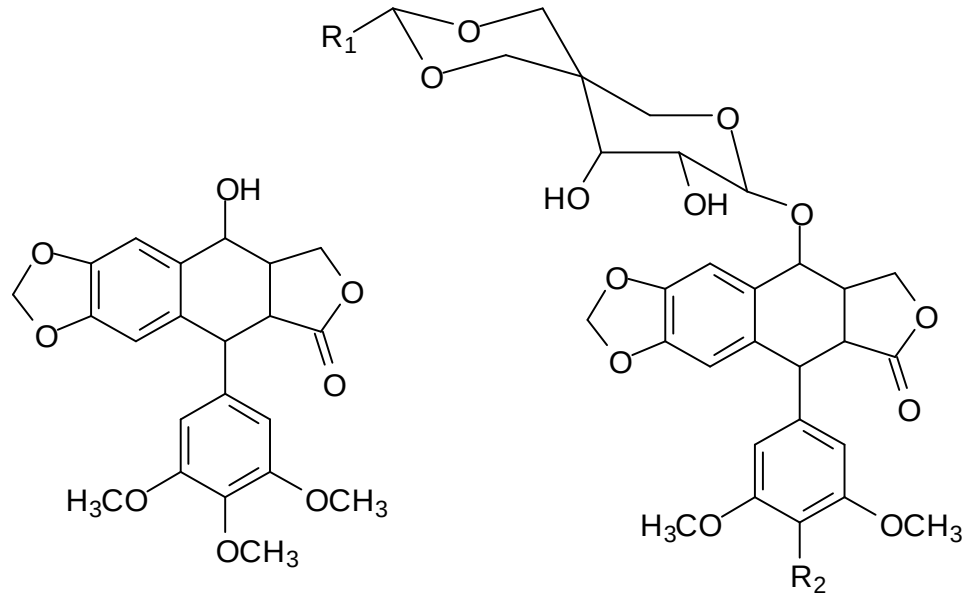

Podophyllotoxin Epipodophyllotoxins

	Etoposide	Teniposide	Etoposide phosphate
R_1	-CH_3	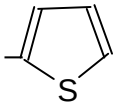	-CH_3
R_2	-OH	-OH	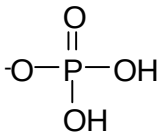

Figure 2.11: Structures of podophyllotoxin and epipodophyllo-toxins[59].

Mitoxantrone: Mitoxantrone (Figure 2.12) produces double-stranded DNA breaks through the inhibition of topoisomerase II. It is primarily used for the treatment of breast and prostate cancer, leukemia and lymphoma. Mitoxantrone has a low toxicity compared to doxorubicin, and it has been incorporated into selected chemotherapy regimens in place of doxorubicin for treatment of breast cancer and lymphoma particularly in patients with a poor performance status, who are believed to be at significant risk for doxorubicin toxicity[59]. Mitoxantrone's primary toxicities are similar to those seen with the anthracyclines: myelosuppression, nausea, vomiting and cardiac toxicity.

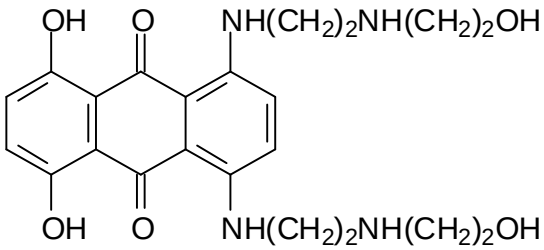

Figure 2.12: Structure of mitoxantrone[59].

2.1.3.1.3 Antimetabolites

The antimetabolites constitute a large group of anticancer drugs that interfere with metabolic processes vital to the physiology and proliferation of cancer cells. They structurally resemble the naturally occurring purines and pyrimidines involved in nucleic acid synthesis. The major classes of the antimetabolites are antifolates, purine analogs and pyrimidine analogs[67].

The era of antimetabolite chemotherapy began in 1948 with the demonstration that aminopterin, the 4-amino analog of folic acid, induced remissions in childhood leukemia[68]. Aminopterin has since been replaced by methotrexate (MTX), the 4-amino-10-methyl analogue of aminopterin (Figure 2.13).

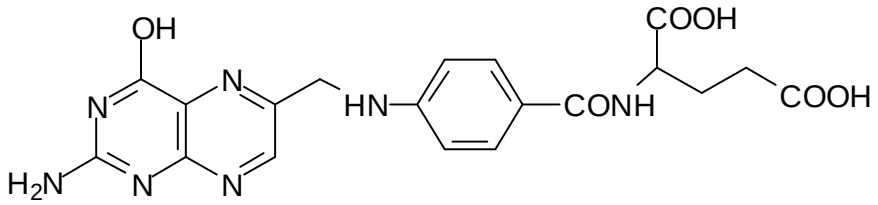

Folic acid

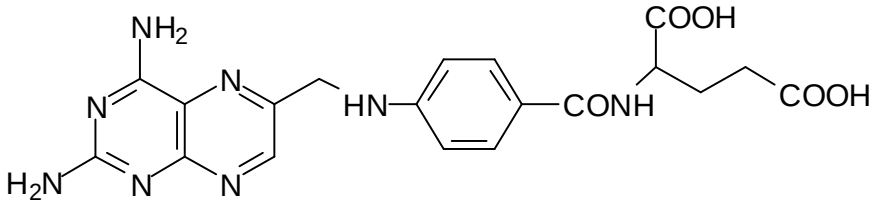

Aminopterin

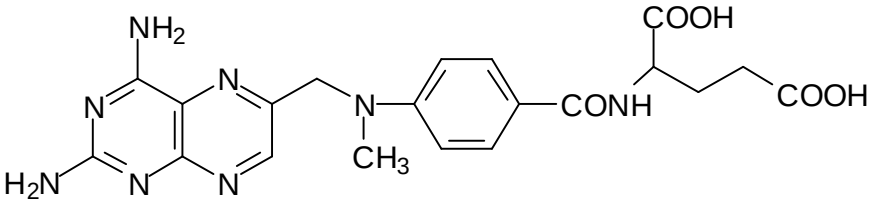

Methotrexate (MTX)

Figure 2.13: Structures of folic acid, aminopterin and MTX[68].

Methotrexate: MTX is the most widely used antifolate in cancer chemotherapy with documented activity against leukemia, breast cancer, head and neck cancer, lymphoma, osteogenic sarcoma and choriocarcinoma[68,69].

The antitumor agent MTX, owes its cytotoxicity to potent inhibition of dihydrofolate reductase (DHFR), a critical enzyme in intracellular folate metabolism. Without the function of DHFR, cells are deprived of key metabolic intermediates needed to form nucleotides and ultimately nucleic acids[68,69]. Intracellular MTX is converted to poly-γ-glutamyl derivatives through the action of folylpolyglutamate synthesis (FPGS), the enzyme that catalyzes peptide-bond elongation of γ-glutamyl residues of folates and

antifolates and thereby promotes intracellular retention[55-57]. In addition to maintaining the ability to inhibit DHFR, polyglutamates of MTX also inhibit other folate-utilizing enzymes such as thymidylate synthase, glycinamide ribonucleotide transformylase, and aminoimidazolecarboxamide ribonucleotide formyltransferase[68].

MTX usage is not unlike that of other cytotoxic antitumor agents in that it suffers major limitations because of its toxic side effects. The primary toxic effects of MTX therapy are myelosuppression and gastrointestinal mucositis. In patients with compromised renal function, even small doses of the drug may result in serious bone marrow toxicity[70].

The development of cellular resistance to MTX remains a major obstacle to it's effective clinical use. Some tumors are naturally resistant to MTX, while others acquire resistance after a period of treatment. Resistance to antifolates may result from several mechanisms including an alteration in antifolate transport into the cell, decreased capacity to form polyglutamate MTX and alteration to the DHFR enzyme, including increased protein expression or decreased binding affinity for the compound[68,71].

2.1.3.1.4 Ferrocenyl drugs

The discovery of ferrocene[72] and the elucidation of its remarkable structure is often considered as the starting point for modern organometallic chemistry. The excellent stability of the ferrocene framework in aqueous aerobic media, the accessibility of a large variety of derivatives and its favorable electrochemical properties have also made ferrocene and its derivatives very popular molecules for biological applications and for conjugation with biomolecules.

In 1984, Köpf and Köpf-Maier together with Neuse[73-75] reported the first iron compounds, ferricenium salts, for which an antiproliferative effect on certain types of cancer cells was demonstrated.

The behavior of the ferrocene complex in the biological environment has in more recent years been identified as eminently challenging with the exact mechanism of action not yet elucidated. Several targets including nuclear DNA, the cell wall and the enzyme topoisomerase II have been proposed. Osella *et al*.[76] showed that ferricenium salts may generate hydroxyl radicals in physiological solutions.

The neutral ferrocene complex readily undergoes one-electron oxidation, transforming to the ferricenium cation (Scheme 2.1). Many biological interactions involve free-radical chemistry, frequently with the participation of reactive oxygen species, and the ferrocene/ferricenium couple, when placed into such biological environment, can be expected to play an active part in it[77-79].

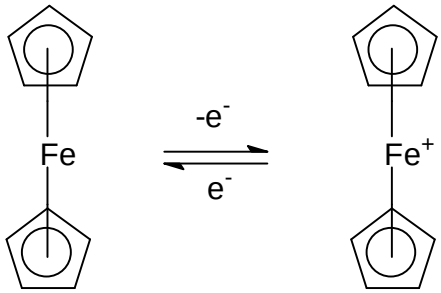

Scheme 2.1: Oxidation of ferrocene to the ferricenium cation[77-79].

Numerous investigations into the behavior and functioning of ferrocene compounds in biological environments have been reported. Pertinent reactions include enzymatically controlled oxidation of ferrocene by hydrogen peroxide[78], ferricenium cation reduction by NADH[79] and, most significantly, recombination of the ferricenium system with attacking free

radicals[77] leading to substituted ferrocenes on proton elimination (Scheme 2.2a). Ferricenium cation reaction with the biologically important superoxide radical anion proceeds with regeneration of ferrocene and dioxygen (Scheme 2.2b). A reverse electron transfer reaction comprises oxidation of the ferrocene complex to its ferricenium counterpart (Scheme 2.2c) in which ferrocenylcarboxylates interact with the aggressive hydroxyl radicals, transforming the latter into harmless hydroxyl anions[79].

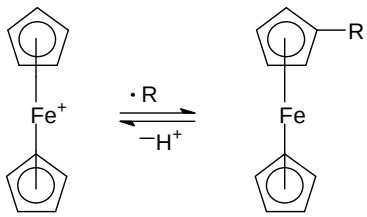

Scheme 2.2a

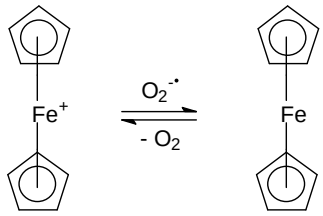

Scheme 2.2b

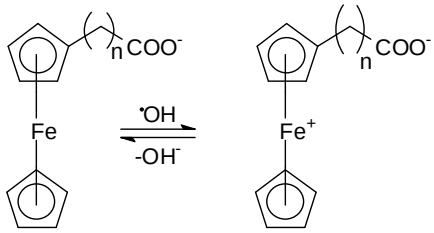

Scheme 2.2c

Scheme 2.2: Reactions ferrocene in biological environments[77-79].

A more recent study confirms the feasibility of $^{\bullet}OH$ generation from ferricenium salt under physiological conditions[79], and the hydroxyl free radical generated is suggested to be the species instrumental in the cell

growth-inhibiting activity of ferricenium salts, leading to oxidative damage of the cellular DNA.

2.2 Polymer-drug conjugation concept

Despite continued efforts to find more potent and more selective compounds for cancer treatment, advances have been disappointing. Many researchers would contend that there are already a plethora of chemicals on the market that have the potential to be antitumor agents. Their limitations can be viewed simply as the inability to deliver them properly[80].

In an effort to improve the outlook for cancer chemotherapy and raise the general drug performance level, advanced pharmaceutical research is focused not just on new drug development, but first and foremost on the design of efficacious drug delivery modalities capable of overcoming the resistance problem and rendering the drug system less toxic and more readily bioavailable. The last two decades have witnessed a worldwide surge of research activities toward this demanding goal. One of the most promising technologies emerging from those efforts is based on the polymer-drug conjugation concept, a strategy designed to take advantage of the pharmacokinetic peculiarities of macromolecular compounds[81]. In fact in the early 1900's, Paul Ehrlich described drugs that could selectively be directed to their site of action as "*the magic bullets*"[82]. The concept of anchoring drugs to polymers has been successfully applied to a wide variety of drugs. Most applications provide[83]:

- Enhanced bioavailability and passage through various biological barriers.
- Increased duration of pharmacological effects.
- Decreased toxicity and adverse properties.
- Increased site-specific delivery.
- Improved stability and solubility properties.

There are principally three approaches to the design of pharmacological polymers. One approach is to prepare a polymerizable monomeric drug and then homopolymerize or copolymerize it with other monomers. A second approach to drug delivery is the use of surgically implantable polymer matrices loaded with chemotherapeutic agents. The matrix is loaded with the desired agent and then implanted within the tumor cavity. The loaded drug is released over a period determined by the characteristics of the polymer. During the last three decades research on drug carriers has focused on the encapsulation of biologically active agents in solid release devices, liposomes and nanoparticles. In a third approach, an active drug species may be complexed or covalently bound to a preformed polymer[80].

2.2.1 Requirements for polymeric drug carrier

Polymers chosen as potential drug carriers should improve a drug's therapeutic effectiveness by being bound to a carrier as opposed to its action in the free state. The basic requirements include solubility in water, degradability, non-immunogenic, and drug anchoring site[79].

2.2.1.1 Solubility

Good solubility in aqueous media is a necessary prerequisite for the polymer-drug conjugate. The presence of intrachain or extrachain hydrophilic entities capable of undergoing effective hydration is therefore required. The amide groups, which are very important linkages in a polymer, as well as the presence of hydroxyl- and amino-terminals are of excellent utility in aqueous media. The possibility of including charged species also leads to improved solubility of the polymer. As such poly(ethylene glycol) (PEG) has found increasing use in the field of polymer therapeutics[84,85]. The addition of PEGs either as part of the polymer backbone or as side groups

imparts numerous properties such as excellent solubility in both aqueous and organic media; ease of chemical modification; and biocompatibility[84].

2.2.1.2 Degradability

Degradation of polymers within an organism is a vital aspect when the functional capabilities of a potential carrier are assessed. To prevent rapid renal excretion observed with low-molecular mass compounds, the carrier must be sufficiently large. However, its backbone needs to include segments amenable to hydrolytic and enzymatic cleavage in order to allow for the biodegradation and resultant catabolic elimination following drug release[86]. Synthetic polymers with a carbon-carbon backbone are generally not biodegradable. In this case, the polymer should have a molecular mass not exceeding the renal threshold of 30 000 to 50 000 in order to avoid deposit and accumulation in various organs. To increase the biodegradability of a polymeric carbon backbone it is necessary to equip it with peptide, saccharide or nucleotide sequences. These links are recognized and biodegraded by the numerous enzymes present in the lysosomal compartment of the cell. They perform two major functions, namely determining the rate of drug release from the polymer, as well as controlling the long-term fate of the polymeric carrier[87].

2.2.1.3 Non-immunogenicity

One of the key requirements for the successful use of the potential macromolecular drug carriers in the biological environment, is their biocompatibility. The carrier must be non-immunogenic, non-toxic, and non-thrombogenic to avoid any carrier-generated toxic, immunogenic and blood-clotting side effects. These requirements will prevent the carrier from attack by the hosts' defense mechanisms, which would render the drug delivery system useless.

PEG has found increasing use in the field of biomedical chemistry as a way for modification of anticancer drugs, in order to improve the solubility and decrease the immunogenic effect of the free drug[88,89]. While PEG is not degraded by mammalian enzymes[90], once in aqueous solution it is heavily hydrated, highly mobile and excludes other polymers including proteins and nucleic acids[83]. As a result, PEGs are non-toxic and non-immunogenic, and molecules coupled to PEG become essentially non-toxic and non-immunogenic. It has been demonstrated that covalent attachment of multiple strands of PEG to proteins produces conjugates with dramatically reduced immunogenicity and antigenicity[91]. PEG also has the lowest levels of protein or cellular adsorption of any known polymer[92].

2.2.1.4 Drug anchoring site

The polymer carrier must include reactive functional groups suitable for drug anchoring and release. The drug can either be part of the polymer backbone, or bound to a side chain. When bound to the polymer backbone, because of the high steric inaccessibility due to the polymeric backbone, most drugs show a reduced or zero biological activity and need to be liberated by complete breakdown of the polymer. In the case where the drug is bound to the carrier *via* a spacer, which is significantly remote from the principal chain, then the active agent can be liberated through increased accessibility by enzymes in the target compartment. Thus, the spacer itself should be stable in the blood stream in order to avoid any premature release before the target. In this case, the polymer carrier must be directed to specific cells. This role can be achieved by incorporating in the polymer specific groups, targeting moieties, such as cationic functions or antibodies[93,94].

2.2.2 Pharmacokinetic benefits of macromolecular conjugates

The concept of polymer-drug conjugation, born in he early 1970s, was forcefully advanced by Ringsdorf[95] (Figure 2.14). This notion of pairing up a bioactive agent with a transporter vehicle is based on a model comprising a linear polymer chain composed of subunits bearing water-solubilizing groups, other subunits equipped with functional groups suitable for reversible drug binding, and still other subunits comprising a homing device, *i.e.* some molecular entity capable of directing the conjugate molecule selectively to the target tissue. The conjugate nearly always represents a prodrug from which the active agent is released in the predestined biological environment (generally the cytoplasmic lysosomes, for anticancer agents) by hydrolysis or through enzymatic action.

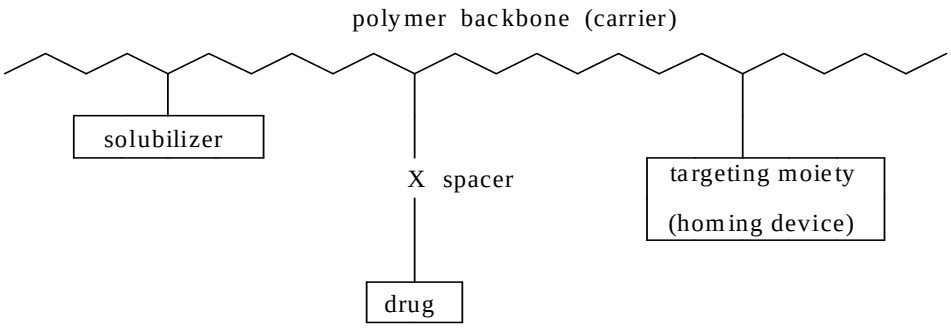

Figure 2.14: General structure of a macromolecular carrier as proposed by Ringsdorf[95].

Drug anchoring to macromolecular carriers has been accepted as a highly practicable approach toward enhancement of drug efficacy[96-98]. Factors contributing to such enhancement include:

(i) The intravenously or intraperitoneally administered polymer-anchored drug, even if inherently hydrophobic and insoluble in water, will be carried immediately into the aqueous phase of the central circulation

system or the intraperitoneum cavity. This will ensure rapid drug distribution in the fluid system.

(ii) The water-soluble polymer-drug conjugate will experience facilitated endocytotic cell entry, thus circumventing potential problems caused by drug polarity or ionicity in the normal process of membrane crossing by passive diffusion common to nonpolymeric solutes. The mechanism is pinocytotic in nature and thus not subject to the limitations imposed by the reticulo-endothelial system on phagocytotically captured particulates[93].

(iii) While in transit in the central circulation system, the polymer-bound drugs will experience temporary protection from enzymatic attack, serum protein binding and other depletion processes. This will lead to reduced renal clearance and prolonged serum life time with substantially enhanced drug bioavailability.

(iv) The dreaded toxic side effects invariably caused by the common, nonpolymeric medicinal agents will be minimized through carrier-attachment, as now the “anchored” agent will be contained in the body and organ while in transit.

(v) Polymer-drug conjugates, in common with macromolecules in general, tend to accumulate in solid tumors because of enhanced intratumoral vascular permeability, allowing for substantial leakage of the polymeric molecules into the tumor tissue. Whereas, in normal tissues, macromolecules in interstitial space are efficiently recovered and eliminated by the lymphatic system, such lymphatic clearance is grossly retarded in tumorous tissue and so represents a weighty factor contributing to the tumoritropic characteristics of macromolecular compounds. This *enhanced permeability and retention* (EPR) effect associated with polymers provides passive targeting and renders polymer-drug conjugate administration more effective while reducing systemic toxicity in other organs.

(vi) Through the expediency of introducing biofissionable segments into the backbone, a polymer can be rendered biodegradable, thus affecting its gradual removal from the body in the form of fragments qualifying for excretion through the body's normal waste removal systems. This process is crucial because high-molecular-mass carriers are not readily eliminated from the body and in the longer term may cause additional toxicity.

Taking advantage of the more favorable pharmacokinetics of macromolecules relative to nonpolymeric compounds, a nonpolymeric, biologically active agent is bioreversibly attached, *conjugated*, to water-soluble polymeric carrier synthesized in strict compliance with biomedical specifications. The water-soluble carrier component in this assembly functions as a vehicle transporting the medical agent. As depicted in Figure 2.15, the pro-drug (conjugate) travels essentially intact from the central circulation through the various body compartments to, and into, the affected target, where the bioactive agent is released for the ultimate biological action[79,99].

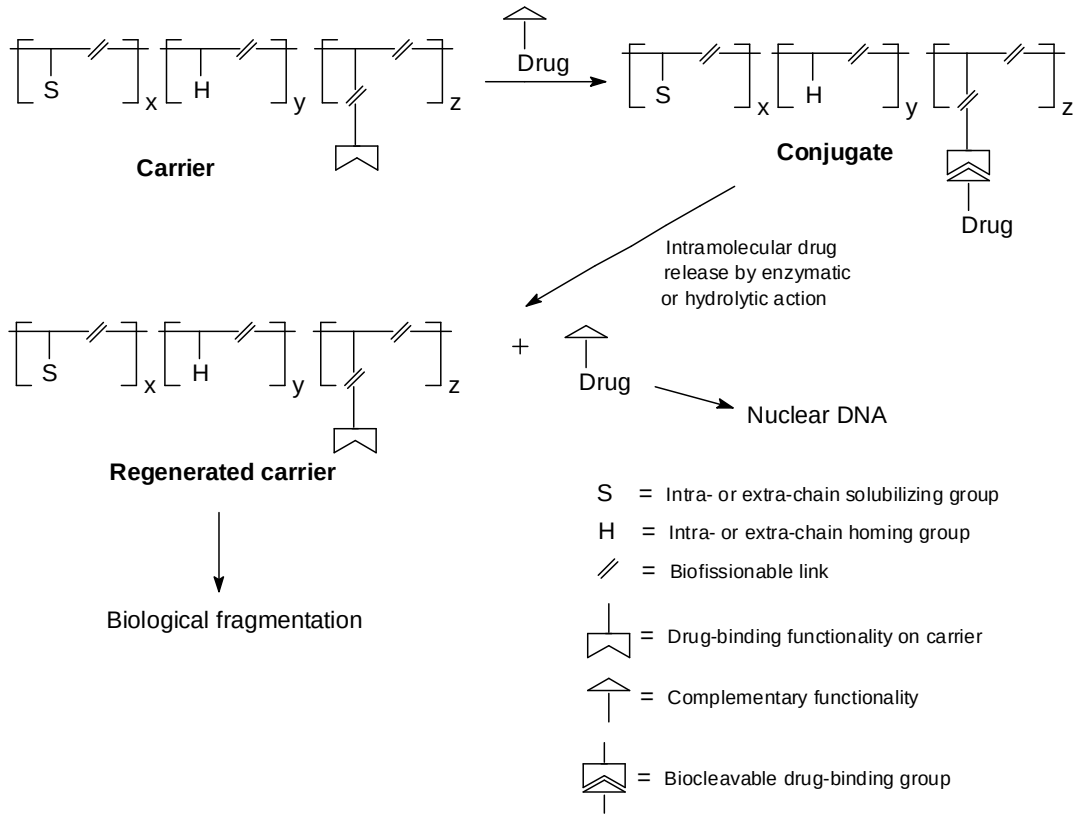

Figure 2.15: Flow chart describing drug conjugate pharmacokinetics[79].

CHAPTER 3

RESULTS AND DISCUSSION

3.1 Synthesis of carrier polymers

In fulfillment of the two objectives of this study (Section 1.2), the synthesis by bioreversible conjugation of selected anticancer drugs with water-soluble macromolecular carriers was undertaken and the biological anticancer activity of the resulting conjugates evaluated in accordance with the necessary prerequisites for any macromolecule intended to serve in the biomedical field (Section 2.2.1). An attempt was made to generate potential macromolecular drug carriers through the design and derivation of several synthetic polymeric structures (Section 3.1). This was additionally motivated by the limited number of naturally occurring counterparts and the possibility to impart the desired functions leading to the accomplishment of the goals. The carrier polymers are to perform the vital function of transporting the medicinal agent from central circulation (the blood pool) through the many body compartments and membranes to the target tissue. Critical design features were specified, and incorporated into the product polymers, as follows:

(i) A nontoxic chain construction amenable to biodegradation to ensure catabolic elimination of the polymer upon drug release.
(ii) A highly flexible backbone and the presence of intrachain type or side group-attached solubilizing groups to ensure conjugate solution in aqueous media required for rapid dissipation in the central circulation system.
(iii) The presence of functional groups as binding sites to ensure proper drug attachment and subsequent release in the biological environment.

(iv) The presence of cationic functions to cause facilitated cell entry by endocytosis, thus circumventing potential problems caused by drug polarity or ionicity. This mode of entry may assume unique importance where drug resistance has been developed by the target cells.

(v) Delayed and controlled drug release involving a polymer-drug connective link, thereby ensuring restriction of drug serum conjugate concentration well within pharmacologically dictated limits, with concomitant reduction of organ toxicity. Features were also built into the molecule that would provide the conjugate stability in the plasma and drug release upon endocytotic cell entry.

The polymeric carriers preferentially used in this project to anchor the selected drug models, to conform to the latter design rules, were of the aliphatic polyamide-type with subunits randomly distributed along the chain (Figure 3.1).

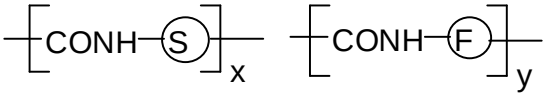

Figure 3.1: Structure of polyamide-type carrier.

In this model the S stands for an extra- or intra-chain type hydrosolubilizing moiety required to provide water solubility of the final conjugate (Figure 3.1). S can be a tertiary amine, hydroxyl or methoxy functionality whilst group F represents an extra- or intra-chain type functionality capable of forming a link with a drug species. In this study, the primary amino group, the dihydroxylato, the dicarboxylato and the carboxylatohydroxylato were adopted as the functional group of choice for drug anchoring, because of the ability to release the drug, even if at different rates, either by passive hydrolysis or enzymatically in the cytoplasmic environment[97]. All efforts were made to design carriers in such a way as to ensure a balance was maintained between the inherently hydrophobic drug species and

solubilizing groups on the polymer, to optimize the hydrophilicity of the drug-carrier conjugate with varying degrees of drug concentration.

Polyaspartamides were the polymers synthesized in this project conforming to the basic carrier model (Figure 3.1) and used for drug conjugation by amide bond formation between the carriers and the carboxylic acid-functionalized platinum drug or by direct coordination between the carriers and the platinum drug. The primary amino group, the dihydroxylato-, the dicarboxylato- and the carboxylatohydroxylato- functional groups of these polymers were introduced as terminals in components **F** for the anchoring of platinum. With the amino group, two different set of carriers were used. In the first set of carriers, all the amino groups were aliphatic amines (polyaspartamides **6** and **7**) using Model 2 (Figure 3.2) for the platination reaction, and in the second set of carriers, all the amino group were aromatic amines (polyaspartamides **1** to **5**) using Model 1 (Figure 3.2) for platination reaction. A different approach was used for the ferrocene drug. It was incorporated in the polymer *via* the amino-functionalized ferrocene drug during the aminolytic ring-opening of the polysuccinimide. The subunits incorporating the binding site form 10 to 20 mol-% of the chains, leaving 80 and 90 mol-% of **S**-labeled subunits of the *ter*-amine or methoxy types for hydrosolubilization. The choice of the compositional specification was based on the necessity to restrict drug loading to levels commensurate with retention of water solubility of the resulting conjugates. This was necessary as previous experiments with carriers containing larger mole percentages of **F**-labeled subunits have demonstrated the need for a disproportionately large excess of drug in the feed for complete drug incorporation. In addition, the resultant coupling products had displayed a propensity for branching and crosslinking with concomitantly decreasing solubility once they had been isolated in the solid state. All polymeric carriers were fractionated by dialysis to remove constituents with a molecular weight substantially below 14 000.

3.1.1 Synthesis of poly-DL-Succinimide

The potential value of polysuccinimide-derived aspartamide polymers for biomedicinal agents was first recognized in the early Seventies by Drobnick *et al*[98] as potential drug carriers, and for a number of years, the Polymer Research Group Laboratory of WITS University (WITS PRG Laboratory) has made use of these macromolecular carriers for a number of antineoplastic drug systems[100-103].

The poly-DL-succinimide (PSI) was synthesized using a method that was first publish by Neri[104], because of its ability to deliver high molecular mass PSI in one step[105]. PSI was obtained by thermal orthophosphoric acid-catalyzed polycondensation of DL-aspartic acid (Scheme 3.1), which was subsequently subjected to dicyclohexylcarbodiimide (DCC) mediated chain extension. A representative polymer had an inherent viscosity of 33 $mL.g^{-1}$ in DMF at 30°C.

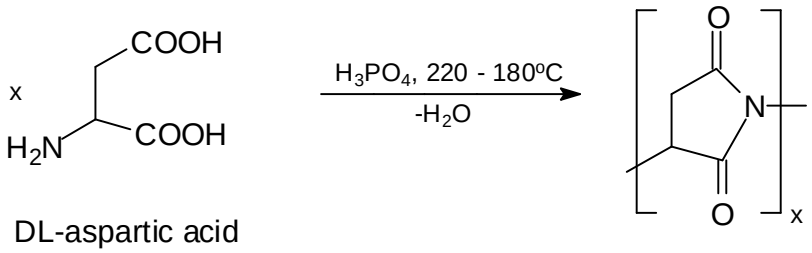

DL-aspartic acid

PSI

Scheme 3.1: Synthesis of poly-DL-succinimide (PSI).

3.1.2 Synthesis of poly-α,β-DL-aspartamides

Polyaspartamides are readily prepared from PSI by aminolytic ring opening carried out under carefully controlled conditions in anhydrous, dipolar aprotic medium producing a mixture of D- and L-enantiomeric forms, of both α- and β-peptidic repeat units (Scheme 3.2)[101]. For convenience, only α-

peptide forms are shown for simplication in further schematic diagrams throughout this dissertation.

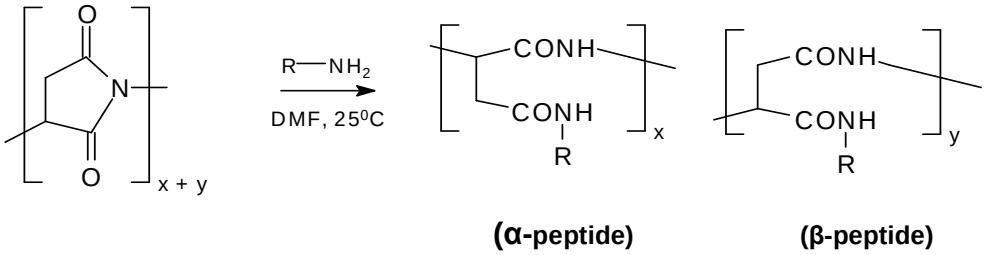

Scheme 3.2: Synthesis of poly-α,β-DL-aspartamide.

The D-type polymers are resistant to enzymatic attack, while the L-type polymers are more liable to enzymatic attack and degradation[101]. Thus, a backbone structure of the D,L- type will ensure delayed enzymatic cleavage and ultimate backbone degradation through hydrolysis.

3.1.3 Synthesis of copolyaspartamides

The aminolytic ring opening reaction of PSI generated a copolymer through a stepwise, sequential addition of two or more different primary amine reactants, R_1–NH_2 and R_2–NH_2, in prearranged stoichiometric feed ratios. The resultant copolyaspartamides are composed of randomly distributed aspartamide repeat units bearing N-attached substituents (R_1, R_2 etc.) as introduced by the amine nucleophiles chosen. Scheme 3.3 depicts this sequence of ring opening steps. In general, R_1 is chosen to represent a hydrosolubilizing group (e.g. hydroxyl, methoxy or tertiary amine), and R_2 represents a drug-anchoring functionality (e.g. carboxyl or primary amine).

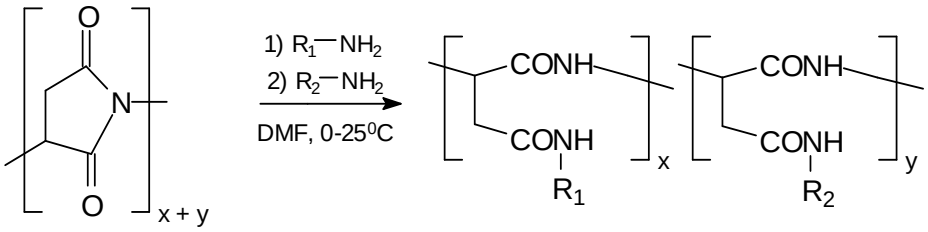

Scheme 3.3: Aminolytic ring opening of polysuccinimide.

In the present project tertiary amines were used as both hydrosolubilizing and cell-selecting group. This choice was motivated by many considerations from previous investigations in this laboratory[106]. There were two main reasons, firstly, tertiary amines are strong bases *per se*, and are readily protonated even under weakly basic conditions. Secondly, the amino groups, being more cationic and positively charged in the protonated state, will favorably approach surfaces of certain types of cancer cells that are negatively charged. This will favor the cellular uptake of the macromolecules by pinocytotic adsorption[107]. In previous investigations from this laboratory, hydroxyl-terminated side chains were used[108-111]. During my MSc project[112], it was noticed that the percentage incorporation of platinum drug was higher than predicted in polymers bearing hydroxyl groups as the hydrosolubilizing moiety. Since platinum has the ability of binding to hydroxyl- or other groups, no discrimination was observed. For this reason, the main focus in this project was the variation of the drug anchoring subunit. Four groups were considered, one was aliphatic (dicarboxylato-) and three were on an aromatic ring (carboxylatohydroxylato-, dihydroxylato-, and primary amine).

The dicarboxylato-ligand was an aspartic acid derivative, derived through a two-step reaction, from aspartic acid by *N*-acryloylation and addition of a diamine to the activated double bond (Schemes 3.30 and 3.31). In the previous work done in the WITS PRG laboratory, aspartic acid was one of the constituents used in an attempt to synthesize water-soluble polymers

with dicarboxylato-anchoring sites[113]. The polymer products were consistently low in the aspartic acid component because of the poor nucleophilicity of the amino group in the aspartic acid. Extended reaction times were tried out, in an effort to enhance the incorporation of the aspartic acid into the polymer backbone with no avail. The aspartic acid derivative was synthesized in an effort to enhance the incorporation of the aspartic acid into the polymer backbone.

The choice of the ligand for platinum(II) chelation was based on the fact that *p*-aminosalicylic acids (PASAs) have been integral medications in the maintenance and induction of remission in inflammatory bowel disease for several decades[114,115]. However, PASA is less well absorbed from colon, resulting in low plasma and urine levels[116], because it is rapidly metabolized, mainly in the gut mucosa, to a pharmacologically inactive metabolite, N-acetyl-5-aminosalicylate[117]. This paper uses PASA not only as a site for platinum(II) anchoring, but also to open an avenue for future work to improve upon the uptake of PASA.

The primary amino group was provided by *p*-aminobenzoic acid (PABA). The choice of the PABA as ligand for platinum anchoring was based on the work done by Esposito *et al*[118]. Over a decade ego this group reported that both procaine and its metabolite *p*-aminobenzoic acid significantly reduce the toxic effects of *cis*-diaminedichloroplatinum(II) (DDP) in mice bearing P388 leukemia, without compromising its antitumor activity[119,120]. These findings helped them prepare platinum(II) complex bearing a PABA ligand[121]. In an effort to achieve further enhancement of the therapeutic effectiveness of complexes of the triamine-coordinated Pt(II)containing a single group type, polymeric conjugates of this type of drug were synthesized.

3.1.4 Copolyaspartamides containing primary amine-terminated side chain as drug anchoring sites

3.1.4.1 Synthesis of p-*aminobenzamidopropylamine*

The *p*-aminobenzamidopropylamine (PABPA or **M1**) derivative was prepared by a one-step reaction (Scheme 3.4), involving the reaction between ethyl 4-aminobenzoate (EAB) and 1,3-diaminopropane (PDA) at 160^{o}C. The ester was chosen instead of the free acid in order to enhance the reaction, formation of the amide bond, as the ethoxy group is a better leaving group compared to the free acid. A large excess of diamine was necessary to minimize any disubstitution on the diamine. The experimental conditions and ^{1}H NMR (Appendix 1a) data are summarized in Tables 3.1 and 3.2, respectively.

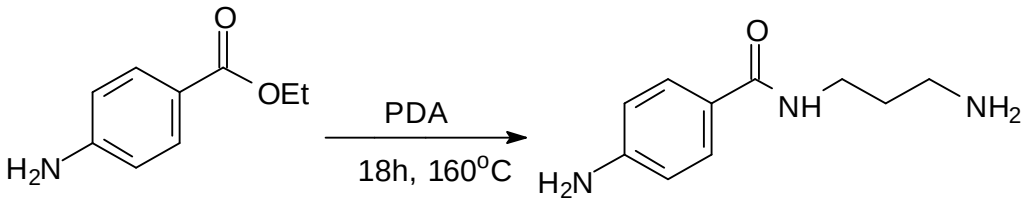

EAB **M1**

Scheme 3.4: Synthesis of *p*-aminobenzamidopropylamine (PABPA).

Table 3.1: Summary of experimental data for **M1**.

Designation	Molar ratio [a, b]		Experimental Conditions	Yield (%)
	EAB	PDA		
M1	1.0	4.0	18h, 160^{o} C	52.1

[a] Base molar for **EAB**
[b] EAB: Ethyl 4-aminobenzoate; PDA: 1,3-diaminopropane

Table 3.2: ^{1}H NMR characterization of **M1**.

Polymer Designation	Assignment	^{1}H NMR [a, b]		
		Shift range δ (ppm)	Proton count	
			Found[c]	Expected
M1	NH_2CH_2**CH_2**CH_2NH	1.7 – 1.5	2 (t, 13.8Hz)	2
	NH_2**CH_2**CH_2CH_2NH	2.8 – 2.7	2 (t, 14.1Hz)	2
	CH_2NHCO	3.4 – 3.3	2 (m)	2
	CH (Aromatic)	6.8	2 (d, 8.7)	2
		7.6 – 7.5	2 (d, 8.7)	2

[a] In D_2O: Deuterium oxide, pD 10 – 11. Chemical shifts, δ (ppm), referenced against internal sodium 3-(trimethylsilyl)-2,2,3,3-d_4-propionate;
[b] Integration error limit ± 10%.
[c] Multiplicity and coupling constant in parenthesis.

3.1.4.2 Copolyaspartamides containing primary amine-terminated side chain

The release of a pharmacologically active agent from a polymeric carrier requires the presence of one or more biofissionable links for the ultimate delivery of a drug at or in its target cell. Amide, urea, urethane, hydrazone and ester groups are typical examples of links that are desirable in a segment connecting a drug to the carrier main chain. The important characteristic of a drug carrier is its ability to retain water solubility after anchoring of a hydrophobic drug.

In the current project, work was carried out where R_1 (Scheme 3.3) represents a group bearing a tertiary amino group capable of imparting water solubility, and unable to participate in any anchoring reactions. The following amines were chosen for the reasons discussed in section 3.1.3: 3-(dimethylamino)propylamine (DMP), 2-(dimethylamino)ethylamine (DMEA), 2-(diethylamino)ethylamine (DEEA), 4-(3-aminopropyl)-morpholine (APM)

and 3-(diethylamino)propylamine (DEP). Whilst, the R_2 (Scheme 3.3) group consists of the aromatic primary amine function possessing drug coupling potential, as well as imparting water-solubility.

The aminolysis of PSI leading to the formation of this class of copolyaspartamides occurred in two steps as depicted in Scheme 3.5. In the first step, PSI was allowed to react with PABPA (**M1**), the drug anchoring moiety, in the presence of triethylamine (TEA) in selected feed molar ratio (x/y) for a 24h period under strict anhydrous conditions in DMF solution at 0-5^{o}C. The -NH_2 on the benzene ring is less nucleophilic than the alkyl NH_2 and the alkyl NH_2 will preferentially open the ring in the PSI. Since long periods were used, typically 1d, very low temperatures were preferred during this step to avoid any possibility of crosslinking, with the consequence of producing a water-insoluble carrier. In the second step, the solubilizing amine (DMP, DMEA, DEEA, APM or DEP) was added in excess to the resultant solution from the first step, to ensure optimal PSI ring opening. The reaction was allowed to continue for 12h at 0-5^{o}C, then at room temperature (RT) for another 3d. The polymeric products were isolated as completely water-soluble solids by a series of procedures, involving precipitation by addition of an ether/hexane (2:1) solution, washing of the precipitate firstly with the precipitant solution, then warm acetone. Purification occurred by stepwise dialysis in water (12 000-14 000 molecular weight cut-off limit), and collection by freeze-drying. As a consequence of the crude fractionation achieved by this dialysis step, yields did not exceed 70%, generally ranging between 54 and 68% (Table 3.3). The highest yield was found with polyaspartamide **5** and the lowest yield with polyaspartamide **3**. The inherent viscosities (η_{inh}) ranged from 10 to 15 mL.g^{-1} with small differences when compared with each other. The highest viscosity was observed with polyaspartamide **3** and the lowest with polyaspartamide **4**. The experimental details and viscosity results are summarized in Table 3.3.

The ^{1}H NMR spectra of polyaspartamides **1**-**5** (Appendix 1f to 1j) measured in D_2O, and recorded at pH 10-11 for elimination of protonation effects, showed characteristic band groups, some of them containing overlapping signals and the significant NMR data is presented in Table 3.4. Thus, the *CH* (methine) signal of the aromatic were found in the 7.7-6.7 ppm region, while the methine signal of the aspartic appeared in the region of 4.7-4.6 ppm and **CH_2**-O (methylene) was found in the region 3.9-3.6 ppm. The methylene protons of CONH-**CH_2** were found in the region of 3.5-3.0 ppm. The protons of CO-**CH_2**, **CH_2**-N (**CH_3**)$_2$, **CH_2**-NH and **CH_2**-NH_2 groups were found in the region of 3.0-2.0 ppm. Methylene protons of CH_2**CH_2**CH_2 groups were in the 1.8-1.5 ppm region. Methyl protons of CH_2**CH_3** groups were found in the region of 1.2-0.8 ppm.

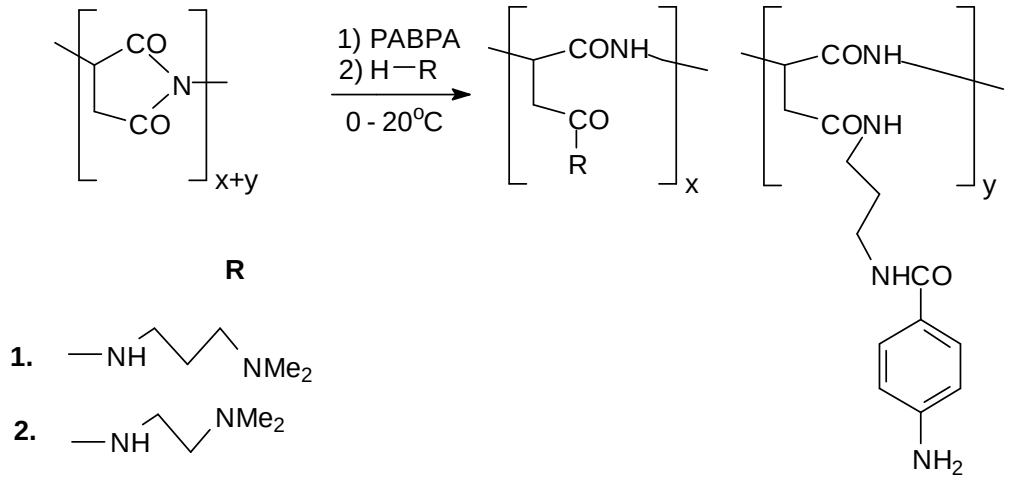

R

1. —NH NMe_2

2. —NH NMe_2

3. —NH NEt_2

4. —NH NEt_2

5. —NH N O

Scheme 3.5: Copolyaspartamide containing primary amine-terminated side chains.

Within this class of copolymers, a carrier containing a DMP side chain as the solubilizing group and 1,3-diaminopropane (PDA) as the drug binding site, was synthesized according to Scheme 3.6. A well established method[122] was used with alteration to the reaction time to improve the result of the product. Two different mole ratios DMP to PDA (80:20 and 90:10) were chosen in order to add variables in terms of drug incorporation. DMP was used as a major reactant (x > y) in a two-step reaction. In the first step, a given amount of DMP was allowed to react with a corresponding amount of PSI according to the desired x/y feed ratio. The mixture was allowed to react for 12h at RT. In the second step, the resulting solution was added to an excess (3 times the stoichiometric amount) of PDA solution, and the reaction continued for 6h at 0-5^{o}C, then for 24h at RT. The large amount of the PDA diamine was necessary to avoid any crosslinking through the involvement of the terminal free primary amines. Anhydrous conditions were observed during both steps in order to avoid any unwanted hydrolytic ring opening leading to formation of carboxylic acid side groups[123]. For this purpose the solvent of choice was N,N'-dimethylformamide (DMF). The final product was isolated as in the forgoing example after precipitation and aqueous dialysis. The water-soluble solids were found to possess inherent viscosities in the range of 14 to 16 mL.g^{-1}. The experimental details and viscosity results are presented in Table 3.3, and the ^{1}H NMR data presented in Table 3.4. The ^{1}H NMR data were in agreement with the structures indicated in Scheme 3.6.

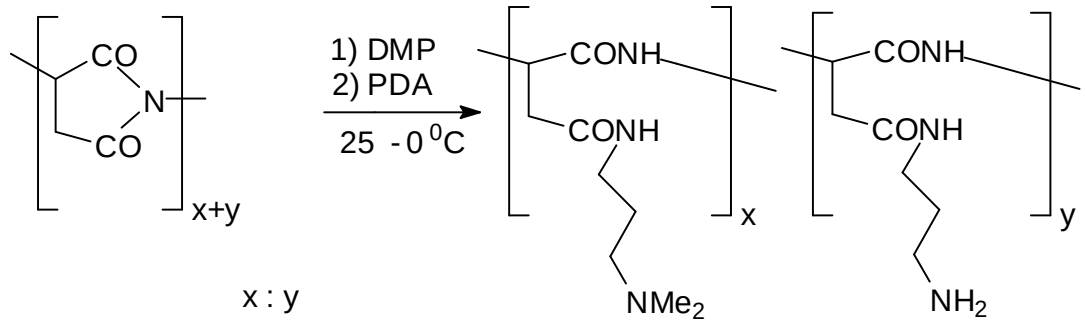

	x : y
6	80 : 20
7	90 : 10

Scheme 3.6: Copolyaspartamides containing primary amine (PDA) terminated side chains.

Table 3.3: Summary of experimental data polyaspartamide bearing an amine side chain as the drug anchoring site.

Designation	Molar Ratios [a, b]								Reaction time & Temperature [c]		Yield (%)	η_{inh} [d] ($mL.g^{-1}$)	x : y [e]
	PSI	M1	DMP	DMEA	DEEA	DEP	APM	PDA	1st Step	2nd Step			
1	1.00	0.20	1.00	-	-	-	-	-	3d, 0-5°C	12h, 0-5°C; 1d, RT	61.2	12.3	90 : 10
2	1.00	0.20	-	1.00	-	-	-	-	3d, 0-5°C	12h, 0-5°C; 1d, RT	58.2	13.1	90 : 10
3	1.00	0.20	-	-	1.00	-	-	-	3d, 0-5°C	12h, 0-5°C; 1d, RT	54.3	14.6	90 : 10
4	1.00	0.20	-	-	-	1.00	-	-	3d, 0-5°C	12h, 0-5°C; 1d, RT	63.2	10.6	90 : 10
5	1.00	0.20	-	-	-	-	1.00	-	3d, 0-5°C	12h, 0-5°C; 1d, RT	67.1	14.2	90 : 10
6	1.00	-	0.80	-	-	-	-	0.60	12h, RT	6h, 0-5°C; 1d, RT	55.9	16.2	80 : 20
7	1.00	-	0.90	-	-	-	-	0.30	12h, RT	6h, 0-5°C; 1d, RT	64.3	14.8	90 : 10

[a] Base molar for **PSI**

[b] PSI: Polysuccinimide; M1: *p*-aminobenzamidopropylamine; DMP: 3-(dimethylamino)propylamine; DMEA: 2-(dimethylamino)ethylamine; DEEA: 2-(diethylamino)ethylamine; DEP: 3-(diethylamino)propylamine; APM: 4-(3-aminopropyl)-morpholine; PDA: 1,3-propylenediamine.

[c] RT: room temperature

[d] At 30.0°C ± 0.5°C in dist H_2O; conc. = 2 $mg.mL^{-1}$

[e] x:y Desired feed ratio, solubilizing moiety to drug binding moiety

Table 3.4: ^{1}H NMR of copolyaspartamides **1** to **7**.

Polymer Designation	Assignment	^{1}H NMR		
		Shift range δ(ppm)	Proton count	
			Found	Expected
1	CH_2**CH_2**CH_2 N**CH_3** **CH_2**N **CH_2**CONH CONH**CH_2** **CH**, (Asp) **CH** (Aromatic)	1.8 – 1.5 2.2 – 2.0 2.4 – 2.2 3.0 – 2.5 3.4 – 3.0 4.7 – 4.6 6.8 7.7 – 7.5	20 55 21 23 22 10 2 2	20 54 18 20 22 10 2 2
2	CH_2**CH_2**CH_2 N**CH_3** **CH_2**N **CH_2**CONH CONH**CH_2** **CH** (Asp) **CH** (Aromatic)	1.8 – 1.5 2.3 – 2.1 2.5 – 2.3 3.0 – 2.5 3.4 – 3.2 4.7 – 4.6 6.8 7.7 – 7.5	2 54 17 22 23 10 1.9 1.9	2 54 18 20 22 10 2 2
3	**CH_3**CH_2 CH_2**CH_2**CH_2 **CH_2**CONH, **CH_2**N CONH**CH_2** **CH**, (Asp) **CH** (Aromatic)	1.2 – 0.9 1.8 – 1.6 3.0 – 2.5 3.5 – 3.2 4.7 – 4.6 6.8 7.8 – 7.6	56 2 78 24 10.2 2 2	54 2 74 22 10 2 2
4	**CH_3**CH_2 CH_2**CH_2**CH_2 **CH_2**N **CH_2**CONH CONH**CH_2** **CH** (Asp) **CH** (Aromatic)	1.1 – 0.9 1.8 – 1.5 2.6 – 2.3 3.0 – 2.6 3.4 – 3.0 4.7 – 4.6 6.8 7.7 – 7.5	54 20 54 23 22 10 2 2	54 20 54 20 22 10 2 2
5	CH_2**CH_2**CH_2 **CH_2**CONH, **CH_2**N CONH**CH_2** **CH_2**-O-**CH_2** **CH** (Asp) **CH** (Aromatic)	1.8 – 1.5 2.9 – 2.0 3.5 – 3.2 3.6 – 3.9 4.7 – 4.6 6.8 7.7 – 7.5	20 76.1 22.6 34.3 10.3 2 2	20 74 22 36 10 2 2

Table 3.4 Continued

6	$CH_2\mathbf{CH_2}CH_2$ $N\mathbf{CH_3}$ $\mathbf{CH_2}N$, $NH_2\mathbf{CH_2}$ $\mathbf{CH_2}CONH$ $CONH\mathbf{CH_2}$ **CH** (Asp)	1.8 – 1.5 2.2 – 2.0 2.4 – 2.2 2.9 – 2.5 3.5 – 3.1 4.7 – 4.6	10 25 11 10 10 5	10 24 10 10 10 5
7	$CH_2\mathbf{CH_2}CH_2$ $N\mathbf{CH_3}$ $\mathbf{CH_2}N$, $NH_2\mathbf{CH_2}$ $\mathbf{CH_2}CONH$ $CONH\mathbf{CH_2}$ **CH** (Asp)	1.8 – 1.5 2.2 – 2.0 2.4 – 2.2 2.9 – 2.5 3.5 – 3.1 4.7 – 4.6	20 54 21 20 20 10	20 54 20 20 20 10

[a] In D_2O, pD 10 – 11. Chemical shifts, δ (ppm), referenced against internal sodium 3-(trimethylsilyl)-2,2,3,3-d_4-propionate
[b] Integration error limit ± 10 %

3.1.5 Copolyaspartamides containing carboxylatohydroxylato ligand as drug anchoring site

This class of copolyaspartamides required special monomers such as Synthesis of *p-N*-(4,8-diaza-octanoyl)salicylic acid (PASA-EDA or **M3**) and *p-N*-(4,8-diaza-heptanoyl)salicylic acid (PASA-PDA or **M4**)

3.1.5.1 Synthesis of p-N-*(4,8-diaza-octanoyl)salicylic acid (PASA-PDA) and* p-N-*(4,8-diaza-heptanoyl)salicylic acid (PASA-EDA)*

The synthesis of *p-N*-(4,8-diaza-octanoyl)salicylic acid (PASA-PDA) and *p-N*-(4,8-diaza-heptanoyl)salicylic acid (PASA-EDA) involved a two-step reaction under experimental conditions similar to previous work performed in our laboratory[124]. In the first step the reaction involved the synthesis of acryloylaminosalicylic acid monomer, as depicted in Scheme 3.7, under very mild conditions. *p*-Aminosalicylic acid was reacted with acryloyl chloride at 0 – 5^{o}C, then RT.

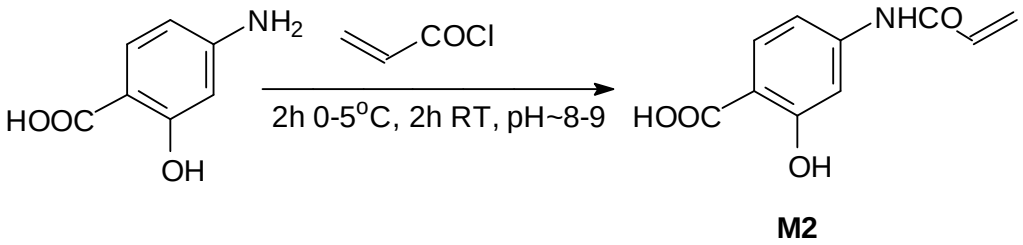

M2

Scheme 3.7: Synthesis of acryloylamidosalicylic acid (**M2**).

The low temperature was necessary during the process to avoid any polymerization of the double bond, since the reaction is exothermic. The pH of the solution was critically maintained at ~8 – 9. Both acidic and more basic conditions would have resulted in the displacement of the chloride ion by water forming an inert carboxylic acid group, or the hydrolysis of the product, forming acrylic acid and *p*-aminosalicylic acid. The experimental conditions and ^{1}H NMR (Appendix 1b) data are summarized in Tables 3.5 and 3.6 respectively.

In the second step, a given amount of acryloylaminosalicylic acid (**M2**) was allowed to react with a 20% excess of PDA for the synthesis of *p*-*N*-(4,8-diaza-octanoyl)salicylic acid or diaminoethane (EDA) for the synthesis of *p*-*N*-(4,8-diaza-heptanoyl)salicylic acid by Michael addition reaction across the active double bond at 65^{o}C, according to Scheme 3.8. The two diamines were chosen as short-chain aliphatic spacers designed to provide spacing between the main chain and the drug and increase the reactivity of the ligand for the binding of the drug during aminolytic ring opening of the polysuccinimide. As can be seen in Table 3.5, the final average yield was 75.2% for the PDA derivative and 64.8% for the EDA derivative. This shows that the PDA was more reactive than the EDA. In addition these high yields suggested a possibility of protection by quaternization. This can be possible in case that the COOH functionality protonated one of the diamine. The ^{1}H NMR spectra of **M2**, **M3** and **M4**, measured in D_2O solutions, were recorded

at pH 10-11 in order to preclude any protonation effects. Prominent band groups were in the regions of 7.7-6.7 ppm (**CH** Aromatic), 6.3 ppm (H**CHCH**CONH), 5.8 ppm (**HC**HCHCONH), 3.0-2.8 ppm (CONH-**CH_2**), 2.6-2.4 (**CH_2CH_2**NH**CH_2**CH_2CO and **CH_2**CH_2**CH_2**NH**CH_2**CH_2CO) and 1.6-1.5 ppm (CH_2**CH_2**CH_2).

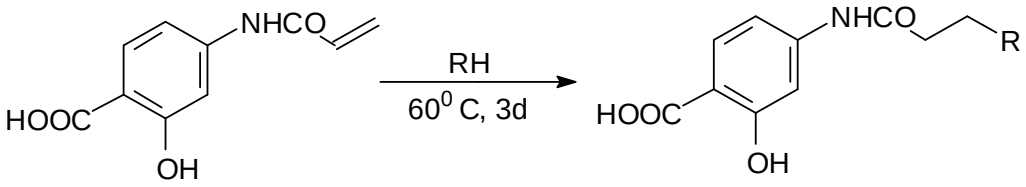

M3: RH = H_2N NH_2 **PASA-EDA**

M4: RH = H_2N NH_2 **PASA-PDA**

Scheme 3.8: Synthesis of *p-N*-(4,8-diaza-octanoyl)salicylic acid (PASA-PDA) and *p-N*-(4,8-diaza-heptanoyl)salicylic acid (PASA-EDA).

Table 3.5: Summary of experimental data for **M2**, **M3** and **M4**.

Designation	Molar ratio [a]					Experimental Conditions [c]	Yield (%)
	PASA	Acryloyl Chloride	M2	PDA	EDA		
M2	1.0	1.2	-	-	-	2h, 0-5°C; 2h, RT	76.3
M3	-	-	1.0	-	1.2	3d, 65°C	64.8
M4	-	-	1.0	1.2	-	3d, 65°C	75.2

[a] Base molar for **PASA** or **M2**
[b] PASA: *p*-aminosalicylic acid; M2: Acryloylamidosalicylic acid; PDA: 1,3-diaminopropane; EDA: 1,2-diaminoethane
[c] RT: room temperature

Table 3.6: ^{1}H NMR analysis of **M2**, **M3** and **M4**.

Designation	Assignment	^{1}H NMR [a, b]		
		Shift range δ (ppm)	Proton count	
			Found[c]	Expected
M2	**HC**HCHCONH H**CHCH**CONH **CH** (Aromatic)	5.8 6.3 6.7 7.4	1 (m) 2 (m) 2 (m) 1 (d, 8.4Hz)	1 2 2 1
M3	**CH_2CH_2**NH**CH_2**CH_2CONH **CH_2**CONH **CH** (Aromatic)	2.6 – 2.4 3.0 – 2.9 6.9 – 6.7 7.6 – 7.5	6 2 2 1	8 2 2 1
M4	CH_2**CH_2**CH_2 **CH_2**CH_2**CH_2**NH**CH_2**CH_2C ONH **CH_2**CONH **CH** (Aromatic)	1.6 – 1.5 2.6 – 2.5 2.9 – 2.8 7.0 – 6.8 7.7 – 7.6	2 6 2 2 1	2 6 2 2 1

[a] In D_2O, pD 10 – 11. Chemical shifts, δ (ppm), referenced against internal sodium 3-(trimethylsilyl)-2,2,3,3-d_4-propionate;
[b] Integration error limit ± 12%.
[c] Multiplicity and coupling constant in parenthesis.

3.1.5.2 Copolyaspartamides containing carboxylatohydroxylato ligand

This class of copolymers is characterized by the presence of a carboxylatohydroxylato ligand in the anchoring subunit of the polymer chain. The advantage of these carriers is that they provide a chelating ligand for *trans*-1,2-diaminocyclohexanediaquaplatinum(II) dinitrate (DACH-Pt). For the synthesis of copolyaspartamide carriers **8** to **17** (Scheme 3.9), two steps were involved. In the first step, a given amount of polysuccinimide (PSI) reacted with an amine bearing a carboxylatohydroxylato group, such as PASA-PDA or PASA-EDA, based on the desired x/y feed ratio in the

presence of triethylamine as base, for a specific time, typically 3d. The use of the base was necessary to liberate the amine since it was used as the hydrochloride salt. In the second step, the second amine bearing a tertiary amine side group was added to the solution, and the experiments were continued and completed after a specific time, typically 1d. This group of reactions was performed at room temperature. Ice-bath temperatures were not required; there was no diamine present among the reactants that could lead to crosslinking. Strictly anhydrous conditions where observed during the two steps in order to avoid any unwanted hydrolytic ring opening leading to formation of carboxylic acid side groups. The polymeric products were isolated as completely water-soluble solids by a succession of operations including precipitation, aqueous dialysis and freeze-drying. These polyaspartamides were obtained in yields ranging between 54 and 68% and possessed inherent viscosities in the range of 10 to 15 $mL.g^{-1}$. As can be seen in Table 3.7, the highest yield was found with polyaspartamide **13** and the lowest yield with polyaspartamide **16**. In the same way the highest viscosity was observed with polyaspartamide **9** and the lowest with polyaspartamide **15**. The analysis of the ^{1}H NMR data of polyaspartamides **8**-**17** indicated the presence of the predicted structures in Scheme 3.9 and Scheme 3.10, through the identification of the aromatic ring. The ^{1}H NMR spectra of these polyaspartamides, measured in D_2O solutions, were recorded at pH 10-11 in order to preclude any protonation effects. They showed several groups of bands, which were occasionally superimposed upon each other. Prominent band groups were in the regions of 7.6-6.6 ppm (**CH** Aromatic), 4.7-4.6 ppm (**CH** Asp), 3.9-3.6 ppm ($\mathbf{CH_2}$-O), 3.5-3.0 ppm (CONH-$\mathbf{CH_2}$), 3.0-2.0 (CO-$\mathbf{CH_2}$, $\mathbf{CH_2}$-N ($\mathbf{CH_3}$)$_2$, $\mathbf{CH_2}$-NH and $\mathbf{CH_2}$-NH_2), 1.8-1.5 ppm ($CH_2\mathbf{CH_2}CH_2$), and 1.2-0.8 ppm ($CH_2\mathbf{CH_3}$). Table 3.7 summarizes the experimental conditions and viscosities, while Table 3.8 presents the ^{1}H NMR (Appendix 1k to 1o) data.

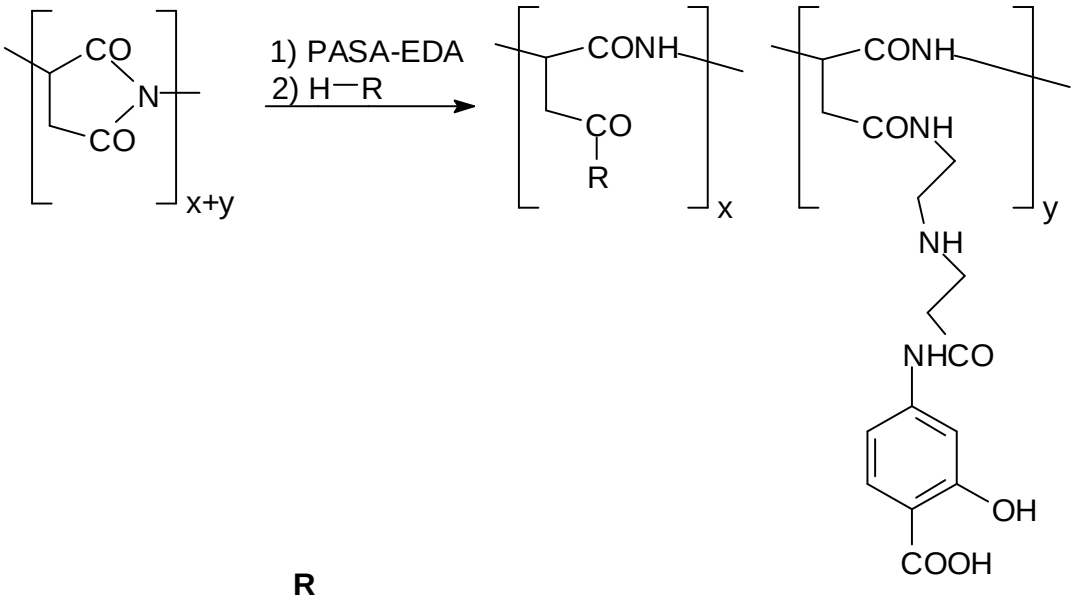

R

8 —NH—(CH2)3—NMe2

9 —NH—(CH2)2—NMe2

10 —NH—(CH2)2—NEt2

11 —NH—(CH2)3—NEt2

12 —NH—(CH2)3—N(CH2CH2)2O

Scheme 3.9: Synthesis of copolyaspartamides **8** to **12**.

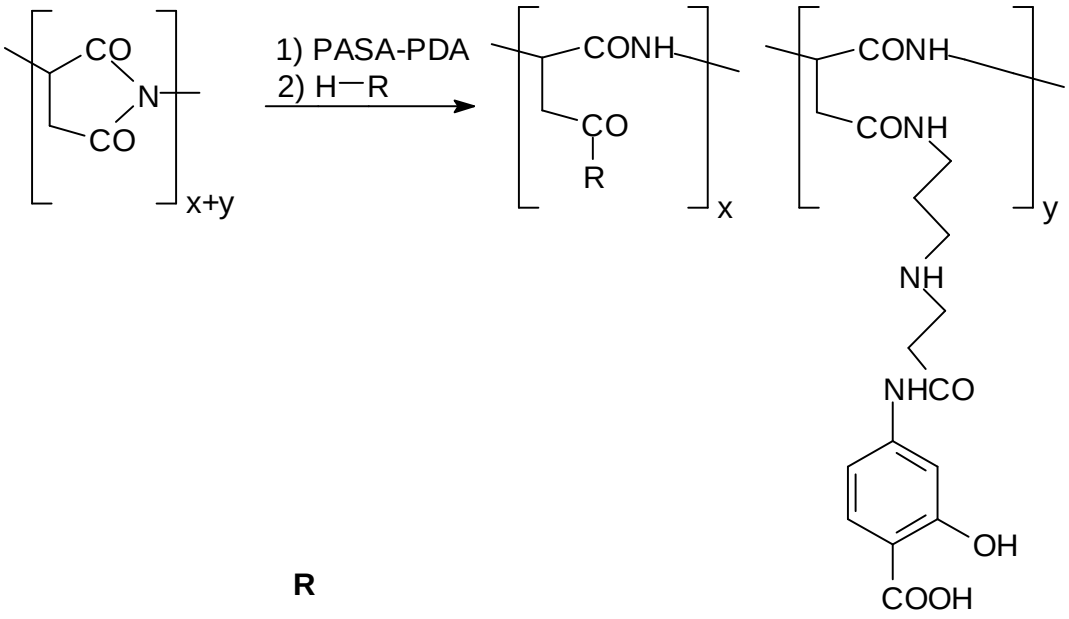

R

13 —NH—NMe_2

14 —NH—NMe_2

15 —NH—NEt_2

16 —NH—NEt_2

17 —NH—N O

Scheme 3.10: Synthesis of copolyaspartamides **13** to **17**.

Table 3.7: Summary of experimental data for polyaspartamide bearing a carboxylatohydroxylato-terminated side chain as the drug anchoring site.

Designation	Molar Ratios[a, b]								Reaction time & Temperature [c]		Yield (%)	η_{inh} [d] ($mL.g^{-1}$)	x : y [e]
	PSI	M3	M4	DMP	DMEA	DEEA	DEP	APM	1st Step	2nd Step			
8	1.00	0.10	-	1.15	-	-	-	-	3d, RT	1d, RT	56.7	13.6	90 : 10
9	1.00	0.10	-	-	1.15	-	-	-	3d, RT	1d, RT	59.8	15.1	90 : 10
10	1.00	0.10	-	-	-	1.15	-	-	3d, RT	1d, RT	61.9	12.6	90 : 10
11	1.00	0.10	-	-	-	-	1.15	-	3d, RT	1d, RT	56.2	13.2	90 : 10
12	1.00	0.10	-	-	-	-	-	1.15	3d, RT	1d, RT	58.1	11.8	90 : 10
13	1.00	-	0.10	1.15	-	-	-	-	3d, RT	1d, RT	67.2	13.6	90 : 10
14	1.00	-	0.10	-	1.15	-	-	-	3d, RT	1d, RT	60.3	14.2	90 : 10
15	1.00	-	0.10	-	-	1.15	-	-	3d, RT	1d, RT	62.1	10.2	90 : 10
16	1.00	-	0.10	-	-	-	1.15	-	3d, RT	1d, RT	54.1	12.4	90 : 10
17	1.00	-	0.10	-	-	-	-	1.15	3d, RT	1d, RT	56.5	10.5	90 : 10

[a] Base molar for **PSI**.
[b] PSI: Polysuccinimide; M3: PASA-PDA; M4: PASA-EDA; DMP: 3-(dimethylamino)propylamine; DMEA: 2-(dimethylamino)ethylamine; DEEA: 2-(diethylamino)ethylamine; DEP: 3-(diethylamino)propylamine; APM: 4-(3-aminopropyl)-morpholine.
[c] RT: room temperature.
[d] At 30.0°C ± 0.5°C in dist H_2O; conc. = 2 $mg.mL^{-1}$.
[e] x:y Desired feed ratio, solubilizing moiety to drug binding moiety.

Table 3.8: ^{1}H NMR analysis of copolyaspartamides **8** to **17**.

Polymer Designation	Assignment	^{1}H NMR		
		Shift range δ(ppm)	Proton count	
			Found	Expected
8	CH_2**CH_2**CH_2 N**CH_3** **CH_2**N, NH**CH_2** **CH_2**CONH CONH**CH_2** **CH** (Asp) **CH** (Aromatic)	1.8 – 1.5 2.2 – 2.1 2.4 – 2.2 3.0 – 2.4 3.4 – 3.0 4.7 – 4.6 6.8 – 6.6 7.5 – 7.3	18 55 20 23 22 10 2 0.9	18 54 22 22 20 10 2 1
9	N**CH_3** **CH_2**N, NH**CH_2**, **CH_2**CONH CONH**CH_2** **CH** (Asp) **CH** (Aromatic)	2.3 – 2.1 3.0 – 2.3 3.4 – 3.1 4.7 – 4.6 6.8 – 6.6 7.5 – 7.3	54 45 22 10 2 1	54 44 20 10 2 1
10	**CH_3**CH_2 **CH_2**N, NH**CH_2**, **CH_2**CONH CONH**CH_2** **CH** (Asp) **CH** (Aromatic)	1.2 – 0.8 3.1 – 2.2 3.4 – 3.0 4.7 – 4.6 6.8 – 6.6 7.6 – 7.3	54 82 23 10 2 1	54 80 20 10 2 1
11	**CH_3**CH_2 CH_2**CH_2**CH_2 **CH_2**CONH, **CH_2**N, NH**CH_2** CONH**CH_2** **CH** (Asp) **CH** (Aromatic)	1.1 – 0.8 1.8 – 1.5 3.0 – 2.3 3.4 – 3.0 4.7 – 4.6 6.8 – 6.6 7.6 – 7.3	58 18 84 22 10 1.9 1	54 18 80 20 10 2 1
12	CH_2**CH_2**CH_2 **CH_2**CONH, **CH_2**N, NH**CH_2** CONH**CH_2** **CH_2**-O-**CH_2** **CH** (Asp) **CH** (Aromatic)	1.8 – 1.5 3.0 – 2.2 3.4 – 3.0 3.9 – 3.6 4.7 – 4.6 6.9 – 6.6 7.6 – 7.3	18 80 23 37 10.2 2 1	18 80 20 36 10 2 1

Table 3.8 Continued.

Polymer Designation	Assignment	^{1}H NMR		
		Shift range δ(ppm)	Proton count	
			Found	Expected
13	CH_2**CH_2**CH_2 N**CH_3** **CH_2**N, NH**CH_2** **CH_2**CONH CONH**CH_2** **CH** (Asp) **CH** (Aromatic)	1.8 – 1.5 2.2 – 2.0 2.4 – 2.2 3.0 – 2.4 3.4 – 3.0 4.7 – 4.6 6.8 – 6.5 7.6 – 7.3	20 54 19 25 23 10 2 1	20 54 22 22 20 10 2 1
14	CH_2**CH_2**CH_2 N**CH_3** **CH_2**N, NH**CH_2**, **CH_2**CONH CONH**CH_2** **CH** (Asp) **CH** (Aromatic)	1.8 – 1.5 2.2 – 2.0 3.0 – 2.2 3.4 – 3.0 4.7 – 4.6 6.8 – 6.5 7.6 – 7.3	2 54 46 22 10 2 0.9	2 54 44 20 10 2 1
15	**CH_3**CH_2 CH_2**CH_2**CH_2 **CH_2**N, NH**CH_2**, **CH_2**CONH CONH**CH_2** **CH** (Asp) **CH** (Aromatic)	0.8 – 1.2 1.8 – 1.5 3.0 – 2.2 3.4 – 3.0 4.7 – 4.6 6.8 – 6.5 7.6 – 7.3	54 2 81 22 10 2 0.9	54 2 80 20 10 2 1
16	**CH_3**CH_2 CH_2**CH_2**CH_2 **CH_2**N, NH**CH_2**, **CH_2**CONH CONH**CH_2** **CH** (Asp) **CH** (Aromatic)	0.8 – 1.2 1.8 – 1.5 3.0 – 2.2 3.4 – 3.0 4.7 – 4.6 6.8 – 6.5 7.6 – 7.3	56 20 83 23 10 1.9 0.9	54 20 80 20 10 2 1
17	CH_2**CH_2**CH_2 **CH_2**N, NH**CH_2**, **CH_2**CONH CONH**CH_2** **CH_2**-O-**CH_2** **CH** (Asp) **CH** (Aromatic)	1.8 – 1.5 3.0 – 2.2 3.4 – 3.0 3.9 – 3.6 4.7 – 4.6 6.8 – 6.5 7.6 – 7.3	20 85 22 38 10 2 1	20 80 20 36 10 2 1

[a] In D_2O, pD 10 – 11. Chemical shifts, δ (ppm), referenced against internal sodium 3-(trimethylsilyl)-2,2,3,3-d_4-propionate

[b] Integration error limit ± 10 %

3.1.6 Polyaspartamide carriers bearing dihydroxyl-functionalised side chain as drug anchoring site

Within this class of copolymers, two distinct types of copolymers, both containing a dihydroxylato-chelating ligand for a Pt containing drug, were synthesized. The first group is bearing one kind of solubilizing moiety; the second having two different solubilizing groups in a predetermined feed ratio.

With one solubilizing moiety (Scheme 3.11), the formation of the copolyaspartamide occurred in a two step reaction. In the first step a given amount of 3-hydroxytyramine (hydrochloride) (dopamine) was reacted with polysuccinimide **(PSI)** at room temperature for a 3d period. A long period and a 15% excess were found to be necessary to get the desired incorporation of the dopamine. In the second step, a solution of a second amine, namely DMP, DMEA, DEEA, DEP or APM, was added to the solution resulting from the first step and allowed to react for 2d. A 25% excess of the second amine was found to be useful to provide the correct balance to ensure complete ring opening of the remaining PSI units. The reaction proceeded under strictly anhydrous conditions in order to prevent undesired hydrolytic ring opening of the succinimide units to form a free carboxylic acid side group[123]. The polymeric products were isolated as completely water-soluble solids by a succession of operations including precipitation with an adequate non-solvent, extensive washing, aqueous dialysis, and freeze drying. As can be seen in Table 3.9, this group of carriers was obtained in typical yields of 58-65%, with inherent viscosities in the range of 10-13 $mL.g^{-1}$. The highest yield was observed with polyaspartamide **21** and the lowest with polyaspartamide **20**. In the same manner, the highest viscosity was observed with polyaspartamide **22** and the lowest viscosity with polyaspartamide **19**. The ^{1}H NMR spectra of polyaspartamides **18**-**22** measured in D_2O, and recorded at pH 10-11 for

elimination of protonation effects, showed characteristic band groups, some of them containing overlapping signals. Thus, the **CH** (methine) signal of the aromatic were found in the 6.7-6.3 ppm region, while the methine signal of the aspartic appeared in the region of 4.7-4.6 ppm and **CH_2**-O (methylene) was found in the region 3.9-3.6 ppm. The methylene protons of CONH-**CH_2** were found in the region of 3.4-3.0 ppm. The protons of CO-**CH_2**, **CH_2**-N (**CH_3**)$_2$, **CH_2**-NH and **CH_2**-NH_2 groups were found in the region of 3.0-2.0 ppm. Methylene protons of CH_2**CH_2**CH_2 groups were in the 1.8-1.5 ppm region. Methyl protons of CH_2**CH_3** groups were found in the region of 1.2-0.8 ppm. Table 3.9 and Table 3.10 summarize the experimental conditions, viscosities and ^{1}H NMR (Appendix 1p to 1t) data.

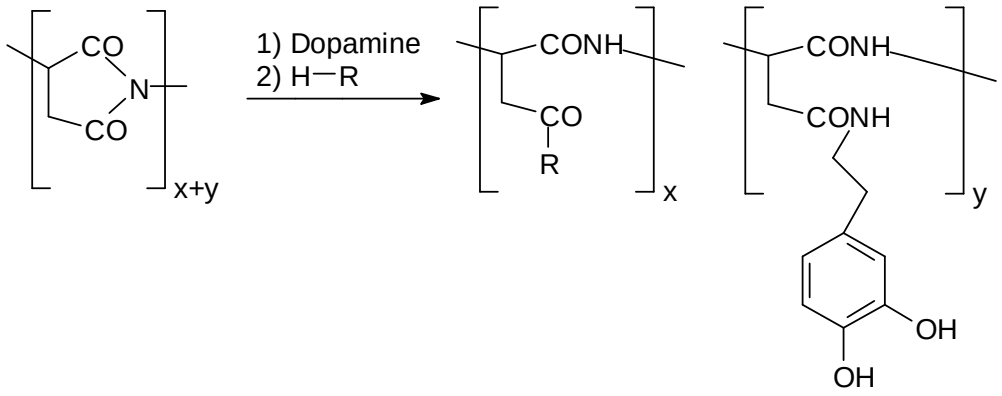

R

18. —NH NMe$_2$

19. —NH NMe$_2$

20. —NH NEt$_2$

21. —NH NEt$_2$

22. —NH N O

Scheme 3.11: Synthesis of copolyaspartamides **18** – **22**

In the case of two solubilizing groups (Scheme 3.12), AEP and DMP were used. This example of two solubilizing groups was motivated by the desire to demonstrate the possibility of improving the water solubility property of a carrier. However it should be noted that AEP can never be used on living patients if the patient is still young, because it will make the patient sterile. During our study it was noticed that all the carriers prepared with AEP alone as a solubilizing group had a poor water solubility. Being a determining criterion for the use of the carrier for further reaction, namely drug anchoring, we suggested the introduction of a second solubilizing group in order to improve the solubility. DMP was chosen for the reason that it is very basic. The reaction was a three-step process. In the first step a given amount of dopamine was allowed to react with polysuccinimide based on the desired x/y/z feed ratio. The reaction was performed at room temperature and under strictly anhydrous conditions. In the second step, 1-(2-aminoethyl)pyridine (AEP) was added to the resulting solution, and the reaction continued for another 1d. Anhydrous conditions were maintained to avoid any hydrolytic ring opening of the PSI units. In the last step, DMP was added in a large excess, twice the required amount, and the reaction proceeded for a further 1d at room temperature, again, strictly anhydrous conditions were observed in order to prevent needless hydrolytic ring opening of the PSI.

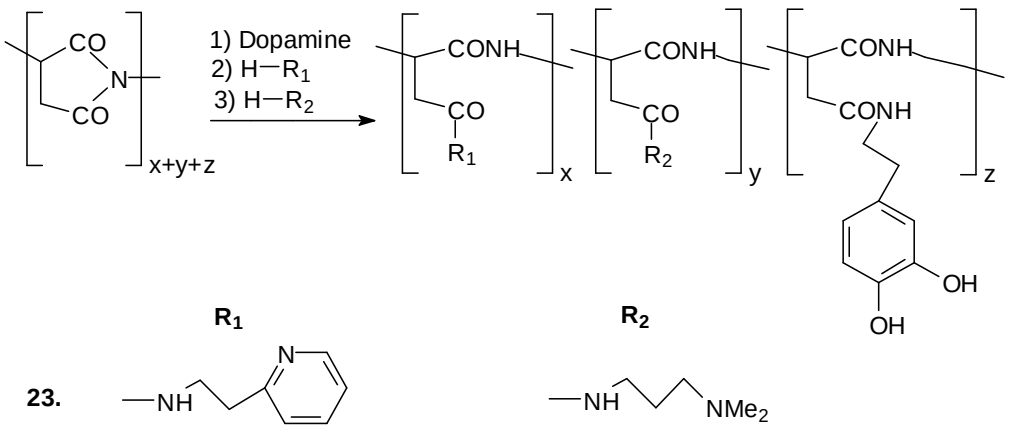

Scheme 3.12: Synthesis of copolyaspartamide **23**

The polymeric product was isolated as a completely water-soluble solid by a series of operations, which included precipitation with a non-solvent, extensive washing, aqueous dialysis, and freeze-drying. The polymers were obtained in a yield of 66.2%, with inherent an viscosity of 11.8 $mL.g^{-1}$. The reaction conditions, viscosity results and 1H NMR (Appendix 1u) are summarized in Tables 3.9 and 3.10. For both groups of carriers (one solubilizing group and two solubilizing groups), the isolated polymers were characterized by ^{1}H NMR as discuss earlier in this section.

Table 3.9: Summary of experimental data Polyaspartamide Bearing a dihydroxylato-ligand Side Chain as Drug Anchoring Site.

Designation	Molar Ratios[a, b]								Reaction time & Temperature[c]		Yield (%)	η_{inh} [d] ($mL.g^{-1}$)	x : y [e] or x : y : z [f]
	PSI	Dopamine	DMP	DMEA	DEEA	DEP	APM	AEP	1st Step	2nd Step			
18	1.00	0.115	1.15	-	-	-	-	-	3d, RT	2d, RT	60.4	12.6	90 : 10
19	1.00	0.115	-	1.15	-	-	-	-	3d, RT	2d, RT	61.3	10.9	90 : 10
20	1.00	0.115	-	-	1.15	-	-	-	3d, RT	2d, RT	58.1	13.2	90 : 10
21	1.00	0.115	-	-	-	1.15	-	-	3d, RT	2d, RT	65.4	12.4	90 : 10
22	1.00	0.115	-	-	-	-	1.15	-	3d, RT	2d, RT	63.5	13.5	90 : 10
23	1.00	0.215	0.60	-	-	-	-	0.50	3d, RT	1d, RT; 1d, RT	66.2	11.8	50:30:20

[a] Base molar for **PSI**

[b] PSI: Polysuccinimide; DMP: 3-(dimethylamino)propylamine; DMEA: 2-(dimethylamino)ethylamine; DEEA: 2-(diethylamino)ethylamine; DEP: 3-(diethylamino)propylamine; APM: 4-(3-aminopropyl)-morpholine; AEP: 1-(2-aminoethyl)pyridine.

[c] RT: room temperature.

[d] At $30.0^{o}C \pm 0.5^{o}C$ in dist H_2O; conc. = 2 $mg.mL^{-1}$.

[e] x:y Desired feed ratio, solubilizing moiety to drug binding moiety (for polyaspartamide 18 to 22).

[f] x:y:z Desired feed ratio, AEP : DMP : Dopamine (for polyaspartamide 23).

Table 3.10: ^{1}H NMR of copolyaspartamides **18** to **23**.

Polymer Designation	Assignment	^{1}H NMR		
		Shift range δ(ppm)	Proton count	
			Found	Expected
18	CH_2**CH_2**CH_2	1.8 – 1.5	18	18
	N**CH_3**	2.2 – 2.0	54	54
	CH_2N, Ar-**CH_2**	2.4 – 2.2	21	20
	CH_2CONH	3.0 – 2.4	23	20
	CONH**CH_2**	3.3 – 3.0	22	20
	CH (Asp)	4.7 – 4.6	10	10
	CH (Aromatic)	6.7 – 6.3	3	3
19	N**CH_3**	2.3 – 2.1	54	54
	CH_2CONH, **CH_2**N, Ar-**CH_2**	3.0 – 2.3	42	40
	CONH**CH_2**	3.5 – 3.1	22	20
	CH (Asp)	4.7 – 4.6	10	10
	CH (Aromatic)	6.7 – 6.3	2.9	3
20	**CH_3**CH_2	1.1 – 0.9	54	54
	CH_2CONH, **CH_2**N, Ar-**CH_2**	3.0 – 2.4	78	76
	CONH**CH_2**	3.5 – 3.1	22	20
	CH (Asp)	4.7 – 4.6	10	10
	CH (Aromatic)	6.7 – 6.3	2.9	3
21	**CH_3**CH_2	1.1 – 0.8	54	54
	CH_2**CH_2**CH_2	1.8 – 1.5	18	18
	CH_2CONH, **CH_2**N, Ar-**CH_2**	3.0 – 2.3	78	76
	CONH**CH_2**	3.4 – 3.0	21	20
	CH (Asp)	4.7 – 4.6	10	10
	CH (Aromatic)	6.7 – 6.3	2.9	3
22	CH_2**CH_2**CH_2	1.8 – 1.5	18	18
	CH_2CONH, **CH_2**N, Ar-**CH_2**	3.0 – 2.2	76	76
	CONH**CH_2**	3.4 – 3.0	22	20
	CH_2-O-**CH_2**	3.9 – 3.6	35.5	36
	CH (Asp)	4.7 – 4.6	10	10
	CH (Aromatic)	6.7 – 6.3	3	3
23	CH_2**CH_2**CH_2	2.0 – 1.8	6	6
	N**CH_3**, **CH_2**CONH, **CH_2**N, Ar-**CH_2**, CONH**CH_2**	3.6 – 2.2	76	78
	CH (Asp)	4.7 – 4.6	9.6	10
	CH (Dopamine)	6.8 – 6.4	5.8	6
	CH (AEP ring)	7.4 – 7.0	9.8	10
		7.8 – 7.5	4.6	5
		8.5 – 8.2	4.9	5

[a] In D_2O, pD 10 – 11. Chemical shifts, δ (ppm), referenced against internal sodium 3-(trimethylsilyl)-2,2,3,3-d_4-propionate

[b] Integration error limit ± 10 %

3.2 Polymer platinum conjugation

Cisplatin, *cis*-diaminedichloroplatinum(II), a square planar Pt^{2+} complex, was the first metal-based agent to enter onto the global market for the clinical treatment of cancer[34,45]. Currently, cisplatin is used either by itself or in combination with other drugs for treating lung, ovarian, bladder, testicular, head and neck, esophageal, colon, gastric, breast, melanoma and prostate cancer. Although sales of cisplatin are presently on the decline, with second- and third-generation analogs being more widely prescribed, cisplatin remains the gold standard to which potential platinum and non-platinum metal-based anticancer drugs are compared[34,39,46].

A major problem with cisplatin in chemotherapy is that repeated exposure to the drug can induce resistance in the cancer being treated, which results in a change in the treatment regimen[31]. While it would seem reasonable to simply increase the dose of the cisplatin administrated to the patient, renal clearance of cisplatin is quite fast[125], and its accumulation in the kidney results in severe renal toxicity. By varying the amine ligands of the cisplatin, it was found that *cis*-dichloroplatinum(II) complexes containing *trans*-1,2-diaminocyclohexane (DACH) showed very high antitumor activity[126]. As salt-like compounds, these complexes cannot efficiently penetrate cell membranes by the passive diffusion mechanism which is generally utilized by nonpolar, neutral compounds.
In comparison with a conventional low-molecular-weight drug, a macromolecular prodrug, such as a polymer-drug conjugate, can be expected to overcome similar problems by improving the distribution of the antitumor agent in the body, through enhanced permeability, retention and pinocytotic entry into cells[127-129].

There is strong scientific evidence that Pt-based drugs should be outstanding candidates for polymer anchoring, *i.e.* the bioreversible conjugation with suitably designed carrier polymers. The literature indeed

provides a plethora of studies in this field. By far the most significant work, dating back to 1983[130-132], has been performed in Carraher's laboratory, and this researcher has presented a comprehensive and proficiently written account of his work and other publications in the field[128]. Also noteworthy are the investigations by Ohya's group[125], Duncan's team[133], and Schechter's laboratory[134]. Initially water-soluble, physically isolated and analytically characterized polymer-platinum conjugates have predominantly been the domain of the WITS PRG Laboratory[135-142]. These conjugates were based on polyaspartamide carrier structures and typically embodied a drug-anchoring design featuring platinum bonding through ethylenediamine chelation, the ligand being attached to short polymer side chains *via* biofissionable amide links. High activity against HeLa cells as well as human liver and lung cancers, paired with excellent cell specificity, was demonstrated *in vitro* for these platinum-conjugates. These encouraging earlier results provided the justification for the present project.

Polymer-platinum conjugation may be brought about by a variety of methods, depending on the type and structure of the metal ligands chosen to serve as the connecting link to the polymer. Fundamentally, platinum may be carrier-bound either *via* the amine ligands or else through the leaving group ligands. This has been an important area of research in this laboratory for a number of years[137,143], and various models for drug anchoring have been established[144]. One practical approach developed at the WITS PRG laboratory[145,146] involved attachment of the ethylenediamine structural unit to the polymer backbone as a side-chain constituent, which may serve as the diamine ligand in subsequent reactions. The conjugates synthesized, of interest as potential antineoplastic agents, contained spacer-incorporated biofissionable amide groups allowing for hydrolytic and enzymatic cleavage in the lysosomal compartment with consequent liberation of the active *cis*-diamineplatinum side-chain component[147].

In this study, platinum complexes anchored *via* a monoamine moiety (Model 1 and Model 2), the leaving group ligands, namely carboxylatohydroxylato (Model 3), dihydroxylato (Model 4), and dicarboxylato (Model 5) ligands are investigated (Figure 3.2). For several decades, a *cis*-diammineplatinum(II) pattern has 'classically' been considered a prerequisite for biological activity, with two ligands left as ready leaving groups critically involved in the biological functioning. However, a few years ago, structures containing charged triamineplatinum(II) complexes were also found to show antineoplastic activity[118]. An outstanding example was the cationic *cis*-diamminechloro-platinum-*p*-aminobenzoic acid complex[121]. Thus, these findings motivated the design of Model 1 and Model 2 in an effort to achieve further enhancement of therapeutic effectiveness of complexes of the triamine-coordinated Pt(II) containing a single leaving group type. These two Models led to the same type of conjugate using two different routes. In Mode 1 DACH-$PtCl_2$ (Scheme 3.13) was used as platination agent and this route required carriers in which the amino side-chains were aromatic amines (Polyaspartamides **1**-**5**). In Model 2 DACH-Pt-PABA (Scheme 3.13) was used as platination agent for carriers in which the amino side-chains were aliphatic amines (polyaspartamides **6** and **7**). The choice of ligands used in Model 3, Model 4 and Model 5 was motivated by the ability of these ligands to chelate the platinum agent upon coordination, forming five- or seven-membered rings stable enough to survive in the central systemic circulation in the cancer patient. From the ultimate conjugate, the release will occur by hydrolytic cleavage of the oxygen-metal bonds at low pH, releasing the *trans*-1,2-diaminocyclohexaneplatinum(II) as an aquated species.

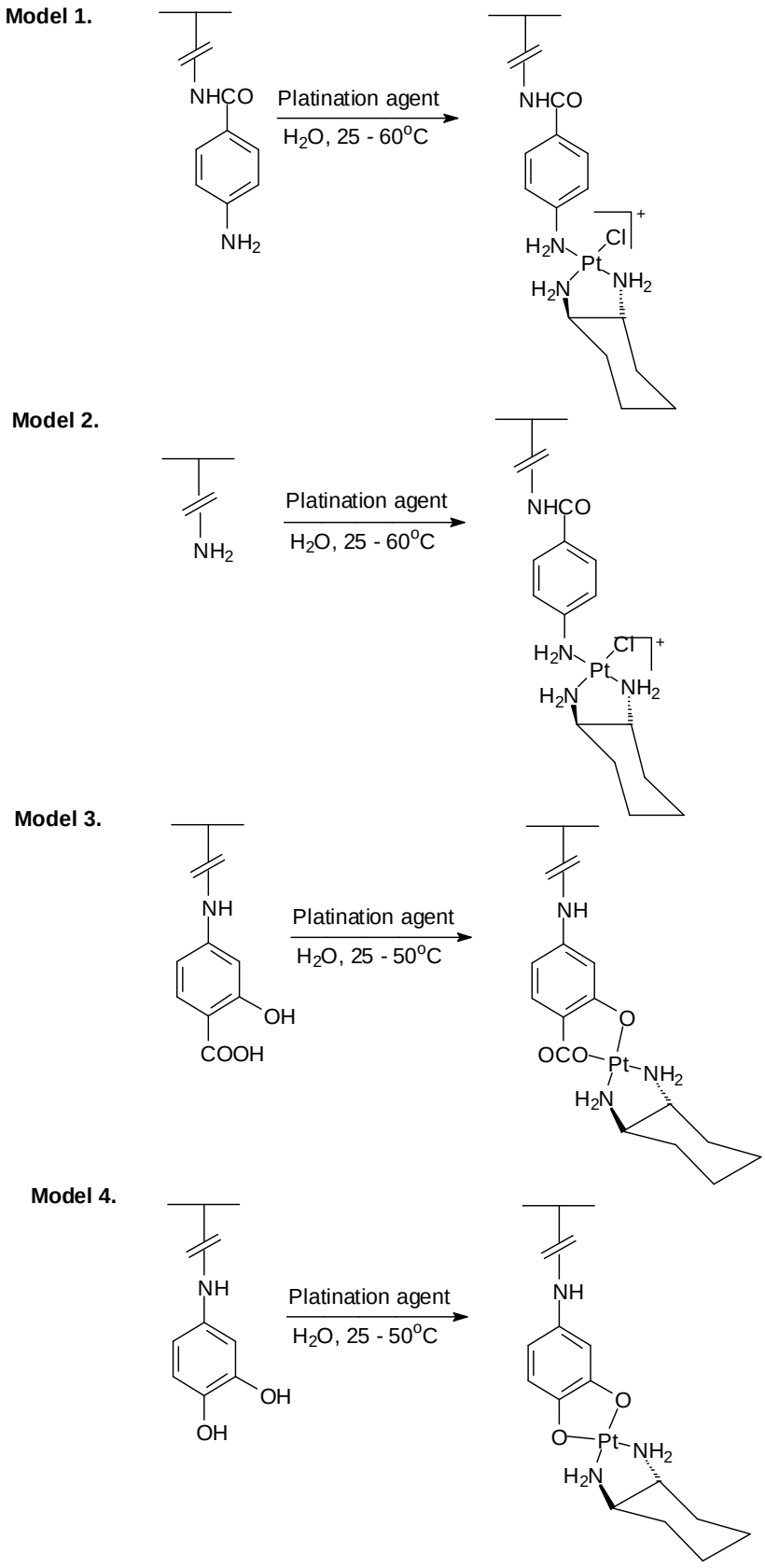

Figure 3.2: Models of platinum conjugates.

Model 5.

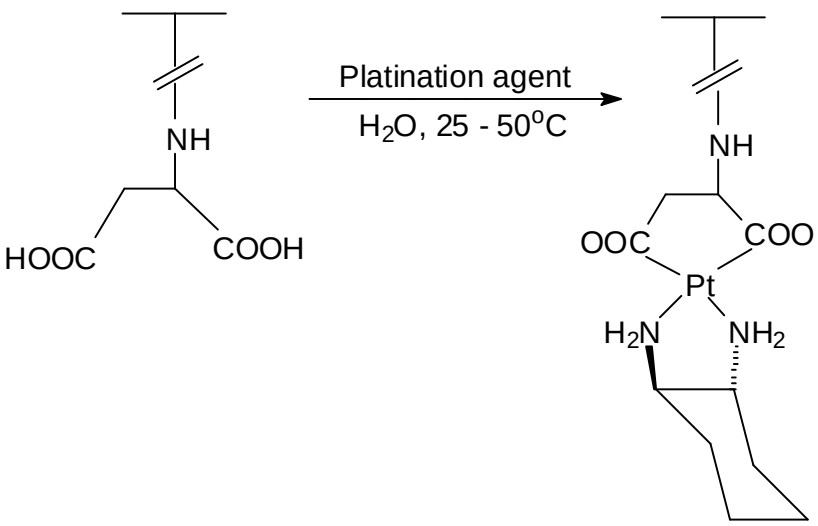

Figure 3.2: Continued

The platination agents, DACH-$PtCl_2$, DACH-Pt and DACH-Pt-PABA were prepared according to published procedures[118,148]. As depicted in Scheme 3.13, a tetrachloroplatinum(II) salt in aqueous solution was treated with *trans*-1,2-diaminocyclohexane, followed by chloro-aqua ligand exchange in the presence of silver nitrate for DACH-Pt or treatment with *p*-aminobenzoic acid at elevated temperature for DACH-Pt-PABA. These three platination agents were chosen based on the synthetic route used and the kind of ligand on the carrier polymer.

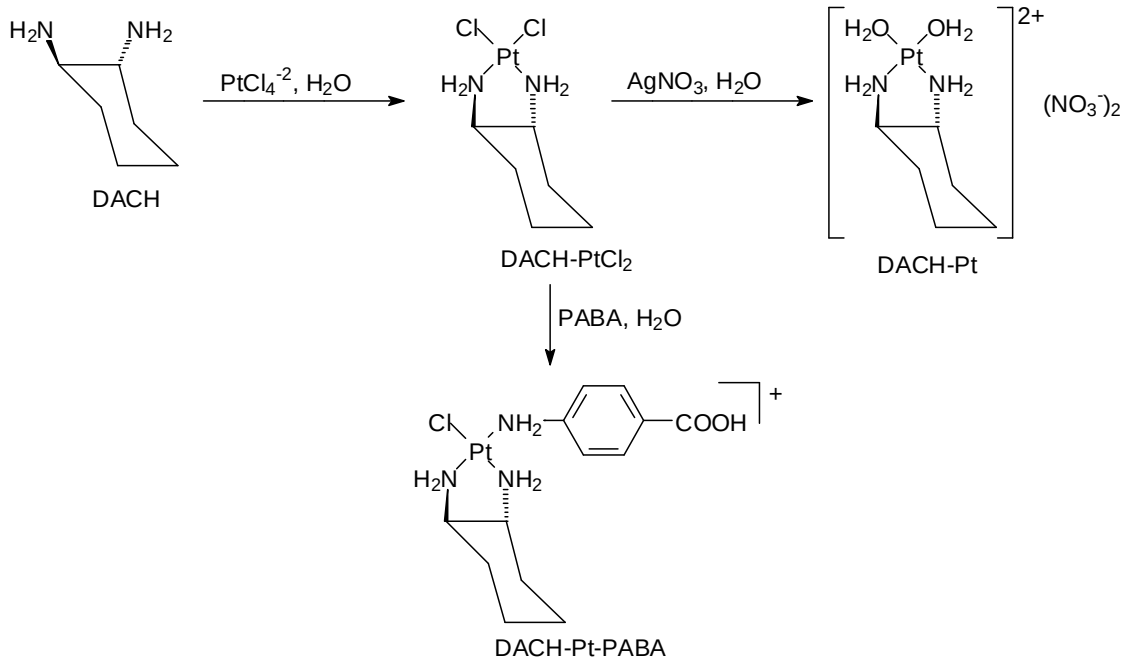

Scheme 3.13: Synthesis of platination agents.

3.2.1 Monoamineplatinum(II) conjugates

Two different routes were used for the preparation of this class of conjugates represented by Model 1 and Model 2.

3.2.1.1 First route

Polyaspartamide **6** and **7** were used in this route (Model 2). The platination agent, DACH-Pt-PABA was directly anchored onto the polymer carriers **6** and **7** *via* the amine and the carboxylic acid groups by using *N*-(3-dimethyl-aminopropyl)-*N*-ethylcarbodiimide hydrochloride (EDC) as coupling agent in aqueous solution as depicted in Schemes 3.14 and 3.15. The reaction was carried out under carefully controlled experimental conditions of time and pH. The pH was monitored during the reaction period and kept between ~5.5 and 6 to prevent crosslinking (higher pH) or hydrolysis (lower pH). Further more, under these conditions the coordination to platinum was preferentially on the monodentate amine group (-NH_2) despite the presence of the tertiary amine (-$N(CH_3)_2$) side chains. The conjugates were dialyzed

for 2d in Spectra/Por 4® (12 000-14 000 molecular weight cut off). Freeze-drying of the retentate resulted in the water-soluble solids with inherent viscosities of 10.8-11.3 mL.g^{-1}. The platinum content was calculated for the structures normalized to y = 1. The molar feed ratio, experimental conditions, viscosities, and platinum content data are summarized in Table 3.11. As a general trend, poor platinum content was observed when this route was used. For all the experiments performed using this route, the platinum incorporations were below 25% regardless of the different ratios of solubilizing moiety to drug binding moiety in the carriers. This suggested a poor EDC-coupling under platination conditions. Thus, only two examples (polyaspartamides **6** and **7**, and conjugates **6**-**Pt** and **7**-**Pt**) were included for illustration. This suggested that the EDC coupling in water was not as good as a method in which coupling was done in other solvent systems such as DMF using 2-(1*H*-benzotriazol-1-yl-)-1,1,3,3-tetramethyluronium fluorophosphates (HBTU). Being an effective coupling agent, HBTU is regularly used in the WITS PRG laboratory[149-151]. In the present study, HBTU was avoided because DMF is a good ligand for platinum and this would have replaced the other ligands and coordinate the platinum. To improve upon the incorporation of platinum into the pro-drug, a second route (Model 2) was proposed.

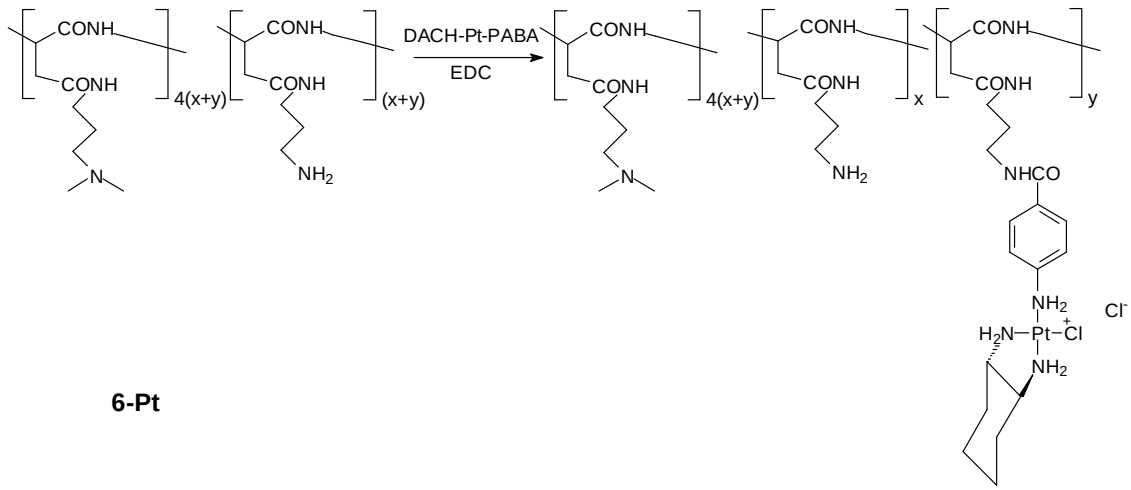

6-Pt

Scheme 3.14: Synthesis of conjugate **6-Pt**.

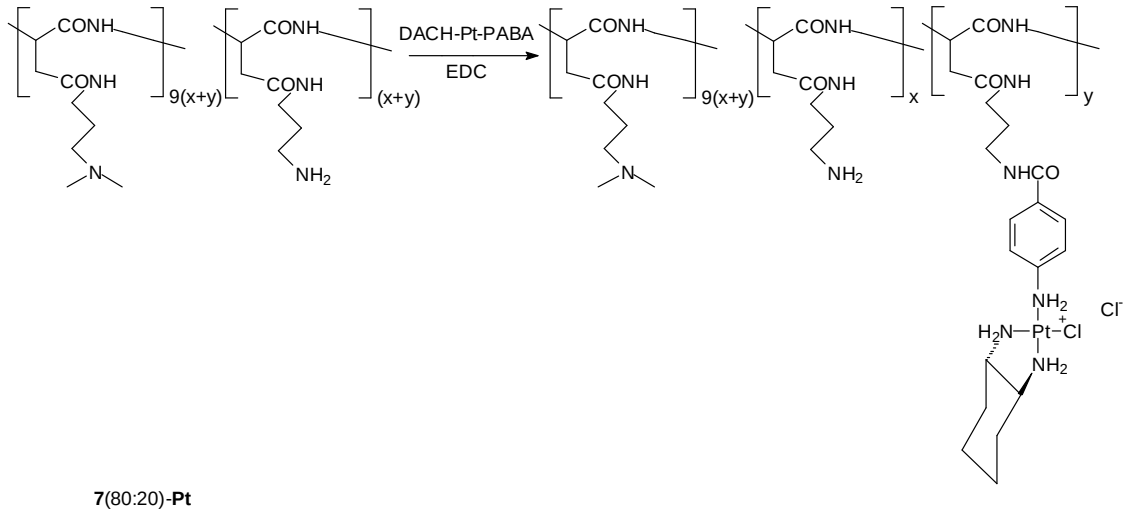

7(80:20)-**Pt**

Scheme 3.15: Synthesis of conjugate **7-Pt**.

3.2.1.2 Second route

The second route or alternative was used in order to improve the percentage of platinum incorporated into the carriers. The preparation of this class of conjugates represented by Model 1 following the second route (Scheme 3.16) involved the treatment of the aromatic amine-functionalized polyaspartamide carriers, in aqueous solution, with excess platination agent (DACH-$PtCl_2$), under well controlled experimental conditions of time, temperature and pH. The conjugates were then dialyzed for the removal of the unbound drug and freeze-dried to give water soluble solids in yields of 46.7-58.1% and with inherent viscosities of 10.8-13.1 $mL.g^{-1}$. The platinum content was calculated for the structure normalized to y = 1. As can be seen in Table 3.11, the ultimate products possessed platinum contents ranging from 5.67 to 7.83%, which correspond to the platinum incorporations ranging between 81.6 and 93.4%, where conjugates **1**-**Pt**, **2**-**Pt** and **3**-**Pt** having the incorporation of above 91%. The highest incorporation was noticed with conjugate **3**-**Pt**, while the lowest with conjugate **5**-**Pt**. Thus, this route was the preferred and adopted route for this class of conjugates because of the high percentage platinum incorporation. To avoid any solid-state interaction of the bound platinum complexes with nearby amines,

leading to crosslink formation and subsequent lost of solubility of the conjugates; the conjugates were stored at 4^{o}C.

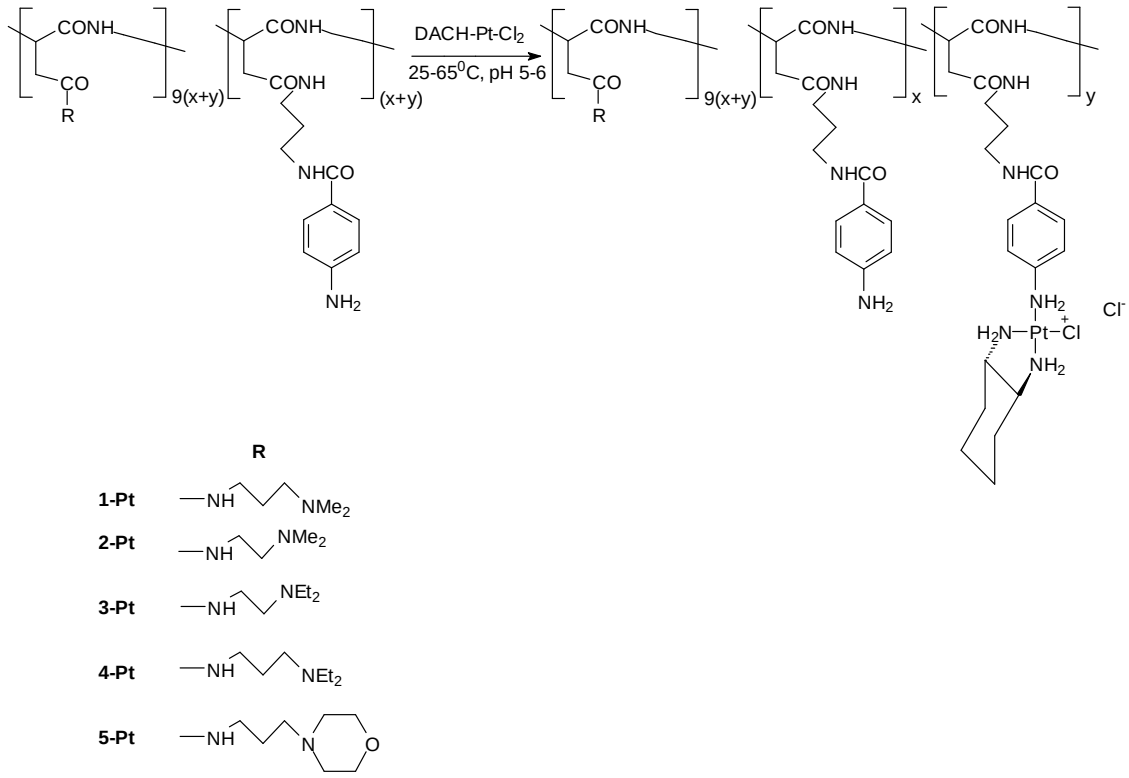

Scheme 3.16: Synthesis of conjugates **1-Pt** to **5-Pt**.

Table 3.11: Preparative and analytical data of conjugates **1-Pt** to **7-Pt**.

Designation	Molar Ratios			Reaction time & Temperature	Yield (%)	Base Molecular Mass[a]	η_{inh}[b] (mL.g^{-1})	x : y [c]	Pt (%)	
	Carrier	DACH-Pt	DACH-Pt-Cl PABA						Found[d]	Calcd[e]
1-Pt	1.0	1.1	-	3d, RT; 1d, 65°C	58.1	2428.0	12.1	90 : 10	7.32	8.03
2-Pt	1.0	1.1	-	3d, RT; 1d, 65°C	52.5	2295.8	10.9	90 : 10	7.83	8.50
3-Pt	1.0	1.1	-	3d, RT; 1d, 65°C	46.7	2554.2	12.6	90 : 10	7.13	7.63
4-Pt	1.0	1.1	-	3d, RT; 1d, 65°C	49.8	2680.5	13.1	90 : 10	6.25	7.28
5-Pt	1.0	1.1	-	3d, RT; 1d, 65°C	48.2	2806.3	11.3	90 : 10	5.67	6.95
6-Pt	1.0	-	1.1	6h, RT; 12h, RT	55.4	1431.9	10.8	80 : 20	2.12	13.62
7-Pt	1.0	-	1.1	6h, RT; 12h, RT	43.2	2428.0	11.3	90 : 10	1.76	8.03

[a] Molecular mass of the simple recurring unit; structures normalized to y = 1.

[b] At 30.0°C ± 0.5°C in distilled water; conc. = 2 mg.mL^{-1}.

[c] Ratio of solubilizing moiety to platinum-drug binding moiety.

[d] Pt content (%) obtained by atomic absorption analysis performed by an outside laboratory.

[e] Pt content (%) for complete incorporation of the drug.

3.2.2 Carboxylatohydroxylato-platinum(II) chelated conjugates

The preparation of this class of conjugates involved the incorporation of the platinum complex as per Model 3 in a chelated form (Schemes 3.17 and 3.18). Conjugates **8-Pt** to **17-Pt** were derived from carriers **8** to **17**. All the carriers of this group contained the carboxylatohydroxylato function, provided by the *p*-aminosalicylic acid component, as a side group; and were treated with *trans*-1,2-diaminocyclohexanediaquaplatinum(II) dinitrate (DACH-Pt) in aqueous solution, under carefully controlled experimental conditions of time, temperature and pH (Schemes 3.17 and 3.18). Dialysis was performed in Spectra/Por 4® for 2d to ensure the removal of non-polymeric salts. The conjugates were isolated as water-soluble solid materials in yields of 42.3-55.4%, with inherent viscosities of 9.8-13.4mL.g^{-1}. As can be seen in Table 3.12, the ultimate products possessed platinum contents ranging from 5.58 to 7.72%, with structures normalized to y = 1 for the calculated values. These platinum contents correspond to the platinum incorporations ranging between 74 and 95%, with conjugates **9**-**Pt**, **11**-**Pt**, **12**-**Pt** and **13**-**Pt** observed the incorporation of above 90%. The highest incorporation was noticed with conjugate **11**-**Pt**, while the lowest with conjugate **8**-**Pt**. A set of experimental conditions and analytical data are summarized in Table 3.12.

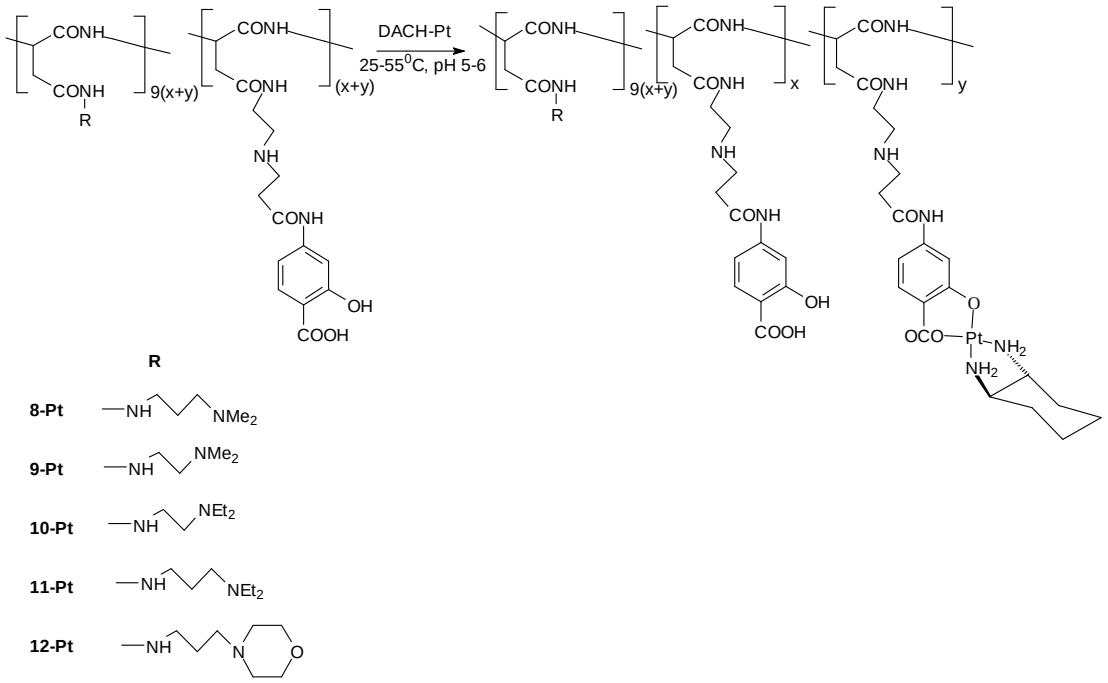

Scheme 3.17: Synthesis of conjugates **8-Pt** to **12-Pt**.

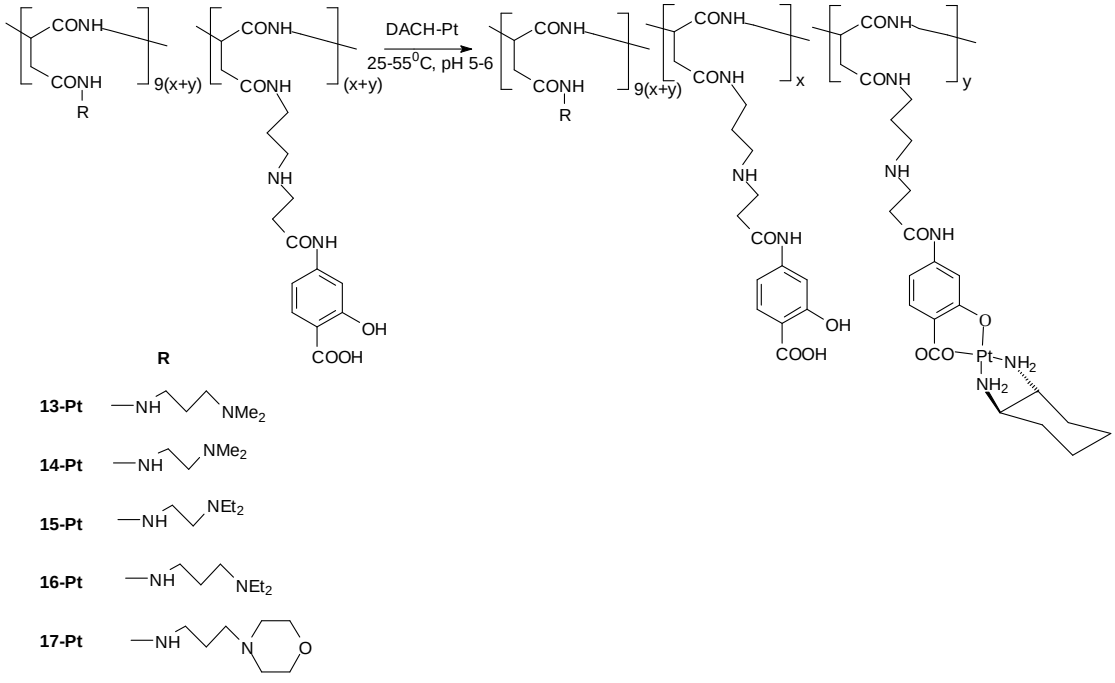

Scheme 3.18: Synthesis of conjugates **13-Pt** to **17-Pt**.

Table 3.12: Preparative and analytical data of platinum-conjugates **8-Pt** to **17-Pt**.

Conjugate Designation	Molar Ratios		Reaction time & Temperature	Yield (%)	Base Molecular Mass [a]	η_{inh} [b] ($mL.g^{-1}$)	x : y [c]	Pt (%)	
	Carrier	DACH-Pt						Found [d]	Calcd [e]
8-Pt	1.0	1.1	3d, RT; 2h, 55°C	48.5	2464.6	13.4	90 : 10	5.86	7.91
9-Pt	1.0	1.1	3d, RT; 2h, 55°C	49.6	2338.3	12.1	90 : 10	7.72	8.34
10-Pt	1.0	1.1	3d, RT; 2h, 55°C	52.8	2590.8	11.3	90 : 10	6.13	7.53
11-Pt	1.0	1.1	3d, RT; 2h, 55°C	54.3	2717.0	12.8	90 : 10	6.84	7.18
12-Pt	1.0	1.1	3d, RT; 2h, 55°C	44.1	2842.9	12.6	90 : 10	6.31	6.86
13-Pt	1.0	1.1	3d, RT; 2h, 55°C	51.2	2478.6	11.5	90 : 10	7.23	7.87
14-Pt	1.0	1.1	3d, RT; 2h, 55°C	42.3	2352.4	9.8	90 : 10	6.92	8.29
15-Pt	1.0	1.1	3d, RT; 2h, 55°C	49.2	2604.8	12.3	90 : 10	5.78	7.49
16-Pt	1.0	1.1	3d, RT; 2h, 55°C	55.5	2731.1	13.1	90 : 10	6.05	7.14
17-Pt	1.0	1.1	3d, RT; 2h, 55°C	52.6	2856.9	12.3	90 : 10	6.12	6.83

[a] Molecular mass of the simple recurring unit; structures normalized to y = 1.

[b] At 30.0°C ± 0.5°C in distilled water; conc. = 2 $mg.mL^{-1}$.

[c] Ratio of solubilizing moiety to platinum-drug binding moiety.

[d] Pt content (%) obtained by atomic absorption analysis performed by an outside laboratory.

[e] Pt content (%) for complete incorporation of the drug.

3.2.3 Dicarboxylato-platinum chelated conjugates

Conjugates **18-Pt** to **23-Pt** were obtained from carriers **18** to **23**, as per Model 4. As depicted in Schemes 3.19 and 3.20, the carriers were treated with DACH-Pt in aqueous medium under well controlled experimental conditions of time, temperature and pH. The same procedure as for preparation of conjugates **8-Pt** to **17-Pt** was used. The work-up was done as discussed in section 3.2.2, and no modification was made to this step. These conjugates were obtained in yields ranging from 42.3 to 56.8% and possessed inherent viscosities in the range of 10.7 to 14.2 mL.g^{-1}. For this group of conjugates, as can be seen in Table 3.13, the platinum contents ranged between 6 and 10%, which corresponded to the platinum incorporation ranging from 71 to 95%. The highest platinum incorporation was observed with conjugate **20**-**Pt** and the lowest with conjugate **23**-**Pt**. The experimental conditions and analytical data are summarized in Table 13.13.

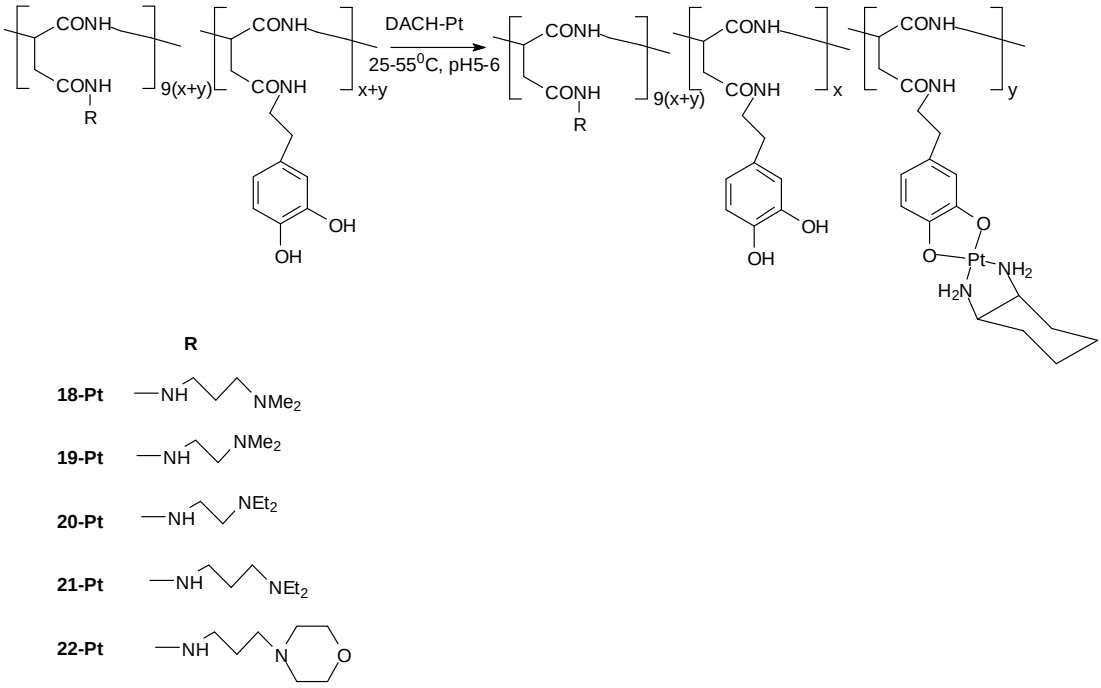

Scheme 3.19: Synthesis of conjugates **18-Pt** to **22-Pt**.

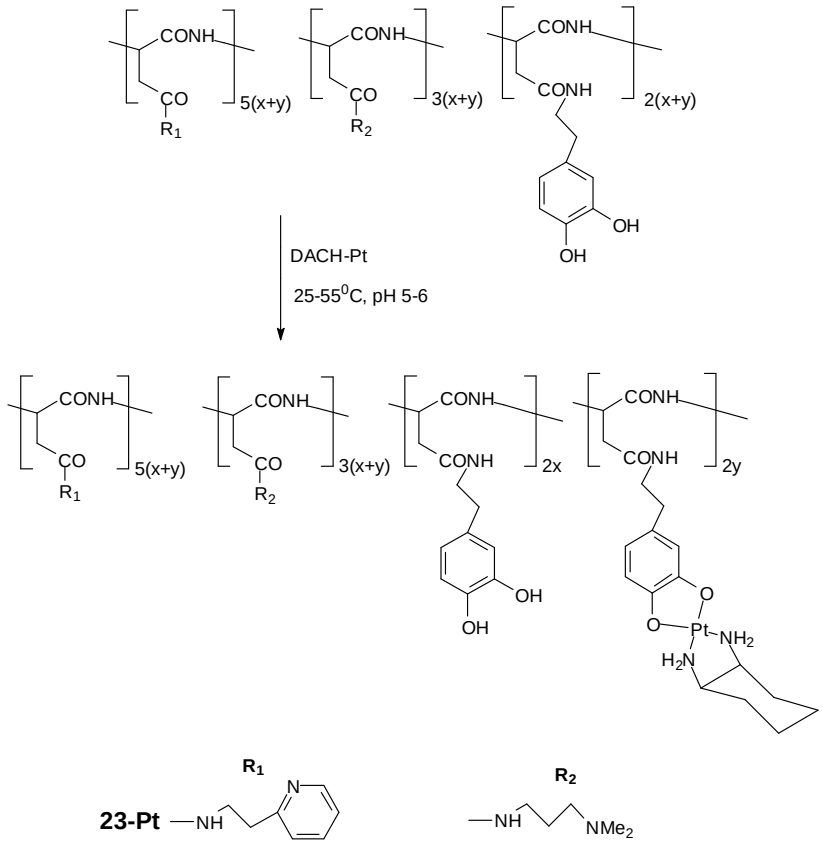

Scheme 3.20: Synthesis of conjugate **23-Pt**.

Table 3.13: Preparative and analytical data of platinum-conjugates **18-Pt** to **23-Pt**

Conjugate Designation	Molar Ratios		Reaction time & Temperature	Yield (%)	Base Molecular Mass [a]	η_{inh} [b] ($mL.g^{-1}$)	x : y [c]	Pt (%)	
	Carrier	DACH-Pt						Found [d]	Calcd [e]
18-Pt	1.0	1.1	3d, RT; 2h, 55°C	56.8	2350.5	14.2	90 : 10	6.89	8.30
19-Pt	1.0	1.1	3d, RT; 2h, 55°C	49.6	2224.2	13.4	90 : 10	8.01	8.77
20-Pt	1.0	1.1	3d, RT; 2h, 55°C	48.3	2476.9	11.1	90 : 10	7.52	7.87
21-Pt	1.0	1.1	3d, RT; 2h, 55°C	51.6	2602.9	13.6	90 : 10	6.26	7.49
22-Pt	1.0	1.1	3d, RT; 2h, 55°C	42.3	2728.9	11.6	90 : 10	6.04	7.15
23-Pt	1.0	1.1	3d, RT; 2h, 55°C	46.8	1481.3	10.7	50:30:20	9.43	13.17

[a] Molecular mass of the simple recurring unit; structures normalized to y = 1.

[b] At 30.0°C ± 0.5°C in distilled water; conc. = 2 $mg.mL^{-1}$.

[c] Ratio of solubilizing moiety to platinum-drug binding moiety.

[d] Pt content (%) obtained by atomic absorption analysis performed by an outside laboratory.

[e] Pt content (%) for complete incorporation of the drug.

3.3 Polymer multi-drug anchoring

During the past decade, many research projects have focused on the sequential and simultaneous delivery of drug combinations to reduce the effects associated with the systemic delivery of anticancer agents[152,153]. It is the fundamental importance of this strategy that additive and even synergistic effects are produced without enhancing overall drug toxicity, and this can potentially lead to reduced doses for each drug administered[154]. One possible route for simultaneous delivery of anticancer drugs is the co-conjugation of two or more of the active agents to a single polymeric carrier *via* biofissionable linkages.

Platinum-based drugs and ferrocene were used to demonstrate the possibility of anchoring two different drugs to the same carrier. The two drugs inhibit cellular growth by two different mechanisms. This study will determine the manner in which the two drugs interact. Since platinum and ferrocene can both be anchored to the same ligand, namely an amine, it was important to find a suitable synthetic approach to incorporate the two drugs in the polymer and control their incorporations. The designed strategy allowed the incorporation of the ferrocene drug during the aminolytic ring opening of the PSI in a well-controlled manner, leaving free the site for platinum anchoring.

3.3.1 Synthesis of 4-ferrocenylbutamidopropylamine (M6)

4-Ferrocenylbutanoic acid was synthesized by reacting ferrocene and succinic anhydride in the presence of aluminum chloride according to a well established procedure used in the WITS PRG laboratory[155]. Two possibilities were reviewed. The standard procedure used in past research[149-151], investigating carriers with side chains bearing a free amino group for ferrocene coupling, was disregarded since platinum (II) complex

and 4-ferrocenylbutanoic acid can both be incorporated into the carrier polymer *via* a free amino group. To gain more control over the drug incorporation, a novel route was designed with the synthesis of 3-[4-ferrocenylbutamido] propylamine to be incorporated in the polysuccinimide during aminolytic ring opening.

3-[4-Ferrocenylbutamido]propylamine was obtained by HSU-DCC coupling under very mild conditions. In the first step, 4-ferrocenylbutanoic acid was reacted with HSU in the presence of DCC at 0-5^{o}C for 4h, then at RT for 2d (Scheme 3.21). The intermediate formed was not isolated after removal of the urea, it was treated with excess PDA at 0-5^{o}C for 1d then at RT for 6h, in the second step. The experimental conditions and ^{1}H NMR (Appendix 1d) data are summarized in Tables 3.14 and 3.15.

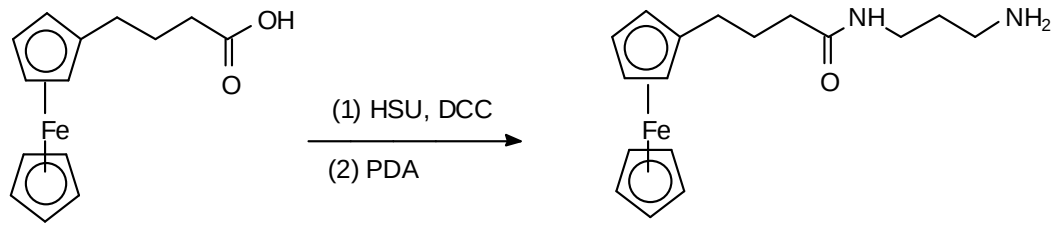

M5 **M6**

Scheme 3.21: Synthesis of 4-ferrocenylbutamidopropylamine

Table 3.14: Summary of experimental data for **M6**.

Designation	Molar ratio [a, b]			Experimental Conditions [c]		Yield (%)
	M5	HSU	PDA	1st Step	2nd Step	
M6	1.0	1.2	4.0	4h, 0-5^{o}C; 2d, RT	1d, 0-5^{o}C; 6h, RT	78.0

[a] Base molar for **M5**

[b] PDA: 1,3-diaminopropane, HSU: N-hydroxysuccinimide

[c] RT: room temperature

Table 3.15: ^{1}H NMR of **M5** and **M6**.

Designation	Assignment	^{1}H NMR [a, b]		
		Shift range δ(ppm)	Proton count	
			Found	Expected
M5	CH_2**CH_2**CH_2 **CH_2**CH_2**CH_2** CH, Ferrocenyl	1.9 – 1.7 2.4 – 2.2 4.25 – 4.1	2 4 8.8	2 4 9
M6	CH_2**CH_2**CH_2 Fc-**CH_2**CH_2, **CH_2**NH_2 **CH_2**CONH CONH**CH_2** **CH**, Ferrocenyl	1.9 – 1.7 2.4 – 2.2 3.0 – 2.9 3.25 – 3.1 4.25 – 4.1	4 4 2 2 9	4 4 2 2 9

[a] In D_2O, pD 10–11. Chemical shifts, δ (ppm), referenced against internal sodium 3-(trimethylsilyl)-2,2,3,3-d_4-propionate;

[b] Integration error limit ± 12%

3.3.2 Co-conjugates coordinated to monoamine platinum and ferrocene

Aminolytic ring-opening of PSI was utilized in order to generate copolyaspartamides containing ferrocene through a stepwise process which involves utilization of three different amine reactants in given stoichiometric feed ratios. The first amine (NH_2 – R) having an anchoring site for platinum complexes, the second amine containing ferrocene (Fc – NH_2), and the last amine (NH_2 – R') used as a solubilizing moiety were incorporated in the PSI in predetermined ratios along the chain. In accordance with the general principle, the solubilizing group was used as a major reactant in the four-step preparative process of these co-conjugates. The first three steps led to an aspartamide-containing ferrocene, as homoconjugate, and the last step

was used for the anchoring of the platinum complex leading to the co-conjugates.

In the first step, to a given amount of PSI under anhydrous conditions was added PABA-PDA according to the desired mole ratio. The reaction was allowed to proceed for 24h under a N_2 atmosphere at 0-5^oC. In the second step, a given amount of Fc–PDA was added and the reaction continued at 0-5^oC for another 24h. In the third step, an excess of the solubilizing amine (DMP, DEEA, DMEA, DEP or APM) was added and the reaction allowed to continue for 6h at 0-5^oC and then for 2d at RT. The long low temperature period was adopted in order to minimize any cross-linking due to the presence of the amino group on the benzene ring. Although this amine is less nucleophilic than the alkyl amino group, longer exposure time would increase the cross-linking chance which would render the product not only insoluble, but also lacking the site for platinum anchoring. All three steps were performed under strictly anhydrous conditions in order to avoid unwanted hydrolytic ring-opening resulting in the generation of free carboxylic acid side groups.

The products (Scheme 3.22) were isolated as completely water-soluble solids by a series of steps which involved precipitation with an adequate non-solvent, washing for the removal of excess amines, dialysis in Spectra/Por 4®, and freeze-drying. As can be seen in Table 3.16, the yields were in the range of 52.7- 67.1%, with inherent viscosity ranging from 11.6 to 15.2 mL/g. As a general trend the yields of the homoconjugates were higher than those of the corresponding co-conjugates. The same trend was observed with the inherent viscosities (Table 3.17) except for conjugate **27**-**Fc** and co-conjugate **27**-**Fc**/**Pt**. These findings suggested that during the platination reaction some hydrolysis of the polymer backbone took place and the lower molecular molecular-weight chains were eliminated during the dialysis process. Drug contents, in percentage by mass, were determined by inductively coupled plasma-atomic emission spectroscopy (ICP-AES)

used exclusively for iron, with the multi-standard solution calibrated at 0.5 ppm in water. The determination of the ferrocene-based drug was determined at two different stages; before and after the addition of the second drug. As a general trend, the ferrocene content was almost the same for both homo- and co-conjugates. This indicated the effectiveness of the method and suggested very little or negligeable hydrolysis of the ferrocene-drug during the platination process. As can be seen in Table 3.17, the ferrocene contents for conjugates **24**-**Fc** to **28**-**Fc** were in the range between 1.98 and 2.41% which correspond to the ferrocene incorporations ranging between 93.8 and 96.2%. The highest incorporation was noticed with conjugate **24**-**Fc**, while the lowest incorporation was observed with conjugate **28**-**Fc**.

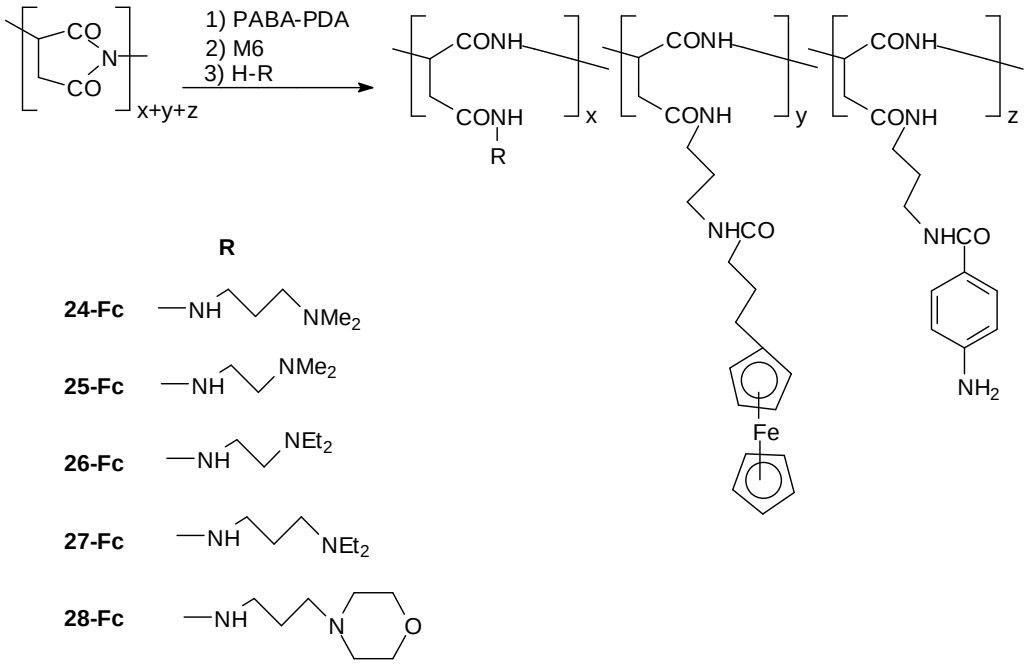

Scheme 3.22: Synthesis of conjugates **24-Fc** – **28-Fc**.

Table 3.16: Preparative data for conjugates **24-Fc** – **28-Fc** and co-conjugates **24-Fc/Pt** – **28-Fc/Pt**.

Designation	Molar Ratios [a, b]										Reaction time & Temperature [c]			Yield (%)	x:y:z [d]
	PSI	Conj.-Fc	M6	M1	DMP	DMEA	DEEA	DEP	APM	DACH-Pt-Cl_2	1st Step	2nd Step	3rd Step		
24-Fc	1.0	-	0.10	0.10	1.15	-	-	-	-	-	1d, RT	2d, 0-5°C	1d, RT	67.1	80:10:10
25-Fc	1.0	-	0.10	0.10	-	1.15	-	-	-	-	1d, RT	2d, 0-5°C	1d, RT	61.4	80:10:10
26-Fc	1.0	-	0.10	0.10	-	-	1.15	-	-	-	1d, RT	2d, 0-5°C	1d, RT	52.7	80:10:10
27-Fc	1.0	-	0.10	0.10	-	-	-	1.15	-	-	1d, RT	2d, 0-5°C	1d, RT	58.3	80:10:10
28-Fc	1.0	-	0.10	0.10	-	-	-	-	1.15	-	1d, RT	2d, 0-5°C	1d, RT	62.4	80:10:10
24-Fc/Pt	-	1.0	-	-	-	-	-	-	-	1.1	3d, RT	1d, 65°C	-	51.2	80:10:10
25-Fc/Pt	-	1.0	-	-	-	-	-	-	-	1.1	3d, RT	1d, 65°C	-	46.3	80:10:10
26-Fc/Pt	-	1.0	-	-	-	-	-	-	-	1.1	3d, RT	1d, 65°C	-	49.5	80:10:10
27-Fc/Pt	-	1.0	-	-	-	-	-	-	-	1.1	3d, RT	1d, 65°C	-	52.6	80:10:10
28-Fc/Pt	-	1.0	-	-	-	-	-	-	-	1.1	3d, RT	1d, 65°C	-	52.6	80:10:10

[a] Base molar for **PSI** or **Conj.-Fc**

[b] PSI: Polysuccinimide; Conj.-Fc: Ferrocene conjugate; M1: p-aminobenzamidopropylamine; DMP: 3-(dimethylamino)propylamine; DMEA: 2-(dimethylamino)ethylamine; DEEA: 2-(diethylamino)ethylamine; DEP: 3-(diethylamino)propylamine; APM: 4-(3-aminopropyl)-morpholine.

[c] RT: room temperature.

[d] x:y:z Ratio of solubilizing moiety to ferrocene-drug binding moiety to platinum-drug binding moiety.

Table 3.17: Analytical data for conjugates **24-Fc** to **28-Fc** and co-conjugates **24-Fc/Pt** to **28-Fc/Pt**.

Designation	Base molar mass [a]	η_{inh} [b] ($mL.g^{-1}$)	x : y : z [c]	Fe (%)		Pt (%)	
				Found [d]	Calcd. [e]	Found [f]	Calcd. [g]
24-Fc	2309.36	15.2	80 : 10 : 10	2.32	2.41	-	-
25-Fc	2197.16	12.6	80 : 10 : 10	2.41	2.54	-	-
26-Fc	2421.57	13.5	80 : 10 : 10	2.18	2.30	-	-
27-Fc	2533.78	12.4	80 : 10 : 10	2.07	2.20	-	-
28-Fc	2645.65	11.6	80 : 10 : 10	1.98	2.11	-	-
24-Fc/Pt	2654.06	10.6	80 : 10 : 10	1.97	2.10	6.93	7.35
25-Fc/Pt	2541.84	12.1	80 : 10 : 10	2.04	2.19	7.24	7.67
26-Fc/Pt	2766.27	11.2	80 : 10 : 10	1.86	2.02	6.81	7.05
27-Fc/Pt	2878.48	13.2	80 : 10 : 10	1.70	1.94	6.46	6.78
28-Fc/Pt	2990.53	9.8	80 : 10 : 10	1.68	1.86	6.19	6.52

[a] Molecular mass of the simple recurring unit; structures normalized to y = 1 and z = 1
[b] At $30.0^{o}C \pm 0.5^{o}C$ in distilled water; conc = 2 $mg.mL^{-1}$
[c] Ratio of solubilizing moiety to ferrocene-drug binding moiety to platinum-drug binding moiety.
[d] Fe content (%) obtained by ICP-AES
[e] Fe content (%) for complete incorporation of the drug.
[f] Pt content (%) obtained by atomic absorption analysis
[g] Pt content (%) for complete incorporation of the drug

The ferrocene conjugates **24-Fc** to **28-Fc** were co-conjugated to DACH-$PtCl_2$ (Scheme 3.23). The same procedure was followed as that used for the preparation of conjugates **1-Pt** to **5-Pt**. The water-soluble solid co-conjugates were obtained in yields of 46.3-52.6%, with inherent viscosity ranging from 9.8 to 13.2 $mL.g^{-1}$. As can be seen in Tables 3.16 and 3.17, these yields and inherent viscosities were lower when compared to those of the corresponding conjugates. This decrease suggested the probability of hydrolysis of the polymer backbone during the platination reaction and the removal of lower molecular-weight polymers during the dialysis process. Table 3.17 also revealed that the ferrocene contents for co-conjugates **24-Fc/Pt** to **28-Fc/Pt** were in the range between 1.68 and 2.04% which correspond to the ferrocene incorporations ranging between 87.6 and 96.6%. The highest incorporation was observed with co-conjugate **25-Fc/Pt**, while the lowest incorporation was observed with co-conjugate **27-Fc/Pt**. These results show that there was no major loss of ferrocene, found to be between 2 and 6%, during the co-conjugation process. The platinum contents of this group of co-conjugates were in the range between 6.19 and 7.24% which corresponds to the platinum incorporations ranging between 94.0 and 95.2%; except for co-conjugate **26-Fc/Pt** for which it was 88.7%. The highest incorporation was observed for co-conjugate **27-Fc/Pt**.

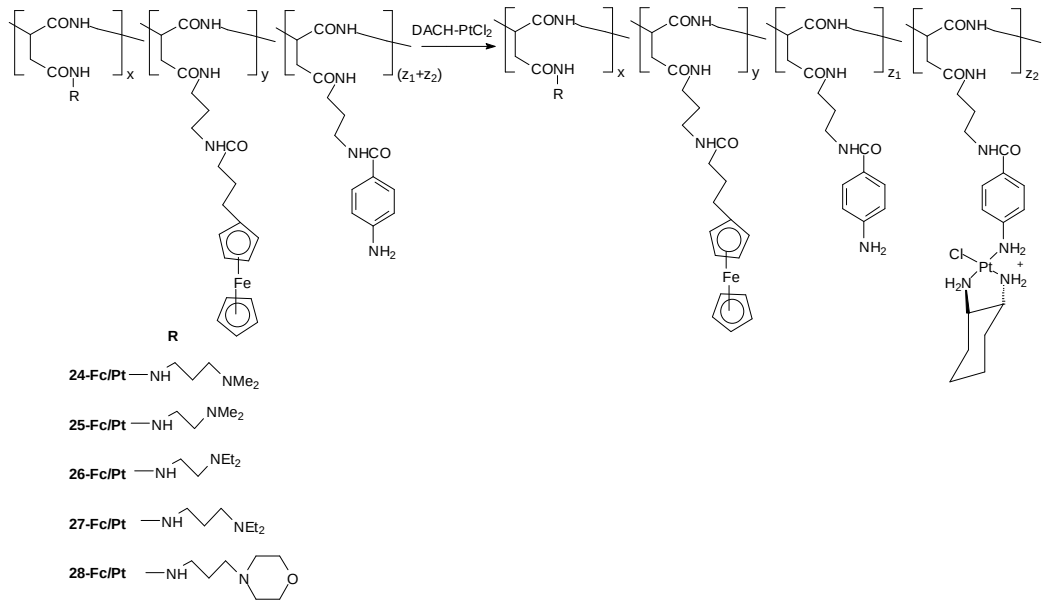

Scheme 3.23: Synthesis of co-conjugates **24-Fc/Pt** to **28-Fc/Pt**.

3.3.3 Co-conjugates coordinated to carboxylatohydroxylato-platinum and ferrocene

The reactions leading to this class of co-conjugates were carried out at RT. As for the ferrocene conjugates **24-Fc** to **28-Fc** (Section 3.3.2), strict anhydrous conditions were observed for the three first steps leading to the ferrocene conjugates **29-Fc**, **30-Fc**, **31-Fc**, **32-Fc** and **33-Fc** in the presence of PASA-PDA (**M4**) (Scheme 3.24), and **34-Fc**, **35-Fc**, **36-Fc**, **37-Fc** and **38-Fc** (Scheme 3.25) in the presence of PASA-EDA (**M3**) in order to avoid any unwanted hydrolytic ring opening. In the first step, a given amount of PASA-PDA or PASA-EDA was added to a stirred solution of PSI in the presence of TEA and allowed to react for 1d. In the second step, Fc–PDA was added and stirred at RT for another 2d. In the third step, the solubilizing group was added in excess and the preparation continued for another 2d. The excess solubilizing moiety was vital for a complete amidation of the PSI. The work-up was similar to that described in section 3.3.2. The products were isolated as completely water-soluble solids in yields ranging between 49.8 and 63.4%, with inherent viscosity in the range of 9.6 – 14.3 $mL.g^{-1}$. As can be

seen in Tables 3.18 and 3.19, as a general trend the yields of conjugates **29**-**Fc** to **38**-**Fc** were higher than those of the corresponding co-conjugates. These findings suggest a probability of hydrolysis of the polymer backbone during the platination reaction and the lower molecular-weight chains were removed during the dialysis process. From Tables 3.20 and 3.21, the ferrocene contents for conjugates **29**-**Fc** to **38**-**Fc** were in the range between 1.89 and 2.32% which corresponded to the ferrocene incorporations ranging between 91.4 and 94.7%. The highest incorporation was observed with conjugate **30**-**Fc**, while the lowest was with conjugate **29**-**Fc**.

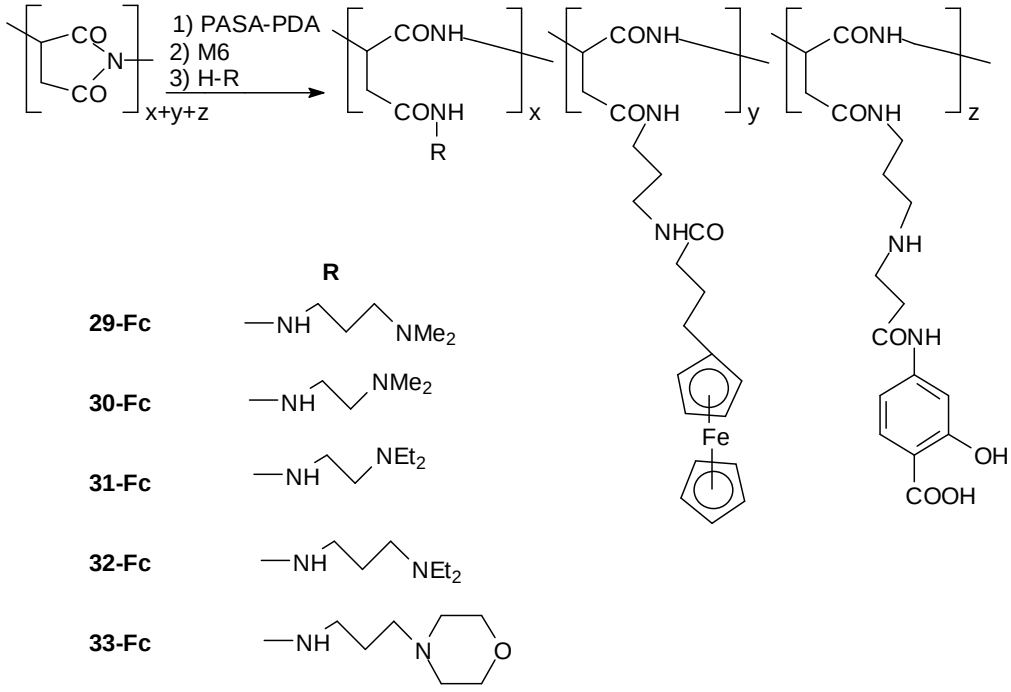

Scheme 3.24: Synthesis of conjugates **29-Fc** to **33-Fc**.

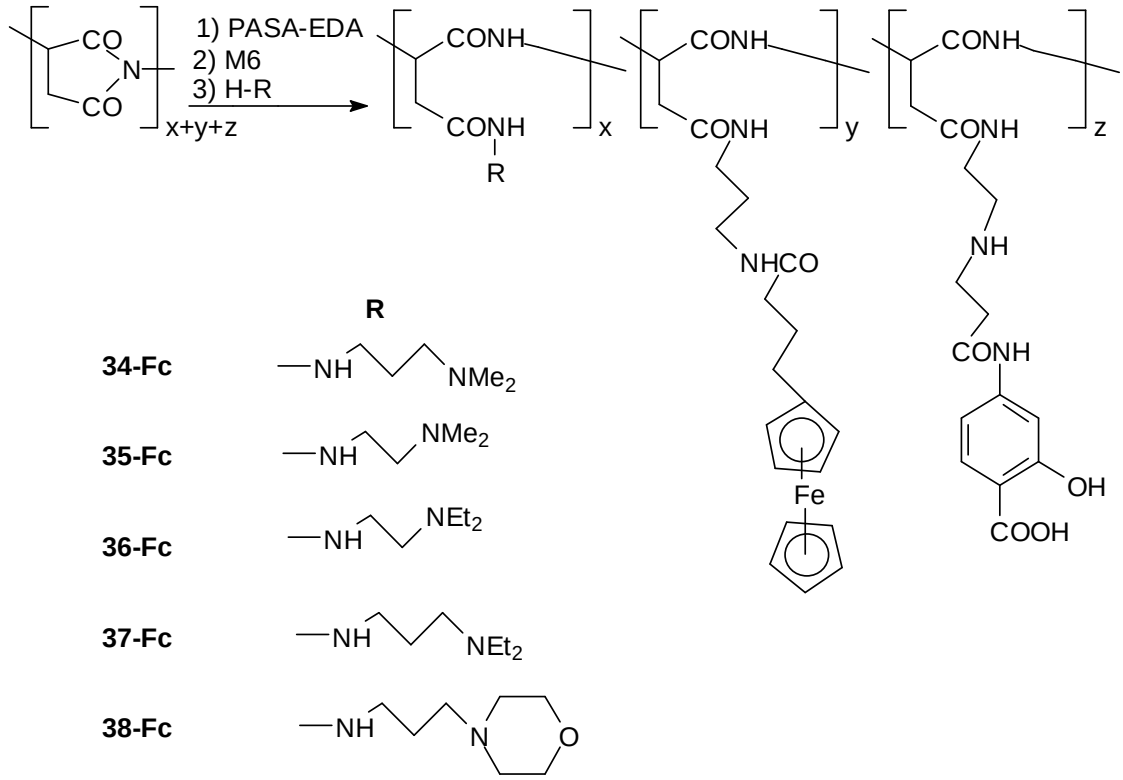

Scheme 3.25: Synthesis of conjugates **34-Fc** to **38-Fc**.

Table 3.18: Preparative data for conjugates **29-Fc** to **33-Fc** and co-conjugates **29-Fc/Pt** to **33-Fc/Pt**.

Designation	Molar Ratios [a, b]										Reaction time & Temperature [c]			Yield (%)	x:y:z [d]
	PSI	Conj.-Fc	M6	M4	DMP	DMEA	DEEA	DEP	APM	DACH-Pt	1st Step	2nd Step	3rd Step		
29-Fc	1.0	-	0.10	0.10	1.15	-	-	-	-	-	1d, RT	2d, RT	2d, RT	56.3	80:10:10
30-Fc	1.0	-	0.10	0.10	-	1.15	-	-	-	-	1d, RT	2d, RT	2d, RT	49.8	80:10:10
31-Fc	1.0	-	0.10	0.10	-	-	1.15	-	-	-	1d, RT	2d, RT	2d, RT	59.5	80:10:10
32-Fc	1.0	-	0.10	0.10	-	-	-	1.15	-	-	1d, RT	2d, RT	2d, RT	54.3	80:10:10
33-Fc	1.0	-	0.10	0.10	-	-	-	-	1.15	-	1d, RT	2d, RT	2d, RT	63.4	80:10:10
29-Fc/Pt	-	1.0	-	-	-	-	-	-	-	1.1	3d, RT	1d, 55°C	-	42.3	80:10:10
30-Fc/Pt	-	1.0	-	-	-	-	-	-	-	1.1	3d, RT	1d, 55°C	-	45.7	80:10:10
31-Fc/Pt	-	1.0	-	-	-	-	-	-	-	1.1	3d, RT	1d, 55°C	-	55.1	80:10:10
32-Fc/Pt	-	1.0	-	-	-	-	-	-	-	1.1	3d, RT	1d, 55°C	-	51.6	80:10:10
33-Fc/Pt	-	1.0	-	-	-	-	-	-	-	1.1	3d, RT	1d, 55°C	-	43.8	80:10:10

[a] Base molar for **PSI** or **Conj.-Fc**

[b] PSI: Polysuccinimide; Conj.-Fc: Ferrocene conjugate; M6: 4-Ferrocenenylbutamidopropylamine; M4: PASA-EDA; DMP: 3-(dimethylamino)propylamine; DMEA: 2-(dimethylamino)ethylamine; DEEA: 2-(diethylamino)ethylamine; DEP: 3-(diethylamino)propylamine; APM: 4-(3-aminopropyl)-morpholine.

[c] RT: room temperature.

[d] x:y:z Ratio of solubilizing moiety to ferrocene-drug binding moiety to platinum-drug binding moiety.

Table 3.19: Preparative data for conjugates **34-Fc** to **38-Fc** and co-conjugates **34-Fc/Pt** to **38-Fc/Pt**.

Designation	Molar Ratios [a, b]										Reaction time & Temperature [c]			Yield (%)	x:y:z [d]
	PSI	Conj.-Fc	M6	M3	DMP	DMEA	DEEA	DEP	APM	DACH-Pt	1st Step	2nd Step	3rd Step		
34-Fc	1.0	-	0.10	0.10	1.15	-	-	-	-	-	1d, RT	2d, RT	2d, RT	60.1	80:10:10
35-Fc	1.0	-	0.10	0.10	-	1.15	-	-	-	-	1d, RT	2d, RT	2d, RT	56.7	80:10:10
36-Fc	1.0	-	0.10	0.10	-	-	1.15	-	-	-	1d, RT	2d, RT	2d, RT	52.4	80:10:10
37-Fc	1.0	-	0.10	0.10	-	-	-	1.15	-	-	1d, RT	2d, RT	2d, RT	58.2	80:10:10
38-Fc	1.0	-	0.10	0.10	-	-	-	-	1.15	-	1d, RT	2d, RT	2d, RT	61.7	80:10:10
34-Fc/Pt	-	1.0	-	-	-	-	-	-	-	1.1	3d, RT	1d, 55°C	-	49.6	80:10:10
35-Fc/Pt	-	1.0	-	-	-	-	-	-	-	1.1	3d, RT	1d, 55°C	-	39.8	80:10:10
36-Fc/Pt	-	1.0	-	-	-	-	-	-	-	1.1	3d, RT	1d, 55°C	-	48.4	80:10:10
37-Fc/Pt	-	1.0	-	-	-	-	-	-	-	1.1	3d, RT	1d, 55°C	-	51.2	80:10:10
38-Fc/Pt	-	1.0	-	-	-	-	-	-	-	1.1	3d, RT	1d, 55°C	-	52.7	80:10:10

[a] Base molar for **PSI** or **Conj.-Fc**

[b] PSI: Polysuccinimide; Conj.-Fc: Ferrocene conjugate; M6: 4-Ferrocenenylbutamidopropylamine; M3: PASA-PDA; DMP: 3-(dimethylamino)propylamine; DMEA: 2-(dimethylamino)ethylamine; DEEA: 2-(diethylamino)ethylamine; DEP: 3-(diethylamino)propylamine; APM: 4-(3-aminopropyl)-morpholine.

[c] RT: room temperature

[d] x:y:z Ratio of solubilizing moiety to ferrocene-drug binding moiety to platinum-drug binding moiety.

Table 3.20: Analytical data for conjugates **29-Fc** to **33-Fc** and co-conjugates **29-Fc/Pt** to **33-Fc/Pt**.

Designation	Base molar mass [a]	η_{inh} [b] ($mL.g^{-1}$)	x : y : z [c]	Fe (%)		Pt (%)	
				Found [d]	Calcd. [e]	Found [f]	Calcld. [g]
29-Fc	2383.40	14.3	80 : 10 : 10	2.14	2.34	-	-
30-Fc	2271.19	12.3	80 : 10 : 10	2.32	2.45	-	-
31-Fc	2495.61	13.8	80 : 10 : 10	2.06	2.23	-	-
32-Fc	2607.81	10.7	80 : 10 : 10	2.02	2.14	-	-
33-Fc	2719.69	13.1	80 : 10 : 10	1.89	2.05	-	-
29-Fc/Pt	2692.70	13.2	80 : 10 : 10	1.72	2.07	6.96	7.24
30-Fc/Pt	2580.50	12.4	80 : 10 : 10	2.01	2.16	6.88	7.26
31-Fc/Pt	2804.90	12.1	80 : 10 : 10	1.70	1.99	6.63	6.95
32-Fc/Pt	2917.11	10.6	80 : 10 : 10	1.74	1.91	6.27	6.68
33-Fc/Pt	3029.0	11.7	80 : 10 : 10	1.65	1.84	6.02	6.44

[a] Molecular mass of the simple recurring unit; structures normalized to y = 1 and z = 1.
[b] At 30.0°C ± 0.5°C in distilled water; conc = 2 $mg.mL^{-1}$.
[c] Ratio of solubilizing moiety to ferrocene-drug binding moiety to platinum-drug binding moiety.
[d] Fe content (%) obtained by ICP-AES.
[e] Fe content (%) for complete incorporation of the drug.
[f] Pt content (%) obtained by atomic absorption analysis.
[g] Pt content (%) for complete incorporation of the drug.

Table 3.21: Analytical data for conjugates **34-Fc** to **38-Fc** and co-conjugates **34-Fc/Pt** to **38-Fc/Pt**.

Designation	Base molar mass [a]	η_{inh} [b] ($mL.g^{-1}$)	x : y : z [c]	Fe (%)		Pt (%)	
				Found [d]	Calcd. [e]	Found [f]	Calcld. [g]
34-Fc	2397.42	12.4	80 : 10 : 10	2.19	2.33	-	-
35-Fc	2285.22	11.3	80 : 10 : 10	2.30	2.44	-	-
36-Fc	2509.63	9.6	80 : 10 : 10	2.07	2.22	-	-
37-Fc	2621.84	12.1	80 : 10 : 10	2.01	2.13	-	-
38-Fc	2733.71	13.6	80 : 10 : 10	1.93	2.04	-	-
34-Fc/Pt	2706.72	12.8	80 : 10 : 10	1.54	1.87	6.92	7.20
35-Fc/Pt	2594.51	9.2	80 : 10 : 10	1.71	1.96	7.18	7.52
36-Fc/Pt	2818.93	11.6	80 : 10 : 10	1.42	1.70	6.12	6.92
37-Fc/Pt	2931.14	13.1	80 : 10 : 10	1.53	1.74	5.87	6.65
38-Fc/Pt	3043.01	12.3	80 : 10 : 10	1.38	1.68	5.63	6.41

[a] Molecular mass of the simple recurring unit; structures normalized to y = 1 and z = 1
[b] At $30.0^{o}C \pm 0.5^{o}C$ in distilled water; conc = $2mg.mL^{-1}$
[c] Ratio of solubilizing moiety to ferrocene-drug binding moiety to platinum-drug binding moiety.
[d] Fe content (%) obtained by ICP-AES
[e] Fe content (%) for complete incorporation of the drug.
[f] Pt content (%) obtained by atomic absorption analysis
[g] Pt content (%) for complete incorporation of the drug.

Ferrocene conjugates **29-Fc** to **38-Fc** were co-conjugated to DACH-Pt (Schemes 3.26 and 3.27) following Model 3 in Figure 3.1. The same procedure used to prepare conjugates **8-Pt** to **17-Pt** (section 3.2.2) was followed. The products were isolated as completely water-soluble solids in yields ranging between 39.8 and 55.1%, with inherent viscosity in the range of 9.2 – 13.2 $mL.g^{-1}$. As can be seen in Tables 3.18 and 3.19, the yields were lower than those of the corresponding conjugates. This drop suggested the probability of hydrolysis of the polymer backbone during the platination reaction and the removal of lower molecular-weight polymers during the dialysis process. Tables 3.20 and 3.21 revealed that the ferrocene contents for co-conjugates **29**-**Fc**/**Pt** to **38**-**Fc**/**Pt** were in the range between 1.38 and 2.01% which corresponded to the ferrocene incorporations ranging between 82.1 and 93.0%. The highest incorporation was observed with co-conjugate **30**-**Fc**/**Pt**, while the lowest incorporation was observed with co-conjugate **38**-**Fc**/**Pt**. The platinum contents of this group of co-conjugates were in the range between 6.02 and 7.18% which corresponds to the platinum incorporations ranging between 87.5 and 96.1%. Co-conjugates **29**-**Fc**/**Pt** to **35**-**Fc**/**Pt** had the platinum incorporation of greater than 93%, while co-conjugates **26**-**Fc**/**Pt** to **38**-**Fc**/**Pt** were below 90% platinum incorporation.

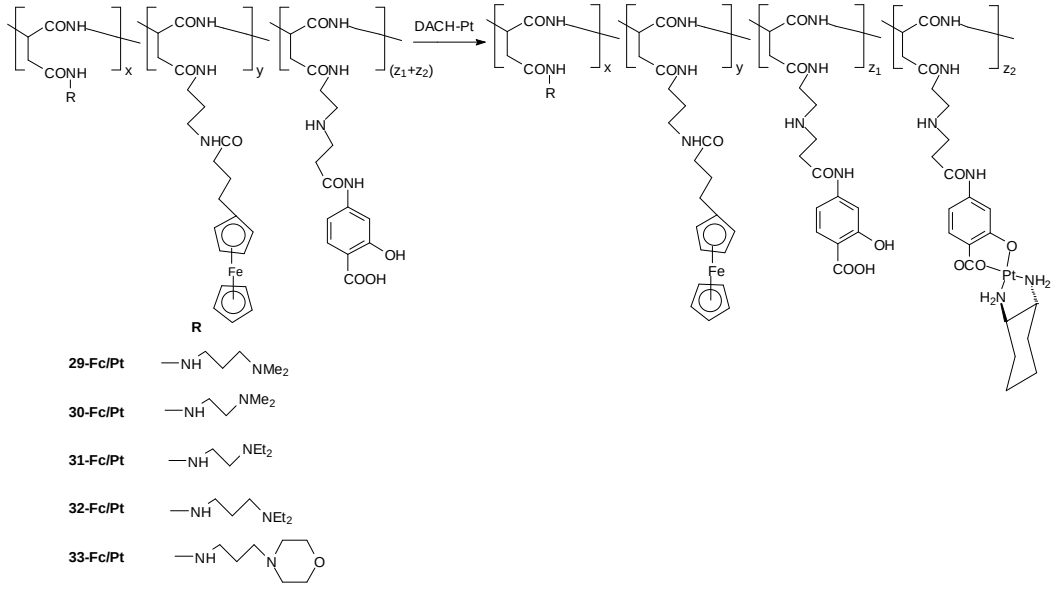

Scheme 3.26: Synthesis of co-conjugates **29-Fc/Pt** to **33-Fc/Pt**.

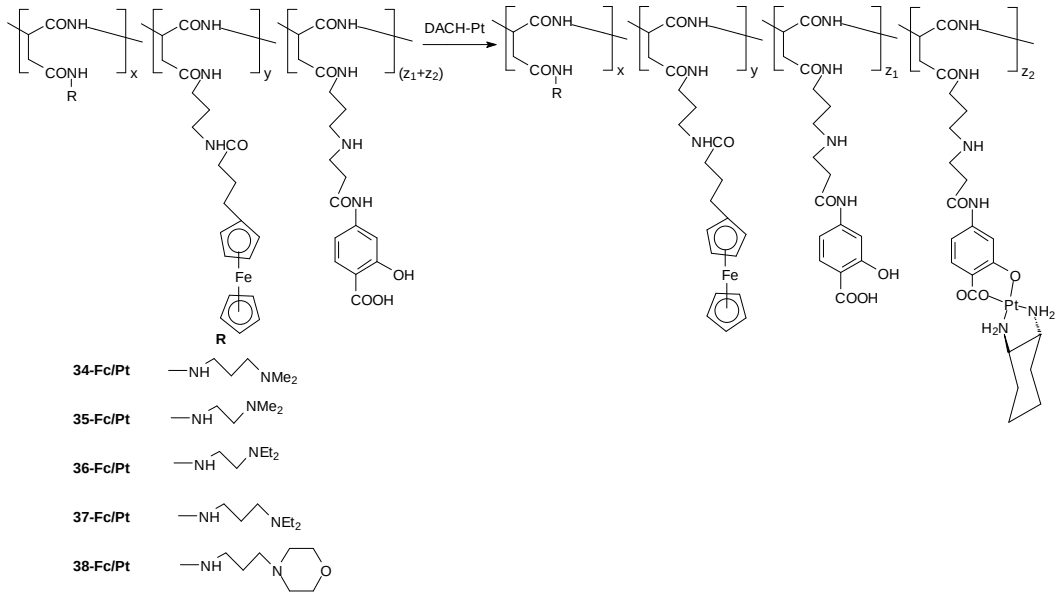

Scheme 3.27: Synthesis of co-conjugates **34-Fc/Pt** to **38-Fc/Pt**.

3.3.4 Co-conjugates coordinated to dihydroxylato-platinum and ferrocene

As described in section 3.3.2, this class of co-conjugates followed the same principle. The synthesis of the related ferrocene conjugates was followed by the synthesis of the corresponding co-conjugates. In the first step conjugates **39**-**Fc**, **40**-**Fc**, **41**-**Fc**, **42**-**Fc** and **43**-**Fc** were synthesized (Scheme 3.28). Three different amines were used. Dopamine was added first to PSI, then Fc-PDA and lastly the solubilizing group in an interval of 1d and 2d, respectively at RT. After the addition of all three amines, the reaction was allowed to continue for a further 2d. Depending on the type of solubilizing group used, ferrocene conjugates **39**-**Fc** to **43**-**Fc** were generated. The work-up process was as described in section 3.3.2. The products were isolated as completely water-soluble solids in yields ranging between 52.8 and 66.1%, with inherent viscosity in the range of 11.3 – 14.2 $mL.g^{-1}$. As can be seen in Table 3.22, as a general trend the yields of the homoconjugates were higher than those of the corresponding co-conjugates. The same trend was observed with the inherent viscosities (Table 3.23) except for conjugate **41**-**Fc** and co-conjugate **41**-**Fc**/**Pt**. These findings suggest probable hydrolysis during the platination reaction of the polymer backbone and the removal of the lower molecular-weight chains during the dialysis process. Table 3.23 shows that the ferrocene contents for conjugates **39**-**Fc** to **43**-**Fc** were in the range between 2.01 and 2.41% which correspond to the ferrocene incorporations ranging between 93.0 and 95.1%. The highest incorporation was noticed with conjugate **39**-**Fc**, while the lowest incorporation was observed with conjugate **40**-**Fc**.

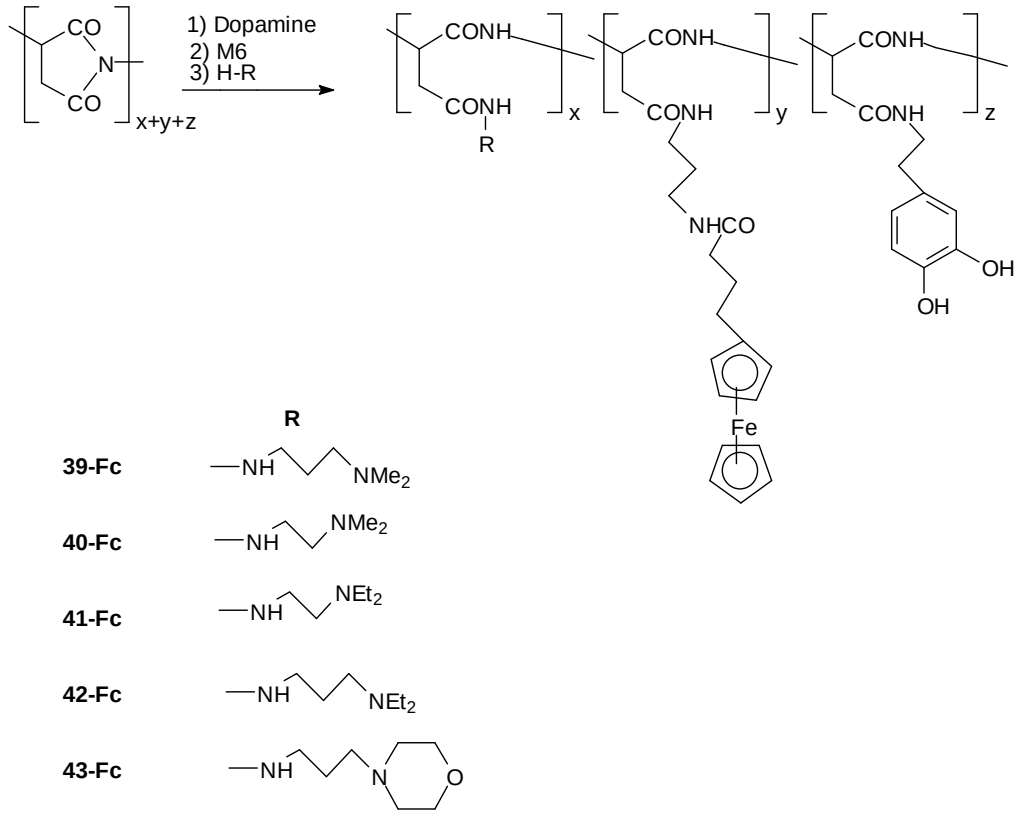

	R
39-Fc	—NH NMe_2
40-Fc	—NH NMe_2
41-Fc	—NH NEt_2
42-Fc	—NH NEt_2
43-Fc	—NH N O

Scheme 3.28: Synthesis of conjugates **39-Fc** – **43-Fc**.

Table 3.22: Preparative data for conjugates **39-Fc** to **43-Fc** and co-conjugates **39-Fc/Pt** to **43-Fc/Pt**.

Designation	Molar Ratios [a, b]										Reaction time & Temperature [c]			Yield (%)	x:y:z [d]
	PSI	Conj.-Fc	M6	Dopamine	DMP	DMEA	DEEA	DEP	APM	DACH-Pt	1st Step	2nd Step	3rd Step		
39-Fc	1.0	-	0.10	0.115	1.15	-	-	-	-	-	1d, RT	2d, RT	2d, RT	66.1	80:10:10
40-Fc	1.0	-	0.10	0.115	-	1.15	-	-	-	-	1d, RT	2d, RT	2d, RT	58.7	80:10:10
41-Fc	1.0	-	0.10	0.115	-	-	1.15	-	-	-	1d, RT	2d, RT	2d, RT	53.6	80:10:10
42-Fc	1.0	-	0.10	0.115	-	-	-	1.15	-	-	1d, RT	2d, RT	2d, RT	55.3	80:10:10
43-Fc	1.0	-	0.10	0.115	-	-	-	-	1.15	-	1d, RT	2d, RT	2d, RT	52.8	80:10:10
39-Fc/Pt	-	1.0	-	-	-	-	-	-	-	1.1	3d, RT	1d, 55°C	-	47.2	80:10:10
40-Fc/Pt	-	1.0	-	-	-	-	-	-	-	1.1	3d, RT	1d, 55°C	-	44.3	80:10:10
41-Fc/Pt	-	1.0	-	-	-	-	-	-	-	1.1	3d, RT	1d, 55°C	-	52.1	80:10:10
42-Fc/Pt	-	1.0	-	-	-	-	-	-	-	1.1	3d, RT	1d, 55°C	-	49.3	80:10:10
43-Fc/Pt	-	1.0	-	-	-	-	-	-	-	1.1	3d, RT	1d, 55°C	-	46.2	80:10:10

[a] Base molar for **PSI** or **Conj.-Fc**

[b] PSI: Polysuccinimide; Conj.-Fc: Ferrocene conjugate; M6: 4-Ferrocenenylbutamidopropylamine; DMP: 3-(dimethylamino)propylamine; DMEA: 2-(dimethylamino)ethylamine; DEEA: 2-(diethylamino)ethylamine; DEP: 3-(diethylamino)propylamine; APM: 4-(3-aminopropyl)-morpholine.

[c] RT: room temperature.

[d] x:y:z Ratio of solubilizing moiety to ferrocene-drug binding moiety to platinum-drug binding moiety.

Table 3.23: Analytical data for conjugates **39-Fc** to **43-Fc** and co-conjugates **39-Fc/Pt** to **43-Fc/Pt**.

Designation	Base molar mass [a]	η_{inh} [b] $mL.g^{-1}$	x : y : z [c]	Fe (%)		Pt (%)	
				Found [d]	Calcd. [e]	Found [f]	Calcd. [g]
39-Fc	2269.30	11.3	80 : 10 : 10	2.34	2.46	-	-
40-Fc	2157.09	11.7	80 : 10 : 10	2.41	2.59	-	-
41-Fc	2381.51	12.5	80 : 10 : 10	2.19	2.34	-	-
42-Fc	2493.71	14.2	80 : 10 : 10	2.13	2.24	-	-
43-Fc	2605.59	12.4	80 : 10 : 10	2.01	2.14	-	-
39-Fc/Pt	2578.60	10.2	80 : 10 : 10	2.01	2.16	7.03	7.56
40-Fc/Pt	2466.40	8.6	80 : 10 : 10	2.04	2.26	7.38	7.91
41-Fc/Pt	2690.80	13.4	80 : 10 : 10	1.88	2.07	6.82	7.25
42-Fc/Pt	2803.01	11.8	80 : 10 : 10	1.80	1.99	6.41	6.96
43-Fc/Pt	2914.88	10.2	80 : 10 : 10	1.82	1.91	6.17	6.69

[a] Molecular mass of the simple recurring unit; structures normalized to y = 1 and z = 1
[b] At $30.0^{o}C \pm 0.5^{o}C$ in distilled water; conc = $2mg.mL^{-1}$
[c] Ratio of solubilizing moiety to ferrocene-drug binding moiety to platinum-drug binding moiety.
[d] Fe content (%) obtained by ICP-AES
[e] Fe content (%) for complete incorporation of the drug.
[f] Pt content (%) obtained by atomic absorption analysis
[g] Pt content (%) for complete incorporation of the drug.

Ferrocene conjugates **39**-**Fc** to **43**-**Fc** were used for the preparation of co-conjugates **39**-**Fc/Pt**, **40**-**Fc/Pt**, **41**-**Fc/Pt**, **42**-**Fc/Pt** and **43**-**Fc/Pt** according to Scheme 3.28. DACH-Pt was used as the platination agent following Model 4 (Figure 3.1) while using the same procedure as for preparation of conjugates **8**-**Pt** to **17**-**Pt** (section 3.2.2). The work-up was as described in section 3.3.2. The water-soluble solid co-conjugates were obtained in yields of 44.3-52.1%, with inherent viscosity ranging from 9.8 to 13.2 $mL.g^{-1}$. As can be seen in Tables 3.22 and 3.23, these yields and inherent viscosities were lower when compared to those of the corresponding conjugates. This drop suggested the probability of hydrolysis of the polymer backbone during the platination reaction and that the lower molecular-weight polymers were removed during the dialysis process. Table 3.23 also revealed that the ferrocene contents for co-conjugates **39**-**Fc**/**Pt** to **43**-**Fc**/**Pt** were in the range between 1.80 and 2.04% which corresponded to the ferrocene incorporations ranging between 90.2 and 95.2%. The highest incorporation was observed with co-conjugate **43**-**Fc**/**Pt**, while the lowest with co-conjugate **40**-**Fc**/**Pt**. These results show that there was no major loss of ferrocene, found to be between 1 and 5%, during the co-conjugation process. The platinum contents of this group of co-conjugates were in the range between 6.17 and 7.38% which corresponded to the platinum incorporations ranging between 92.0 and 94.0%. The highest incorporation was observed with co-conjugate **41**-**Fc**/**Pt** and the lowest with co-conjugate **42**-**Fc**/**Pt**.

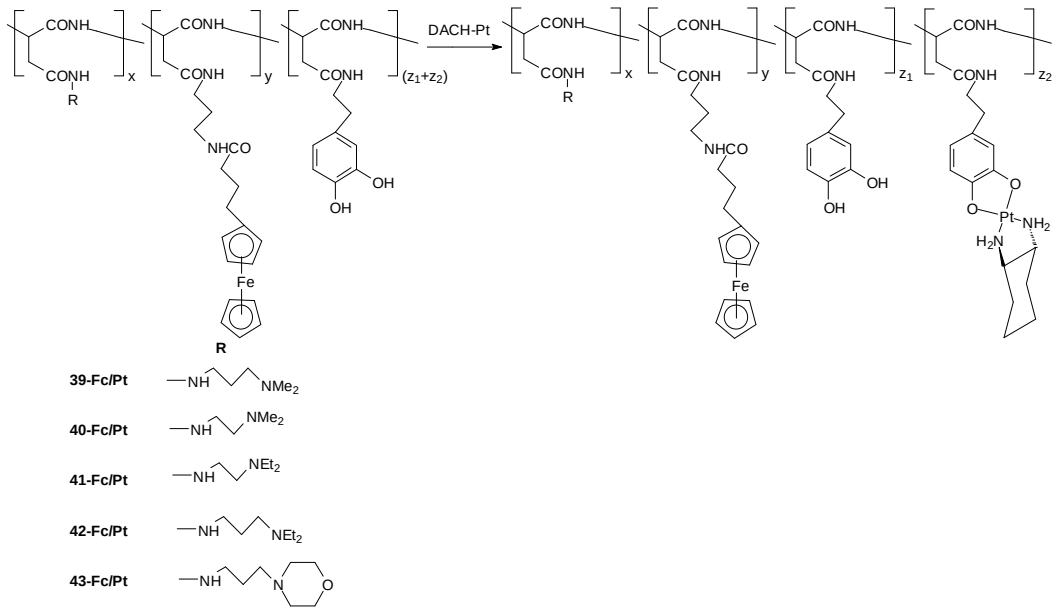

Scheme 3.29: Synthesis of co-conjugates **39-Fc/Pt** to **43-Fc/Pt**.

3.3.5 Co-conjugates coordinated to dicarboxylato-platinum and ferrocene

This class of co-conjugates required the synthesis of a special monomer, namely *N*-(4,8-diaza-octanoyl)aspartic acid (ACRYASP-PDA), for platinum chelation.

3.3.5.1 Synthesis of N-*(4,8-diaza-octanoyl)aspartic acid*

The preparation of *N*-(4,8-diaza-octanoyl)aspartic acid (ACRYASP-PDA or **M8**) was a two step reaction under experimental conditions similar to previous research performed in the WITS PRG laboratory. The same procedure as described for macromonomer *p-N*-(4,8-diazaheptanoyl)-salicylic acid (PASA-PDA) was used (section 3.1.5.1). In the first step, the reaction involved the synthesis of acryloylaspartic acid monomer (**M7**) in the presence of acryloyl chloride under very mild conditions (Scheme 3.30).

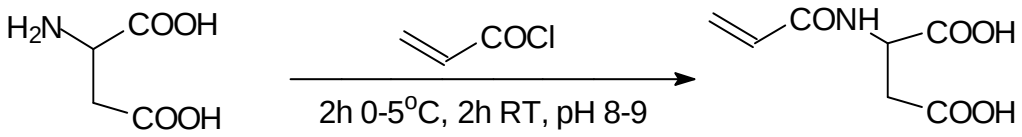

Scheme 3.30: Synthesis of acryloylaspartic acid (**M7**).

In the second step, the isolated product from the first step, namely acryloylaspartic acid, was reacted with an excess of the diamine (PDA) by the Michael addition reaction across the active double bond at 60°C (Scheme 3.31). The final product was isolated after removing the free amine with boiling toluene and acetone, followed by re-crystallization from MeOH at pH 3 – 4. Several crops were combined for a total yield of 72.4%. Identical products from different runs were mixed in the batch. The experimental conditions and ^{1}H NMR data are summarized in Tables 3.25 and 3.26, respectively.

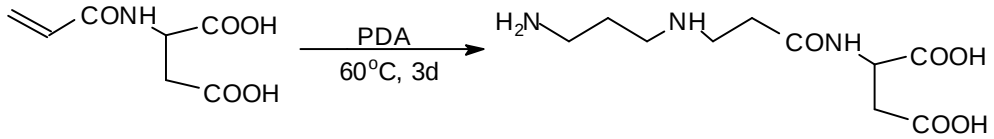

Scheme 3.31: Synthesis of ACRYASP-PDA (**M8**).

Table 3.25: Summary of experimental data for **M6** and **M7**.

Designation	Molar ratio [a, b]				Experimental Conditions [c]	Yield (%)
	Aspartic acid	Acryloyl Chloride	M7	PDA		
M7	1.0	1.2	-	-	2h, 0-5°C; 2h,RT	78.0
M8	-	-	1.0	1.2	3d, 60°C	72.4

[a] Base molar for aspartic acid or **M7**

[b] PDA: 1,3-diaminopropane

[c] RT: room temperature

Table 3.26: ^{1}H NMR analysis of **M7** and **M8**.

Polymer Designation	Assignment	^{1}H NMR [a, b]		
		Shift range δ (ppm)	Proton count	
			Found	Expected
M7	**CH_2** (Asp)	2.4 – 2.2	2	2
	CH (Asp)	4.2 – 4.1	1	1
	HCHCHCONH	5.5 – 5.4	0.9	1
	H**CHCH**CONH	6.1 – 5.8	1.9	2
M8	NH_2CH_2**CH_2**CH_2NH	2.0 – 1.7	2.3	2
	NH_2**CH_2**CH_2**CH_2**NH**CH_2**; **CH_2** (Asp); **CH_2**CONH	3.2 – 2.4	10.4	10
	CH (Asp)	4.5 – 4.3	1	1

[a] In D_2O, pD 10 – 11. Chemical shifts, δ (ppm), referenced against internal sodium 3-(trimethylsilyl)-2,2,3,3-d_4-propionate;

[b] Integration error limit ± 12%

3.3.5.2 Co-conjugates coordinated to dicarboxylato- Pt and ferrocene

The co-conjugates coordinated to dicarboxylato-platinum and ferrocene were synthesized from PSI in a two-step reaction. The first step involved the incorporation of ferrocene-PDA and ACRYASP-PDA in the PSI by aminolytic ring-opening, and the second step involved the platinum coupling (Scheme 3.32).

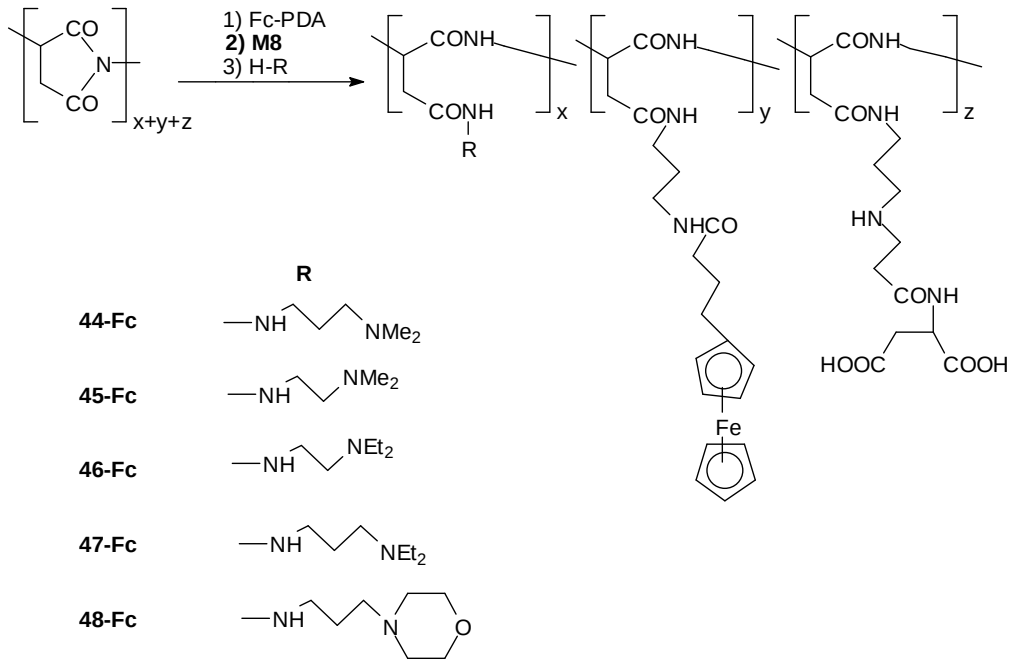

Scheme 3.32: Synthesis of conjugates **44-Fc** to **48-Fc**.

In the first step, three different amines were used in a pre-determined mole ratio to PSI (Scheme 3.32). Ferrocene-PDA was added first to a solution of PSI and allowed to react for 1d at RT, this was followed by the addition of ACRYASP-PDA, and the reaction mixture was stirred for 2d at RT before the addition of the last amine. This last amine was the solubilizing moiety and it was added in excess to achieve a complete ring opening of PSI. The work-up was as described in section 3.3.2. The ferrocene conjugates, **44**-**Fc**, **45**-**Fc**, **46**-**Fc**, **47**-**Fc** and **48**-**Fc** obtained were isolated as water-soluble solids in yields ranging from 54.3 to 70.3%, and inherent viscosities in the range of 10.3 and 12.3 $mL.g^{-1}$. As can be seen in Table 3.3.27, the yields of the homoconjugates were higher than those of the corresponding co-conjugates. Table 3.28 revealed that the ferrocene contents for conjugates **44**-**Fc** to **48**-**Fc** were in the range between 1.78 and 2.46% which corresponded to the ferrocene incorporations ranging between 89.8 and 92.8%. The highest incorporation was observed with conjugate **46**-**Fc**, while the lowest with conjugate **45**-**Fc**.

The ferrocene conjugates **44**-**Fc** to **48**-**Fc** were co-conjugated to DACH-Pt (Scheme 3.33). A similar procedure as used for conjugates **8**-**Pt** to **17**-**Pt** was followed (section 3.2.2). The work-up steps were essentially the same as described in section 3.3.2. The co-conjugates obtained were isolated as completely water-soluble products in yields of 42.1-56.3%, with inherent viscosity ranging from 9.7 to 12.6 $mL.g^{-1}$. As can be seen in Tables 3.28 these yields were lower than those of the corresponding conjugates. This drop suggested the probable hydrolysis of the polymer backbone during the platination reaction and the removal of the lower molecular-weight polymers during the dialysis process. Table 3.28 also revealed that the ferrocene contents for co-conjugates **44**-**Fc**/**Pt** to **48**-**Fc**/**Pt** were in the range between 1.84 and 2.17% which corresponded to the ferrocene incorporations ranging between 85.6 and 91.0%. The highest incorporation was noticed with co-conjugate **47**-**Fc**/**Pt**, while the lowest incorporation was observed with co-conjugate **44**-**Fc**/**Pt**. These results show that there was no major loss of ferrocene, found to be between 1.5 and 5.0%, during the co-conjugation process. The platinum contents of this group of co-conjugates were in the range between 5.33 and 7.03% which corresponded to the platinum incorporations ranging between 81.8 and 93.8%. The highest incorporation was observed with co-conjugate **44**-**Fc**/**Pt** and the lowest with co-conjugate **47**-**Fc**/**Pt**.

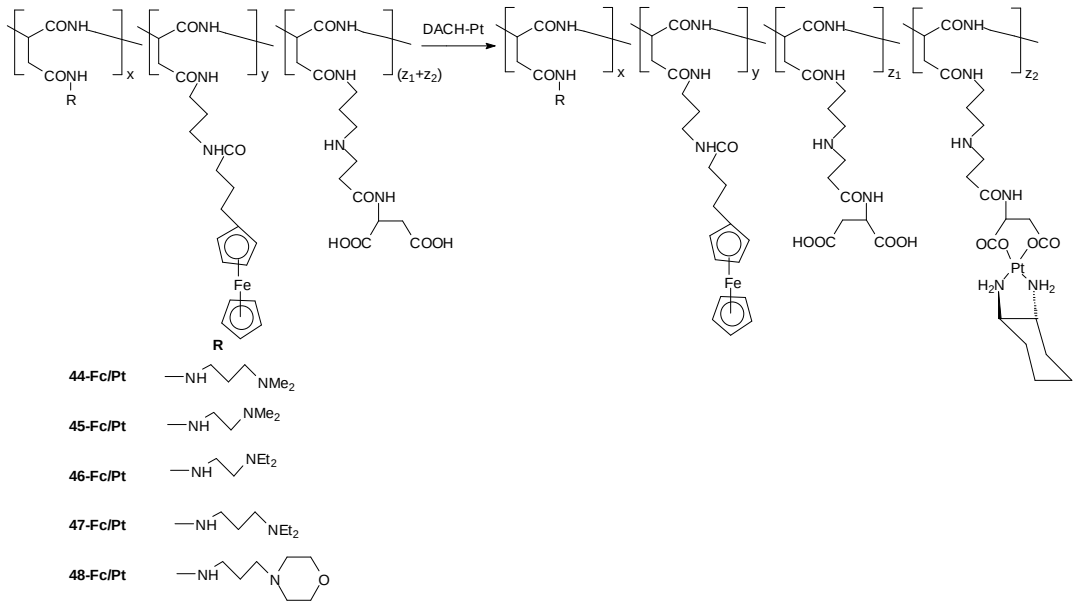

Scheme 3.33: Synthesis of co-conjugates **44-Fc/Pt** to **48-Fc/Pt**.

Table 3.27: Preparative data for conjugates **44-Fc** to **48-Fc** and co-conjugates **44-Fc/Pt** to **48-Fc/Pt**.

Designation	Molar Ratios [a, b]										Reaction time & Temperature [c]			Yield (%)	x:y:z [d]
	PSI	Conj.-Fc	M6	M8	DMP	DMEA	DEEA	DEP	APM	DACH-Pt	1st Step	2nd Step	3rd Step		
44-Fc	1.0	-	0.10	0.10	1.15	-	-	-	-	-	1d, RT	2d, RT	2d, RT	61.4	80:10:10
45-Fc	1.0	-	0.10	0.10	-	1.15	-	-	-	-	1d, RT	2d, RT	2d, RT	70.3	80:10:10
46-Fc	1.0	-	0.10	0.10	-	-	1.15	-	-	-	1d, RT	2d, RT	2d, RT	56.2	80:10:10
47-Fc	1.0	-	0.10	0.10	-	-	-	1.15	-	-	1d, RT	2d, RT	2d, RT	54.3	80:10:10
48-Fc	1.0	-	0.10	0.10	-	-	-	-	1.15	-	1d, RT	2d, RT	2d, RT	57.4	80:10:10
44-Fc/Pt	-	1.0	-	-	-	-	-	-	-	1.1	3d, RT	1d, 55°C	-	56.3	80:10:10
45-Fc/Pt	-	1.0	-	-	-	-	-	-	-	1.1	3d, RT	1d, 55°C	-	51.4	80:10:10
46-Fc/Pt	-	1.0	-	-	-	-	-	-	-	1.1	3d, RT	1d, 55°C	-	42.1	80:10:10
47-Fc/Pt	-	1.0	-	-	-	-	-	-	-	1.1	3d, RT	1d, 55°C	-	45.8	80:10:10
48-Fc/Pt	-	1.0	-	-	-	-	-	-	-	1.1	3d, RT	1d, 55°C	-	49.2	80:10:10

[a] Base molar for **PSI** or **Conj.-Fc**

[b] PSI: Polysuccinimide; Conj.-Fc: Ferrocene conjugate; M6: 4-Ferrocenenylbutamidopropylamine; M8: ACRYASP-PDA; DMP: 3-(dimethylamino)propylamine; DMEA: 2-(dimethylamino)ethylamine; DEEA: 2-(diethylamino)ethylamine; DEP: 3-(diethylamino)propylamine; APM: 4-(3-aminopropyl)-morpholine.

[c] RT: room temperature. [d] x:y:z Ratio of solubilizing moiety to ferrocene-drug binding moiety to platinum-drug binding moiety.

Table 3.28: Analytical data for conjugates **44-Fc** to **48-Fc** and co-conjugates **44-Fc/Pt** to **48-Fc/Pt**.

Designation	Base molar mass [a]	η_{inh} [b] ($mL.g^{-1}$)	x : y : z [c]	Fe (%)		Pt (%)	
				Found [d]	Calcd. [e]	Found [f]	Calcld. [g]
44-Fc	2377.40	10.3	80 : 10 : 10	2.13	2.35	-	-
45-Fc	2265.19	12.3	80 : 10 : 10	2.21	2.46	-	-
46-Fc	2489.60	10.6	80 : 10 : 10	2.08	2.24	-	-
47-Fc	2601.81	11.2	80 : 10 : 10	1.98	2.14	-	-
48-Fc	2713.68	10.6	80 : 10 : 10	1.87	2.06	-	-
44-Fc/Pt	2686.70	12.5	80 : 10 : 10	1.78	2.08	6.81	7.26
45-Fc/Pt	2574.48	9.7	80 : 10 : 10	1.90	2.17	7.03	7.57
46-Fc/Pt	2798.90	11.4	80 : 10 : 10	1.78	1.99	6.22	6.97
47-Fc/Pt	2911.11	12.6	80 : 10 : 10	1.74	1.91	5.48	6.70
48-Fc/Pt	3023.0	10.9	80 : 10 : 10	1.60	1.84	5.33	6.45

[a] Molecular mass of the simple recurring unit; structures normalized to y = 1 and z = 1.
[b] At $30.0^{o}C \pm 0.5^{o}C$ in distilled water; conc = 2 $mg.mL^{-1}$
[c] Ratio of solubilizing moiety to ferrocene-drug binding moiety to platinum-drug binding moiety.
[d] Fe content (%) obtained by ICP-AES.
[e] Fe content (%) for complete incorporation of the drug.
[f] Pt content (%) obtained by atomic absorption analysis.
[g] Pt content (%) for complete incorporation of the drug.

3.4 Cell culture testing

Selected compounds arising from this work were screened in *in vitro* studies in collaboration with Professor R. van Zyl from the Pharmacology Division in the Department of Pharmacy and Pharmacology, University of the Witwatersrand. The pro-drugs were tested for antineoplastic activity against the MCF-7 human breast cancer cell line in accordance with the previously published procedure[156,157]. Free cisplatin and ferrocene were also tested under the same conditions for comparison. With one cell line available at the time of the testing, the results presented in this section will only be estimative in terms of performance of the conjugates. Since the resistance factor is defined as the ratio of IC_{50}'s of two different cell lines, this will not be included in the discussion.

MCF-7 cells were cultured and maintained as a monolayer in Dulbecco's modified Eagle's medium (DMEM) supplemented with 10% of fetal calf serum and antibiotics (100 $IU.mL^{-1}$ of penicillin and 100 $\mu g.mL^{-1}$ of streptomycin). All cells were cultured at 37℃ in a 100% humidity atmosphere and 5% CO_2 and exponentially growing viable cells were plated at 100,000 $cells.mL^{-1}$ into 96-well plates. Stock solutions of compounds were initially dissolved in 50% (v/v) DMSO to sterilize the compounds and further diluted with culture medium. The growth inhibitory effects of the compounds were measured using a standard tetrazolium MTT assay [156]. After 24 h of incubation at 37^{o}C, 20 µL of MTT (5 $mg.mL^{-1}$) in PBS (pH 7.4) was added to each well. The plates were incubated at 37^{o}C for 2 h. At the end of the incubation period, the medium was replaced with 100 µL DMSO to terminate the reaction and dissolve the formazan crystals. The metabolised MTT product was quantified by reading the absorbance at 540 nm with a reference wavelength of 690 nm in a plate reader[158]. The % cell viability was calculated using the necessary controls and the concentration required to inhibit 50% of the cells (IC_{50} values) were determined from log

sigmoid dose response curves using GraphPad® Prism. All assays were performed in at least triplicate and averages and standard deviation (s.d.) calculated.

The results in Table 3.29 are given in terms of IC_{50}, the drug concentration required to kill 50% of the cells relative to drug-free control. The table also contains an entry for the activity factor (AF) defined as the ratio of IC_{50}[free drug] over IC_{50}[conjugate or co-conjugate]. In the calculation of the AF, the IC_{50} of cisplatin (free drug) was used for platinum conjugates and platinum/ferrocene co-conjugates, and IC_{50} of ferrocene (free drug) was used for ferrocene conjugates.

Table 3.29: Antiproliferative activity of conjugates and co-conjugates.

Designation	% Cell viability at 100 µg.mL^{-1}		IC_{50} value (µg.mL^{-1})		AF[a]
	AVE.	S.D.	AVE.	S.D.	
1-Pt	55.90	9.55	94.61	19.78	1.09
3-Pt	69.37	8.24	281.37	10.85	0.37
13-Pt	47.80	8.93	48.92	6.10	2.11
24-Fc	69.05	12.56	149.69	23.30	0.45
24-Fc/Pt	82.30	12.34	-	-	-
25-Fc	67.07	5.79	-	-	-
25-Fc/Pt	38.39	3.36	83.86	12.36	1.23
34-Fc	24.75	8.89	13.18	2.49	5.11
34-Fc/Pt	34.44	4.09	6.22	4.64	16.60
44-Fc	21.32	4.69	33.54	5.43	2.01
44-Fc/Pt	6.44	4.02	15.52	3.69	6.65
Cisplatin	69.71	6.55	103.23	8.49	-
Ferrocene	48.94	4.92	67.33	13.49	-
Dopamine	153.96	6.22	262.05	46.03	-

[a] AF: Activity factor

Conjugate **13-Pt** is a polymeric chelate in which the Pt atom is anchored through the carboxylatohydroxylato ligand system on a benzene ring, while **1-Pt** and **3-Pt** are anchored to the Pt atom through an amino-group on a benzene ring. For the three conjugates **1-Pt**, **3-Pt** and **13-Pt**, the IC_{50} values were derived from plots of cell growth relative to control versus conjugate concentration expressed in terms of µg $Pt.mL^{-1}$. The data analysis reveals that the IC_{50} values for **13-Pt** is significantly lower than that for cisplatin, while **1-Pt** of **3-Pt** do not improve upon the anticancer properties of cisplatin. By looking at the activity factors, it can be concluded that **13-Pt** is some 2-fold more active than the free drug, followed by **1-Pt**. **3-Pt** was not as effective as the free drug, being almost three times less active. Almost the same trend was noticed with the ferrocene homoconjugate samples (**44-Fc**, **24-Fc** and **34-Fc**). **34-Fc** was the most active with an AF of 5.11, followed by **44-Fc** with an AF of 2.01. **24-Fc** was less active than the free drug. This suggests that **34-Fc** was five times more active than free ferrocene and **44-Fc**, two times more active than the free ferrocene, while **24-Fc** was two times less active than the free ferrocene. It is apparent that the *tert*-amine DMP functionality in conjugates **44-Fc**, **34-Fc** and **13-Pt** exerts a positive influence on the *in vitro* cytotoxic data. In a biological environment, DMP is partially protonated, rendering the polymer fairly basic and may thus facilitate pinocytotic cell entry with resultant activity enhancement[144]. Larger sample numbers and different cell lines will be required, however, to substantiate this explanation. In addition, it should be ascertained to whether these conjugates and co-conjugates are selective for cancerous cells or do affect normal (non-cancerous) tissue, which could contribute to potential adverse effects.

A series of dopamine-containing carriers and platinum conjugates were also tested against the MCF-7 cell line. Dopamine is a neurotransmitter found in the brain that regulates movement and affects behavior. A report by Sarkar *et al*[158] shows that dopamine increases the efficacy of anticancer drugs in

breast cancer. The test performed in this study did not show any *in vitro* cytotoxic activity for both carriers and conjugates. A reasonable conclusion should be made after considering other cell lines.

The antiproliferative activity of the co-conjugates was also evaluated against the MCF-7 cell line. The procedure was similar to that used for the homoconjugate cell culture testing experiments. Ferrocene conjugates were directly compared to corresponding co-conjugates; **24-Fc** with **24-Fc/Pt**, **25-Fc** with **25-Fc/Pt**, **34-Fc** with **34-Fc/Pt** and **44-Fc** with **44-Fc/Pt**. The general observation of AF (Table 3.29) showed an increase in activity for the co-conjugates when compared to corresponding homoconjugates. The AF increased from 2 to 6-fold for **44-Fc/Pt** and from 5 to 16-fold for **34-Fc/Pt**. **25-Fc** did not give any IC_{50} value, however the corresponding co-conjugate **25-Fc/Pt** had an AF of 1.23. This shows that the trend is maintained. On the other hand, **24-Fc** was half as active as the free ferrocene drug and its corresponding co-conjugate **24-Fc/Pt** did not yield any IC_{50} value. Both prodrugs containing the dicarboxylato or the carboxylatohydroxylato ligands gave promising results, with the dicarboxylato being the best. In the case of tri-amino platinum with one amino group link platinum-carrier, very poor biological results were recorded. However any of these considerations can only be preliminary, only one cell line and few structures were used. Thus, it would be too early to draw a clear structure-activity relationship for these prodrugs.

Chapter 4

EXPERIMENTAL

4.1 Chemical synthesis

4.1.1 General procedures

^{1}H NMR spectra (300 MHz or 400 MHz unless otherwise specified) were taken in D_2O solutions. Chemical shifts, δ in ppm, were given relative to sodium 3-(trimethylsilyl)-2,2,3,3-d_4-propionate. Integration error limits were 12–15%. In order to eliminate protonation effects, spectral sample solutions were adjusted to pD 10–11 with NaOH.

Inherent viscosities, η_{inh} expressed as $mL.g^{-1}$, were determined in triplicate at 30.0 ± 0.5^{o}C in Cannon-Fenske tubes. Deionized water was used as the solvent; the concentration was 0.2 g/100 mL. Dialysis was performed with the aid of cellulose membranes (Spectrum Industry Inc., Los Angeles, USA) of type Spectra/Por 4®, with molecular mass cut-off limit of 12 000–14 000, against several batches of distilled water. The pH of the carriers was adjusted to desirable value with conc. hydrochloric acid by using a 1 mL micro-syringe. Where necessary the pH was measured with the pH-meter.

For freeze drying operations, a Virtis Bench Top 3 freeze drier (-40^{o}C, 10 – 15 Pa) was used. The freeze-dried polymer samples were post-dried in an infrared drying apparatus and kept in a desiccator. Analytical samples of the conjugates were normally dried for 2 days at 55–60^{o}C under reduced pressure in an Abderhalden apparatus ($CaCl_2$ as the drying agent). The platinum determinations were undertaken at De Bruyn Spectroscopic Solutions, Bryanston, Johannesburg and CHEMTECH Laboratory services, Monument Park, Pretoria. The analysis was performed by ICP–OES using matrix matched standards. Yttrium (Y) was used as internal standard to compensate for viscosity effects.

4.1.2 Solvents and reagents

Distilled water was used for all preparative work. The reaction solvent, *N,N'*-dimethylformamide (DMF), was distilled under reduced pressure in a faint stream of N_2, with a fore-run of around 10% being discarded, and was dried over 4Å molecular sieves. All other solvents were laboratory grade, received from commercial sources.

The monomeric reagent, acryloyl chloride (Fluka Chemie) and the amines, chemical grade (Aldrich Chemie, Fluka AG), were used as received. These included: 3-hydroxy-tyramine-hydrochloride (Dopamine), DL-aspartic acid, *N,N'*-dicyclohexylcarbodiimide (DCC), 3-(dimethylamino)propylamine (DMP), 2-dimethylaminoethylamine (DMEA), 2-diethylaminoethylamine (DEEA), 1,3-diaminopropane (PDA), diaminoethane (EDA) and ethyl 4-aminobenzoate (EAB). Potassium tetrachloroplatinate (K_2PtCl_4) was in part donated by the Western Platinum Refinery.

4.1.3 Preparation of monomers

4.1.3.1 Synthesis of p-aminobezamidopropylamine ***M1***

Ethyl 4-aminobenzoate (EAB: 1.65 g, 10 mmol) was dissolved in 1,3-diaminopropylamine (PDA: 2.964 g, 40 mmol). Sodium carbonate (Na_2CO_3: 0.106 g, 1.0 mmol) was added to the solution, then the mixture was flashed with N_2. The mixture was refluxed for 18h at 160^{o}C. Thereafter the mixture was filtered and water added to the filtrate. The unreacted salt was removed by filtration and the volume of filtrate reduced to an oily viscous solution by rotary evaporation under reduced pressure at 50^{o}C. The latter was dissolved in methanol (MeOH: 2 mL) and acidified to pH ~3-4 with conc. HCl. Different fractions were obtained and the final product was found in the final mother liquor. After solvent removal, the product was dried to afford 0.109 g, (56.8%) a white powder.

^{1}H NMR (D_2O), (Appendix 1a), δ/ppm (expected proton counts in parentheses): 1.761-1.688, 2H (2H, NH_2CH_2**CH_2**CH_2NH, m); 2.683-2.636, 2H (2H, NH_2**CH_2**CH_2CH_2NH, t, 14.1Hz); 3.402-3.356, 2H (2H, **CH_2**CONH, t, 13.8Hz); 6.851-7.822, 2H (2H, CH Aromatic, d, 8.7Hz); 7.603-7.574, 2H (2H, CH Aromatic, d, 8.7Hz).

*4.1.3.2 Synthesis of acryloylamidosalicylic acid **M2***

To a rapidly stirring solution (60 mL) of *p*-aminosalicylic acid (1.532 g, 10.0 mmol), Na_2CO_3 (0.530 g, 5.0 mmol) and hydroquinone (5 mg), a solution of acryloyl chloride (1.086 g, 12.0 mmol) in dichloromethane (2 mL) was added dropwise. The pH of the solution was maintained at pH~8-9 by addition of drops of 2 M solution of Na_2CO_3. The solution was stirred at ice bath temperature for 2h, then for another 2h at RT. The solution was acidified to pH~3-4 with conc. HCl and extracted with ethyl acetate. Several crops were collected and similar crops were pulled together in a yield of 1.581 g (76.3%) of a whitish solid; mp 126-128^{o}C.

^{1}H NMR (D_2O), (Appendix 1b), δ/ppm (expected proton counts in parentheses): 5.835-5.797, 1H (1H, **HC**HCHCONH, m); 6.3-6.2, 2H (2H, H**CHCH**CONH, m); 6.7-6.6, 2H (2H, **CH** Aromatic, m); 7.442-7.414, 1H (**CH** Aromatic, d, 8.4Hz).

*4.1.3.3 Synthesis of **M3***

1,2-Diaminoethane (EDA) (311 mg, 5.180 mmol) was added to **M2** (723 mg, 3.9 mmol) and Na_2CO_3 (410 mg, 3.9 mmol) in H_2O (1 mL). The solution was stirred in an incubator for 4d at 65 ^{0}C. The solution was concentrated on a rotary evaporator under reduced pressure and then washed with boiling toluene several times and re-washed with hot acetone to remove the excess PDA. Thereafter it was slurried in MeOH (3mL) and acidified to pH~3 with conc. HCl. The solution was reconcentrated on the rotary evaporator and re-dissolved in MeOH (8 mL). The product was collected from MeOH as crystallized crops of whitish solids in a total yield of 702 mg (67.4%).

^{1}H NMR (D_2O), δ/ppm (expected proton counts in parentheses): 1.6-1.5, 2H (2H, CH_2**CH_2**CH_2); 2.6-2.5, 6H (6H, **CH_2**CH_2**CH_2**NH**CH_2**CH_2CONH); 2.9-2.8, 2H (2H, **CH_2**CONH), 7.0-6.8, 2H (2H, **CH** Aromatic); 7.7-7.6, 1H (1H, **CH** Aromatic).

*4.1.3.4 Synthesis of **M4***

To an aqueous solution of **M2** (500 mg, 2.7 mmol) in H_2O (1 mL), Na_2CO_3 (285 mg, 2.7 mmol) and 1,3-diaminopropane (PDA: 291 mg, 3.925 mmol) were added and stirred for 4d at 65^{o}C. The solution was concentrated and washed before the **M4** product was collected as described for **M3** (section 4.1.3.3). The yield of the product was 618 mg (64.8%) of a whitish solid.

^{1}H NMR (D_2O), (Appendix 1c), δ/ppm (expected proton counts in parentheses): 2.6-2.4, 6H (6H, **$CH_2$$CH_2$**NH**$CH_2$**$CH_2$CONH); 3.0-2.9, 2H (2H, **CH_2**CONH); 6.9-6.7, 2H (2H, **CH** Aromatic); 7.6-7.5, 1H (1H, **CH** Aromatic).

*4.1.3.5 Synthesis of 4-ferrocenylbutanoic acid **M5***

4-Ferrocenylbutanoic acid (**M5**) was prepared according to a procedure described in the literature[155].

^{1}H NMR (D_2O), δ/ppm (expected proton counts in parentheses): 1.9-1.7, 2H (2H, CH_2**CH_2**CH_2); 2.4-2.2, 4H (4H, **CH_2**CH_2**CH_2**), 4.3-4.1, 8.8H (9H, **CH** ferrocenyl);.

*4.1.3.6 Synthesis of 4-ferrocenylbutamidepropylamine (Fc-PDA or **M6**)*

4-Ferrocenylbutanoic acid (**M5**: 2.73 g, 10 mmol) was dissolved in THF (20 mL). To the stirred solution HSU (1.38 g, 12 mmol) was added in small portions at RT, and stirring continued at ice-bath temperature for 15min. There after DCC (2.48 g, 12 mmol) in THF (5 mL) was added dropwise and stirring continued in the ice-water bath for 4h then at RT for 2d. The solid was filtered off, and washed with THF. The filtrate and washings were combined and added dropwise to a stirred solution of PDA (2.99 g, 40 mmol) in THF (25 mL). Stirring continued for 24h in an ice-water bath and

for another 6h at RT. The solid was filtered off and washed with THF. The filtrate and washes were combined and solvent removed to leave an oily viscous liquid. The oily liquid was dissolved in MeOH (4mL) and acidified to pH~3-4 with conc. HCl. Thereafter the material was purified by flash chromatography (silica gel column) using MeOH. The solution solvent was removed under reduced pressure to give a product that was an orange viscous at RT, in a yield of 2.511 g (76.3%).

^{1}H NMR (D_2O), (Appendix 1d), δ/ppm (expected proton counts in parentheses): 1.9-1.7, 4H (4H, CH_2**CH_2**CH_2); 2.4-2.2, 4 (4, Fc-**CH_2**CH_2, **CH_2**NH_2); 2.8-2.9, 2H (2H, **CH_2**$CONH_2$); 3.25-3.1, 2H (2H, CONH**CH_2**); 4.1-4.25, 9H (9H, **CH**, Ferrocenyl).

*4.1.3.7 Synthesis of **M7***

A Solution of acryloyl chloride (1.52 mL, 1.88 mmol) in dichloromethane (4 mL) was added to a vigorously stirred solution of aspartic acid (2.08 g, 1.56 mmol), Na_2CO_3 (1.66 g, 1.56 mmol) and hydroquinone (20 mg) in 80 mL of H_2O at 0–5^{o}C. The pH of the solution was kept at pH ~8–9 by drop wise addition of 2M Na_2CO_3 solution. After the addition of acryloyl chloride, stirring was continued at 0–5^{o}C for 2h and then for another 2h at RT. The solution was acidified to pH~3with conc. HCl and then extracted with ethyl acetate. The product (**M7**) was crystallized from ethyl acetate in a total yield of 2.28 g (78.0%) of whitish solids; mp: 161-163^{o}C.

^{1}H NMR (D_2O), δ/ppm (expected proton counts in parentheses): 2.4-2.2, 2H (2H, **CH_2** (Asp)); 4.2-4.1, 1H (1H, **CH** (Asp)); 5.5-5.4, 0.9H (1H, **HC**HCHCONH); 6.1-5.8, 1.9 (2H, H**CHCH**CONH).

*4.1.3.8 Synthesis of **M8***

PDA (0.36 mL, 4.2 mmol) was added to an aqueous solution (1 mL) of **M7** (0.72 g, 3.9 mmol) and sodium carbonate (20%). The solution was stirred in an incubator for 3d at 65^{o}C. The solution volume was reduced under reduced pressure at 60^{o}C and then washed with boiling toluene and

thereafter re-washed with hot acetone. The residue was slurried in MeOH (3 mL) and acidified to pH~3 with conc. HCl. The product was crystallized from MeOH in a total yield of 0.741 g (72.4%) of whitish solids.

^{1}H NMR (D_2O), (Appendix 1e), δ/ppm (expected proton counts in parentheses): 2.0-1.7, 2.3H (2H, NH_2CH_2**CH_2**CH_2NH); 3.2-2.4, 10.4H (10, NH_2**CH_2**CH_2**CH_2**NH**CH_2**; **CH_2** (Asp); **CH_2**CONH); 4.5-4.3, 1H (1H, **CH** (Asp)).

4.1.4 Poly-DL-succinimide

Poly-DL-succinimide (PSI) was prepared by the method of Neri and Antoni[99]. This method involved the polymerization of DL-aspartic acid in the presence of orthophosphoric acid at 220^{o}C for 30min then 180^{o}C for 2h. The polymer was subjected to carbodiimide chain extension. The products of approximately equal viscosity were pooled from different runs and thoroughly mixed to give a master batch with inherent viscosity (in DMF) of 28.5 mL.g^{-1}.

4.1.5 Preparation of polymeric carriers

*4.1.5.1 Carriers containing **M1***

*4.1.5.1.1 Polyaspartamide **1***

M1 (59.1 mg, 0.3059 mmol) in DMF (5 mL) and triethylamine (TEA: 31.0 mg, 0.3059 mmol) were added to a stirred solution of PSI (300 mg, 3.059 mmol) in DMF (8 mL) at ice-bath temperature. The solution was saturated with N_2 and stirred for 1d at ice-bath temperature (0–5^{o}C). Then 3-(*N,N*-dimethylamino)propylamine (DMP: 313 mg, 3.059 mmol) in DMF (3 mL) was added in one portion to the stirred solution at 0–5^{o}C. The solution was resaturated with N_2 and stirred at the same temperature for 12h and then for another 1d at room temperature (RT). The solution was concentrated by

rotary evaporation, before the polymeric product was precipitated out with 15 mL diethyl ether:hexane (2:1), and thoroughly washed, firstly with the precipitant, then with hot acetone to eliminate any unreacted amine, and finally dissolved in 15 mL H_2O. The pH was adjusted to pH~8 with concentrated HCl and the solution dialyzed for 3d in 12 000-14 000 molecular mass cut-off limit tubing against distilled water, which was replaced several times during this period. The retentate was freeze-dried to afford 390 mg (61.2%) of beige water-soluble material; η_{inh} (H_2O): 12.3 $mL.g^{-1}$.

^1H NMR (D_2O), (Appendix 1f), δ/ppm (expected proton counts in parentheses): 1.8-1.5, 20H (20H, CH_2**CH_2**CH_2); 2.2-2.0, 55H (54H, N**CH_3**); 2.4-2.2, 21H (18, **CH_2**N); 3.0-2.5, 23H (20H, **CH_2**CONH); 3.4-3.0, 22H (22H, CONH**CH_2**); 4.7-4.6, 10H (10H, **CH**, Asp); 6.8, 2H (2H, **CH**, Aromatic); 7.7-7.5, 2H (2H, **CH**, Aromatic).

*4.1.5.1.2 Polyaspartamide **2***

Polyaspartamide **2**, a variant of polyaspartamide **1**, was prepared using the same procedure as for polyaspartamide **1** (section 4.1.4.2). Thus, PSI (310 mg, 3.161 mmol), **M1** (61.1 mg, 0.3161 mmol), TEA (32.0 mg, 0.3161 mmol) and 2-(dimethylamino)ethylamine (DMEA: 326 mg, 3.700 mmol) afforded poly-aspartamide **2** in a yield of 360 mg (58.2%) as beige water-soluble material; η_{inh} (H_2O): 13.1 $mL.g^{-1}$.

^1H NMR (D_2O), (Appendix 1g), δ/ppm (expected proton counts in parentheses): 1.8-1.5, 2H (2H, CH_2**CH_2**CH_2); 2.3-2.1, 54H (54H, N**CH_3**); 2.5-2.3, 17H (18, **CH_2**N); 3.0-2.5, 22H (20H, **CH_2**CONH); 3.4-3.2, 23H (22H, CONH**CH_2**); 4.7-4.6, 10H (10H, **CH**, Asp); 6.8, 1.9H (2H, **CH**, Aromatic); 7.7-7.5, 1.9H (2H, **CH**, Aromatic).

*4.1.5.1.3 Polyaspartamide **3***

The same procedure used for polymer **1** (section 4.1.4.2) was used to prepare polyaspartamide **3**. DMP was replaced with 2-

(diethylamino)ethylamine (DEEA). PSI (313 mg, 3.191 mmol), **M1** (61.6 mg, 0.3191 mmol), TEA (32.3 mg, 0.3191 mmol) and DEEA (418 mg, 3.600 mmol) were allowed to react. The reaction conditions as well as the work up were as previously described. This produced the copolymer **3** in a yield of 407 mg (54.3%) of beige material, η_{inh} (H_2O): 14.6 $mL.g^{-1}$.

^1H NMR (D_2O), (Appendix 1h), δ/ppm (expected proton counts in parentheses): 1.2-0.9, 56H (54H, **CH_3**CH_2); 1.8-1.6, 2H (2H, CH_2**CH_2**CH_2); 3.0-2.5, 78H (74H, **CH_2**CONH, **CH_2**N); 3.5-3.2, 24H (22H, CONH**CH_2**); 4.7-4.6, 10.2H (10H, **CH**, Asp); 6.8, 2H (2H, **CH**, Aromatic); 7.8-7.6, 2H (2H, **CH**, Aromatic).

*4.1.5.1.4 Polyaspartamide **4***

Polyaspartamide **4** was prepared analogously to polyaspartamide **1**. PSI (305 mg, 3.110 mmol), **M1** (60.1 mg, 0.3110 mmol), TEA (31.5 mg, 0.3110 mmol) and 3-(diethylamino)-propylamine (DEP: 456 mg, 3.500 mmol) were reacted and polyaspartamide **4** was obtained in a yield of 459 mg (63.2%) of beige material, η_{inh} (H_2O): 10.6 $mL.g^{-1}$.

^1H NMR (D_2O), (Appendix 1i), δ/ppm (expected proton counts in parentheses): 1.1-0.9, 54H (54H, **CH_3**CH_2); 1.8-1.5, 20H (20H, CH_2**CH_2**CH_2); 2.6-2.3, 54H (54H, **CH_2**N); 3.0-2.6, 23H, (20H, **CH_2**CONH,); 3.4-3.0, 22H (22H, CONH**CH_2**); 4.7-4.6, 10H (10H, **CH**, Asp); 6.8, 2H (2H, **CH**, Aromatic); 7.7-7.5, 2H (2H, **CH**, Aromatic).

*4.1.5.1.5 Polyaspartamide **5***

By a similar procedure as for polyaspartamide **1** (section 4.1.4.2), polyaspartamide **5** was synthesized. PSI (320 mg, 3.262 mmol), **M1** (63.0 mg, 0.3262 mmol), TEA (33.0 mg, 0.3262 mmol) and 4-(3-aminopropyl)-morpholine (APM: 526 mg, 3.650 mmol) were reacted. The polymer was obtained in a yield of 539 mg (67.1%) of beige material, η_{inh} (H_2O): 14.2 $mL.g^{-1}$.

^{1}H NMR (D_2O), (Appendix 1j), δ/ppm (expected proton counts in parentheses): 1.8-1.5, 20H (20H, CH_2**CH_2**CH_2); 2.9-2.0, 76.1H (74H, **CH_2**CONH, **CH_2**N); 3.5-3.2, 22.6H (22H, CONH**CH_2**); 3.6-3.9, 34.3H (36H, **CH_2**-O-**CH_2**); 4.7-4.6, 10.3H (10H, **CH**, Asp); 6.8, 2H (2H, **CH**, Aromatic); 7.7-7.5, 2H (2H, **CH**, Aromatic).

4.1.5.2 Carriers containing PDA

A modified procedure was used to prepare polyaspartamides **6** and **7**. Instead of **M1**, 1,2-diaminopropylamine (PDA) was used.

*4.1.5.2.1 Polyaspartamide **6***

Polyaspartamide **6** was obtained by reacting PSI (311 mg, 3.171 mmol), DMP (259 mg, 2.537 mmol) and PDA (141 mg, 1.903 mmol). To a stirred PSI solution in DMF (8 mL) was added DMP in DMF (5 mL). The resulting solution was saturated with N_2 and stirred at RT for 12h. To PDA in DMF (10 mL) at 0–5^{o}C was added dropwise the PSI-DMP solution over 1h. The resulting solution was saturated with N_2 and stirred for 6h at 0–5^{o}C and another 1d at RT. The work up and the purification process were similar to polyaspartamide **1** (section 4.1.5.1.1). This process afforded 171 mg (55.9%) of a beige water-soluble polymer; η_{inh} (H_2O): 16.2 mL.g^{-1}.

^{1}H NMR (D_2O), δ/ppm (expected proton counts in parentheses): 1.8-1.5, 10H (10H, CH_2**CH_2**CH_2); 2.2-2.0, 25H (24H, N**CH_3**); 2.4-2.2, 11H (10H, **CH_2**N, NH_2**CH_2**); 2.9-2.5, 10H (10H, **CH_2**CONH); 3.5-3.1, 10H (10H, CONH**CH_2**); 4.7-4.6, 5H (5H, **CH**, Asp).

*4.1.5.2.2 Polyaspartamide **7***

For polyaspartamide **7**, PSI (313 mg, 3.191 mmol), DMP (293 mg, 2.872 mmol) and PDA (70.9 mg, 0.9573 mmol) were used. The same procedure as for polyaspartamide **6** (section 4.1.5.2.1) was followed and the polyaspartamide **7** was obtained in a yield of 403 mg (64.3%) of beige material; η_{inh} (H_2O): 14.8 mL.g^{-1}.

^{1}H NMR (D_2O), δ/ppm (expected proton counts in parentheses): 1.8-1.5, 20H (20H, CH_2**CH_2**CH_2); 2.2-2.0, 54H (54H, N**CH_3**); 2.4-2.2, 21H (20H, **CH_2**N, NH_2**CH_2**); 2.9-2.5, 20H (20H, **CH_2**CONH); 3.5-3.1, 20H (20H, CONH**CH_2**); 4.7-4.6, 10H (10H, **CH**, Asp).

*4.1.5.3 Carriers containing **M3***

*4.1.5.3.1 Polyaspartamide **8***

M3 (83.4 mg, 0.3120 mmol) in DMF (2 mL) was added with stirring to PSI (306 mg, 3.120 mmol) pre-dissolved in DMF (8 mL), and TEA (31.6 mg, 0.3120 mmol) was added. The resulting solution was saturated with N_2, the flask tightly stoppered to preclude any moisture penetrating, and stirring continued for 3d at RT. DMP (357 mg, 3.500 mmol) in DMF (4 mL) was added in one portion to the stirred solution. The resultant solution was resaturated with N_2, and stirred at RT for another 1d. The solution was concentrated using a rotary evaporator at reduced pressure at 65^{o}C. The polymeric product was obtained by precipitation with diethyl ether:hexane (2:1) and washed with the precipitant, before hot acetone, and finally dissolved in water (15mL). The pH was adjusted to pH~8 with conc. HCl, and the polymeric solution was dialyzed for 3d in 12 000-14 000 molecular mass cut-off limit tubing against distilled water, which was replaced several times during this period. The polymer was obtained as a beige water-soluble solid after freeze-drying, in a yield of 381 mg (56.7%); η_{inh} (H_2O): 13.6 mL.g^{-1}.

^{1}H NMR (D_2O), (Appendix 1k), δ/ppm (expected proton counts in parentheses): 1.8-1.5, 18H (18H, CH_2**CH_2**CH_2); 2.2-2.1, 55H (54H, N**CH_3**); 2.4-2.2, 20H (22H, **CH_2**N, NH**CH_2**); 3.0-2.4, 23H (22H, **CH_2**CONH); 3.4-3.0, 22H (20H, CONH**CH_2**); 4.7-4.6, 10H (10H, **CH**, Asp); 6.8-6.6, 2H (2H, **CH**, Aromatic); 7.5-7-3, 0.9H (1H, **CH**, Aromatic).

*4.1.5.3.2 Polyaspartamide **9***

The same procedure as described for polyaspartamide **8** (section 4.1.4.8) was used to prepare polyaspartamide **9**. **M3** (84.5 mg, 0.3161 mmol) and TEA (32.0 mg, 0.3161 mmol) in DMF (2 mL) were added to PSI (310 mg, 3.161 mmol) dissolved in DMF (8 mL). The solution was saturated with N_2 and stirred for 3d, thereafter DMEA (308 mg, 3.500 mmol) in DMF (3 mL) was added and the solution re-saturated with N_2 and stirred for 1d at RT. This reaction yielded 384 mg (59.8%) of polyaspartamide **9** as beige material; η_{inh} (H_2O): 15.1 $mL.g^{-1}$.

^1H NMR (D_2O), (Appendix 1l), δ/ppm (expected proton counts in parentheses): 2.3-2.1, 54H (54H, N**CH_3**); 3.0-2.3, 45H (44H, **CH_2**N, NH**CH_2**, **CH_2**CONH); 3.4-3.1, 22H (20H, CONH**CH_2**); 4.7-4.6, 10H (10H, **CH**, Asp); 6.8-6.6, 2H (2H, **CH**, Aromatic); 7.5-7-3, 1H (1H, **CH**, Aromatic).

*4.1.5.3.3 Polyaspartamide ***10***

Using a similar procedure as for polyaspartamide **8** (section 4.1.4.8), **M3** (83.6 mL, 0.3130 mmol) and TEA (31.7 mg, 0.3130 mmol) in DMF (2 mL) were added to PSI (307 mg, 3.130 mmol) dissolved in DMF (8 mL). The solution was saturated with N_2 and stirred for 3d, thereafter DEEA (407 mg, 3.500 mmol) in DMF (3 mL) was added, the solution re-saturated with N_2 and stirred for 1d at RT. This resulted in polyaspartamide **10** with a yield of 442 mg (61.9%) beige material, and η_{inh} (H_2O): 12.6 $mL.g^{-1}$.

^1H NMR (D_2O), (Appendix 1m), δ/ppm (expected proton counts in parentheses): 1.2-0.8, 54H (54H, **CH_3**CH_2); 3.1-2.2, 82H (80H, **CH_2**N, NH**CH_2**, **CH_2**CONH); 3.4-3.0, 23H (20H, CONH**CH_2**); 4.7-4.6, 10H (10H, **CH**, Asp); 6.8-6.6, 2H (2H, **CH**, Aromatic); 7.6-7-3, 1H (1H, **CH**, Aromatic).

*4.1.5.3.4 Polyaspartamide ***11***

Based on the procedure used to synthesized polyaspartamide **8** (section 4.1.4.8), polyaspartamide **11** was prepared by treating PSI (313 mg, 3.191 mmol) in DMF (8 mL) with **M3** (85.3 mg, 0.3191 mmol) and TEA (32.3 mg,

0.3191 mmol). DEP (456 mg, 3.500 mmol) in DMF (3 mL) was added to the stirred solution and the resultant solution was treated as in section 4.1.4.8 to yield a beige water-soluble solid product in a yield of 432 mg (56.2%); η_{inh} (H_2O): 13.2 $mL.g^{-1}$.

^1H NMR (D_2O), δ/ppm (expected proton counts in parentheses): 1.1-0.8, 58H (54H, **CH_3**CH_2); 1.8-1.5, 18H (18H, CH_2**CH_2**CH_2); 3.0-2.3, 84H (80H, **CH_2**CONH, **CH_2**N, NH**CH_2**); 3.4-3.0, 22H (20H, CONH**CH_2**); 4.7-4.6, 10H (10H, **CH**, Asp); 6.8-6.6, 1.9H (2H, **CH**, Aromatic); 7.6-7-3, 1H (1H, **CH**, Aromatic).

*4.1.5.3.5 Polyaspartamide **12***

The same procedure as for polyaspartamide **8** (section 4.1.4.8) was followed here. PSI (321 mg, 3.273 mmol) in DMF (8 mL) was treated with **M3** (87.5 mg, 0.3273 mmol) and TEA (32.7 mg, 0.3273 mmol) in DMF (2 mL) in the first step, and APM (526 mg, 3.650 mmol) in DMF (3 mL) in the second step. This reaction produced a beige water-soluble solid with a yield of 482 mg (58.1%); η_{inh} (H_2O): 11.8 $mL.g^{-1}$.

^1H NMR (D_2O), (Appendix 1n), δ/ppm (expected proton counts in parentheses): 1.8-1.5, 18H (18H, CH_2**CH_2**CH_2); 3.0-2.2, 80H (80H, **CH_2**CONH, **CH_2**N, NH**CH_2**); 3.4-3.0, 23H (20H, CONH**CH_2**); 3.9-3.6, 37H (36H, **CH_2**-O-**CH_2**); 4.7-4.6, 10H (10H, **CH**, Asp); 6.8-6.6, 1.9H (2H, **CH**, Aromatic); 7.6-7-3, 1H (1H, **CH**, Aromatic).

*4.1.5.4 Carriers containing **M4***

Polyaspartamides **13** to **17** were obtained by the same procedure used to prepare polymer **8** to **12**, except the amine **M3** was replaced with **M4.** The reactions conditions were maintained.

*4.1.5.4.1 Polyaspartamide **13***

Polyaspartamide **13** was prepared from PSI (317 mg, 3.232 mmol), **M4** (90.9 mg, 0.3232 mmol), TEA (32.7 mg, 0.3232 mmol) and DMP (357 mg,

3.500 mmol). The reaction mixture was treated as in section 4.1.5.3.1 to produce a beige water-soluble solid in a yield of 471 mg (67.2%); η_{inh} (H_2O): 13.6 $mL.g^{-1}$.

^1H NMR (D_2O), (Appendix 1o), δ/ppm (expected proton counts in parentheses): 1.8-1.5, 20H (20H, CH_2**CH_2**CH_2); 2.2-2.0, 54H (54H, **CH_3**N); 2.4-2.2, 19H (22H, **CH_2**N, NH**CH_2**); 3.0-2.4, 25H (22H, **CH_2**CONH,); 3.4-3.0, 23H (20H, CONH**CH_2**); 4.7-4.6, 10H (10H, **CH**, Asp); 6.8-6.5, 2H (2H, **CH**, Aromatic); 7.6-7.3, 1H (1H, **CH**, Aromatic).

*4.1.5.4.2 Polyaspartamide **14***

This polyaspartamide was prepared and treated as in section 4.1.5.3.1, where, PSI (308 mg, 3.140 mmol), **M4** (88.3 mg, 0.3140 mmol), TEA (31.8 mg, 0.3140 mmol) and DMEA (308 mg, 3.500 mmol) were used. The beige water-soluble polymer was in a yield of 0.387 mg (60.3%); η_{inh} (H_2O): 14.2 $mL.g^{-1}$.

^1H NMR (D_2O), δ/ppm (expected proton counts in parentheses): 1.8-1.5, 2H (2H, CH_2**CH_2**CH_2); 2.2-2.0, 54H (54H, N**CH_3**); 3.0-2.2, 46H (44H, **CH_2**CONH, **CH_2**N, NH**CH_2**); 3.4-3.0, 22H (20H, CONH**CH_2**); 4.7-4.6, 10H (10H, **CH**, Asp); 6.8-6.5, 2H (2H, **CH**, Aromatic); 7.6-7.3, 0.9H (1H, **CH**, Aromatic).

*4.1.5.4.3 Polyaspartamide **15***

Polyaspartamide **15** was prepared in a similar manner to polyaspartamide **8**, where PSI (312 mg, 3.181 mmol), **M4** (89.5 mg, 0.3181 mmol), TEA (32.2 mg, 0.3181 mmol) and DEEA (406 mg, 3.500 mmol) were reacted together and the solution was treated as described in section 4.1.5.3.1. The yield was 454 mg (62.1%) of a beige water-soluble solid; η_{inh} (H_2O): 10.2 $mL.g^{-1}$.

^1H NMR (D_2O), δ/ppm (expected proton counts in parentheses): 0.8-1.2, 56H (54H, **CH_3**CH_2); 1.8-1.5, 2H (2H, CH_2**CH_2**CH_2); 3.0-2.2, 81H (80H, **CH_2**CONH, **CH_2**N, NH**CH_2**); 3.4-3.0, 22H (20H, CONH**CH_2**); 4.7-4.6, 10H

(10H, **CH**, Asp); 6.8-6.5, 2H (2H, **CH**, Aromatic); 7.6-7.3, 0.9H (1H, **CH**, Aromatic).

*4.1.5.4.4 Polyaspartamide **16***

Using the procedure leading to polyaspartamide **8** (section 4.1.5.3.1), this carrier was prepared from PSI (320 mg, 3.262 mmol), **M4** (91.8 mg, 0.3262 mmol), TEA (33.0 mg, 0.3262 mmol) and DEP (469 mg, 3.600 mmol). The solution was treated as described in section 4.1.5.3.1 and yielded 427 mg (54.1%) of a beige water-soluble solid; η_{inh} (H_2O): 12.4 $mL.g^{-1}$.

^1H NMR (D_2O), δ/ppm (expected proton counts in parentheses): 0.8-1.2, 56H (54H, **CH_3**CH_2); 1.8-1.5, 20H (20H, CH_2**CH_2**CH_2); 3.0-2.2, 83H (80H, **CH_2**CONH, **CH_2**N, NH**CH_2**); 3.4-3.0, 23H (20H, CONH**CH_2**); 4.7-4.6, 10H (10H, **CH**, Asp); 6.8-6.5, 1.9H (2H, **CH**, Aromatic); 7.6-7.3, 0.9H (1H, **CH**, Aromatic).

*4.1.5.4.5 Polyaspartamide **17***

As described for polymer **8** (section 4.1.5.3.1), polyaspartamide **17** was synthesized from PSI (313 mg, 3.191 mmol), **M4** (89.8 mg, 0.3191 mmol), TEA (32.3 mg, 0.3191 mmol) and APM (505 mg, 3.500 mmol) were used. The solution was treated as in section 4.1.5.3.1. This reaction yielded 459 mg (56.5%) of a beige water-soluble solid; η_{inh} (H_2O): 10.5 $mL.g^{-1}$.

^1H NMR (D_2O), δ/ppm (expected proton counts in parentheses): 1.8-1.5, 20H (20H, CH_2**CH_2**CH_2); 3.0-2.2, 85H (80H, **CH_2**CONH, **CH_2**N, NH**CH_2**); 3.4-3.0, 22H (20H, CONH**CH_2**); 3.9-3.6, 38H (36H, **CH_2**-O-**CH_2**); 4.7-4.6, 10H (10H, **CH**, Asp); 6.8-6.5, 2H (2H, **CH**, Aromatic); 7.6-7.3, 1H (1H, **CH**, Aromatic).

4.1.5.5 Carriers containing dopamine

*4.1.5.5.1 Polyaspartamide **18***

To a stirred solution of PSI (310 mg, 3.161 mmol) in DMF (10 mL), 3-hydroxytyramine hydrochloride (dopamine: 58.1 mg, 0.3793 mmol) in DMF

(2 mL) and TEA (38.4 mg, 0.3793 mmol) were added. The resulting solution was saturated with N_2 before being stirred for 3d at RT. DMP (357 mg, 3.500 mmol) dissolved in DMF (3 mL), was added whilst being stirred. Following re-saturation with N_2, the suspension was stirred for another 2d at RT. The suspension was then filtered and the filtrate was concentrated in a rotary evaporator under reduced pressure at 65^{o}C. The polymeric product was precipitated with diethyl ether:hexane (2:1), and then washed with the latter precipitant followed by hot acetone. The solid was then dissolved in H_2O (15 mL) and the pH was adjusted to pH~8 with conc. HCl. The solution was dialyzed for 3d in 12 000-14 000 molecular mass cut-off limit tubing. Freeze-drying of the retentate yielded 390 mg (60.4%) of brownish water-soluble solid polymer; η_{inh} (H_2O): 13.6 mL.g^{-1}.

^{1}H NMR (D_2O), (Appendix 1p), δ/ppm (expected proton counts in parentheses): 1.8-1.5, 18H (18H, CH_2**CH_2**CH_2); 2.2-2.0, 54H (54H, N**CH_3**); 2.4-2.2, 21H (22H, **CH_2**N, Ar-**CH_2**); 3.0-2.4, 23H (20, **CH_2**CONH); 3.3-3.0, 22H (20H, CONH**CH_2**); 4.7-4.6, 10H (10H, **CH**, Asp); 6.7-6.3, 3H (3H, **CH**, Aromatic).

*4.1.5.5.2 Polyaspartamide **19***

Based on the procedure for the synthesis of polyaspartamide **18** (section 4.1.5.5.1), polyaspartamide **19** was prepared from PSI (313 mg, 3.191 mmol), dopamine (58.7 mg, 0.3829 mmol), TEA (38.7 mg, 0.3829 mmol) and DMEA (308 mg, 3.500 mmol). The process resulted in the brownish water-soluble polymer **19** in a yield of 375 mg (61.3%); η_{inh} (H_2O): 10.9 mL.g^{-1}.

^{1}H NMR (D_2O), (Appendix 1q), δ/ppm (expected proton counts in parentheses): 2.3-2.1, 54H (54H, N**CH_3**); 3.0-2.3, 42H (40H, **CH_2**CONH, **CH_2**N, Ar-**CH_2**); 3.5-3.1, 22H (20H, CONH**CH_2**); 4.7-4.6, 10H (10H, **CH**, Asp); 6.7-6.3, 2.9H (3H, **CH**, Aromatic).

*4.1.5.5.3 Polyaspartamide **20***

Following the same procedure as for polymer **18** (section 4.1.5.5.1), PSI (316 mg, 3.222 mmol), dopamine (59.6 mg, 0.3866 mmol), TEA (39.1 mg, 0.3866 mmol) and DEEA (412 mg, 3.550 mmol) were treated as described in section 4.1.5.5.1. The process yielded 406 mg (58.1%) of **20** as a brownish water-soluble solid; η_{inh} (H_2O): 13.2 $mL.g^{-1}$.

^1H NMR (D_2O), (Appendix 1r), δ/ppm (expected proton counts in parentheses): 1.1-0.9, 54H (54H, **CH_3**CH_2); 3.0-2.4, 78H (76H, **CH_2**CONH, **CH_2**N, Ar-**CH_2**); 3.5-3.1, 22H (20H, CONH**CH_2**); 4.7-4.6, 10H (10H, **CH**, Asp); 6.7-6.3, 2.9H (3H, **CH**, Aromatic).

*4.1.5.5.4 Polyaspartamide **21***

The same procedure as described for polyaspartamide **18** (section 4.1.5.5.1) was followed to produce polyaspartamide **21**, whereby PSI (314 mg, 3.201 mmol), dopamine (59.2 mg, 0.3841 mmol), TEA (38.9 mg, 0.3841 mmol) and DEP (456 mg, 3.500 mmol) were allowed to react, and yielded 480 mg (65.4%) of a brownish water-soluble solid; η_{inh} (H_2O): 12.4 $mL.g^{-1}$.

^1H NMR (D_2O), (Appendix 1s), δ/ppm (expected proton counts in parentheses): 1.1-0.8, 54H (54H, **CH_3**CH_2); 1.8-1.5, 18H (18H, CH_2**CH_2**CH_2); 3.0-2.3, 78H (76H, **CH_2**CONH, **CH_2**N, Ar-**CH_2**); 3.4-3.0, 21H (20H, CONH**CH_2**); 4,7-4.6, 10H (10H, **CH**, Asp); 6.7-6.3, 2.9H (3H, **CH**, Aromatic).

*4.1.5.5.5 Polyaspartamide **22***

This polymer was synthesized as polyaspartamide **18** (section 4.1.5.5.1), PSI (304 mg, 3.099 mmol), dopamine (56.9 mg, 0.3719 mmol), TEA (37.6 mg, 0.3719 mmol) and APM (505 mg, 3.500 mmol) were reacted and yielded 476 mg (63.5%) of polyaspartamide **22** as a brownish water-soluble solid; η_{inh} (H_2O): 13.5 $mL.g^{-1}$.

^1H NMR (D_2O), (Appendix 1t), δ/ppm (expected proton counts in parentheses): 1.8-1.5, 18H (18H, CH_2**CH_2**CH_2); 3.0-2.2, 76H (76H,

CH_2CONH, **CH_2**N, Ar-**CH_2**); 3.4-3.0, 22H (20H, CONH**CH_2**); 3.9-3.6, 35.5H (36H, **CH_2**-O-**CH_2**); 4.7-4.6, 10H (10H, **CH**, Asp); 6.7-6.3, 3H (3H, **CH**, Aromatic).

*4.1.5.5.6 Polyaspartamide **23***

The procedure used to synthesized polyaspartamide **18** (section 4.1.5.5.1) was slightly modified in order to synthesize polyaspartamide **23** where two solubilizing groups were used instead of one.

Thus, PSI (306 mg, 3.120 mmol) was dissolved in DMF (10 mL) whilst stirring dopamine (106 g, 0.6864 mmol) and TEA (69.4 mg, 0.6864 mmol) in DMF (2 mL) were added. The resultant mixture was saturated with N_2, the flask tightly stoppered and stirred continuously for 1d at RT. Thereafter 1-(2-aminoethyl)pyridine (AEP: 190 mg, 1.560 mmol) in DMF (2 mL) was added to the stirred mixture and the reaction was allowed to continue for another 2d following re-saturation with N_2. In the last step DMP (127 mg, 1.248 mmol) in DMF (2 mL) was added, once again the flask was re-saturated with N_2 and the reaction continued for 1d. The resultant suspension was treated as previously described in section 4.1.5.5.1; such that the collected product was a brownish water-soluble solid in a yield of 453 mg (66.2%); η_{inh} (H_2O): 11.8 $mL.g^{-1}$.

^{1}H NMR (D_2O), (Appendix 1u), δ/ppm (expected proton counts in parentheses): 2.0-1.8, 6H (6H, CH_2**CH_2**CH_2); 3.7-2.2, 76H (78H, N**CH_3**, **CH_2**CONH, **CH_2**N, Ar-**CH_2**), CONH**CH_2**); 4.7-4.6, 9.6H (10H, **CH**, Asp); 6.8-6.4, 5.8H (6H, **CH**, Dopamine); 7.4-7.0, 9.8H (10H, **CH**, AEP ring); 7.8-7.5, 4.6H (5H, **CH**, AEP ring); 8.5-8.2, 4.9H (5H, **CH**, AEP ring).

4.1.6 Polymer platinum conjugation

The platination of the polymeric carriers was achieved as described in section 3.2, with several minor modifications where different platination agents were used depending on the type of carrier. For polyaspartamides **1**

to **5**, DACH-$PtCl_2$ was used, and DACH-PtCl-PABA was used for polyaspartamides **6** and **7**. For polymer carriers **8** to **23**, the platination agent was *trans*-1,2-diaminocyclohexane-diaquaplatinum(II)-dinitrate (DACH-Pt). The platination agents were prepared by literature methods[119,148] .

*4.1.6.1 Platination of polyaspartamides **1** to **5***

This group of polyaspartamides was platinated using Model 1 (Figure 3.1).

*4.1.6.1.1 Conjugate **1-Pt***

The light protected nitrogen-saturated solution (8 mL) of polyaspartamide **1** (200 mg, 0.0960 mmol) was treated with DACH-$PtCl_2$ (35.2 mg, 0.100 mmol). The resulting solution was stirred at RT for 3d, with the pH of the solution monitored and maintained at pH~6. The solution was then stirred for another 1d at 65^{o}C, with the pH carefully monitored and kept at pH~5-6. The solution was filtered and the filtrate dialyzed for 3d in 12 000-14 000 molecular mass cut-off limit tubing. The conjugate was isolated by freeze-drying as brownish water-soluble solid in a yield of 133 mg (58.1%); η_{inh} (H_2O): 12.1 mL.g^{-1}.

Anal. Calcd. for $(C_{101}H_{185}O_{21}N_{33}ClPt)_n$ $(2428.0)_n$ Pt (calcd), 8.03%; Pt (found), 7.32%.

*4.1.6.1.2 Conjugate **2-Pt***

The same procedure as described for conjugate **1-Pt** (section 4.1.6.1.1) was used for the synthesis of conjugate **2-Pt**. Polyaspartamide **2** (200 mg, 0.1022 mmol) was treated with DACH-$PtCl_2$ (39.6 mg, 0.1124 mmol) to afford conjugate **2-Pt** in a yield of 122 mg (52.5%) of brownish material; η_{inh} (H_2O): 10.9 mL.g^{-1}.

Anal. Calcd. for $(C_{92}H_{167}O_{21}N_{33}ClPt)_n$ $(2295.8)_n$ Pt (calcd), 8.50%; Pt (found), 7.83%.

*4.1.6.1.3 Conjugate **3-Pt***

The same procedure as described for conjugate **1-Pt** (section 4.1.6.1.1) was used for the synthesis of conjugate **3-Pt**. Polyaspartamide **3** (200 mg, 0.0905 mmol) and DACH-$PtCl_2$ (35.0 mg, 0.0995 mmol) reacted to afford conjugate **3-Pt** as a brownish water-soluble solid in a yield of 106 mg (46.7%); η_{inh} (H_2O): 12.6 $mL.g^{-1}$.

Anal. Calcd. for $(C_{110}H_{203}O_{21}N_{33}ClPt)_n$ $(2554.2)_n$ Pt (calcd), 7.63%; Pt (found), 7.13%.

*4.1.6.1.4 Conjugate **4-Pt***

The same procedure as described for conjugate **1-Pt** (section 4.1.6.1.1) was used for the synthesis of conjugate **4-Pt**. Carrier **4** (200 mg, 0.0856 mmol) and DACH-$PtCl_2$ (33.2 mg, 0.0942 mmol) reacted to afford conjugate **4-Pt** as a brownish water-soluble solid in a yield of 113 mg (49.8%); η_{inh} (H_2O): 13.1$mL.g^{-1}$.

Anal. Calcd. for $(C_{119}H_{221}O_{21}N_{33}ClPt)_n$ $(2680.5)_n$ Pt (calcd), 7.28%; Pt (found), 6.25%.

*4.1.6.1.5 Conjugate **5-Pt***

The same procedure as described for conjugate **1-Pt** (section 4.1.6.1.1) was used for the synthesis of conjugate **5-Pt**. Carrier **5** (200 mg, 0.08124 mmol) and DACH-$PtCl_2$ (31.5 mg, 0.0894 mmol) reacted to afford conjugate **5-Pt** as a brownish water-soluble solid in a yield of 108 mg (48.2%); η_{inh} (H_2O): 11.3$mL.g^{-1}$.

Anal. Calcd. for $(C_{119}H_{203}O_{30}N_{33}ClPt)_n$ $(2806.3)_n$ Pt (calcd), 6.95%; Pt (found), 5.67%.

*4.1.6.2 Platination of polyaspartamides **6-Pt** and **7-Pt***

Conjugates **6-Pt** and **7-Pt** were prepared by a different procedure as described for the previous conjugates using a coupling agent (EDC) and DACH-PtCl-PABA as platination agent according to Model 2 (Figure 3.1).

*4.1.6.2.1 Conjugate **6-Pt***

Conjugate **6-Pt** was prepared by reacting polyaspartamide **6** (200 mg, 0.2066 mmol) in water (5 mL) and DACH-PtCl-PABA (99.3 mg, 0.2273 mmol) dissolved in water (2 mL) in the presence of EDC (41.7 mg, 0.2066 mmol). The reaction was protected from light, saturated with N_2 and stirred at RT for 6h. Thereafter 20% EDC was added and the solution re-saturated with nitrogen and stirred for another 12h, and the pH of the solution was kept between pH 5 and 6. The solution was freeze-dried, the post-dried residue washed with hot acetone and re-dissolved in water (10 mL) and dialyzed in 12 000-14 000 molecular mass cut-off limit for 2d with a regular change of the outer water. The product was obtained after freeze drying as brownish water-soluble solid in a yield of 160 mg (55.4%); η_{inh} (H_2O): 10.8 $mL.g^{-1}$.

Anal. Calcd. for $(C_{56}H_{100}O_{11}N_{16}ClPt)_n$ $(1431.9)_n$ Pt (calcd), 13.62%; Pt (found), 2.12%.

*4.1.6.2.2 Conjugate **7-Pt***

Conjugate **7-Pt** was obtained by the same procedure as for conjugate **6-Pt**. Polyaspartamide **7** (200 mg, 0.1018 mmol), DACH-PtCl-PABA (48.9 mg, 0.1120 mmol) and EDC (20.5 mg, 0.1018 mmol) afforded 105 mg (43.2%) of a brownish water-soluble solid; η_{inh} (H_2O): 11.3 $mL.g^{-1}$.

Anal. Calcd. for $(C_{101}H_{185}O_{21}N_{33}ClPt)_n$ $(2428.0)_n$ Pt (calcd), 8.03%; Pt (found), 1.76%.

*4.1.6.3 Platination of polyaspartamides **8** to **12***

*4.1.6.3.1 Conjugate **8-Pt***

To the light protected and N_2 saturated solution of polyaspartamide **8** (200 mg, 0.09270 mmol) in H_2O (7 mL), DACH-Pt (45.0 mg, 0.1020 mmol) in H_2O (4 mL) was added. Upon re-saturation with nitrogen the solution was stirred for 3 d at RT with the pH of the solution maintained at ~5.5 – 6. The

reaction was then stirred for 2h at 55°C. The solution was filtered and dialyzed for 2d in 12 000-14 000 molecular mass cut-off limit 4 tubing. The retentate was freeze-dried, to afford 109 mg (48.5%) of a brownish water-soluble solid **8-Pt**; η_{inh} (H_2O): 13.4 $mL.g^{-1}$.

Anal. Calcd. for $(C_{103}H_{187}O_{24}N_{33}Pt)_n$ $(2464.6)_n$ Pt (calcd), 7.91%; Pt (found), 5.86%.

*4.1.6.3.2 Conjugate **9-Pt***

To the light protected and N_2 saturated solution of polyaspartamide **9** (200 mg, 0.09846 mmol), DACH-Pt (47.8 mg, 0.1083 mol) was added. The solution was treated and worked up as for conjugate **8-Pt** (section 4.1.6.3.1), giving conjugate **9-Pt** as a brownish water-soluble solid in a yield of 123 mg (49.6%); η_{inh} (H_2O): 12.1 $mL.g^{-1}$.

Anal. Calcd. for $(C_{94}H_{169}O_{24}N_{33}Pt)_n$ $(2338.3)_n$ Pt (calcd), 8.34%; Pt (found), 7.72%.

*4.1.6.3.3 Conjugate **10-Pt***

To the light protected and N_2 saturated solution of polyaspartamide **10** (200 mg, 0.0876 mmol), DACH-Pt (42.5 mg, 0.09636 mmol) was added. The solution was treated and worked up as for conjugate **8-Pt** (section 4.1.6.3.1), giving conjugate **10-Pt** as a brownish water-soluble solid in a yield of 118 mg (52.8%); η_{inh} (H_2O): 11.3 $mL.g^{-1}$.

Anal. Calcd. for $(C_{112}H_{205}O_{24}N_{33}Pt)_n$ $(2590.8)_n$ Pt (calcd), 7.53%; Pt (found), 6.13%.

*4.1.6.3.4 Conjugate **11-Pt***

To the light protected and N_2 saturated solution of polyaspartamide **11** (200 mg, 0.08299 mmol), DACH-Pt (40.3 mg, 0.09130 mmol) was added. The solution was treated and worked up as for conjugate **8-Pt** (section 4.1.6.3.1), giving conjugate **11-Pt** as a brownish water-soluble solid in a yield of 121 mg (54.3%); η_{inh} (H_2O): 12.8 $mL.g^{-1}$.

Anal. Calcd. for $(C_{121}H_{223}O_{24}N_{33}Pt)_n$ $(2717.0)_n$ Pt (calcd), 7.18%; Pt (found), 6.84%.

*4.1.6.3.5 Conjugate **12-Pt***

To the light protected and N_2 saturated solution of polyaspartamide **12** (200 mg, 0.07887 mmol), DACH-Pt (38.3 mg, 0.08676 mmol) was added. The solution was treated and worked up as for conjugate **8-Pt** (section 4.1.6.3.1), giving conjugate **12-Pt** as a brownish water-soluble solid in a yield of 97.9 mg (44.1%); η_{inh} (H_2O): 12.6 $mL.g^{-1}$.

Anal. Calcd. for $(C_{121}H_{169}O_{33}N_{33}Pt)_n$ $(2842.9)_n$ Pt (calcd), 6.86%; Pt (found), 6.31%.

*4.1.6.4 Platination of polyaspartamides **13** to **17***

*4.1.6.4.1 Conjugate **13-Pt***

To a stirred aqueous solution (7 mL) of polyaspartamide **13** (200 mg, 0.09210 mmol), saturated with N_2 and light protected, DACH-Pt (44.7 mg, 0.1013 mmol) was added. The solution was re-saturated with nitrogen, stirred for 3d at RT and then stirred for another 2h in the incubator at 55^0C. During the process, the pH was carefully monitored and maintained at pH~5.5 - 6. The routinely filtered solution was dialyzed in 12 000-14 000 molecular mass cut-off limit tubing for 2d, and the conjugate isolated as a brownish water-soluble solid by freeze-drying in a yield of 116 mg (51.2%); η_{inh} (H_2O): 11.5 $mL.g^{-1}$.

Anal. Calcd. for $(C_{104}H_{189}O_{24}N_{33}Pt)_n$ $(2478.6)_n$ Pt (calcd), 7.87%; Pt (found), 7.23%.

*4.1.6.4.2 Conjugate **14-Pt***

To a stirred aqueous solution of polyaspartamide **14** (200 mg, 0.09779 mmol), saturated with N_2 and light protected, DACH-Pt (47.5 mg, 0.1076 mmol) was added. The solution was treated and worked up as for conjugate

13-Pt (section 4.1.6.4.1), and conjugate **14-Pt** was afforded as a brownish water-soluble solid in a yield of 96.1 mg (42.3%); η_{inh} (H_2O): 9.8 $mL.g^{-1}$.
Anal. Calcd. for $(C_{95}H_{171}O_{24}N_{33}Pt)_n$ $(2352.4)_n$ Pt (calcd), 8.29%; Pt (found), 6.92%.

*4.1.6.4.3 Conjugate **15-Pt***

To a stirred aqueous solution of polyaspartamide **15** (200 mg, 0.08704 mmol), saturated with N_2 and light protected, DACH-Pt (42.2 mg, 0.09574 mmol) was added. The solution was treated and worked up as for conjugate **13-Pt** (section 4.1.6.4.1), and conjugate **15-Pt** was afforded as a brownish water-soluble solid in a yield of 110 mg (49.2%); η_{inh} (H_2O): 12.3 $mL.g^{-1}$.
Anal. Calcd. for $(C_{113}H_{207}O_{24}N_{33}Pt)_n$ $(2604.8)_n$ Pt (calcd), 7.49%; Pt (found), 5.78%.

*4.1.6.4.4 Conjugate **16-Pt***

To a stirred aqueous solution of polyaspartamide **16** (200 mg, 0.8251 mmol), saturated with N_2 and light protected, DACH-Pt (40.0 mg, 0.09076 mmol) was added. The solution was treated and worked up as for conjugate **13-Pt** (section 4.1.6.4.1), giving conjugate **16-Pt** as a brownish water-soluble solid in a yield of 123 mg (55.5%). η_{inh} (H_2O): 13.1 $mL.g^{-1}$.
Anal. Calcd. for $(C_{121}H_{225}O_{24}N_{33}Pt)_n$ $(2731.1)_n$ Pt (calcd), 7.14%; Pt (found), 6.05%.

*4.1.6.4.5 Conjugate **17-Pt***

To a stirred aqueous solution of polyaspartamide **17** (200 mg, 0.07844 mmol), DACH-Pt (38.1 mg, 0.08628 mmol) was added. The solution was treated and worked up as for conjugate **13-Pt** (section 4.1.6.4.1) and afforded a brownish water-soluble solid conjugate **17-Pt** in a yield of 116 mg (52.6%); η_{inh} (H_2O): 12.3 $mL.g^{-1}$.
Anal. Calcd. for $(C_{122}H_{171}O_{33}N_{33}Pt)_n$ $(2856.9)_n$ Pt (calcd), 6.83%; Pt (found), 6.12%.

*4.1.6.5 Platination of polyaspartamides **18** to **23***

*4.1.6.5.1 Conjugate **18-Pt***

The light protected solution of polyaspartamide **18** (200 mg, 0.09788 mmol) was treated with a solution of DACH-Pt (47.5 mg, 0.1077 mmol). The solution was treated and worked up as for conjugate **13-Pt** (section 4.1.6.4.1) and afforded conjugate **18-Pt** as a brown water-soluble solid in a yield of 129 mg (56.8%); η_{inh} (H_2O): 14.2 $mL.g^{-1}$.

Anal. Calcd. for $(C_{99}H_{183}O_{22}N_{31}Pt)_n$ $(2350.5)_n$ Pt (calcd), 8.30%; Pt (found), 6.89%.

*4.1.6.5.2 Conjugate **19-Pt***

The light protected solution of polyaspartamide **19** (200 mg, 0.1043 mmol) was treated with a solution of DACH-Pt (50.6 mg, 0.1147 mmol). The solution was treated and worked up as for conjugate **13-Pt** (section 4.1.6.4.1). The brown water-soluble solid conjugate **19-Pt** was isolated in a yield of 113 mg (49.6%); η_{inh} (H_2O): 13.4 $mL.g^{-1}$.

Anal. Calcd. for $(C_{90}H_{165}O_{22}N_{31}Pt)_n$ $(2224.2)_n$ Pt (calcd), 8.77%; Pt (found), 8.01%.

*4.1.6.5.3 Conjugate **20-Pt***

The light protected solution of polyaspartamide **20** (200 mg, 0.09219 mmol) was treated with a solution of DACH-Pt (44.8 mg, 0.1014 mmol). The solution was treated and worked up as for conjugate **13-Pt** (section 4.1.6.4.1). The brown water-soluble conjugate **20-Pt** was afforded in a yield of 109 mg (48.3%); η_{inh} (H_2O): 11.1 $mL.g^{-1}$.

Anal. Calcd. for $(C_{108}H_{201}O_{22}N_{31}Pt)_n$ $(2476.9)_n$ Pt (calcd), 7.87%; Pt (found), 7.52%.

*4.1.6.5.4 Conjugate **21-Pt***

The light protected solution of polyaspartamide **21** (200 mg, 0.08712 mmol) was treated with a solution of DACH-Pt (42.3 mg, 0.09583 mmol). The

solution was treated and worked up as for conjugate **13-Pt** (section 4.1.6.4.1), and afforded conjugate **21-Pt** in a yield of 115 mg (51.6%) as brown water-soluble material; η_{inh} (H_2O): 13.6 $mL.g^{-1}$.
Anal. Calcd. for $(C_{117}H_{219}O_{22}N_{31}Pt)_n$ $(2602.9)_n$ Pt (calcd), 7.49%; Pt (found), 6.26%.

*4.1.6.5.5 Conjugate **22-Pt***
The light protected solution of polyaspartamide **22** (200 mg, 0.08259 mmol) was treated with a solution of DACH-Pt (40.1 mg, 0.09085 mmol). The solution was treated and worked up as for conjugate **13-Pt** (section 4.1.6.4.1), and gave conjugate **22-Pt** as a brown water-soluble solid in a yield of 94 mg (42.3%); η_{inh} (H_2O): 11.6 $mL.g^{-1}$.
Anal. Calcd. for $(C_{117}H_{165}O_{31}N_{31}Pt)_n$ $(2728.2)_n$ Pt (calcd), 7.15%; Pt (found), 6.04%.

*4.1.6.5.6 Conjugate **23-Pt***
The light protected solution of polyaspartamide **23** (200 mg, 0.09115 mmol) was treated with a solution of DACH-Pt (44.2 mg, 0.1002 mmol). The solution was treated and worked up as for conjugate **13-Pt** (section 4.1.6.4.1), and gave a brown water-soluble conjugate **23-Pt** in a yield of 105 mg (46.8%); η_{inh} : 10.7 $mL.g^{-1}$.
Anal. Calcd. for $(C_{59}H_{81}O_{17}N_{16}Pt)_n$ $(1481.3)_n$ Pt (calcd), 13.17%; Pt (found), 9.43%.

4.1.7 Synthesis of co-conjugates

Polymer-drug co-conjugation was a major part of this work with two drugs. Ferrocene and platinum derivatives were used. The conjugates were synthesized in a two-step process. The first step consisted of the incorporation of ferrocene to the polymeric carrier *via* aminolytic ring opening of the succinimide, a novel route developed in this study for

ferrocene incorporation. The anchoring of the second drug, platinum derivatives, was brought about by the method as described in section 4.1.6.

*4.1.7.1 Conjugates **24-Fc** to **28-Fc***

*4.1.7.1.1 Conjugate **24-Fc***

Fc-PDA (101 mg, 0.3069 mmol) in DMF (2 mL) was added dropwise with stirring to PSI (301 mg, 3.069 mmol) dissolved in DMF (8 mL). The solution was saturated with nitrogen and stirred for 1d at RT. Then PABA-PDA (59.3 mg, 0.3069 mmol) and TEA (31.0 mg, 0.3069 mmol) in DMF (5 mL) was added to the stirred solution at ice-water bath temperature. The solution was re-saturated with nitrogen and stirred for 2d in ice-water bath. Then DMP (357 mg, 3.500 mmol) in DMF (3 mL) was added dropwise to the stirred solution before being re-saturated with N_2 and stirred for another 1d at RT. The solution was concentrated on a rotary evaporator and the product obtained by precipitation with ether:hexane (2:1). The precipitate was firstly washed with the precipitant, then with hot acetone. The precipitate was dissolved in water (15 mL), before the pH was adjusted to pH~7.5-8 with conc. HCl. The solution was dialyzed for 3d in 12 000-14 000 molecular mass cut-off limit tubing. The retentate was freeze dried to give 457 mg (67.1%) of **24-Fc** as a yellow water-soluble solid; η_{inh} (H_2O): 15.2 $mL.g^{-1}$.
Anal. Calcd. for $(C_{107}H_{181}O_{22}N_{31}Fe)_n$ $(2309.36)_n$ Fe (calcd), 2.41%; Fe (found), 2.32%.

*4.1.7.1.2 Conjugate **25-Fc***

Conjugate **25-Fc** was prepared using the same procedure as for conjugate **24-Fc** (section 4.1.7.1.1). Thus, PSI (306 mg, 3.120 mmol), Fc-PDA (103 mg, 0.3120 mmol), PABA-PDA (60.3 mg, 0.3120 mmol), TEA (31.6 mg, 0.3120) and DMEA (308 mg, 3.500 mmol) afforded conjugate **25-Fc** in a yield of 421 mg (61.4%) as yellow water-soluble material; η_{inh} (H_2O): 12.6 $mL.g^{-1}$.

Anal. Calcd. for $(C_{97}H_{165}O_{22}N_{31}Fe)_n$ $(2197.16)_n$ Fe (calcd), 2.54%; Fe (found), 2.41%.

*4.1.7.1.3 Conjugate **26-Fc***

Conjugate **26-Fc** was prepared using the same procedure as for conjugate **24-Fc** (section 4.1.7.1.1). DMP was replaced by 2-(diethylamino)ethylamine (DEEA). PSI (305 mg, 3.110 mmol), Fc-PDA (102 mg, 0.3110 mmol), PABA-PDA (60.1 mg, 0.3110 mmol), TEA (31.5 mg, 0.3110 mmol) and DEEA (407 mg, 3.500 mmol) were allowed to react under the same reaction conditions. This gave the conjugate **26-Fc** in yield of 397 mg (52.7%) as yellow water-soluble material, η_{inh} (H_2O): 13.5 $mL.g^{-1}$.

Anal. Calcd. for $(C_{115}H_{197}O_{22}N_{31}Fe)_n$ $(2421.57)_n$ Fe (calcd), 2.30%; Fe (found), 2.18%.

*4.1.7.1.4 Conjugate **27-Fc***

Conjugate **27-Fc** was prepared using the same procedure as for conjugate **24-Fc** (section 4.1.7.1.1). PSI (304 mg, 3.099 mmol), Fc-PDA (102 mg, 0.3099 mmol), PABA-PDA (59.9 mg, 0.3099 mmol), TEA (31.4 mg, 0.3099 mmol) and DEP (456 mg, 3.500 mmol). Conjugate **27-Fc** was obtained in a yield of 457 mg (58.3%) as yellow water-soluble material, η_{inh} (H_2O): 12.4 $mL.g^{-1}$.

Anal. Calcd. for $(C_{123}H_{213}O_{22}N_{31}Fe)_n$ $(2533.78)_n$ Fe (calcd), 2.20%; Fe (found), 2.07%.

*4.1.7.1.5 Conjugate **28-Fc***

Conjugate **28-Fc** was prepared using the same procedure as for conjugate **24-Fc** (section 4.1.7.1.1). PSI (306 mg, 3.120 mmol), Fc-PDA (103 mg, 0.3120 mmol), PABA-PDA (60.3 mg, 0.3120 mmol), TEA (31.6 mg, 0.3120 mmol) and APM (512 mg, 3.550 mmol) were reacted. The conjugate was obtained in a yield of 515 mg (62.4%) as yellow water-soluble material, η_{inh} (H_2O): 11.6 $mL.g^{-1}$.

Anal. Calcd. for $(C_{123}H_{197}O_{30}N_{31}Fe)_n$ $(2645.65)_n$ Fe (calcd), 2.11%; Fe (found), 1.98%.

*4.1.7.2 Conjugates **29-Fc** to **33-Fc***

*4.1.7.2.1 Conjugate **29-Fc***

To a stirred and nitrogen saturated solution of PSI (300 mg, 3.059 mmol) dissolved in DMF (8 mL), Fc-PDA (101 mg, 0.3059 mmol) in DMF (3 mL) was added. The solution was re-saturated with N_2 and allowed to proceed for 1d at RT. Then PASA-PDA (81.8 mg, 0.3059 mmol) and TEA (31.0 mg, 0.3059 mmol) in DMF (2 mL) was added, and the solution re-saturated with N_2; before being stirred for another 1d at RT. Lastly, DMP (357 mg, 3.500 mmol) in DMF (2 mL) was added; and then re-saturated with N_2 and stirring continued for 1d. The work up and the purification process were similar to that described before (section 4.1.7.1.1). This process afforded 410 mg (56.3%) of a yellow water-soluble polymer; η_{inh} (H_2O): 14.3 $mL.g^{-1}$.

Anal. Calcd. for $(C_{109}H_{183}O_{25}N_{31}Fe)_n$ $(2383.40)_n$ Fe (calcd), 2.34%; Fe (found), 2.14%.

*4.1.7.2.2 Conjugate **30-Fc***

Conjugate **30-Fc** was prepared using the same procedure as for conjugate **29-Fc** (section 4.1.7.2.1). PSI (301 mg, 3.069 mmol), Fc-PDA (101 mg, 0.3069 mmol), PASA-PDA (82.0 mg, 0.3069 mmol), TEA (31.0 mg, 0.3069 mmol) and DMEA (308 mg, 3.500 mmol) were used. This afforded 347 mg (49.8%) of conjugate **30-Fc** as a yellow water-soluble solid; η_{inh} (H_2O): 12.3 $mL.g^{-1}$.

Anal. Calcd. for $(C_{99}H_{167}O_{25}N_{31}Fe)_n$ $(2271.19)_n$ Fe (calcd), 2.45%; Fe (found), 2.32%.

*4.1.7.2.3 Conjugate **31-Fc***

Conjugate **31-Fc** was prepared using the same procedure as for conjugate **29-Fc** (section 4.1.7.2.1). PSI (305 mg, 3.110 mmol), Fc-PDA (102 mg, 0.3110 mmol), PASA-PDA (83.1 mg, 0.3110 mmol), TEA (31.5 mg, 0.3110 mmol) and DEEA (412 mg, 3.550 mmol) were allowed to react; this resulted in conjugate **31-Fc** as yellow water-soluble solid in a yield of 461 mg (59.5%); η_{inh} (H_2O): 13.8 $mL.g^{-1}$.

Anal. Calcd. for $(C_{117}H_{199}O_{25}N_{31}Fe)_n$ $(2495.61)_n$ Fe (calcd), 2.23%; Fe (found), 2.06%.

*4.1.7.2.4 Conjugate **32-Fc***

Conjugate **32-Fc** was prepared using the same procedure as for conjugate **29-Fc** (section 4.1.7.2.1). PSI (308 mg, 3.140 mmol), Fc-PDA (103 mg, 0.3140 mmol), PASA-PDA (83.9 mg, 0.3140 mmol), TEA (31.8 mg, 0.3140 mmol) and DEP (462 mg, 3.550 mmol) were reacted. The resultant solution was treated and worked up as before. Conjugate **32-Fc** was obtained as a yellow water-soluble solid in a yield of 444 mg (54.3%); η_{inh} (H_2O): 10.7 $mL.g^{-1}$.

Anal. Calcd. for $(C_{125}H_{215}O_{25}N_{31}Fe)_n$ $(2607.81)_n$ Fe (calcd), 2.14%; Fe (found), 2.02%.

*4.1.7.2.5 Conjugate **33-Fc***

Conjugate **33-Fc** was prepared using the same procedure as for conjugate **29-Fc** (section 4.1.7.2.1). PSI (307 mg, 3.130 mmol), Fc-PDA (103 mg, 0.3130 mmol), PASA-PDA (83.6 mg, 0.3130 mmol), TEA (31.7 mg, 0.3130 mmol) and APM (512 mg, 3.550 mmol) were allowed to react, and this afforded a yellow water-soluble solid in a yield of 539 mg (63.4%); η_{inh} (H_2O): 13.1 $mL.g^{-1}$.

Anal. Calcd. for $(C_{125}H_{199}O_{33}N_{31}Fe)_n$ $(2719.69)_n$ Fe (calcd), 2.05%; Fe (found), 1.89%.

*4.1.7.3 Conjugates **34-Fc** to **38-Fc***

Conjugates **34-Fc** to **38-Fc** were obtained by the same procedure used to prepare conjugate **29-Fc**, with PASA-PDA being replaced by PASA-EDA; the reactions conditions were maintained.

*4.1.7.3.1 Conjugate **34-Fc***

Conjugate **34-Fc** was prepared using the same procedure as for conjugate **29-Fc** (section 4.1.7.2.1). PSI (303 mg, 3.089 mmol), Fc-PDA (102 mg, 0.3089 mmol), PASA-EDA (86.9 g, 0.3089 mmol), TEA (31.3 mg, 0.3089 mmol) and DMP (357 mg, 3.500 mmol) were used. The reaction mixture was treated and worked up as before. The conjugate was isolated as a yellow water-soluble solid in a yield of 445 mg (60.1%); η_{inh} (H_2O): 12.4 $mL.g^{-1}$.

Anal. Calcd. for $(C_{110}H_{185}O_{25}N_{31}Fe)_n$ $(2397.42)_n$ Fe (calcd), 2.33%; Fe (found), 2.19%.

*4.1.7.3.2 Conjugate **35-Fc***

Conjugate **35-Fc** was prepared using the same procedure as for conjugate **29-Fc** (section 4.1.7.2.1). PSI (304 mg, 3.099 mmol), Fc-PDA (102 mg, 0.3099 mmol), PASA-EDA (87.2 mg, 0.3099 mmol), TEA (31.4 mg, 03099 mmol) and DMEA (308 mg, 3.500 mmol) were used. The yellow water-soluble polymer was in a yield of 401 mg (56.7%); η_{inh} (H_2O): 11.3 $mL.g^{-1}$.

Anal. Calcd. for $(C_{100}H_{169}O_{25}N_{31}Fe)_n$ $(2285.22)_n$ Fe (calcd), 2.44%; Fe (found), 2.30%.

*4.1.7.3.3 Conjugate **36-Fc***

Conjugate **36-Fc** was prepared using the same procedure as for conjugate **29-Fc** (section 4.1.7.2.1). PSI (302 g, 3.079 mmol), Fc-PDA (101 mg, 0.3079 mmol), PASA-EDA (86.6 mg, 0.3079 mmol), TEA (31.1 mg, 0.3079 mmol) and DEEA (406 mg, 3.500 mmol) were used. The solution was

treated and worked up as before. The yield was 405 mg (52.4%) of a yellow water-soluble solid; η_{inh} (H_2O): 9.6 $mL.g^{-1}$.

Anal. Calcd. for $(C_{118}H_{201}O_{25}N_{31}Fe)_n$ $(2509.63)_n$ Fe (calcd), 2.22%; Fe (found), 2.07%.

*4.1.7.3.4 Conjugate **37-Fc***

Conjugate **37-Fc** was prepared using the same procedure as for conjugate **29-Fc** (section 4.1.7.2.1). PSI (301 mg, 3.069 mmol), Fc-PDA (101 mg, 0.3069 mmol), PASA-EDA (86.3 mg, 0.3069 mmol), TEA (31.0 mg, 0.3069 mmol) and DEP (456 mg, 3.500 mmol) were used. The solution was treated and worked up as before, and afforded 468 mg (58.2%) of a yellow water-soluble solid; η_{inh} (H_2O): 12.1 mL/g.

Anal. Calcd. for $(C_{126}H_{217}O_{25}N_{31}Fe)_n$ $(2621.84)_n$ Fe (calcd), 2.13%; Fe (found), 2.01%.

*4.1.7.3.5 Conjugate **38-Fc***

Conjugate **38-Fc** was prepared using the same procedure as for conjugate **29-Fc** (section 4.1.7.2.1). PSI (304 mg, 3.099 mmol), Fc-PDA (102 mg, 0.3099 mmol), PASA-EDA (87.2 mg, 0.3099 mmol), TEA (31.4 mg, 0.3099 mmol) and APM (504 mg, 3.500 mmol) were used and the solution was treated and worked up as before, giving 522 mg (61.7%) of a yellow water-soluble solid; η_{inh} (H_2O): 13.6 $mL.g^{-1}$.

Anal. Calcd. for $(C_{126}H_{201}O_{33}N_{31}Fe)_n$ $(2733.71)_n$ Fe (calcd), 2.04%; Fe (found), 1.93%.

*4.1.7.4 Conjugates **39-Fc** to **43-Fc***

*4.1.7.4.1 Conjugate **39-Fc***

To the stirred solution of PSI (305 mg, 3.110 mmol) in DMF (15 mL), dopamine (47.6 mg, 0.3110 mmol) in DMF (2 mL) and TEA (31.4 mg, 0.3110 mmol) were added. The resulting solution was saturated with N_2 and

was stirred for 2d at RT. Fc-PDA (102 mg, 0.3110 mmol) was added and the solution re-saturated with N_2, then stirred for another 2d. DMP (357 mg, 3.500 mmol) dissolved in DMF (3 mL) was added whilst stirring, and following re-saturation with N_2 the solution was stirred for another 2d at RT. The solution was concentrated on a rotary evaporator under reduced pressure at 65^{o}C, and the polymeric product was precipitated with Et_2O:hexane (2:1). The precipitate was washed with precipitant then hot acetone; the solid was dissolved in H_2O (15 mL) and the pH was adjusted to pH~8 with conc. HCl. The solution was dialyzed for 3d in 12 000-14 000 molecular mass cut-off limit tubing. Freeze-drying of the retentate gave 466 mg (66.1%) of brown water-soluble solid polymer; η_{inh} (H_2O): 11.3 mL.g^{-1}.
Anal. Calcd. for $(C_{105}H_{177}O_{23}N_{29}Fe)_n$ $(2269.30)_n$ Fe (calcd), 2.46%; Fe (found), 2.34%.

*4.1.7.4.2 Conjugate **40-Fc***

Conjugate **40-Fc** was prepared using the same procedure as for conjugate **39-Fc** (section 4.1.7.4.1). PSI (306 mg, 3.120 mmol), dopamine (47.8 mg, 0.3120 mmol), TEA (31.6 mg, 0.3120 mmol), Fc-PDA (103 mg, 0.3120 mmol) and DMEA (313 mg, 3.550 mmol) were reacted and the process afforded the brown water-soluble conjugate **40-Fc** in a yield of 395 mg (58.7%); η_{inh} (H_2O): 11.7 mL.g^{-1}.
Anal. Calcd. for $(C_{95}H_{161}O_{23}N_{29}Fe)_n$ $(2157.09)_n$ Fe (calcd), 2.59%; Fe (found), 2.41%.

*4.1.7.4.3 Conjugate **41-Fc***

Conjugate **41-Fc** was prepared using the same procedure as for conjugate **39-Fc** (section 4.1.7.4.1). PSI (307 mg, 3.130 mmol), dopamine (48.0 mg, 0.3130 mmol), TEA (31.7 mg, 0.3130 mmol), Fc-PDA (103 mg, 0.3130 mmol) and DEEA (412 mg, 3.550 mmol) were reacted and worked up as before. The process afforded 399 mg (53.6%) of conjugate **41-Fc** as a brown water-soluble solid; η_{inh} (H_2O): 12.5 mL.g^{-1}.

Anal. Calcd. for $(C_{113}H_{193}O_{23}N_{29}Fe)_n$ $(2381.51)_n$ Fe (calcd), 2.34%; Fe (found), 2.19%.

*4.1.7.4.4 Conjugate **42-Fc***

Conjugate **42-Fc** was prepared using the same procedure as for conjugate **39-Fc** (section 4.1.7.4.1). PSI (306 mg, 3.120 mmol), Dopamine (47.8 mg, 0.3120 mmol), TEA (31.6 mg, 0.3120 mmol), Fc-PDA (103 mg, 0.3120 mmol) and DEP (456 mg, 3.500 mmol) were allowed to react, and afforded 430 mg (55.3%) of a brown water-soluble solid; η_{inh} (H_2O): 14.2 $mL.g^{-1}$.

Anal. Calcd. for $(C_{121}H_{209}O_{23}N_{29}Fe)_n$ $(2493.71)_n$ Fe (calcd), 2.24%; Fe (found), 2.13%.

*4.1.7.4.5 Conjugate **43-Fc***

Conjugate **43-Fc** was prepared using the same procedure as for conjugate **39-Fc** (section 4.1.7.4.1). PSI (301 mg, 3.069 mmol), dopamine (47.0 mg, 0.3069 mmol), TEA (31.0 mg, 0.3069 mmol), Fc-PDA (101 mg, 0.3069 mmol) and APM (505 mg, 3.500 mmol) reacted and afforded 422 mg (52.8%) of conjugate **43-Fc** as a brown water-soluble solid; η_{inh} (H_2O): 12.4 $mL.g^{-1}$.

Anal. Calcd. for $(C_{121}H_{193}O_{31}N_{29}Fe)_n$ $(2605.59)_n$ Fe (calcd), 2.14%; Fe (found), 2.01%.

*4.1.7.5 Conjugates **44-Fc** to **48-Fc***

*4.1.7.5.1 Conjugate **44-Fc***

To a N_2 saturated solution of PSI (300 mg, 3.059 mmol) dissolved in DMF (8 mL) Fc-PDA (101 mg, 0.3059 mmol) in DMF (3 mL) was added. The solution was re-saturated with N_2 and stirred for 1d at RT. Then ACRYASP-PDA (79.6 mg, 0.3059 mmol) and TEA (31.0 mg, 0.3059 mmol) in DMF (2 mL) were added. The solution was re-saturated with N_2 and stirred for another 2d at RT. Lastly, DMP (357 mg, 3.500 mmol) in DMF (2 mL) was

added before the reaction was re-saturated with nitrogen and stirred for 1d at RT. The work up and the purification process were similar to those described in section 4.1.7.4.1. This process afforded 446 mg (61.4%) of a yellow water-soluble polymer; η_{inh} (H_2O): 10.3 $mL.g^{-1}$.

Anal. Calcd. for $(C_{107}H_{185}O_{26}N_{31}Fe)_n$ $(2377.40)_n$ Fe (calcd), 2.35%; Fe (found), 2.13%.

*4.1.7.5.2 Conjugate **45-Fc***

Conjugate **45-Fc** was prepared using the same procedure as for conjugate **44-Fc** (section 4.1.7.5.1). PSI (302 mg, 3.079 mmol), Fc-PDA (101 mg, 0.3079 mmol), ACRYASP-PDA (80.1 mg, 0.3079 mmol), TEA (31.2 mg, 0.3079 mmol) and DMEA (308 mg, 3.500 mmol) were used. This afforded 490 mg (70.3%) of conjugate **45-Fc** as a yellow water-soluble solid; η_{inh} (H_2O): 12.3 $mL.g^{-1}$.

Anal. Calcd. for $(C_{97}H_{169}O_{26}N_{31}Fe)_n$ $(2265.19)_n$ Fe (calcd), 2.46%; Fe (found), 2.21%.

*4.1.7.5.3 Conjugate **46-Fc***

Conjugate **46-Fc** was prepared using the same procedure as for conjugate **44-Fc** (section 4.1.7.5.1). PSI (308 mg, 3.140 mmol), Fc-PDA (103 mg, 0.3140 mmol), ACRYASP-PDA (81.7 mg, 0.3140 mmol), TEA (31.8 mg,0.3140 mmol) and DEEA (412 mg, 3.550 mmol) were allowed to react; this resulted in conjugate **46-Fc** as yellow water-soluble solid in a yield of 439 mg (56.2%), and η_{inh} (H_2O): 10.2 $mL.g^{-1}$.

Anal. Calcd. for $(C_{115}H_{201}O_{26}N_{31}Fe)_n$ $(2489.60)_n$ Fe (calcd), 2.24%; Fe (found), 2.08%.

*4.1.7.5.4 Conjugate **47-Fc***

Conjugate **45-Fc** was prepared using the same procedure as for conjugate **44-Fc** (section 4.1.7.5.1). PSI (309 mg, 3.150 mmol), Fc-PDA (104 mg, 0.315 mmol), ACRYASP-PDA (82.0 mg, 0.3150 mmol), TEA (31.9 mg,

0.3150) and DEP (462 mg, 3.550 mmol) were reacted. The resultant solution was treated and worked up as before. Conjugate **47-Fc** was obtained as a yellow water-soluble solid in a yield of 445 mg (54.3%); η_{inh} (H_2O): 11.2 $mL.g^{-1}$.

Anal. Calcd. for $(C_{123}H_{217}O_{26}N_{31}Fe)_n$ $(2601.81)_n$ Fe (calcd), 2.14%; Fe (found), 1.98%.

*4.1.7.5.5 Conjugate **48-Fc***

Conjugate **45-Fc** was prepared using the same procedure as for conjugate **44-Fc** (section 4.1.7.5.1). PSI (306 mg, 3.120 mmol), Fc-PDA (103 mg, 0.3120 mmol), ACRYASP-PDA (81.2 mg, 0.3120 mmol), TEA (31.6 mg, 0,3120 mmol) and APM (512 mg, 3.550 mmol) were allowed to react, and this afforded a yellow water-soluble solid in a yield of 486 mg (57.4%); η_{inh} (H_2O): 10.6 $mL.g^{-1}$.

Anal. Calcd. for $(C_{123}H_{201}O_{34}N_{31}Fe)_n$ $(2713.68)_n$ Fe (calcd), 2.06%; Fe (found), 1.87%.

*4.1.7.6 Co-conjugates **24-Fc/Pt** to **28-Fc/Pt***

*4.1.7.6.1 Co-conjugate **24-Fc/Pt***

The light protected, N_2-saturated solution (8 mL) of conjugate **24-Fc** (200 mg, 0.09016 mmol) was treated with DACH-$PtCl_2$ (35.2 mg, 0.100 mmol). The resulting solution was stirred at RT for 3d with the pH of the solution monitored and maintained at pH~6. The solution was then stirred for another 1d at 65 ^{0}C, with the pH carefully monitored and kept at pH~5-6. The solution was filtered and the filtrate dialyzed for 3d in 12 000-14 000 molecular mass cut-off limit tubing. The conjugate was isolated by freeze-drying as a brown water-soluble solid in a yield of 117 mg (51.2%); η_{inh} (H_2O): 10.6 $mL.g^{-1}$.

Anal. Calcd. for $(C_{113}H_{195}O_{22}N_{33}ClFePt)_n$ $(2654.06)_n$ Fe: (calcd) 2.10%, (found) 1.97%; Pt: (calcd) 7.35%, (found) 6.93%.

*4.1.7.6.2 Co-conjugate **25-Fc/Pt***

The same procedure as described for co-conjugate **24-Fc/Pt** (section 4.1.7.6.1) was followed for the preparation of co-conjugate **25-Fc/Pt**. Conjugate **25-Fc** (201 mg, 0.09148 mmol) was treated with DACH-$PtCl_2$ (35.4 mg, 0.1006 mmol) to afford co-conjugate **25-Fc/Pt** in a yield of 106 mg (46.3%) as brown water-soluble mayerial; η_{inh} (H_2O): 12.1 $mL.g^{-1}$.

Anal. Calcd. for $(C_{103}H_{179}O_{22}N_{33}ClFePt)_n$ $(2541.84)_n$ Fe: (calcd) 2.19%, (found) 2.04%; Pt: (calcd) 7.67%, (found) 7.24%.

*4.1.7.6.3 Co-conjugate **26-Fc/Pt***

The same procedure as described for co-conjugate **24-Fc/Pt** (section 4.1.7.6.1) was followed for the preparation of co-conjugate **26-Fc/Pt**. Conjugate **26-Fc** (203 mg, 0.08383 mmol) and DACH-$PtCl_2$ (32.5 mg, 0.09221 mmol) reacted to afford co-conjugate **26-Fc/Pt** as a brown water-soluble solid in a yield of 113 mg (49.5%); η_{inh} (H_2O): 11.2 $mL.g^{-1}$.

Anal. Calcd. for $(C_{121}H_{211}O_{22}N_{33}ClFePt)_n$ $(2766.27)_n$ Fe: (calcd) 2.02%, (found) 1.86%; Pt: (calcd) 7.05%, (found) 6.81%.

*4.1.7.6.4 Co-conjugate **27-Fc/Pt***

The same procedure as described for co-conjugate **24-Fc/Pt** (section 4.1.7.6.1) was followed for the preparation of co-conjugate **27-Fc/Pt**. Conjugate **27-Fc** (202 mg, 0.07972 mmol) and DACH-$PtCl_2$ (30.9 mg, 0.8769 mmol) reacted to afford co-conjugate **27-Fc/Pt** as a brown water-soluble solid in a yield of 119 mg (52.6%); η_{inh} (H_2O): 13.2 $mL.g^{-1}$.

Anal. Calcd. for $(C_{129}H_{227}O_{22}N_{33}ClFePt)_n$ $(2878.48)_n$ Fe: (calcd) 1.94%, (found) 1.70%; Pt: (calcd) 6.78%, (found) 6.46%.

*4.1.7.6.5 Co-conjugate **28-Fc/Pt***

The same procedure as described for co-conjugate **24-Fc/Pt** (section 4.1.7.6.1) was followed for the preparation of co-conjugate **28-Fc/Pt**. Conjugate **28-Fc** (201 mg, 0.07597 mmol) and DACH-$PtCl_2$ (29.4 mg,

0.8356 mmol) reacted to afford co-conjugate **28-Fc/Pt** as a brown water-soluble solid in a yield of 113 mg (52.6%); η_{inh} (H_2O): 9.8 $mL.g^{-1}$.
Anal. Calcd. for $(C_{129}H_{211}O_{33}N_{33}ClFePt)_n$ $(2990.35)_n$ Fe: (calcd) 1.86%, (found) 168%; Pt: (calcd) 6.52%, (found) 6.19%.

*4.1.7.7 Co-conjugates **29-Fc/Pt** to **48-Fc/Pt***

The experimental details which follow describe the standard procedure adopted for the platination of conjugates **29-Fc/Pt** to **48-Fc/Pt** using *trans*-1,2-diaminocyclohexanediaquaplatinum(II)-dinitrate (DACH-Pt).

*4.1.7.7.1 Co-conjugate **29-Fc/Pt:***

To the light protected and N_2 saturated solution of conjugate **29-Fc** (204 mg, 0.08559 mmol) in H_2O (7 mL), DACH-Pt (41.5 mg, 0.09415 mmol) in H_2O (4 mL) was added. Upon re-saturation with N_2, the solution was stirred for 3d at RT with the pH of the solution maintained at ~5.5 – 6. The reaction was then stirred for 2h at 55 ^{0}C. The solution was filtered and dialyzed for 2d in 12 000-14 000 molecular mass cut-off limit tubing. The retentate was freeze-dried to afford 95.8 mg (42.3%) of a brown water-soluble solid co-conjugate **29-Fc/Pt**; η_{inh} (H_2O): 13.2 $mL.g^{-1}$.
Anal. Calcd. for $(C_{115}H_{197}O_{25}N_{33}FePt)_n$ $(2692.70)_n$ Fe: (calcd) 2.07%, (found) 1.72%; Pt: (calcd) 7.24%, (found) 6.96%.

*4.1.7.7.2 Co-conjugate **30-Fc/Pt***

The same procedure as described for co-conjugate **29-Fc/Pt** (section 4.1.7.7.1) was followed for the preparation of co-conjugate **30-Fc/Pt**. Conjugate **30-Fc** (202 mg, 0.08894 mmol) and DACH-Pt (43.2 mg, 0.09783 mmol) were allowed to react. The solution was treated and worked up as before, giving co-conjugate **30-Fc/Pt** as a brown water-soluble solid in a yield of 103 mg (45.7%); η_{inh} (H_2O): 12.4 $mL.g^{-1}$.
Anal. Calcd. for $(C_{105}H_{181}O_{25}N_{33}FePt)_n$ $(2580.50)_n$ Fe: (calcd) 2.16%, (found) 2.01%; Pt: (calcd) 7.26%, (found) 6.88%.

*4.1.7.7.3 Co-conjugate **31-Fc/Pt***

The same procedure as described for co-conjugate **29-Fc/Pt** (section 4.1.7.7.1) was followed for the preparation of co-conjugate **31-Fc/Pt**. Conjugate **31-Fc** (203 mg, 0.08134 mmol) reacted with DACH-Pt (39.5 mg, 0.08947 mmol). The solution was treated and worked up as before, giving co-conjugate **31-Fc/Pt** as a brown water-soluble solid in a yield of 123 mg (55.1%); η_{inh} (H_2O): 12.1 $mL.g^{-1}$.

Anal. Calcd. for $(C_{123}H_{213}O_{25}N_{33}FePt)_n$ $(2804.90)_n$ Fe: (calcd) 1.99%, (found) 1.70%; Pt: (calcd) 6.95%, (found) 6.63%.

*4.1.7.7.4 Co-conjugate **32-Fc/Pt***

The same procedure as described for co-conjugate **29-Fc/Pt** (section 4.1.7.7.1) was followed for the preparation of co-conjugate **32-Fc/Pt**. A solution of conjugate **32-Fc** (201 mg, 0.07707 mmol) was treated with DACH-Pt (37.4 mg, 0.08478 mmol) and afforded a brown water-soluble co-conjugate **32-Fc/Pt** in a yield of 114 mg (51.6%); η_{inh} (H_2O): 10.6 $mL.g^{-1}$.

Anal. Calcd. for $(C_{131}H_{229}O_{25}N_{33}FePt)_n$ $(2917.11)_n$ Fe: (calcd) 1.91%, (found) 1.74%; Pt: (calcd) 6.68%, (found) 6.27%.

*4.1.7.7.5 Co-conjugate **33-Fc/Pt***

The same procedure as described for co-conjugate **29-Fc/Pt** (section 4.1.7.7.1) was followed for the preparation of co-conjugate **33-Fc/Pt**. Conjugate **33-Fc** (202 mg, 0.07427 mmol) was reacted with DACH-Pt (36.0 g, 0.08170 mmol). The solution was treated and worked up as before, giving co-conjugate **33-Fc/Pt** as a brown water-soluble solid in a yield of 97.0 mg (43.8%); η_{inh} (H_2O): 11.7 $mL.g^{-1}$.

Anal. Calcd. for $(C_{131}H_{213}O_{33}N_{33}FePt)_n$ $(3029.0)_n$ Fe: (calcd) 1.84%, (found) 1.65%; Pt: (calcd) 6.44%, (found) 6.02%.

*4.1.7.7.6 Co-conjugate **34-Fc/Pt***

The same procedure as described for co-conjugate **29-Fc/Pt** (section 4.1.7.7.1) was followed for the preparation of co-conjugate **34-Fc/Pt**. Conjugate **34-Fc** (200 mg, 0.08342 mmol) was treated with DACH-Pt (40.5 mg, 0.09176 mmol) and afforded a brown water-soluble co-conjugate **34-Fc/Pt** in a yield of 110 mg (49.6%); η_{inh} (H_2O): 12.8 $mL.g^{-1}$.

Anal. Calcd. for $(C_{116}H_{199}O_{25}N_{33}FePt)_n$ $(2706.72)_n$ Fe: (calcd) 2.06%, (found) 1.54%; Pt: (calcd) 7.20%, (found) 6.92%.

*4.1.7.7.7 Co-conjugate **35-Fc/Pt***

The same procedure as described for co-conjugate **29-Fc/Pt** (section 4.1.7.7.1) was followed for the preparation of co-conjugate **35-Fc/Pt**. Conjugate **35-Fc** (206 mg, 0.09014 mmol) and DACH-Pt (43.7 mg, 0.09915 mmol) were used. The solution was treated and worked up as before, and co-conjugate **35-Fc/Pt** was afforded as a brown water-soluble solid in a yield of 91.4 mg (39.8%); η_{inh} (H_2O): 9.2 $mL.g^{-1}$.

Anal. Calcd. for $(C_{106}H_{183}O_{25}N_{33}FePt)_n$ $(2594.51)_n$ Fe: (calcd) 2.15%, (found) 1.71%; Pt: (calcd) 7.52%, (found) 7.18%.

*4.1.7.7.8 Co-conjugate **36-Fc/Pt***

The same procedure as described for co-conjugate **29-Fc/Pt** (section 4.1.7.7.1) was followed for the preparation of co-conjugate **36-Fc/Pt**. A solution of conjugate **36-Fc** (205 mg, 0.08168 mmol) was treated with DACH-Pt (39.6 mg, 0.0985 mmol) and resulted in a brown water-soluble co-conjugate **36-Fc/Pt** in a yield of 109 mg (48.4%); η_{inh} (H_2O): 11.6 $mL.g^{-1}$.

Anal. Calcd. for $(C_{124}H_{215}O_{25}N_{33}FePt)_n$ $(2818.93)_n$ Fe: (calcd) 1.98%, (found) 1.42%; Pt: (calcd) 6.92%, (found) 6.12%.

*4.1.7.7.9 Co-conjugate **37-Fc/Pt***

The same procedure as described for co-conjugate **29-Fc/Pt** (section 4.1.7.7.1) was followed for the preparation of co-conjugate **37-Fc/Pt**.

Conjugate **37-Fc** (201 mg, 0.7666 mmol) and DACH-Pt (37.2 mg, 0.08432 mmol) were used. The solution was treated and worked up as before, giving co-conjugate **37-Fc/Pt** as a brown water-soluble solid in a yield of 113 mg (51.2%). η_{inh} (H_2O): 13.1 $mL.g^{-1}$.

Anal. Calcd. for $(C_{132}H_{131}O_{25}N_{33}FePt)_n$ $(2931.14)_n$ Fe: (calcd) 1.90%, (found) 1.53%; Pt: (calcd) 6.65%, (found) 5.87%.

*4.1.7.7.10 Co-conjugate **38-Fc/Pt***

The same procedure as described for co-conjugate **29-Fc/Pt** (section 4.1.7.7.1) was followed for the preparation of co-conjugate **38-Fc/Pt**. Conjugate **38-Fc** (202 mg, 0.07389 mmol) was treated with DACH-Pt (35.8 mg, 0.08180 mmol) and afforded a brown water-soluble solid co-conjugate **38-Fc/Pt** in a yield of 118 mg (52.7%); η_{inh} (H_2O): 12.3 $mL.g^{-1}$.

Anal. Calcd. for $(C_{132}H_{215}O_{33}N_{33}FePt)_n$ $(3043.01)_n$ Fe: (calcd) 1.83%, (found) 1.38%; Pt: (calcd) 6.41%, (found) 5.63%.

*4.1.7.7.11 Co-conjugate **39-Fc/Pt***

The same procedure as described for co-conjugate **29-Fc/Pt** (section 4.1.7.7.1) was followed for the preparation of co-conjugate **39-Fc/Pt**. Conjugate **39-Fc** (203 mg, 0.08945 mmol) was allowed to react with DACH-Pt (43.4 mg, 0.09839 mmol). The solution was treated and worked up as before and afforded co-conjugate **39-Fc/Pt** as a brown water-soluble solid in a yield of 107 mg (47.2%); η_{inh} (H_2O): 10.2 $mL.g^{-1}$.

Anal. Calcd. for $(C_{111}H_{191}O_{23}N_{31}FePt)_n$ $(2578.60)_n$ Fe: (calcd) 2.16%, (found) 2.01%; Pt: (calcd) 7.56%, (found) 7.03%.

*4.1.7.7.12 Co-conjugate **40-Fc/Pt***

The same procedure as described for co-conjugate **29-Fc/Pt** (section 4.1.7.7.1) was followed for the preparation of co-conjugate **40-Fc/Pt**. Conjugate **40-Fc** (204 mg, 0.09457 mmol) and DACH-Pt (45.9 mg, 0.1040 mmol) were allowed to react. The solution was treated and worked up as

before. The brown water-soluble solid co-conjugate **40-Fc/Pt** was isolated in a yield of 102 mg (44.3%); η_{inh} (H_2O): 8.6 $mL.g^{-1}$.

Anal. Calcd. for $(C_{101}H_{175}O_{23}N_{31}FePt)_n$ $(2466.40)_n$ Fe: (calcd) 2.26%, (found) 2.04%; Pt: (calcd), 7.91%, 7.38%.

*4.1.7.7.13 Co-conjugate **41-Fc/Pt***

The same procedure as described for co-conjugate **29-Fc/Pt** (section 4.1.7.7.1) was followed for the preparation of co-conjugate **41-Fc/Pt**. Conjugate **41-Fc** (202 mg, 0.08482 mmol) and DACH-Pt (41.2 mg, 0.09330 mmol) afforded the brown water-soluble co-conjugate **41-Fc/Pt** in a yield of 117 mg (52.1%); η_{inh} (H_2O): 13.4 $mL.g^{-1}$.

Anal. Calcd. for $(C_{119}H_{207}O_{23}N_{31}FePt)_n$ $(2690.80)_n$ Fe: (calcd) 2.07%, (found) 1.88%; Pt: (calcd) 7.25%, 6.82%.

*4.1.7.7.14 Co-conjugate **42-Fc/Pt***

The same procedure as described for co-conjugate **29-Fc/Pt** (section 4.1.7.7.1) was followed for the preparation of co-conjugate **42-Fc/Pt**. Conjugate **42-Fc** (202 mg, 0.08140 mmol) was treated with DACH-Pt (39.5 mg, 0.08954 mmol) and afforded co-conjugate **42-Fc/Pt** in a yield of 111 mg (49.3%) brown water-soluble material; η_{inh} (H_2O): 11.8 $mL.g^{-1}$.

Anal. Calcd. for $(C_{127}H_{223}O_{23}N_{31}FePt)_n$ $(2803.01)_n$ Fe: (calcd) 1.99%, (found) 1.80%; Pt: (calcd) 6.96%, (found) 6.41%.

*4.1.7.7.15 Co-conjugate **43-Fc/Pt***

The same procedure as described for co-conjugate **29-Fc/Pt** (section 4.1.7.7.1) was followed for the preparation of co-conjugate **43-Fc/Pt**. Conjugate **43-Fc** (205 mg, 0.07867 mmol) and DACH-Pt (38.2 mg, 0.08654 mmol) gave co-conjugate **43-Fc/Pt** as a brown water-soluble solid in a yield of 105 mg (46.2%); η_{inh} (H_2O): 10.2 $mL.g^{-1}$.

Anal. Calcd. for $(C_{127}H_{207}O_{31}N_{31}FePt)_n$ $(2914.88)_n$ Fe: (calcd) 1.91%, (found) 1.82%; Pt: (calcd) 6.69%, (found) 6.17%.

*4.1.7.7.16 Co-conjugate **44-Fc/Pt***

The same procedure as described for co-conjugate **29-Fc/Pt** (section 4.1.7.7.1) was followed for the preparation of co-conjugate **44-Fc/Pt**. Conjugate **44-Fc** (206 mg, 0.08665 mmol) and DACH-Pt (42.1 mg, 0.09531 mmol) gave a brown water-soluble co-conjugate **44-Fc/Pt** in a yield of 129 mg (56.3%); η_{inh} (H_2O): 12.5 $mL.g^{-1}$.

Anal. Calcd. for $(C_{113}H_{199}O_{26}N_{33}FePt)_n$ $(2686.70)_n$ Fe: (calcd) 2.08%, (found) 1.78%; Pt: (calcd) 7.26%, (found) 6.81%.

*4.1.7.7.17 Co-conjugate **45-Fc/Pt***

The same procedure as described for co-conjugate **29-Fc/Pt** (section 4.1.7.7.1) was followed for the preparation of co-conjugate **45-Fc/Pt**. Conjugate **45-Fc** (209 mg, 0.09226 mmol) and DACH-Pt (44.8 mg, 0.1015 mmol) were used. The reaction mixture was treated and worked up as before. The co-conjugate was isolated as a brown water-soluble solid in a yield of 121 mg (51.4%); η_{inh} (H_2O): 9.7 $mL.g^{-1}$.

Anal. Calcd. for $(C_{103}H_{183}O_{26}N_{33}FePt)_n$ $(2574.48)_n$ Fe: (calcd) 2.17%, (found) 1.90%; Pt: (calcd) 7.57%, (found) 7.03%.

*4.1.7.7.18 Co-conjugate **46-Fc/Pt***

The same procedure as described for co-conjugate **29-Fc/Pt** (section 4.1.7.7.1) was followed for the preparation of co-conjugate **46-Fc/Pt**. Conjugate **46-Fc** (204 mg, 0.08194 mmol) and DACH-Pt (39.8 mg, 0.09013 mmol) were used. The brown water-soluble co-conjugate was isolated in a yield of 95.5 mg (42.1%); η_{inh} (H_2O): 11.4 $mL.g^{-1}$.

Anal. Calcd. for $(C_{121}H_{215}O_{26}N_{33}FePt)_n$ $(2798.90)_n$ Fe: (calcd) 1.99%, (found) 1.78%; Pt: (calcd) 6.97%, (found) 6.22%.

*4.1.7.7.19 Co-conjugate **47-Fc/Pt***

The same procedure as described for co-conjugate **29-Fc/Pt** (section 4.1.7.7.1) was followed for the preparation of co-conjugate **47-Fc/Pt**.

Conjugate **47-Fc** (203 mg, 0.07802 mmol) and DACH-Pt (37.9 mg, 0.08582 mmol) were used. The solution was treated and worked up as before. The yield was 103 mg (45.8%) of a brown water-soluble solid; η_{inh} (H_2O): 12.6 $mL.g^{-1}$.

Anal. Calcd. for $(C_{129}H_{231}O_{26}N_{33}FePt)_n$ $(2911.11)_n$ Fe: (calcd) 1.91%, (found) 1.74%; Pt: (calcd) 6.70%, (found) 5.48%.

*4.1.7.7.20 Co-conjugate **48-Fc/Pt***

The same procedure as described for co-conjugate **29-Fc/Pt** (section 4.1.7.7.1) was followed for the preparation of co-conjugate **48-Fc/Pt**. Conjugate **48-Fc** (205 mg, 0.07554 mmol) and DACH-Pt (36.6 mg, 0.08309 mmol) were reacted. The solution was treated and worked up as before, and afforded 111 mg (49.2 %) of a brown water-soluble solid; η_{inh} (H_2O): 10.9 mL/g.

Anal. Calcd. for $(C_{129}H_{215}O_{34}N_{33}FePt)_n$ $(3023.0)_n$ Fe: (calcd) 1.84%, (found) 1.60%; Pt: (calcd) 6.45%, (found) 5.33%.

CHAPTER 5

CONCLUSION

Cancer is an ancient affliction and through the centuries many therapeutic measures have been developed to treat it, including surgery, chemotherapy and immunotherapy. Despite these advances, it remains one of the most life changing diagnoses a doctor can render to a patient. The statistics of cancer prevalence is very high. Chemotherapy is one of the most widely used cancer treatment methods. Although novel anticancer agents have been successful in inhibiting cancer, the agents have failed to make it to the market due to their inability to be delivered effectively to the tumor cells because of their lack of cell specificity, blood solubility, metabolic stability and bio-availability. Over the years, ongoing research indicated that the limitations could be overcome by using polymeric drug carriers for drug delivery. From a clinical view point, the most interesting consequence of polymer-drug conjugation is the opportunity to capitalize on altered drug pharmacokinetics at the whole-body and cellular level. In this thesis, as part of an ongoing program in the School of Chemistry, water-soluble synthetic polymers were prepared as potential targetable carriers for drug delivery in cancer chemotherapy. Key monomers that were incorporated on the polymer backbone as side chain units for drug conjugation were synthesized. These key monomers of choice included aspartic acid derivatives and benzene ring derivatives. The latter included *p*-aminobenzoic acid, *p*-aminosalicylic acid and dopamine derivatives, and these were utilized as new drug anchors. These monomers were synthesized in the first and main step of the project, under critically controlled conditions of pH, temperature, time and choice of solvents.

The polymers synthesized in this project bearing the key monomers were aliphatic polyaspartamides capable of forming a link to a drug species.

Careful design of the polymer systems allowed for the inclusion of hydrosolubilizing moieties and possible targeting residues within a biodegradable backbone. The molecular mass range was controlled in such a way that it was sufficiently large to retard renal clearance, yet small enough to prevent inherent polymer toxicity. The synthetic methodology, based in part on experience gained in previous programs, included polyaspartamide formation by aminolytic ring opening in polysuccinimide. Two different types of prodrugs were prepared, the homoconjugates and the co-conjugates. Carriers leading to the formation of homoconjugate were prepared in a way such that three different drug binding sites were incorporated. The first group contained carriers modified with free amine functionalities from *p*-aminobenzoic acid derivative; the second group contained carriers modified with carboxylhydroxyl functionalities from *p*-aminosalicylic acid derivatives; and the third group contained carriers modified with dihydroxyl functionalities from dopamine. These three groups of carriers were used for the anchoring of platinum drugs. Three types of platination agents, DACH-$PtCl_2$, DACH-Pt and DACH-Pt-PABA, were used.

The polyaspartamides leading to the formation of co-conjugates were prepared in two steps. A novel method developed in this project was used. Three amines were used instead of two, one of them being the modified ferrocene, 3-[4-ferrocenylbutyramido]propylamine. In the first step, the homoconjugate was prepared with a desired percentage of ferrocene. Ferrocene was introduced directly in the polysuccinimide through its functionalization by aminolytic ring opening. At this stage the amine-functionalized ferrocene was treated as any other amine. The second step involved the platination of the different ferrocene homoconjugates, using the same platination agents as for the homoconjugates.

In fulfillment of the goals set out in this project, a chosen number of conjugates were submitted to the Division of Pharmacology of WITS

University for preliminary biological screening. *In vitro* tests were performed against the MCF-7 human breast cancer cell line. Although it is difficult to depict a clear preliminary biological activity with one cancer cell line, it can be concluded that the simultaneous incorporation of ferrocene and platinum in the polymeric carriers, apart from exemplifying the co-drug construction, represents a tool for the delivery of two anticancer drugs with different mechanisms of biological activity. The inhibitory concentrations reveal that the co-conjugates were more active than homo-conjugates as growth inhibitors against the MCF-7 cell line. These are very promising anti-proliferative results. Despite the fact that the preliminary activity data presented here confirm our expectations of enhanced activity, a considerably larger number of exemplifying polymer structures possessing a wide range of side groups and spacer attachment designs will have to be investigated in order to establish significant structure-performance relationships. In addition, biological studies should be performed on a larger number of different cancer cell lines and DMP polymers have been proposed to be included in future publications outside this dissertation.

The proof of principle has been shown for these polymer-bound drug models and the strategy offers interesting perspectives for the conjugation of various other antineoplastic agents.

REFERENCES

1. A.S-Y. Leong and G-W. Leong, *Cancer Explained: Causes, Diagnosis, Treatment and Prevention,* P G Publishing, Singapore, Chap.1 (1989).
2. P. Rubin, J.P. Williams, P. Okunieff, J.D. Rosenblatt, J.V. Sitzmann, In *Clinical oncology: A multidisciplinary approach for physicians and students,* 8 Ed, P. Rubin, Ed, W.B. Saunders company, USA, Chap. 1 (2001).
3. A.J. Neal, P.J. Hoskin, *Clinical oncology: Basic principles and practice*, 2 Ed, Arnold, USA, Chap. 1 (1997).
4. World Health Organization, *Fact sheet,* **297**, February 2006.
5. M.M. Ciranowisz, D.D. DeCarolis, C. Ferrante, R. Pazdur, *Neoplastic disorders*, Springhouse, Pennsylvania, Chap. 1 (1995).
6. P.F. Spitalnik, P.A. Sant'Agnese, In *Clinical oncology: A multidisciplinary approach for physicians and students,* 8 Ed, P. Rubin, Ed, W.B. Saunders company, USA, Chap. 3 (2001).
7. M.B. Ford, M.F. Mitchell, In *Primary care oncology*, K.L. Boyer, M.B. Ford, A.F. Judkins, B. Levin, Eds, W.B. Saunders company, USA, Chap. 1 (1999).
8. W.B. Ober, Kaposi: In *Kaposi's Sarcoma: a Text and Atlas,* G. Gottlieb and A.B. Ackerman, Eds, LEA & FEBIGER, Philadelphia, USA, Chap.2 (1988).
9. C.M. Haskell, In *Cancer treatment, 4th Ed.*, C.M. Haskell, Ed, W.B. Saunders company, USA, Chap.1 (1995).
10. K.C. Calman, J.F. Smyth, M.H.N. Tattersall, *Basic Principles of cancer Chemotherapy.,* Macmillan Press, London, (1980)
11. E. Pan, M.D. Prados, In *Cancer Medicine*, 6 Ed, Vol. **2**, D.W. Kufe, R.E. Pollock, R.R. Weichselbaum, R.C. Bast, T.S. Gansler, J.F. Holland, E. Frei, Eds., American Cancer Society, London, Chap. 83 (2003).

12. T.M. Becker, *Cancer Chemotherapy: a manual for nurses,* Little, Brown Pub., University of Mishigan, Mishigan, Chap. 1 (1981).
13. R.E. Pollock, D.L. Morton, In *Cancer Medicine*, 6 Ed, Vol. **1**, D.W. Kufe, R.E. Pollock, R.R. Weichselbaum, R.C. Bast, T.S. Gansler, J.F. Holland, E. Frei, Eds., American Cancer Society, London, Chap. 38 (2003).
14. D.F. Easton, D.T. Bishop, D. Ford, B.P. Crocford, *Am. J. Hum. Genet.*, **52**, 678 (1993).
15. A.J. Neal, P.J. Hoskin, *Clinical oncology: Basic principles and practice*, 2 Ed, Arnold, USA, Chap. 8 (1997).
16. L.S. Friedman, E.A. Ostermeyer, C.I. Szabo, P. Dowd, E.D. Lynch, S.E. Rowell, M.C. King, *Nat. Genet.,* **8**, 399 (1994).
17. E.R. Sigurdson, J.A. Ridge, R.J. Ginsberg, In *Clinical oncology: A multidisciplinary approach for physicians and students,* 8 Ed, P. Rubin, Ed, W.B. Saunders company, USA, Chap. 4 (2001).
18. M.P. Boente, D.S. Chi, W.J. Hoskins, *Semin Oncol*, **25**, 326 (1998).
19. D.L. Larson, J.R. Sanger, *Semin Surg Oncol*, **11**, 190 (1995).
20. C.A. Perez, L.W. Brady, J.L. Roti Roti, In *Principles and practice of radiation oncology,* 3 Ed, C.A. Perez, L.W. Brady, (eds.), Lippincott-Raven publishers, Philadelphia, Chap. 1 (1997).
21. W.C. Dewey, J.S. Bedford, In *Textbook of radiation oncology*, 2 Ed, S.A. Leibel, T.L. Phillips, (eds), Saunders, Elsevier Inc., Chap.1 (2004).
22. C.J. McGinn, T.S. Lawrence, In *Principles and practice of radiation oncology,* 3 Ed, C.A. Perez, L.W. Brady, (eds.), Lippincott-Raven publishers, Philadelphia, Chap. 74 (1997).
23. A.J. Mundt, P.M. Bruch, B. Wyman, C. Chotipradit, J.C. Roeske, In *Intensity Modulated radiation therapy: A clinical perspective,* A.J. Mundt, J.C. Roeske, (eds.), BC Decker Inc., Hamilton, London, Chap.1 (2005).
24. I. Krakoff, *CA Cancer J Clin*, **46**, 134 (1996).

25. L. Tenenbaum (ed), *Cancer Chemotherapy and Biotherapy: Reference Guide,* 2 Ed, Philadelphia: W.B. Saunders, (1994).
26. R. Epstein, *J Clin Oncol*, **8** (1987) 2062-2084.
27. M.J. Cline, C.M. Haskel, *Cancer chemotherapy*, 3 Ed., W.B. Saunders Company, Philadelphia, Chap. 2 (1980).
28. M. Bower, J. Waxman, *Lecture notes: Oncology*, Blackwell publishing, Massachusetts, USA, Chap.3 (2006).
29. K.C. Ingwersen, In *Cancer Chemotherapy: A Nursing Process Approach,* M. Barton-Burke, G.M. Wilkes, K. Ingwersen, Eds., Jones & Bartlett Publishers, Chap. 2 (2001).
30. M. Barton-Burke, G.M. Wikes, In *Cancer Therapies*, M. Barton-Burke, G.M. Wilkes, Eds., Jones & Bartlett Publishers, Chap. 2 (2006).
31. M. Colvin, In *Cancer Medicine*, 6 Ed, Vol. **1**, D.W. Kufe, R.E. Pollock, R.R. Weichselbaum, R.C. Bast, T.S. Gansler, J.F. Holland, E. Frei, Eds., American Cancer Society, London, Chap. 51 (2003).
32. J.A. Montgomery, In *Cancer chemotherapeutic agents*, W.O. Foye (Ed), American Chemical Society, Washington, DC, 111 (1995).
33. I. Kostova, *Recent Patents on Anti-Cancer Drug Discovery,* **1**, 1 (2006).
34. D.W. Siegmann-Louda, C.E. Carraher, In *Macromolecules containing metal-like elements,* Volume 3: Biomedical applications*,* A.S. Abd-El-Aziz, C.E. Carraher, C.U. Pittman, J.E. Sheats, M. Zeldin, Eds., Wiley & Sons, New York, Chap. 7 (2004).
35. B. Rosenberg, L. Van Camp, T. Krigas, *Nature*, **205**, 698 (1965).
36. B. Rosenberg, L. Van Camp, J.E Trosco., et al., Nature, **222**, 385 (1969).
37. E.W. Neuse, M.G. Meirim, H.M. Netshifhefhe, W.-C. Shen, *40th Microsymposium "Polymers in Medicine"*, Prague, 17-20; Abstr. P34 (July 2000).
38. D.J. Higby, H.J. Wallace, D.J. Albert, J.F. Holland. *Cancer*; **33**, 1219 (1974).

39. B. Rosenberg, in *Metal Ions in biological systems,* Vol. 11, H. Sigel, Ed., Marcel Dekker, New York, 127 (1980).
40. M. Rozencweig, D.D. Von Hoff, R. Abele, F.M. Muggia, In *Cancer Chemotherapy Annual* **2**, H.M. Pinedo, Ed., Excerpta Medical Amsterdam, 107 (1982).
41. C.F.J. Bernard, M.J. Cleare, P.C. Hydes, *Chem. Brit.,* **22**, 1001 (1986).
42. J.H. Burchenal, K. Kalaher, K. Dew, L. Lokys, G. Gale, *Biochimie,* **60**, 961 (1978).
43. E.W. Neuse, *S. Afr. J. Sci.,* **95**, 1 (1999).
44. W.R. Waud, In *Cancer chemotherapeutic agents*, W.O. Foye (Ed), American Chemical Society, Washington, DC, 121 (1995).
45. J.C. Dabrowiak, *Metals in medicine*, John Wiley & Sons, Ltd, UK Chap. 4 (2009).
46. S.J. Berners-Price, T.G. Appleton, In *Platinum-Based Drugs in Cancer Therapy,* L.R. Kelland, N.P. Farell, Eds., Humana Press Inc., Totwa, Chap. 1 (2000).
47. M.E. Heim, In *Metal complexes in camcer chemotherapy,* B.K. Keppler, Ed., VCH, New York, 1 (1993).
48. J. Arpalahti, In *Perspectives on Bioinorganic Chemistry, Volume 4*, R.Ed. Hay, J.R. Dilworth, K.B. Nolan, Eds., Elsevier, 165 (1999).
49. J.C. Dabrowiak, *Metals in medicine*, John Wiley & Sons, Ltd, UK Chap. 3 (2009).
50. A. Gelasco, S.J. Lippard, in *Metallopharmaceuticals I DNA interactions: Topics in Biological Inorganic Chemistry,* **1**, M.J. Clarke, P.J. Sadler, Eds., Springer, New York, 1 (1999).
51. D.P. Bancroft, C.A. Lepre, S.J. Lippard, *J. Am. Chem. Soc.,* **112**, 6860 (1990).
52. S.K.C. Elmroth, S.J. Lippard, *J. Am. Chem. Soc.,* **116**, 3633 (1994).

53. M.J. McKeage, L.R. Kelland, in *Molecular Aspects of Drug-DNA interactions,* S. Meidle, M.J. Waring, Eds., MacMillan, New York, 1 (1992).
54. M.E. Heim, in *Metal complexes in cancer chemotherapy*, Keppler, B.K. Ed., VCH, New York, 1 (1993).
55. W.I. Sundquist, S.J. Lippard, B.D. Stollar, Biochemistry: *Proc. Natl. Acad. Sci.* USA **84**, 8225 (1987).
56. B. Schechter, R. Arnon, M. Wilchek, *Reactive Polymers,* **25**, 167 (1995).
57. D. Avichezer, B. Schechter, R. Arnon, *Reactive & Functional Polymers,* **36**, 59 (1998).
58. J.E. Schuring, W.T. Brandner, J.B. Haftalen, G.J. Doyle, T.A. Gylus, in *Cisplatin: Current Status and New Development,* A.W. Prestayko, S.T. Crooke, S.K. Carter (Eds.), Academic Press, New York, 227 (1980).
59. E.H. Rubin, W.N. Hait, In *Cancer Medicine*, 6 Ed, Vol. **1**, D.W. Kufe, R.E. Pollock, R.R. Weichselbaum, R.C. Bast, T.S. Gansler, J.F. Holland, E. Frei, Eds., American Cancer Society, London, Chap. 52 (2003).
60. H.M. Sobell, S.C. Jain, *J Mol Biol*, **68**, 21 (1972).
61. X. Liu, H. Chen, D.J. Patel, *J Biomol*, **1**, 323 (1991).
62. C.Yu, Y.Y. Tseng, *Eur J Biochem*, **209**, 181 (1992).
63. D.E. Seigler, A. Preti, In *Primary care oncology*, K.L. Boyer, M.B. Ford, A.F. Judkins, B. Levin, Eds, W.B. Saunders company, USA, Chap. 17 (1999).
64. A.Ritty, A. Preti, In *Primary care oncology*, K.L. Boyer, M.B. Ford, A.F. Judkins, B. Levin, Eds, W.B. Saunders company, USA, Chap. 18 (1999).
65. G.L. Chen, L. Yang, T.C Rowe, *et al*, *J Biol Chem*, **259**, 13360 (1984).

66. P.J. O'Dwyer, S.A. King, C.L. Fortner, B. Leyland-Jones, *J Clin Oncol*, **4**, 1262 (1986).
67. J.A. Montgomery, In *Cancer chemotherapeutic agents*, W.O. Foye (ed), American Chemical Society, Washington, DC, 47 (1995).
68. B.A. Kamen, P.D. Cole, J.R. Bertino, In *Cancer Medicine*, 6 Ed, Vol. **1**, D.W. Kufe, R.E. Pollock, R.R. Weichselbaum, R.C. Bast, T.S. Gansler, J.F. Holland, E. Frei, Eds., American Cancer Society, London, Chap. 49 (2003).
69. J.R. Piper, In *Cancer chemotherapeutic agents*, W.O. Foye (ed), American Chemical Society, Washington, DC, 96 (1995).
70. L.E. Jolly, H.P. Fletcher, *Toxicol Appl Pharmacol*, **39**, 23 (1977).
71. J.R. Bertino,(Ed) *Ann. N.Y. Acad. Sci.*, **186** (1971).
72. G. Wilkinson, M. Rosenblum, M.C. Whiting, R.B. Woodward, *J. Am. Chem. Soc.*, **74**, 2123 (1952).
73. P. Köpf-Maier, H. Köpf, E.W. Neuse, *Angew. Chem.,***96**, 446 (1984).
74. P. Köpf-Maier, H. Köpf, E.W. Neuse, *Angew. Chem., Int. Ed.,* **23**, 456 (1984).
75. P. Köpf-Maier, H. Köpf, E.W. Neuse, *J. Cancer Res. Clin. Oncol.,* **108**, 336 (1984).
76. D. Ossela, M. Ferrali, P. Zanello *et al, Inorg. Chim. Acta*, **306**, 42 (2000).
77. E.W. Neuse, *Macromol. Synmp.,* **80**, 111 (1994).
78. E.W. Neuse, *Macromol. Synmp.,* **172**, 127 (2001).
79. E.W. Neuse, In *Macromolecules containing metal and metal-like elements,* **3**: *Biomedical applications*, A.S. Abd-el-Aziz, C.E. Carraher Jr, C.U. Pittman Jr, J.E. Sheats, M. Zeldin, (Eds), John Wileys & Sons, Inc. Chap. 6 (2004).
80. R. Duncan, J. Kopeček, *Adv. Polym. Sci.,* **57** 53 (1984).
81. R. Satchi-Fainaro, R. Duncan, C.M. Barnes, *Adv. Polym. Sci.,* **193**, 1 (2006).

82. R. Mulcahy, *Diseases: Finding the Cure*, The Oliver Press, Inc., Chap. 4 (1996).
83. M.D. Maree, E.W. Neuse, E. Erasmus, J.C. Swarts, *Metal-Based Drugs,* volume 2008, Hindawi Publishing Corporation, ID 217573, (2008).
84. J.M.J. Haris, In *Macromol. Sci. rev. Macromol. Chem. Phys.,* Chap. 25 (1985).
85. R.L. Davidson, K.A. O'Malley, T.B. Wheeler, *Somatic Cell Genetics,* **2**, 271 (1976).
86. K. Ulbrich, J. Kopeèek, *Prog. Polym. Sci.,* **9**, 1 (1983).
87. M.J. Poznansky, D. Bhardwaj, In *Design of prodrugs,* H. Bundhard, (Ed), Elsevier Scientific publishers, Amsterdam, 317 (1985).
88. A. Pendri, C.W. Gilbert, S. Soundarajan, D. Bolikal, R.G.L. Shorr, R.B. greenwald, *J. Bioact. Comp. Polym.,* **11**, 122 (1996).
89. Y. Ohya, H. Kuroda, K. Hirat, T. Ouchi, *J. Bioact. Comp. Polym.,* **10**, 51 (1995).
90. S. Zalipsky, C. Lee, In *Poly(ethylene glycol) Chemistry: Biotechnical and Biomedical Applications,* J. Milton-Harris, (Ed), Plenum press, New York, 121 (1982).
91. J. Milton-Harris, J.M. Dust, R.A. Harris, M.J. Edgell. R.M. Sedaghat-Herati, L.J. Karr, D.L. Donnely, In *Water-soluble polymers,* S.W. Shalaby, C.L. McCormick, G.B. Butler, (Eds), ACS, 418 (1991).
92. G. Hooftman, S. Herman, E. Schacht, *J. Bioact. Comp. Polym.,* **11**, 135 (1996).
93. M.G. Meirim, *MSc. Thesis*, University of the Witwatersrand, (2002).
94. A.I. Mufula, E.W. Neuse, *J. Inorg. Organomet. Polym. Mat.*, **22**, 134 (2012).
95. H. Ringsdorf. *J. Polym. Sci. Symp.,* **51**, 135 (1975).
96. K. Kono, M. Liu, J.M.J. Fréchet, *Bioconjugate Chem.,* **10**, 1115 (1999).

97. Soyer, H., Schacht, E. and Vanderkerken, S. *Adv. Drug Delivery Rev*., **21**, 81 (1984).
98. J. Drobník, V. Saudek, J. Vlasák, and J. Kala, *J. Polym. Sci., Polym. Symp.,* **66**, 65 (1979).
99. A. Gelasco, S.J. Lippard, In *Metallopharmaceuticals I DNA interactions: Topics in Biological Inorganic Chemistry,* **1**, M.J. Clarke, P.J. Sadler, Eds., Springer, New York, 1 (1999).
100. E.W. Neuse, C.W.N. Mbonyana, In *Inorganic and Metal-Containing Polymeric Materials,* J. Sheats *et al*., (Eds.), Plenum Press, New York, 139 (1990).
101. E.W. Neuse, *Encyl. Polym. Sci. Technol. Chem.,* **8** (1968) 667.
102. M.G. Meirim, E.W. Neuse, G. Caldwell, *J. Inorg. Organomet. Polym.,* **8**, 225 (1998).
103. J. Barianga, M.T. Johnson, E.M. Mmutlane, E.W. Neuse, *J. Inorg. Organomet. Polym. Mat.*, vol. 15, **3**, 335 (2005).
104. Neri, P.; and Antoni, G.; *Macromol. Synt.,* **8**, 25 (1982).
105. M. Tomida, T. Nakoto, S. Matsunami, T. Kakuchi, *Polymer* , **38**, 4733 (1997).
106. A.I. Mufula, B.A. Aderibigbe, E.W. Neuse, H.E. Mukaya, *J. Inorg. Organomet. Polym.,* **22**, 423 (2012).
107. W.C. Shen, B. Ballou, H.J.P. Ryser, T.R. Hakala, *Cancer Res*., **46**, 3912 (1986).
108. G. Caldwell, M.G. Meirim, E.W. Neuse, C.E.J. van Rensburg, *Appl. Organometal. Chem.*, **12**, 793 (1998).
109. E.W. Neuse, A.G. Perlwitz, S. Schmitt, *Angew. Makromol. Chem.*, **192**, 35 (1991).
110. D.D. N'Da, E.W. Neuse, C.E.J. van Rensburg, *S. Afr. Chem.*, **59**, 135 (2006).
111. E.W. Neuse, *Polym. Adv. Technol.,* **9**, 786 (1998).
112. H.E. Mukaya, *MSc. Thesis*, University of the Witwatersrand, (2008).
113. E.W. Neuse, G. Caldwell, *S. Afr. J. Chem,* **45** (4), 93 (1992).

114. T. Orchard, C.S. Probert, S. Keshav, *Aliment Pharmacol. Ther.*, **2**, 17 (2006).
115. A. Ireland, D.P. Jewell, *Clinical Science*, **78**, 119 (1990).
116. S.R. Ritland, J.A. Leighton, R.E. Hirsch, *et al.*, *Clin. Cancer Res.*, **5**, 855 (1999).
117. Y. Cheng, P. Desreumaux, *World J. Gastroenterol.*, **11** (**3**), 309 (2005).
118. B. Parodi *et al*., *Cancer Res.*, **15**, 895 (1995).
119. M. Esposito *et al*., *J. Natl. Cancer Inst.,* **82**, 677 (1990)
120. M. Esposito *et al*., *Carcinogenesis,* **14**, 2595 (1993).
121. S. Cafaggi *et al*., *Anticancer Res.*, **12**, 2285 (1992).
122. D.D. N'Da, E.W. Neuse, *J. Inorg. Organomet. Polym.,* **20**, 468 (2010).
123. U. Chiba, E.W. Neuse, J.C. Swarts, G.J. Lamprecht, *Angew. Makromol. Chem.*, **214**, 137 (1994).
124. L.L. Komane, E.H. Mukaya, E.W. Neuse, C.E.J. van Rensburg, *J. Inorg. Organomet. Polym.,* **18**, 111 (2008).
125. Y. Ohya, H. Oue, K. Nagatomi, T. Ouchi, *Biomacromolecules,* **2**, 927 (2001).
126. Y. Ohya, K. Nagatomi, T. Ouchi, *Macromol. Biosci.,* **1**, 355 (2001).
127. I. Kostova, *Recent Patents on Anti-Cancer Drug Discovery,* **1**, 1 (2006).
128. D.W. Siegmann-Louda, C.E. Carraher, in *Macromolecules containing metal-like elements,* Volume 3: Biomedical applications*,* A.S. Abd-El-Aziz, C.E. Carraher, C.U. Pittman, J.E. Sheats, M. Zeldin, Eds., Wiley & Sons, New York, Chap. 7 (2004).
129. B. Rosenberg, L. Van Camp, T. Krigas, *Nature*, **205**, 698 (1965).
130. C. Carraher, C. Ademu – John, J. Fortman, D. Giron, R. Linville, *Polym. Mater. Sci. Eng.,* **49**, 210 (1983).

131. C. Carraher, W. Scott, D. Giron, in *Bioactive Polymeric Systems,* G. Gebelein, C. Carraher, Eds., Plenum Press, New York, Chap. 20 (1985).
132. C. Carraher, C. Ademu-John, J. Fortman, D. Giron, in *Metal-containing Polymeric Systems,* J. Sheats *et al*. Eds., Plenum Press, New York, 1985. See also: *Polm. Mater. Sci. Eng.*, **51**, 307 (1984).
133. R. Duncan, N. Malik, E. Evagorou, *Anti-cancer Drugs,* **10**, 767 (1999).
134. L. Chen, B. Schechter, R. Arnon, M. Witchek, *Drug Dev. Res.,* **50**, 258 (2000).
135. B.A. Aderibigbe, E.W. Neuse, *J. Inorg. Organomet. Polym.*, **22**, 429 (2012).
136. E.W. Neuse, M.G. Meirim, N.F. Blom, *Organometallics*, **7**, 2562 (1988).
137. C.W.N. Mbonyana, E.W. Neuse, A.G. Perlwitz, *Appl. Organomet. Chem.*, **7**, 279 (1993).
138. E.W. Neuse, A.G. Perlwitz, G. Caldwell, *J. Inorg. Organometal. Polym.,* **5** (1995) 195.
139. E.W. Neuse, G. Caldwell, A.G. Perlwitz, *J. Inorg. Organometal. Polym.*, **7**, 867 (1996).
140. W.C. Shen, K. Beloussow, M.G. Meirim, E.W. Neuse, *J. Inorg. Organometal. Polym.,* **10**, 51 (2000).
141. G. Caldwell, E.W. Neuse, C.E. van Rensburg, *Appl. Organomet. Chem.,* **13**, 189 (1999).
142. M.T. Johnson, E.W. Neuse, C.E. van Rensburg, E. Kreft, *J.Inorg. Organometal. Polym.,* **13**, 55 (2003).
143. E.W. Neuse, *S. Afr. J. Sci.*, vol. 95, **11**-**12**, 509 (1999).
144. E.W. Neuse, *Metal-Based Drugs*, vol. 2008, Hindawi Publishing Corporation, Art. ID 469531, doi:10.1155/2008/469531 (2008).
145. E.W. Neuse, B.B. Patel, C.W.N. Mbonyana, *J. Inorg. Organomet. Polym.*, vol. 1, **2**, 147 (1991).

146. E.W. Neuse, G. Caldwell, A.G. Perlwitz, *J. Inorg. Organomet. Polym.*, vol. 5, **3**, 195 (1995).
147. J.C. Swarts, D.M. Swarts, D.M. Maree, *Anticancer Res.*, vol. 21, **3B** 2033 (2001).
148. J.D. Hoeschele, N. Farell, W.R. Turner, C.D. Rithner, *Inorg. Chem.,* **27**, 4106 (1988).
149. G. Caldwell, E.W. Neuse, A. Stephanou, *J. Appl. Polym. Sci.,* **50**, 393 (1993).
150. M.G. Meirim, E.W. Neuse, D.D. N'Da, *J. Appl. Polym. Sci.*, **82**, 1844 (2001).
151. G. Caldwell, E.W. Neuse, *S. Afr. J. Chem.*, **45**, 93 (1992).
152. A.U. Buzdar, G.N. Hortobagyi, *Sem. Oncol.*, **26**, 21 (1999).
153. MC.A. Presant, W. Wolf, V. Walush, C.L. Wiseman, I. Weitz, J. Shani, *J. Clin. Oncol.*, **18**, 255 (2000).
154. G. Von Minckwitz, S.D. Costa, W. Eiermann, J.U. Blohmer, A.H. Tulusan, C. Jackish, M. Kaufmann, *J. Clin. Oncol.*, **17**, 121 (1999).
155. N.F. Blom, E.W. Neuse, H.G. Thomas, *Transition. Met. Chem.*, **12**, 301 (1987).
156. T. Mosmann, *J. Immunol. Meth.*, **65**, 55 (1983).
157. R.L. van Zyl, S.T. Seatlholo, A.M. Viljoen, *S. Afr. J. Bot.*, **76**, 662 (2010).
158. C. Sarkar, D. Chakroborty, U.R. Chowdhury, *et al.*, *Clin. Cancer Res.*, **14**, 2502 (2008).

APPENDIX:

^{1}H NMR SPECTRA

Appendix 1a: ^{1}H NMR of **M1**.

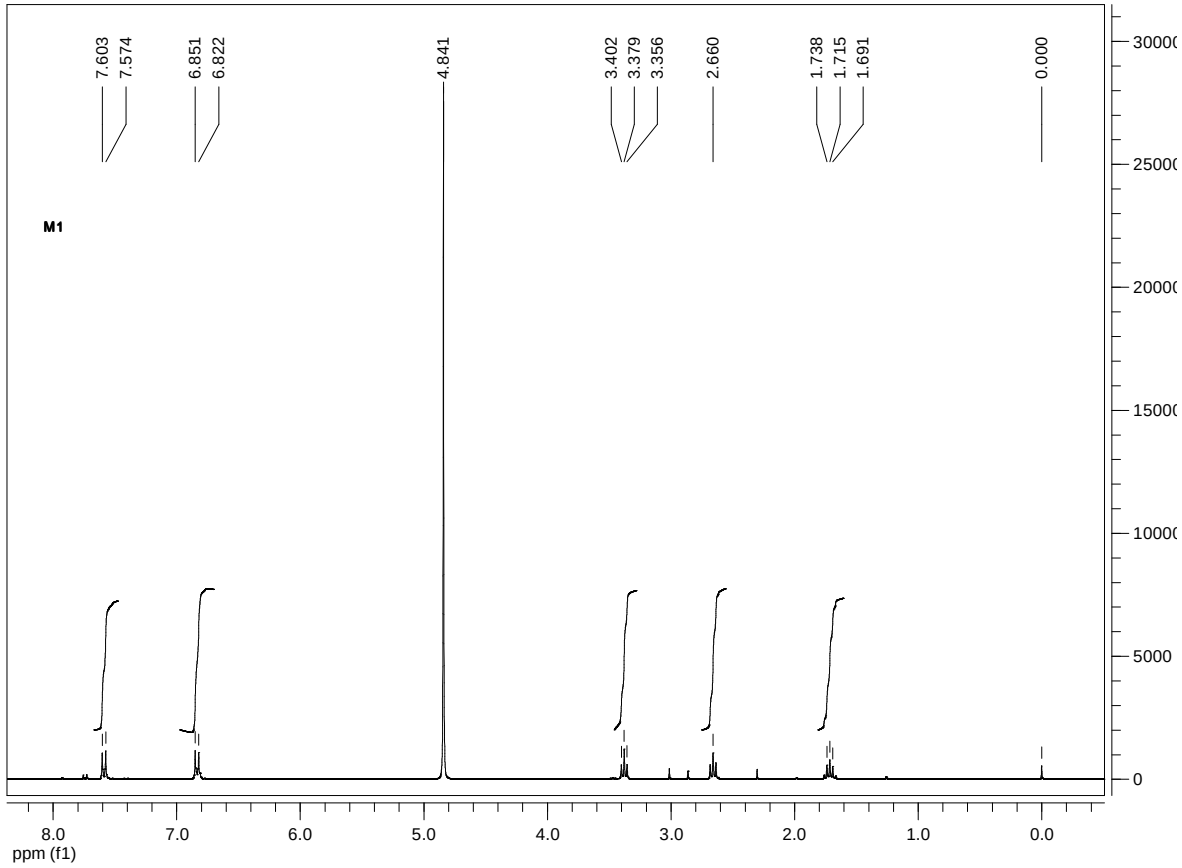

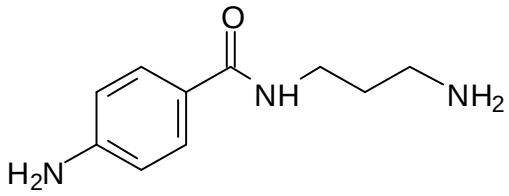

Appendix 1b: ^{1}H NMR of **M2**.

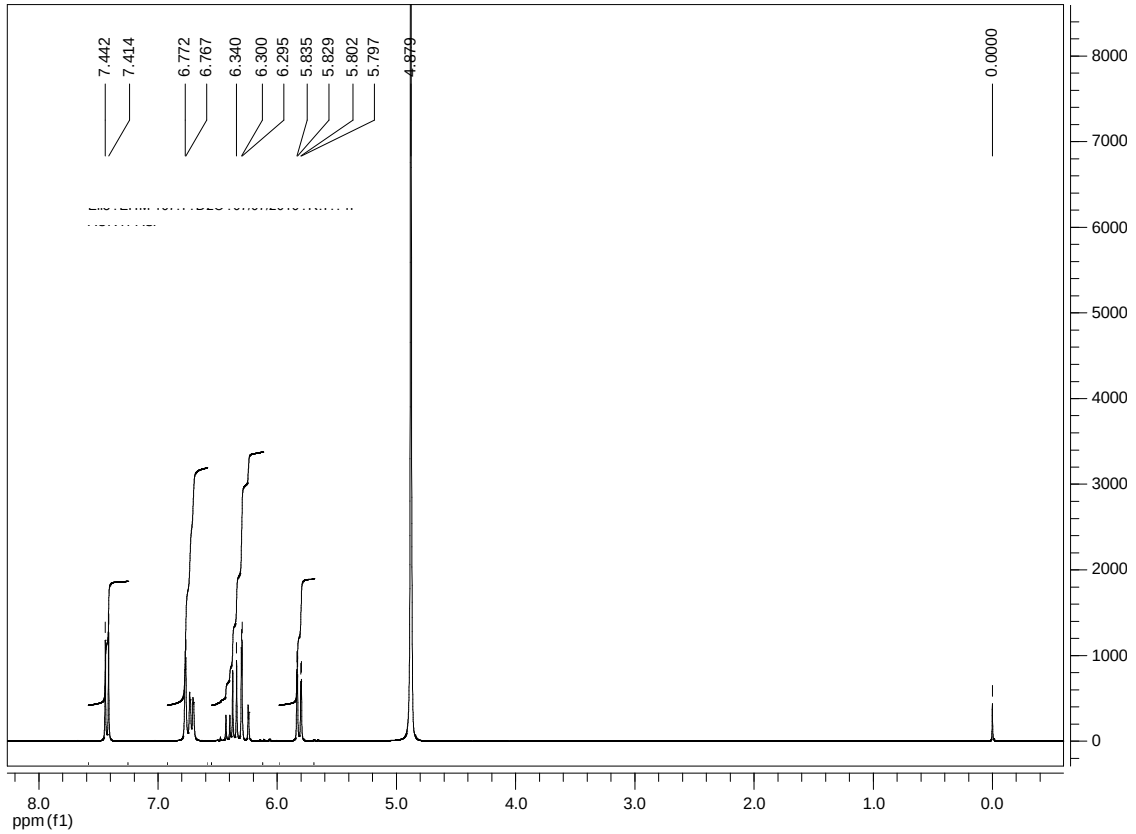

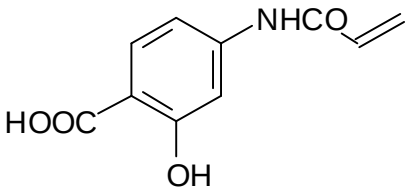

Appendix 1c: ^{1}H NMR of **M4**.

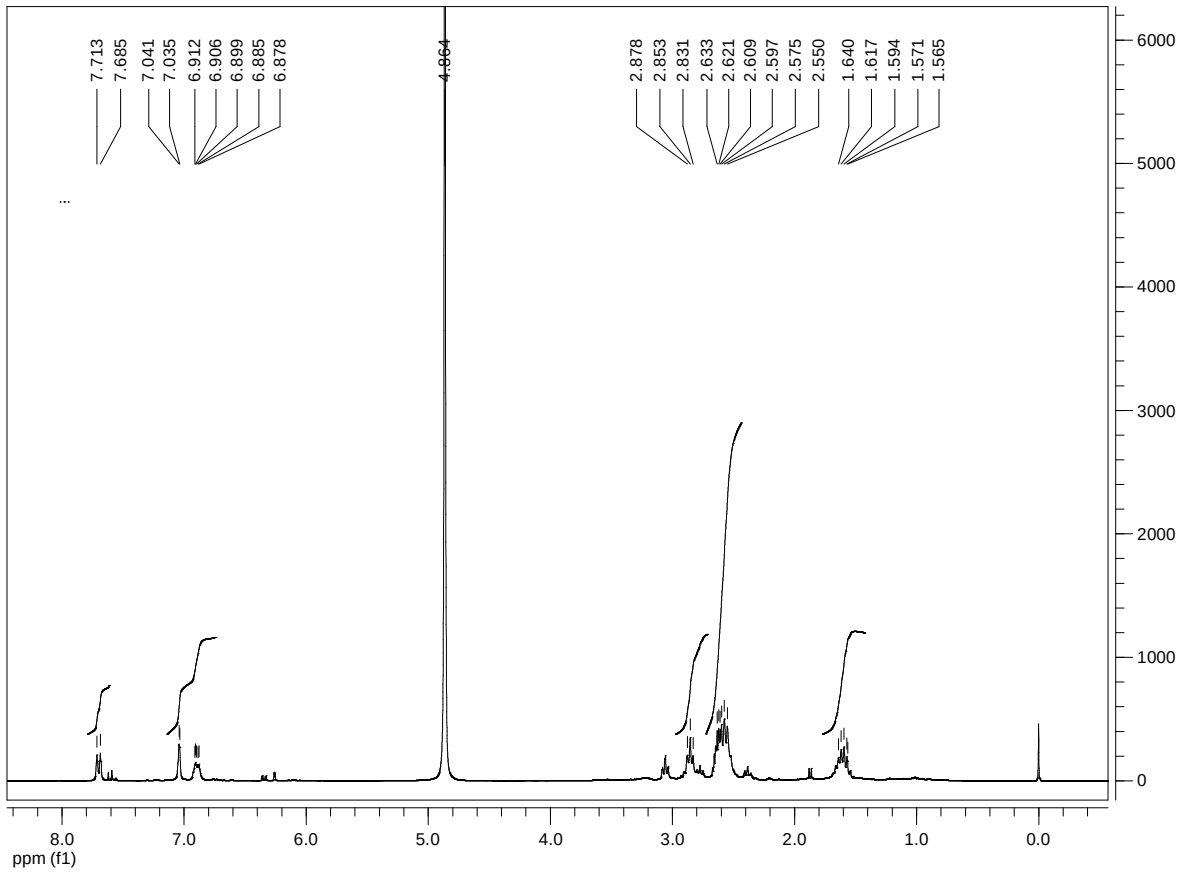

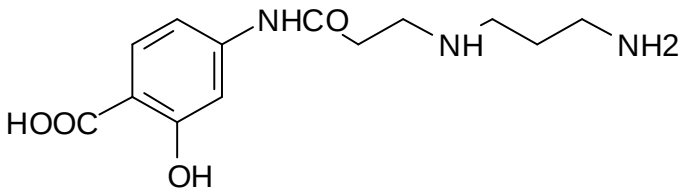

Appendix 1d: ^{1}H NMR of **M6**.

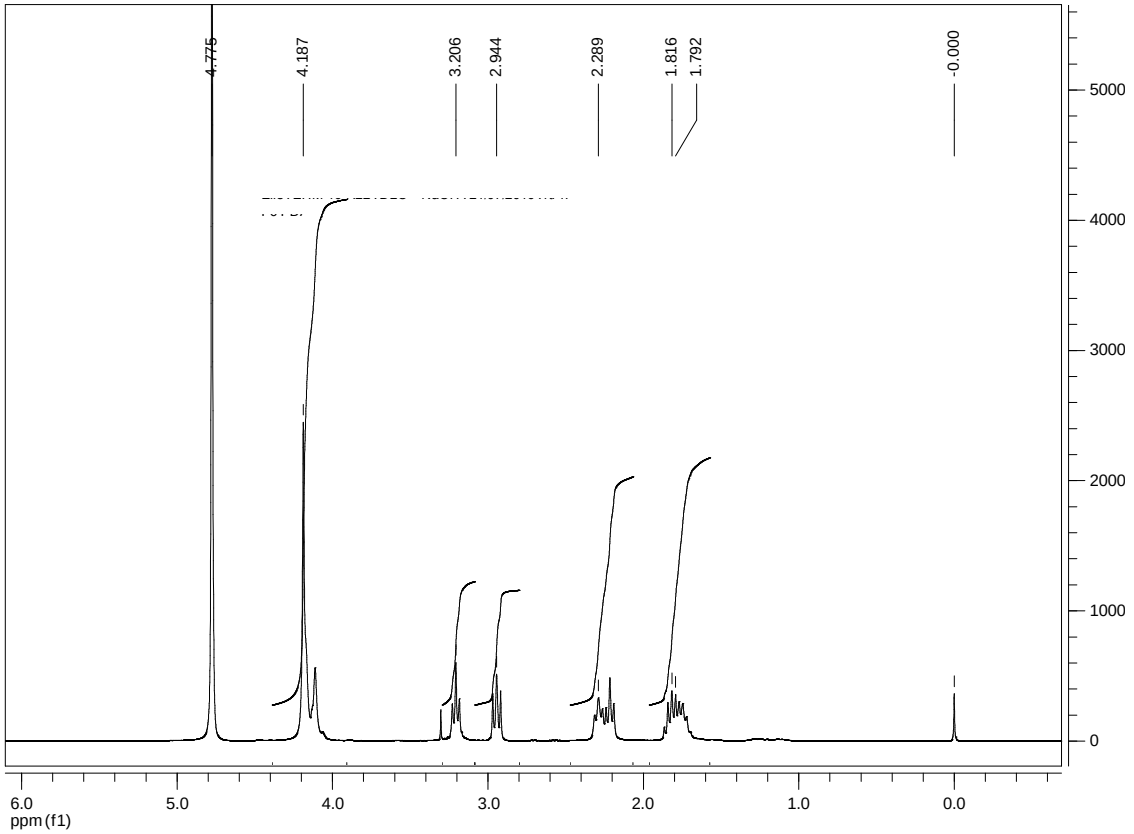

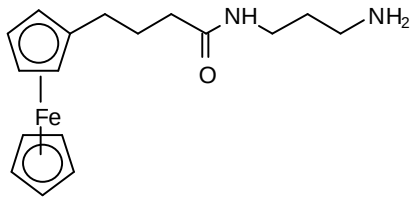

Appendix 1e: ^{1}H NMR of **M8**.

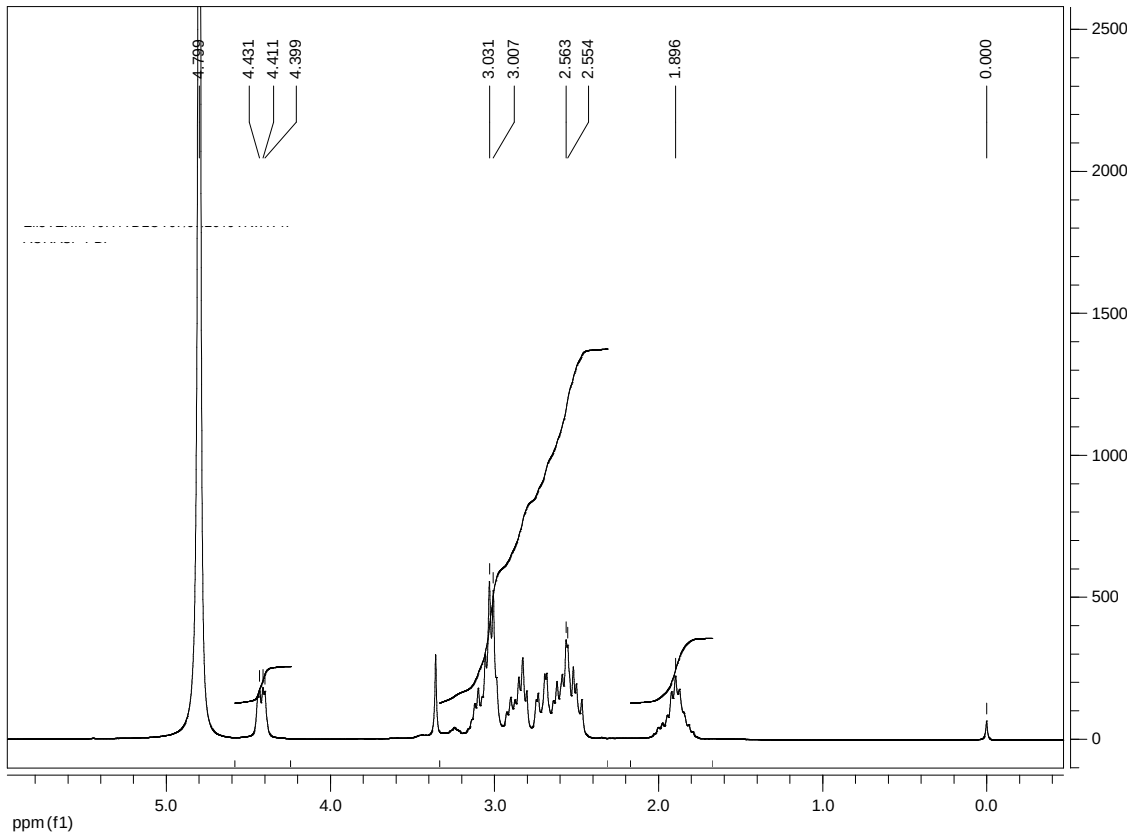

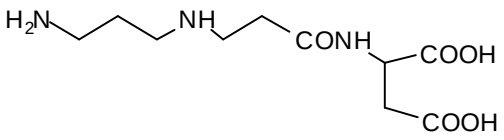

Appendix 1f: ^{1}H NMR of polyaspartamide **1**.

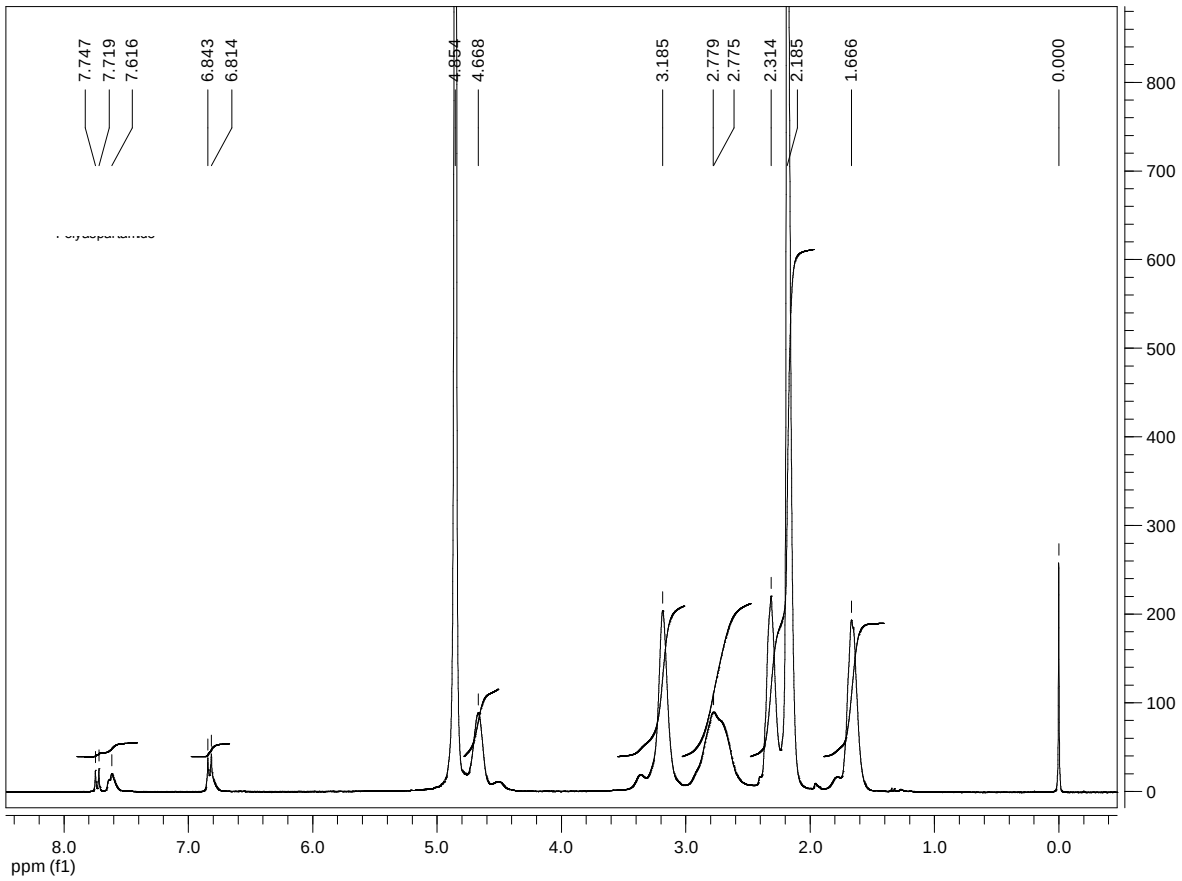

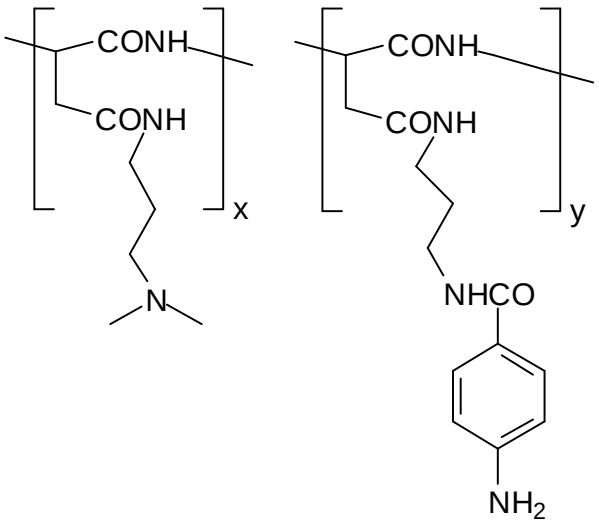

Appendix 1g: ^{1}H NMR of polyaspartamide **2**.

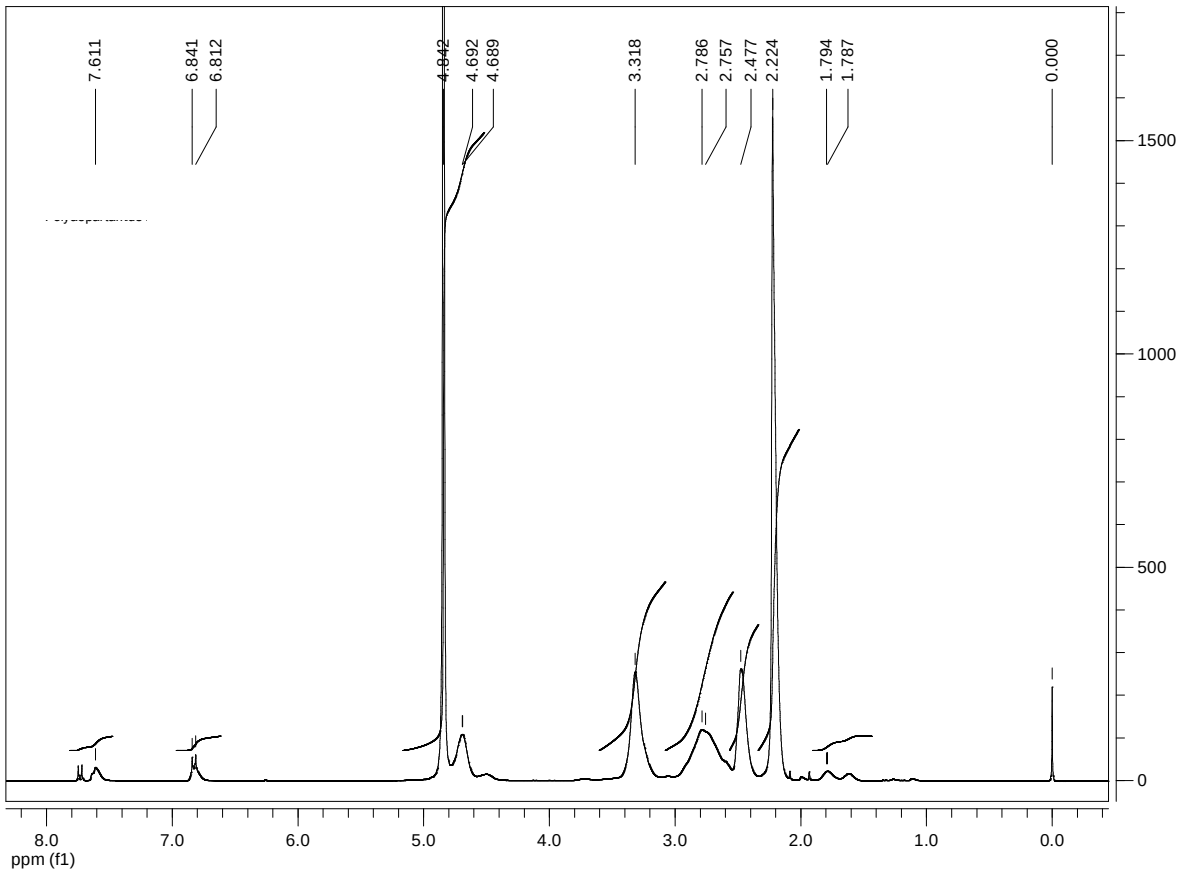

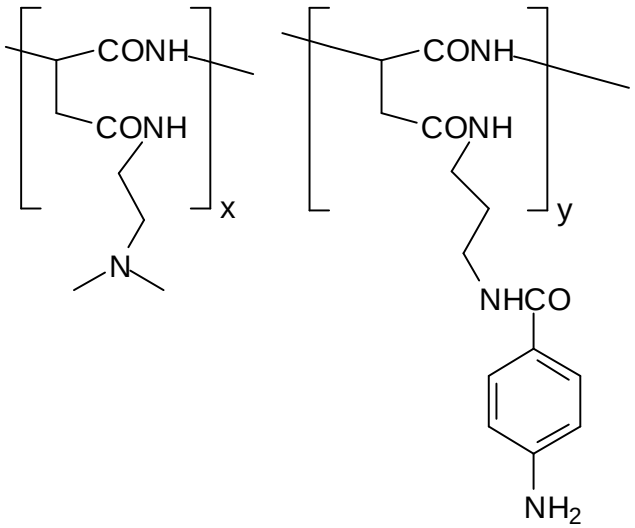

Appendix 1h: ^{1}H NMR of polyaspartamide **3**.

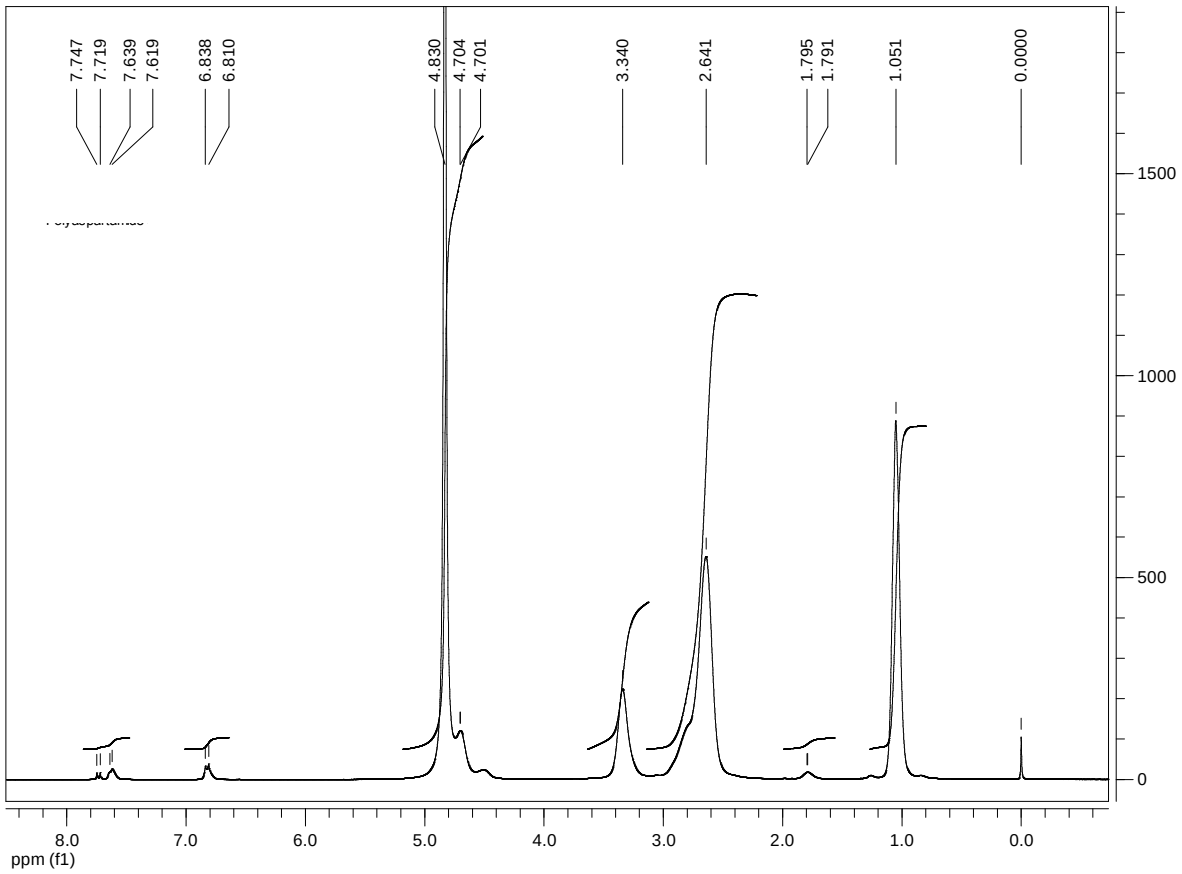

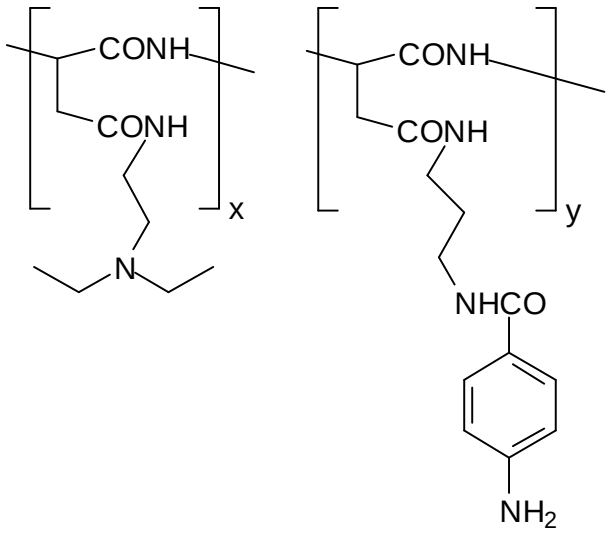

Appendix 1i: ^{1}H NMR of polyaspartamide **4**.

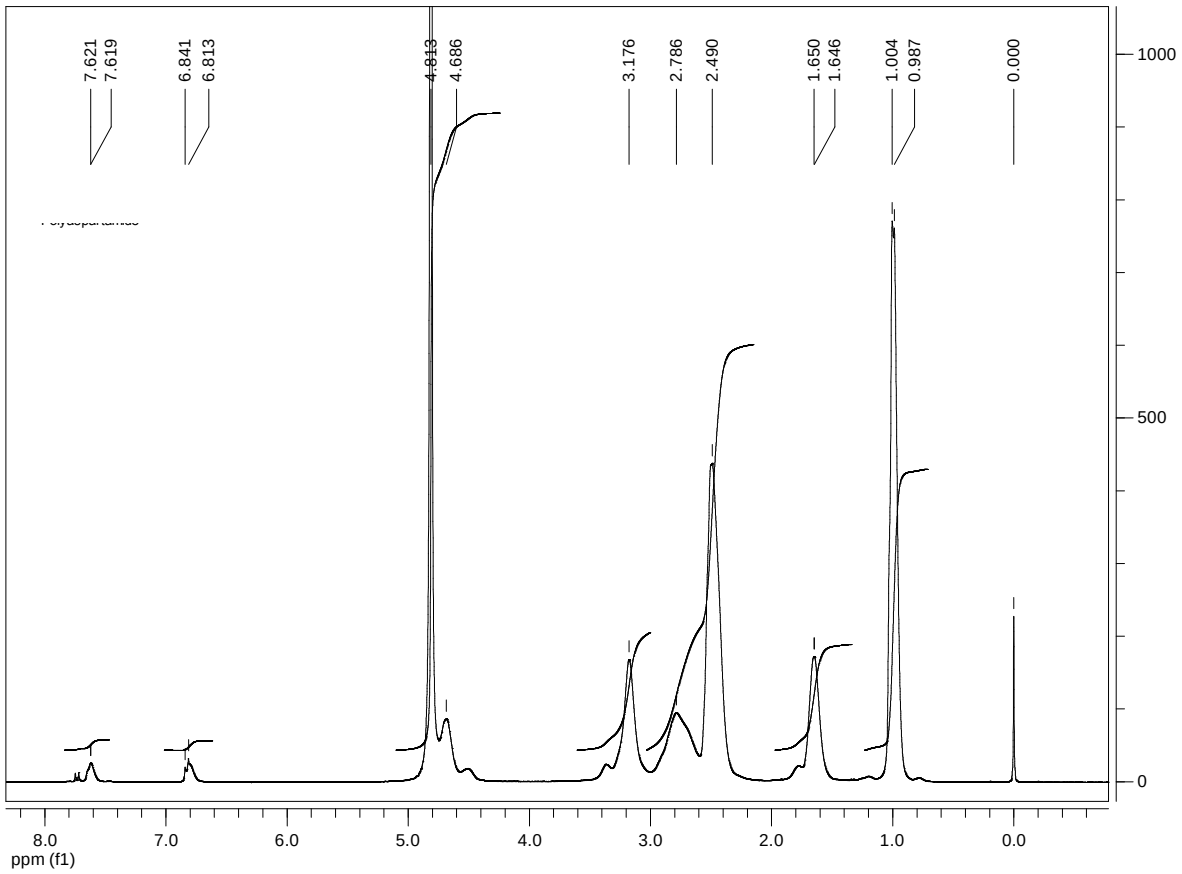

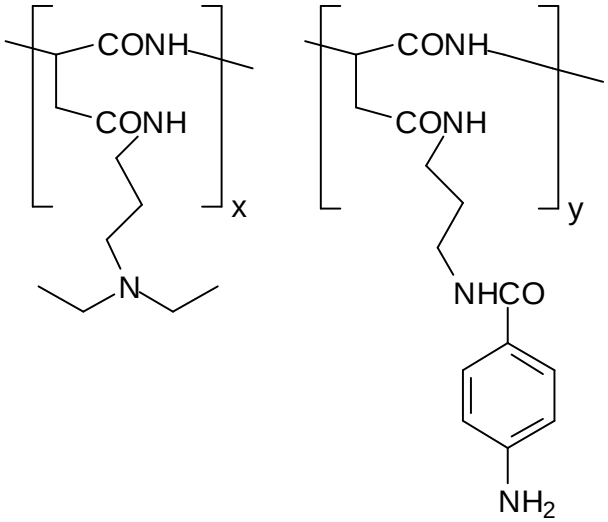

Appendix 1j: ^{1}H NMR of polyaspartamide **6**.

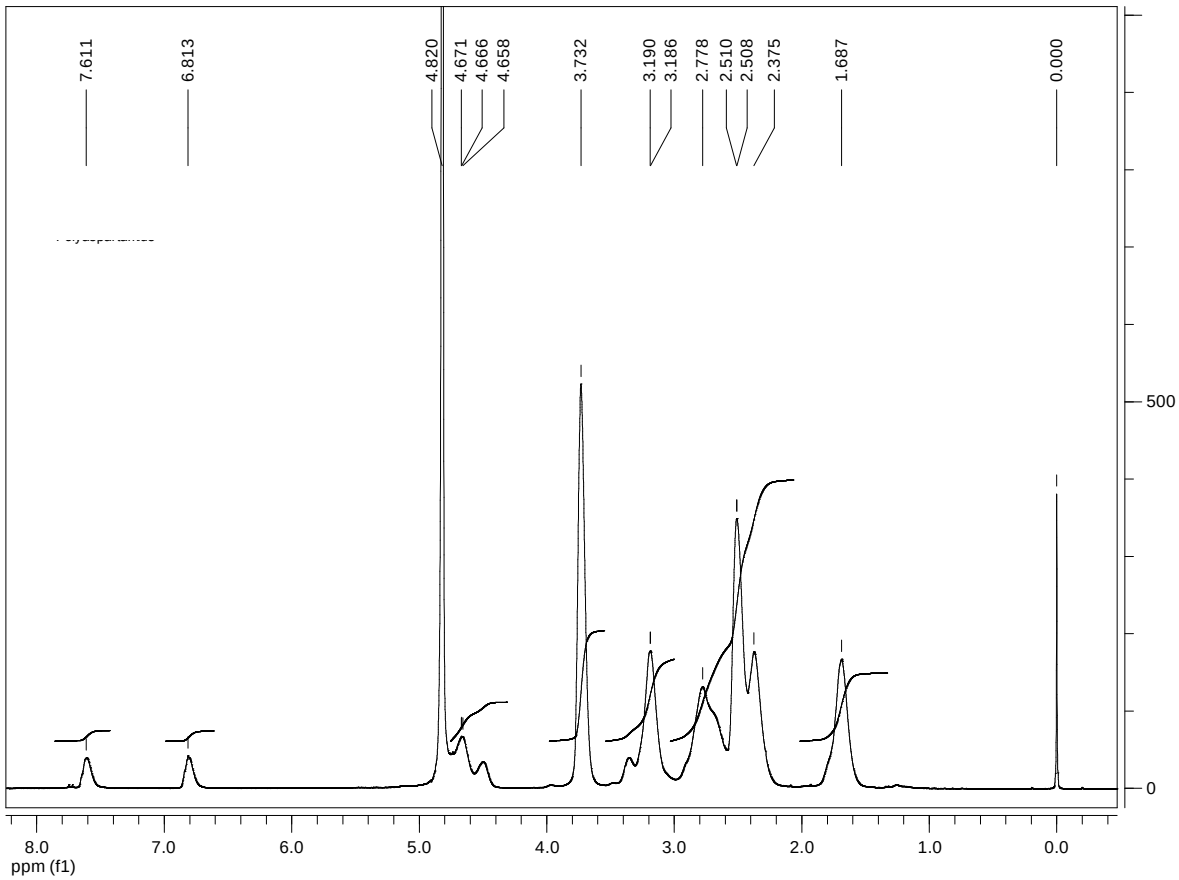

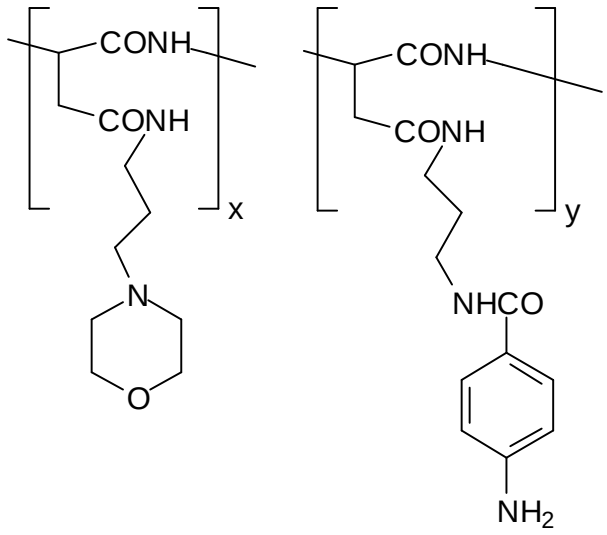

Appendix 1k: ^{1}H NMR of polyaspartamide **8**.

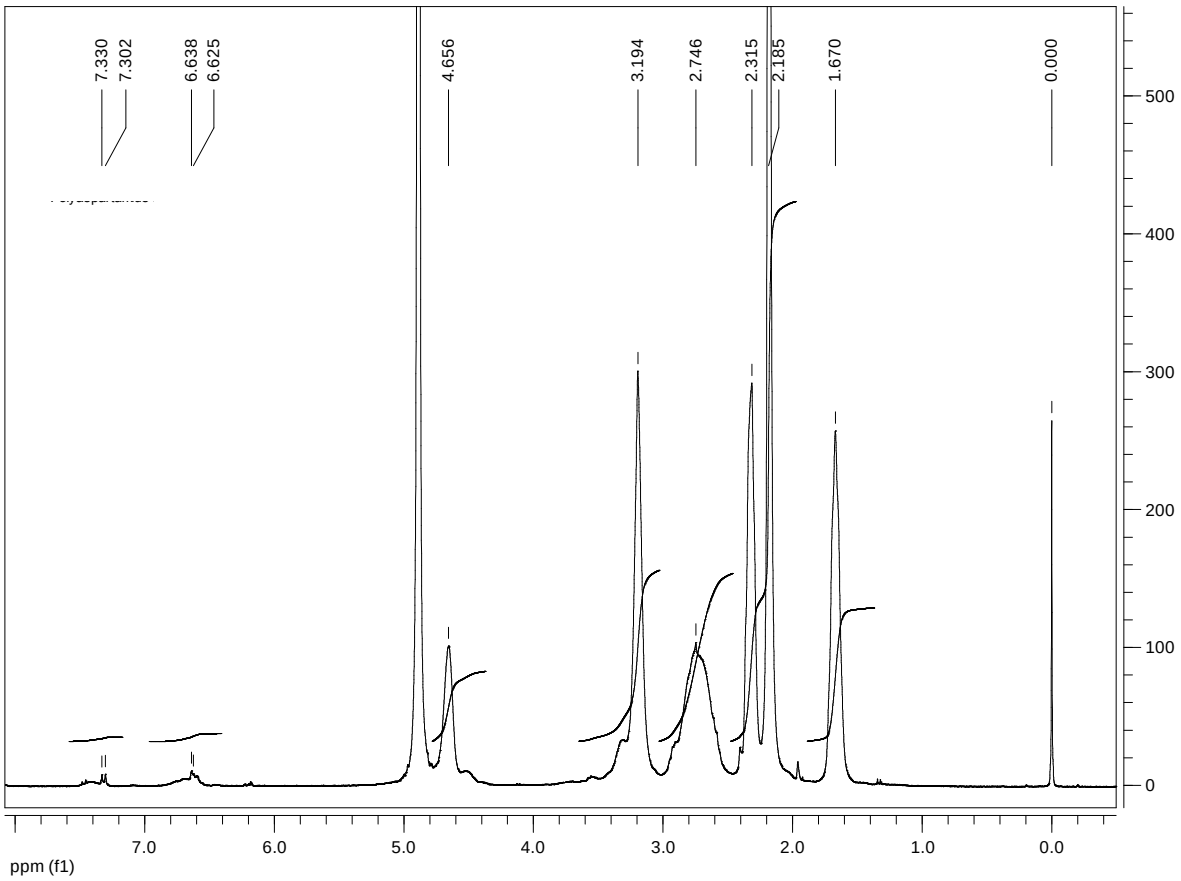

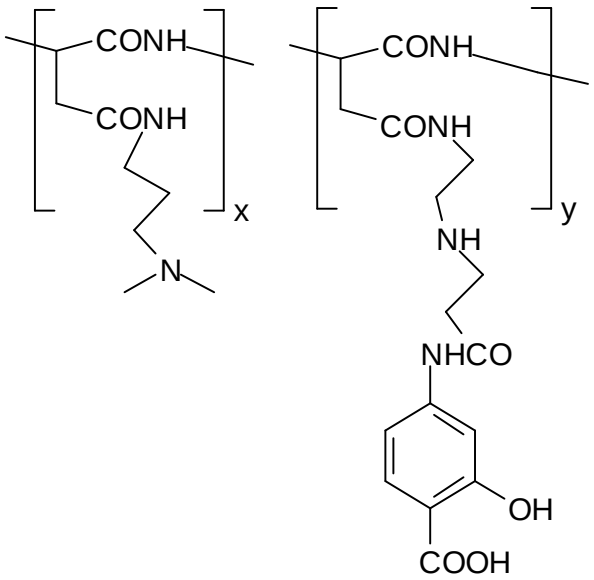

Appendix 1l: ^{1}H NMR of polyaspartamide **9**.

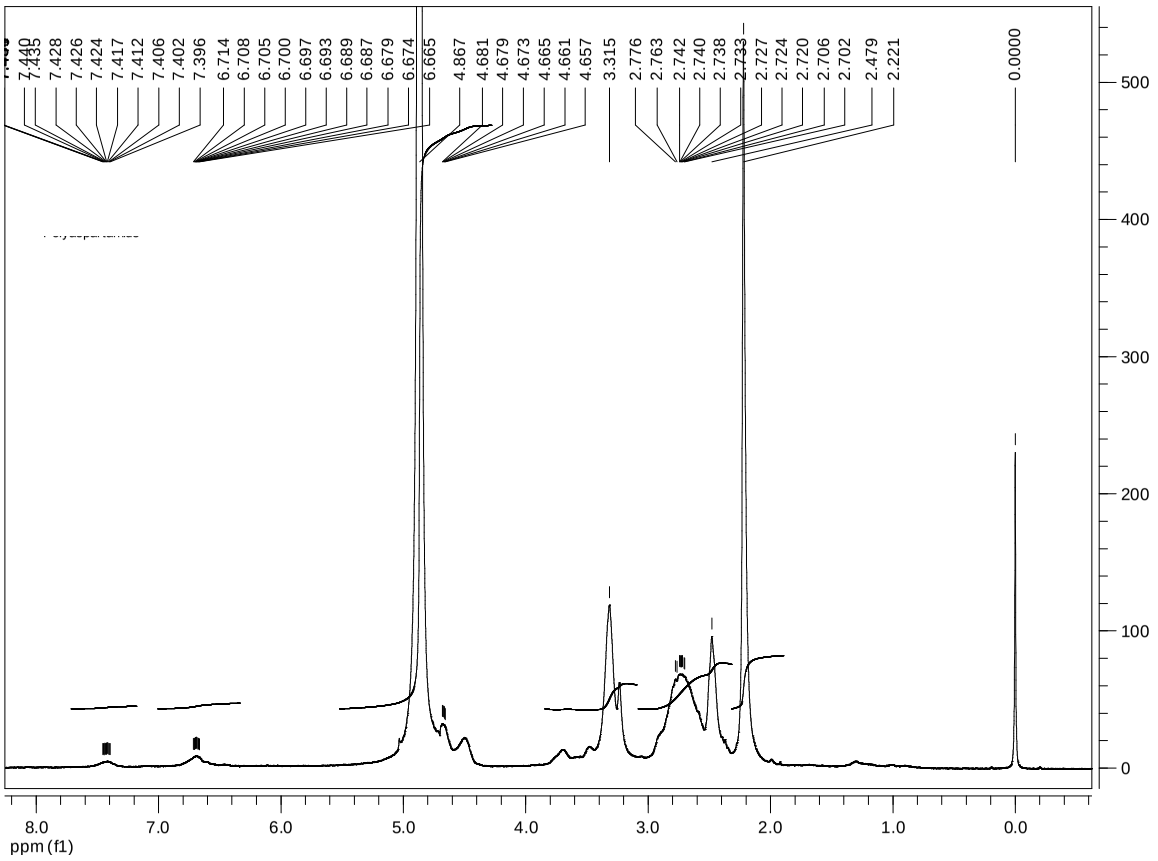

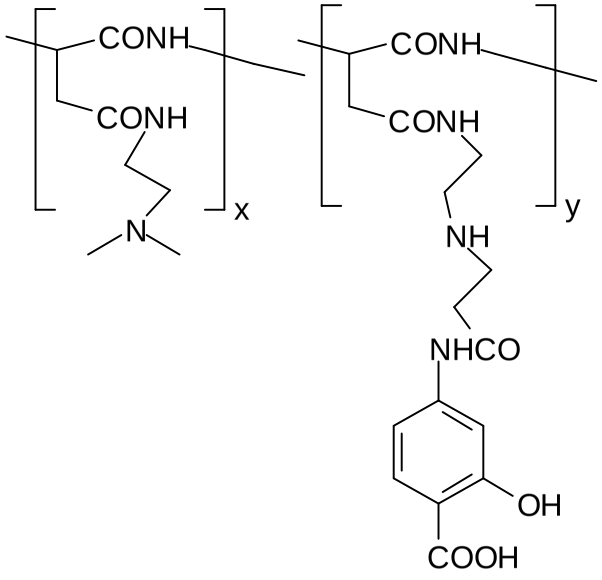

Appendix 1m: ^{1}H NMR of polyaspartamide **10**.

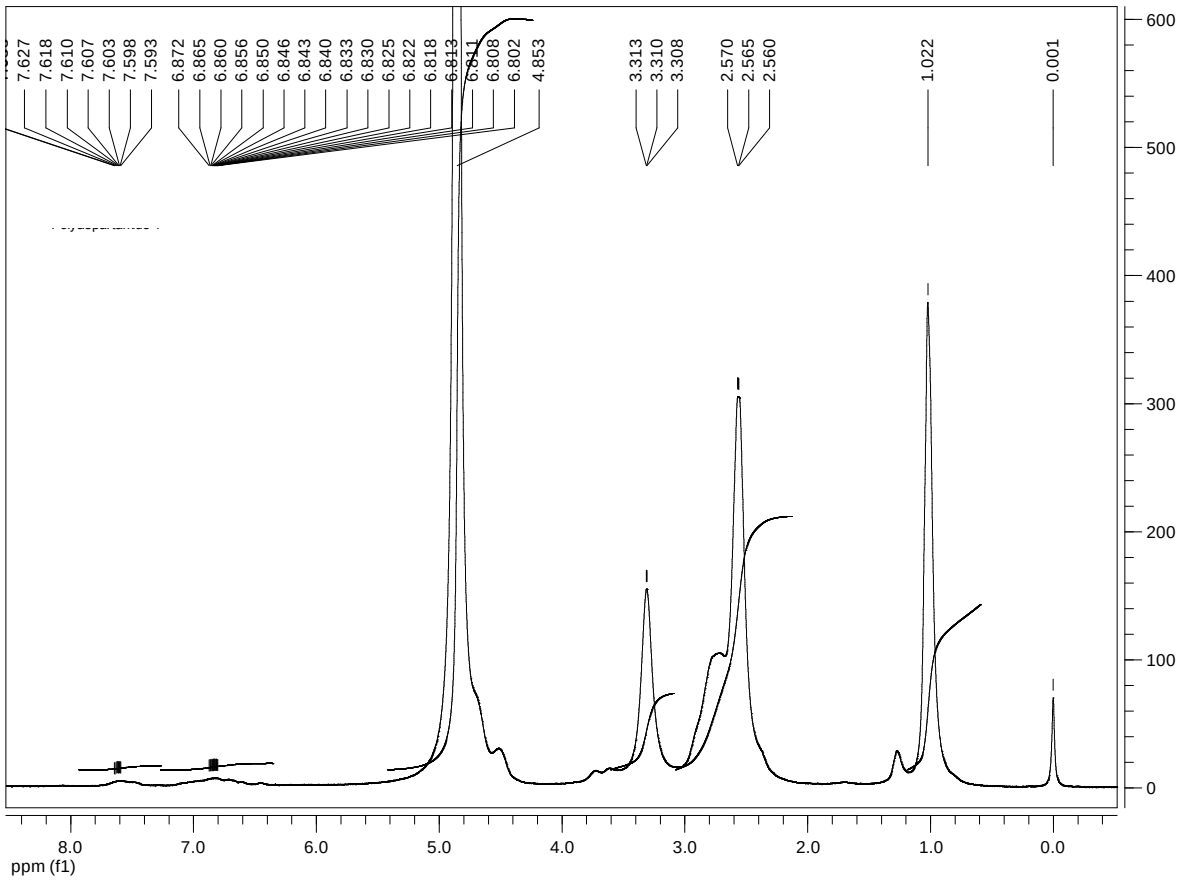

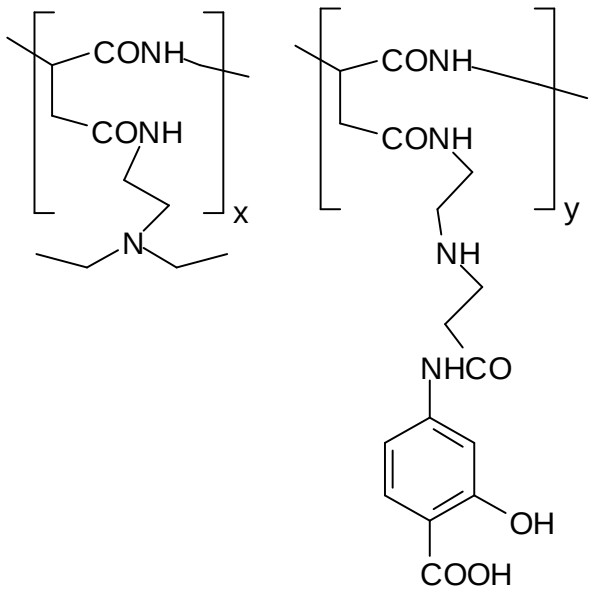

Appendix 1n: ^{1}H NMR of polyaspartamide **12**.

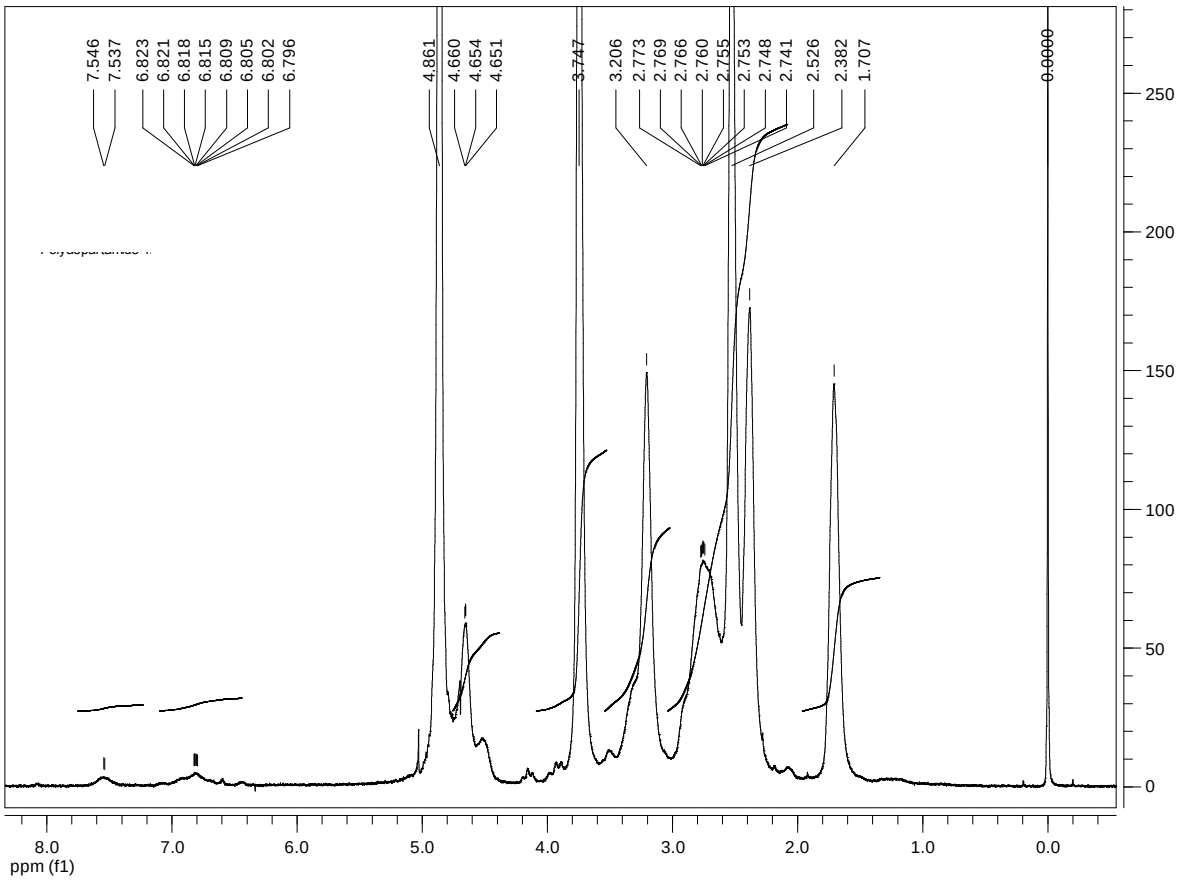

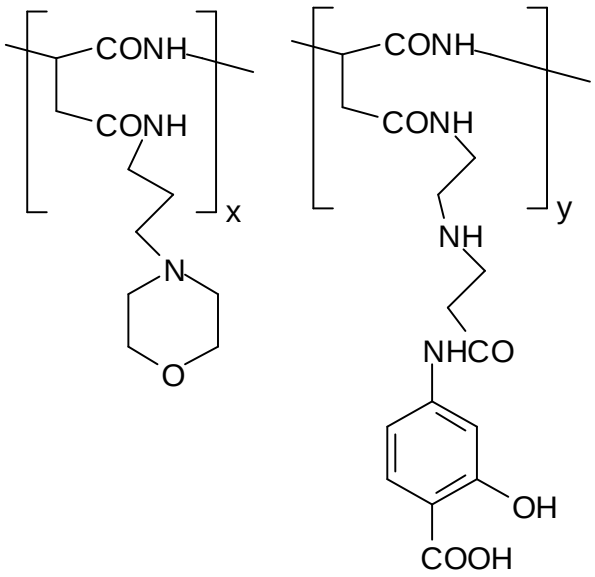

Appendix 1o: ^{1}H NMR of polyaspartamide **13**.

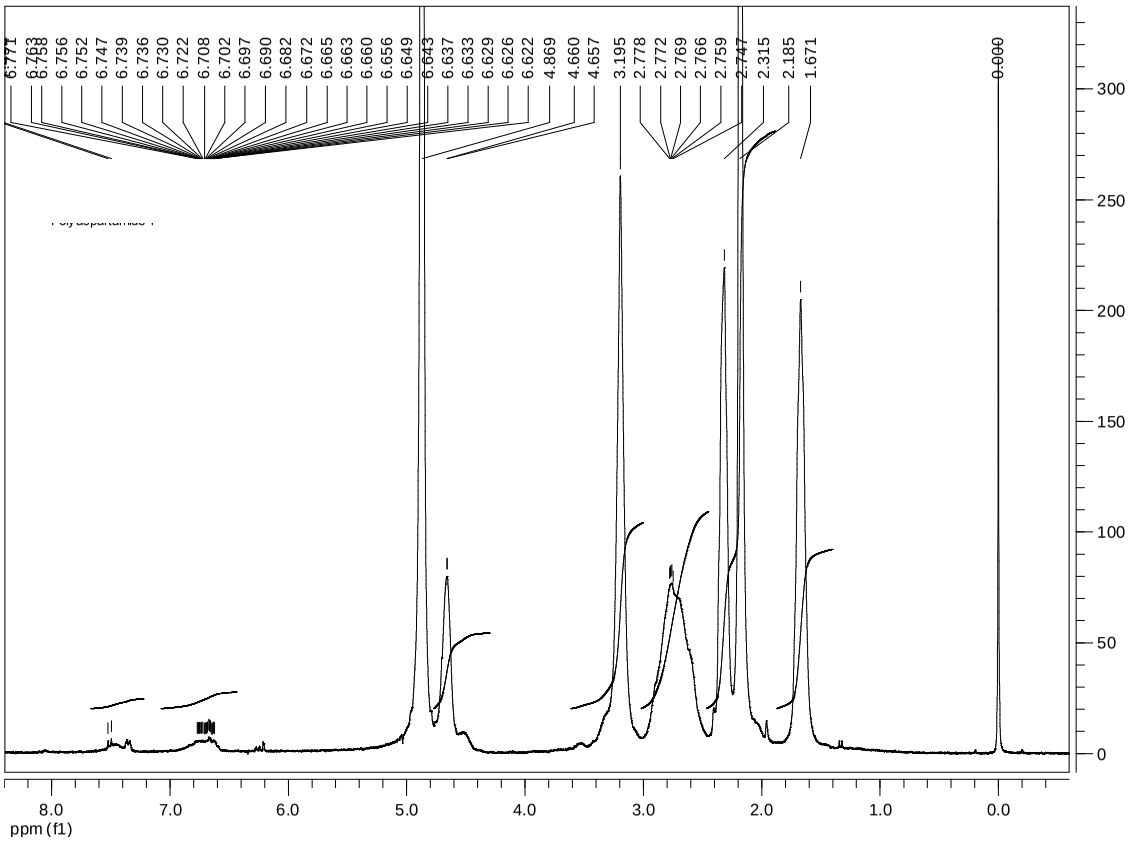

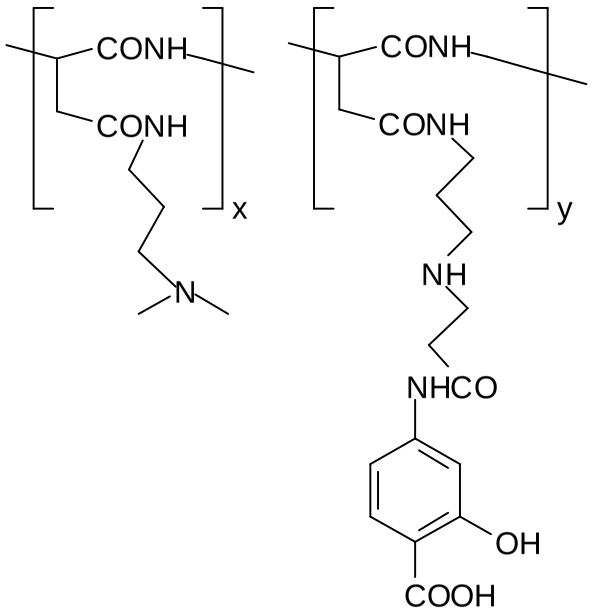

Appendix 1p: ^{1}H NMR of polyaspartamide **18**.

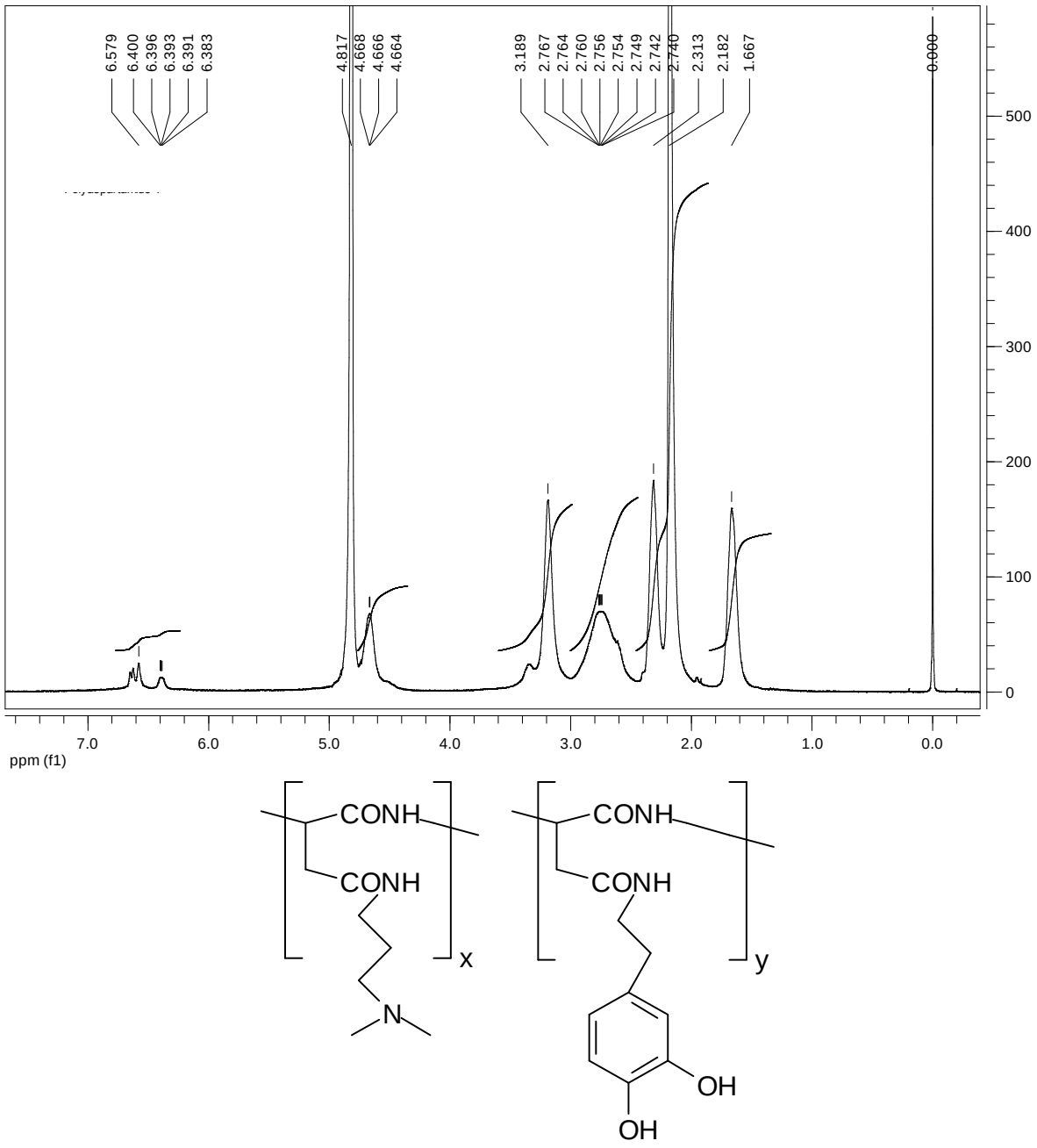

Appendix 1q: ^{1}H NMR of polyaspartamide **19**.

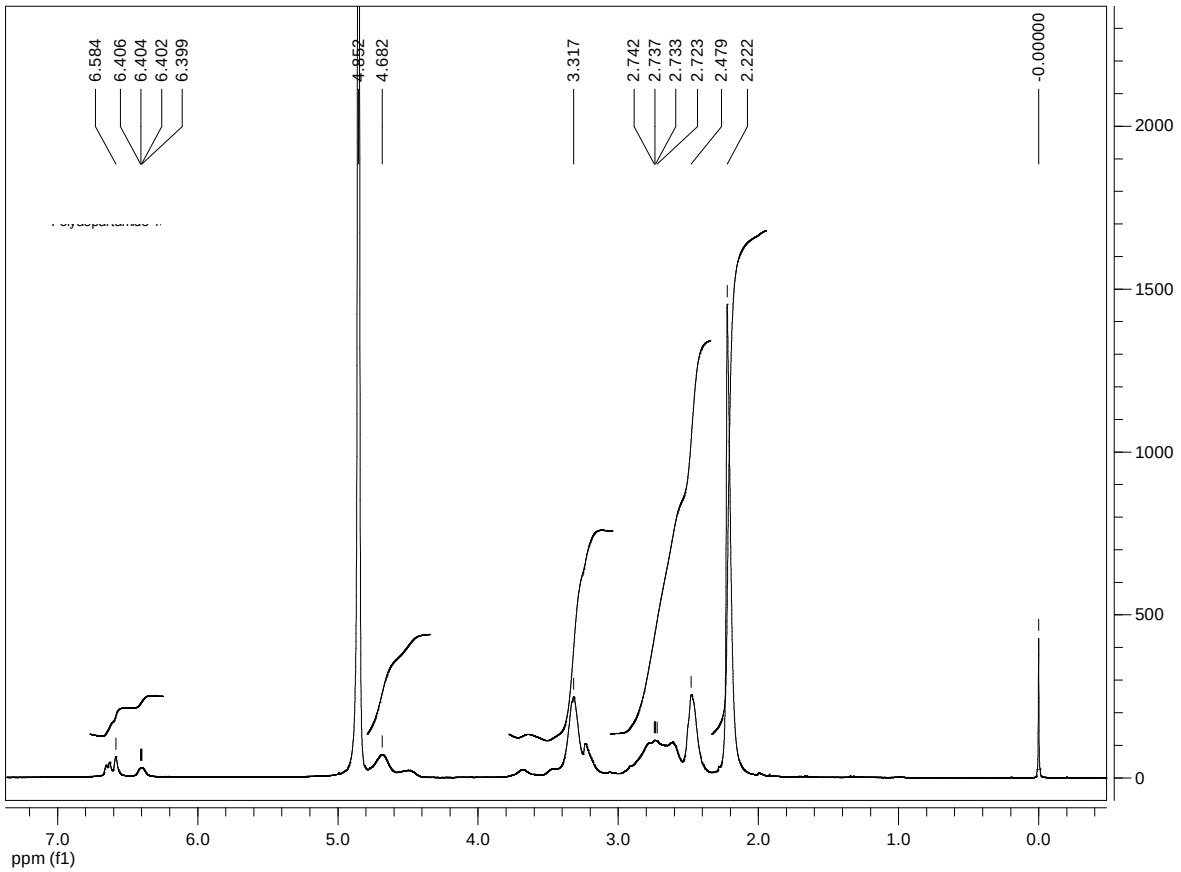

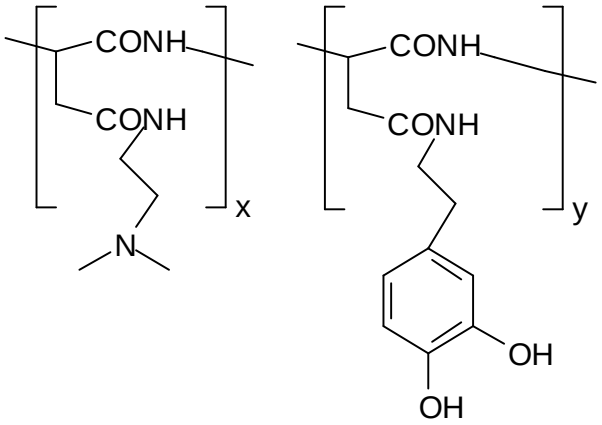

Appendix 1r: ^{1}H NMR of polyaspartamide **20**.

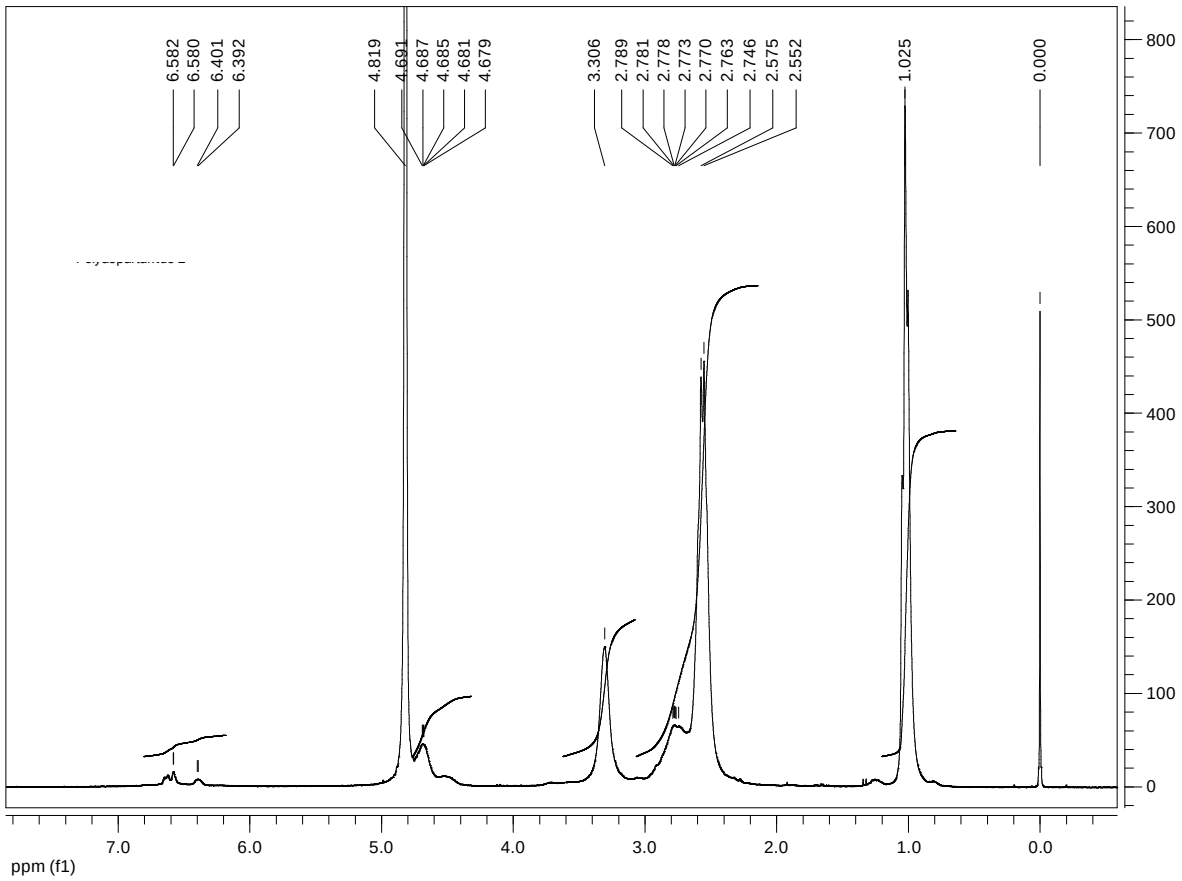

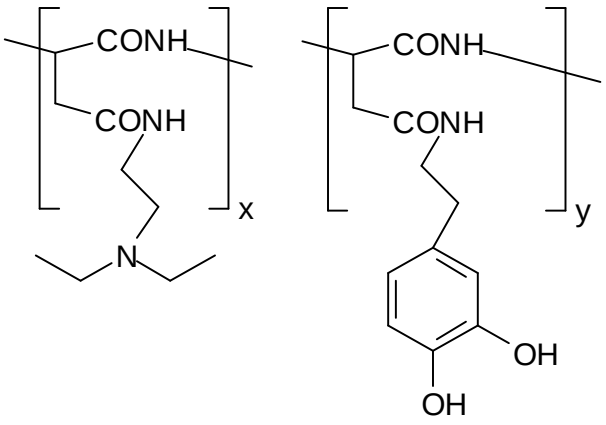

Appendix 1s: ^{1}H NMR of polyaspartamide **21**.

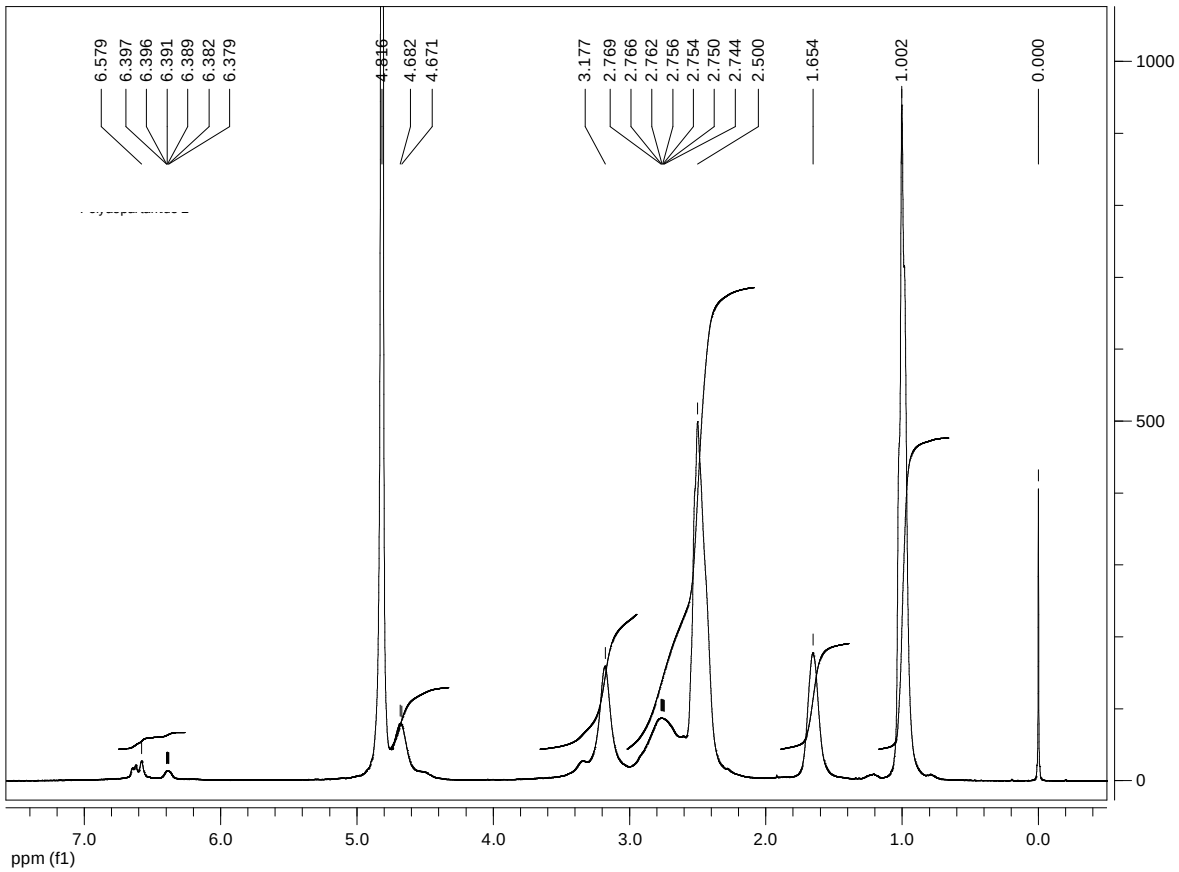

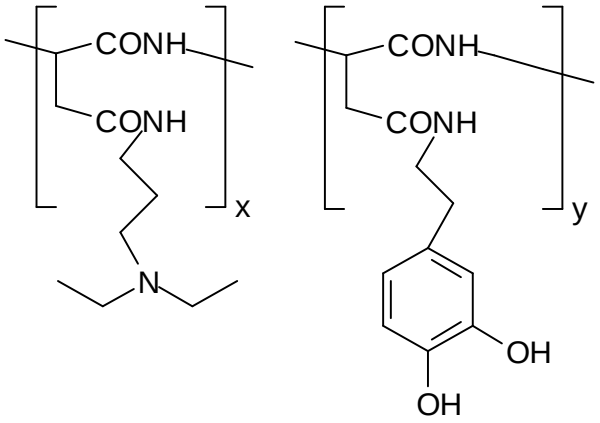

Appendix 1t: ^{1}H NMR of polyaspartamide **22**.

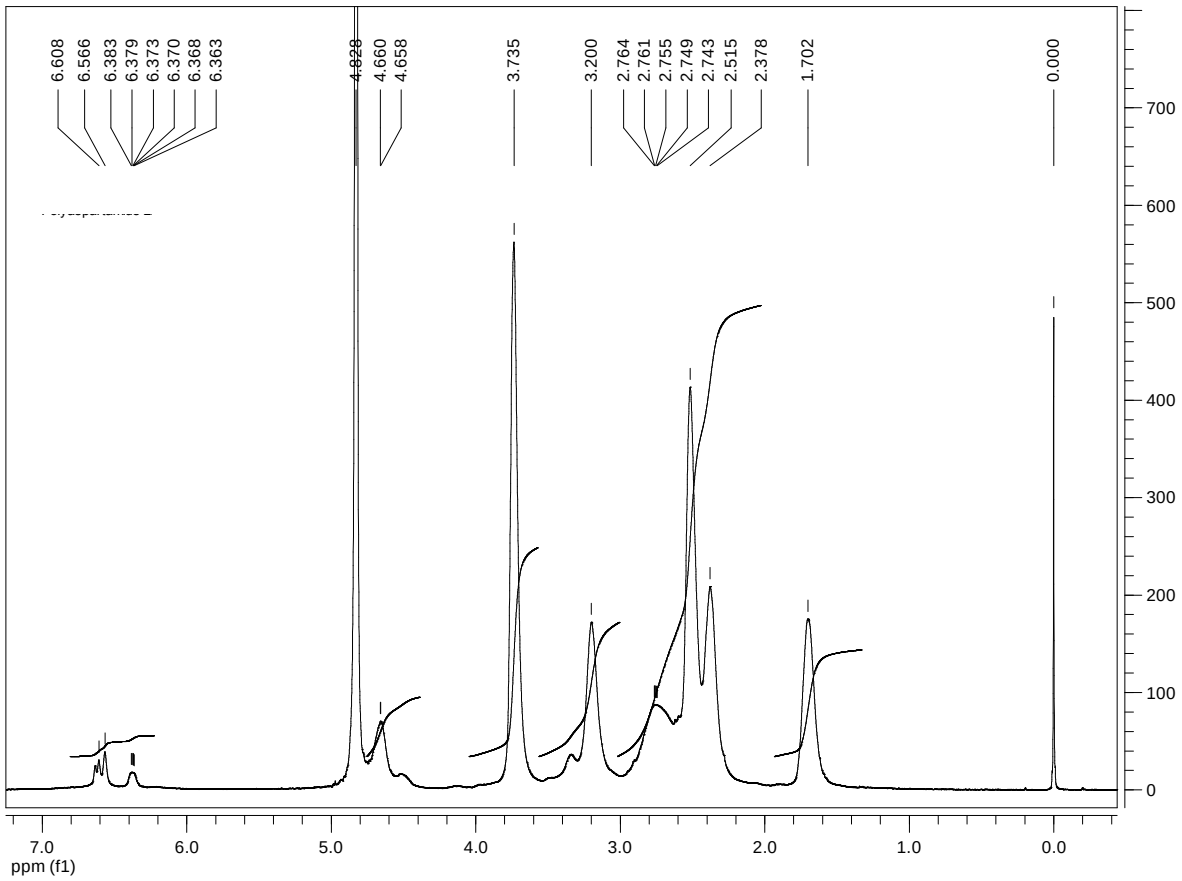

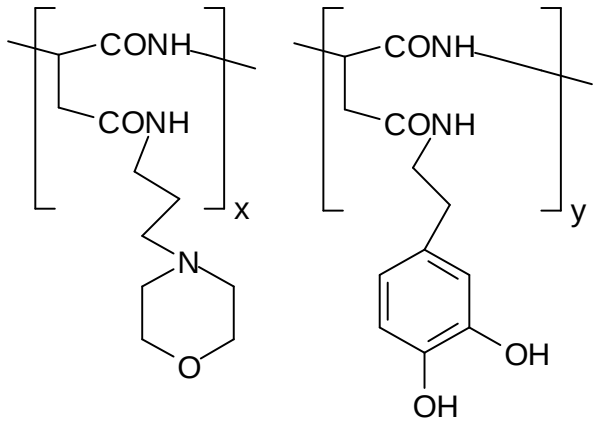

Appendix 1u: ^{1}H NMR of polyaspartamide **23**.